The role of *Xylella fastidiosa* extracellular vesicles and sRNAs in cell-to-cell communication

Dissertation zur Erlangung des

naturwissenschaftlichen Doktorgrades Dr. rer. nat.

an der Fakultät für Biologie

der Ludwig-Maximilians-Universität München

vorgelegt von Alessa Ruf

Munich, November 2025

Diese Dissertation wurde angefertigt unter der Leitung von Prof. Dr. Silke Robatzek im Bereich der Genetik der Fakultät für Biologie an der Ludwig-Maximilians-Universität München.

Erstgutachter/in: Prof. Dr. Silke Robatzek

Zweitgutachter/in: Prof. Dr. Daniel Unterweger

Tag der Abgabe: 26. November 2025

Tag der mündlichen Prüfung: 13. Februar 2026

Eigenständigkeitserklärung

Eigenständigkeitserklärung

Hiermit versichere ich an Eides statt, dass die vorliegende schriftliche Dissertation / Masterarbeit / Bachelorarbeit / Zulassungsarbeit mit dem Titel

The role of Xylella fastidiosa extracellular vesicles and sRNAs in cell-to-cell communication

von mir selbstständig verfasst wurde und dass keine anderen als die angegebenen Quellen und Hilfsmittel benutzt wurden. Die Stellen der Arbeit, die anderen Werken dem Wortlaut oder dem Sinne nach entnommen sind, wurden in jedem Fall unter Angabe der Quellen (einschließlich des World Wide Web und anderer elektronischer Text- und Datensammlungen) kenntlich gemacht. Weiterhin wurden alle Teile der Arbeit, die mit Hilfe von Werkzeugen der künstlichen Intelligenz de novo generiert wurden, durch Fußnote/Anmerkung an den entsprechenden Stellen kenntlich gemacht und die verwendeten Werkzeuge der künstlichen Intelligenz gelistet. Die genutzten Prompts befinden sich im Anhang. Diese Erklärung gilt für alle in der Arbeit enthaltenen Texte, Graphiken, Zeichnungen, Kartenskizzen und bildliche Darstellungen.

München, 17.11.2025

(Ort / Datum)

Alessa Ruf

(Vor und Nachname in Druckbuchstaben)

Alessa Ruf

(Unterschrift)

Affidavit

Herewith I certify under oath that I wrote the accompanying Dissertation / MSc thesis / BSc thesis / Admission thesis myself.

Title: The role of Xylella fastidiosa extracellular vesicles and sRNAs in cell-to-cell communication

In the thesis no other sources and aids have been used than those indicated. The passages of the thesis that are taken in wording or meaning from other sources have been marked with an indication of the sources (including the World Wide Web and other electronic text and data collections). Furthermore, all parts of the thesis that were de novo generated with the help of artificial intelligence tools were identified by footnotes/annotations at the appropriate places and the artificial intelligence tools used were listed. The prompts used were listed in the appendix. This statement applies to all text, graphics, drawings, sketch maps, and pictorial representations contained in the Work.

München, 17.11.2025

(Location/date)

Alessa Ruf

(First and last name in block letters)

Alessa Ruf

(Signature)

Regeln für den Einsatz von Werkzeugen der Künstlichen Intelligenz (KI) für prüfungsrelevante Tätigkeiten

1. Der Einsatz von KI-Werkzeugen für prüfungsrelevante Leistungen ist möglich.

2. Der Einsatz von KI-Werkzeugen zur Optimierung, Übersetzung, Korrektur von Rechtschreibung und Grammatik von selbstgenerierten Texten und zur Optimierung von Designaspekten selbstgenerierter Abbildungen ist ohne Kennzeichnung zulässig.

3. Von KI-Werkzeugen de novo generierte und in der Arbeit verwendete Textabschnitte und Abbildungen sind durch Fußnoten/Anmerkungen an den entsprechenden Stellen deutlich zu kennzeichnen und das KI-Tool ist analog zu Literaturquellen anzugeben. Die verwendeten Prompts sind im Anhang zu listen.

4. Textabschnitte, die durch den iterativen Einsatz von KI-Tools erzeugt wurden, sind zu kennzeichnen.

5. Die Autorin / der Autor ist für die Korrektheit und korrekte Darstellung in schriftlichen Leistungen und Präsentationen verantwortlich.

6. Quellen / Referenzen müssen nach den Regeln der guten wissenschaftlichen Praxis zitiert werden.

Rules for the use of artificial intelligence (AI) tools for examination-relevant activities

1. The use of AI tools for examination-relevant performances is possible.

2. The use of AI tools to optimize, translate and correct the spelling and grammar of self-generated texts and to optimize self-generated illustrations is permitted without indication.

3. Text sections and illustrations de novo generated by AI tools and used in the thesis must be clearly marked by footnotes/annotations at the appropriate places and the AI tool must be indicated analogously to literature sources. The prompts used have to be listed in the appendix.

4. Sections of the text generated through iterative use of AI tools should be marked.

5. The author is responsible for the correctness and proper presentation in written performances and presentations.

6. Sources / references must be cited in accordance with the rules of good scientific practice.

Erklärung über frühere Promotionsversuche

Erklärung
Declaration

Hiermit erkläre ich, *
Hereby I declare

☒ dass die Dissertation nicht ganz oder in wesentlichen Teilen einer anderen Prüfungskommission vorgelegt worden ist.
that this work, complete or in parts, has not yet been submitted to another examination institution

☒ dass ich mich anderweitig einer Doktorprüfung ohne Erfolg **nicht** unterzogen habe.
*that I did **not** undergo another doctoral examination without success*

☐ dass ich mich mit Erfolg der Doktorprüfung im Hauptfach
that I successfully completed a doctoral examination in the main subject

und in den Nebenfächern
and in the minor subjects

bei der Fakultät für
at the faculty of _____

der
at _____
(Hochschule/*University*)

unterzogen habe.

☐ dass ich ohne Erfolg versucht habe, eine Dissertation einzureichen oder mich der Doktorprüfung zu unterziehen.
that I submitted a thesis or did undergo a doctoral examination without success

München, 17.11.2025 _____ Alessa Ruf _____
Ort, Datum/*place, date* Unterschrift/*signature*

*) Nichtzutreffendes streichen/
delete where not applicable

Table of Content

List of Figures

Abbreviations

AGO	Argonaute
ALS	Almond Leaf Scorch
At	*Arabidopsis thaliana*
ATP	Adenosine triphosphate
AvrPphB	Avirulence protein of *Pseudomonas syringae* pv. *PHaseolicola* B
BAK1	BRI1-Associated receptor Kinase 1
Bc	*Botrytis cinerea*
BigR	Biofilm Growth-Associated Repressor
BIK1	Botrytis-induced Kinase 1
BRI1	Brassinosteroid Insensitive 1
c-di-GMP	cyclic di-guanylate monophosphate
Ca^{2+}	Calcium
CC-NBS-LRR; CNL	Coiled Coil domain-Nucleotide Binding Site-Leucine Rich Repeat
ckRNAi	cross-kingdom RNA interference
CLS	Coffee Leaf Scorch
CME	Clathrin-Mediated Endocytosis
Col-0	Colombia-0
ComE/A	Competence proteins E/A
CPK	Calcium-dependent Proteinase Kinase
CSP	Cold Shock Protein
CVC	Citrus-Variegated Chlorosis
CWDE	Cell Wall Degrading Enzyme
DAMPs	Danger-associated molecular pattern
DBP	DNA-Binding Protein
DCL	Dicer-Like endonuclease
DNA	DeoxyriboNucleic Acid
DNA-seq	DNA sequencing
DSF	Diffusible Signal Factor
dsRNA	double-stranded RNA
E. coli	*Escherichia coli*
eDNA	Environmental DNA
EDS1	Enhanced Disease Susceptibility 1
EF-Tu	Elongation-Factor Tu
EFR	EF-Tu Receptor
elf18	epitope of EF-Tu
EPS	Exopolysaccharides
ER	Endoplasmic Reticulum
ETI	Effector-Triggered Immunity
EV	Extracellular Vesicle
exDNA	Extracellular DNA
exRNA	Extracellular RNA
FarS	Fatty Acids regulated sRNA
FimT3	Fimbrial protein T3; Minor pilin of TIV pilus
flg22	epitope of flagellin
FLS2	Flagellin-Sensing 2
GFP	Green Fluorescent Protein
GI	Genomic Island
HEN1	Hua Enhancer 1
Hfq	Host Factor for phage Qβ replication
HGT	Horizontal Gene Transfer
HopT1-1	Hrp Outer Protein T1-1
HR	Hypersensitive Response
HrpG/HrpX	Hypersensitive Response and Pathogenicity protein G/X
IM	Inner Membrane
LesA	Lipase/Esterase A
LPS	Lipopolysaccharides
MAMP	Microbe-Associated Molecular Pattern
MAPK	Mitogen-Activated Protein Kinase
miRNA	micro RNA
mRNA	messenger RNA
MVB	Multivesicular Body
NAD+	Nicotinamide Adenine Dinucleotide
NBS-LRR; NLR	Nucleotide Binding Site-Leucine Rich Repeat Receptor
ncRNA	non-coding RNA
nt	nucleotides
ObfA	Outer membrane-associated Biofilm Facilitating protein A
OIMV	Outer Inner Membrane Vesicle
OM	Outer Membrane
OMV	Outer Membrane Vesicle
OQDS	Olive Quick Decline Syndrome
Pa	*Pseudomonas aeruginosa*
PAD4	Phytoalexin Deficient 4
PCW	Primary Cell Wall
PD	Pierce's Disease
PD2/PD3	Pierce's Disease medium 2/3
phasiRNA	Phased Small Interfering RNA
PhoP/Q/R	Phosphate regulon proteins P/Q/R

Abbreviations

PilY	Pilus Y
PRR	Pattern Recognition Receptor
Pst	*Pseudomonas syringae* pv. *tomato*
PTI	Pattern-Triggered Immunity
Pto DC3000	*Pseudomonas syringae* pv. *tomato* strain DC3000
pv.	pathovar
QS	Quorum Sensing
R protein	Resistance protein
RBP	RNA-Binding Protein
RBS	Ribosome Binding Site
RDR	RNA-Dependent RNA polymerase
RecA	Recombinase A
RISC	RNA-Induced Silencing Complex
RLCK	Receptor-Like Cytoplasmic Kinases
RMS	Restriction-Modification Systems
RNA	RiboNucleic Acid
RNA-seq	RNA sequencing
RNAi	RNA interference
RnE	Ribonuclease E
ROS	Reactive Oxygen Species
RpfF	Regulator of Pathogenicity Factor F
RPS5	Resistance to Pseudomonas Syringae 5
rRNA	ribosomal RNA
SA	Salicylic Acid
SAG101	Senescence-Associated Gene 101
SBR	Syndrome Basses Richesses
SCW	Secondary Cell Wall
SERK1	Somatic Embryogenesis Receptor-like Kinase 1
siRNAs	small interfering RNA
sRNA	small RNA
sRNA-seq	small RNA sequencing
sRNA-*Xcc1*	class of Xanthomonas sRNA
SS	Secretion Systems
subsp.	subspecies
sXF	class of *Xf* sRNAs, homologues of sRNA-*Xcc1*
T0/2/3/4/6SS	Type-0/2/3/4/6 secretion system
T4-pilus	Type-IV pilus
TALE	Transcription Activator-Like Effectors
Tet8	Tetraspanin-8
TF	Transcription Factors
TIR-NBS-LRR/TNL	Toll/Interleukin-1 Receptor (TIR)-Nucleotide Binding Site-Leucine Rich Repeat
TOE1/2	Target Of Eat1/2
tRFs	tRNA-derived RNA fragments
tRNA	transfer RNA
UTR	Untranslated Regions
VACs	Vessel-Associated parenchyma Cells
Vc	*Vibrio cholerea*
Vd	*Verticillium dahlia*
Vv	*Vitis vinifera*
Xcc / *Xco*	*Xanthomonas campestris* pathovar *campestris*/*oryzae*
Xf / *Xff* / *Xfp* / *Xfm*	*Xylella fastidiosa* (subspecies *fastidiosa*/*pauca*/*multiplex*)
Xff Tem1	*Xylella fastidiosa* subspecies *fastidiosa* strain 'Temecula1'
Xfp DD	*Xylella fastidiosa* subspecies *pauca* strain 'DeDonno'
Xoo	*Xanthomonas oryzae* pathovar oryzicola
ZAR1	HopZ-Activated Resistance 1

List of publications

Accepted publications

1. **Ruf**, Alessa, Patrick Blumenkamp, Christina Ludiwg, Anne Lippegaus, Andreas Brachmann, Andreas Klingl, Alexander Goesmann, Karina Brinkrolf, Kai Papenfort, Silke Robatzek, 'Extracellular vesicles from *Xylella fastidiosa* carry sRNAs and genomic islands, suggesting roles in recipient cells.', *Journal of Extracellular Vesicles* (May **2025**): https://doi.org/10.1002/jev2.70102. (Reproduced with permission under the license CC BY 4.0 https://creativecommons.org/licenses/by/4.0/)

2. **Ruf,** Alessa*, Hannah Thieron*, Sabrine Nasfi*, Bernhard Lederer, Sebastian Fricke, Trusha Adeshara, Johannes Postma, Patrick Blumenkamp, Seomun Kwon, Karina Brinkrolf, Michael Feldbrügge, Alexander Goesmann, Julia Kehr, Jens Steinbrenner, Ena Šečić, Vera Göhre, Arne Weiberg, Karl-Heinz Kogel, Ralph Panstruga, Silke Robatzek, on behalf of the exRNA consortium 'Broad-scale Phenotyping in Arabidopsis Reveals Varied Involvement of RNA Interference across Diverse Plant-microbe Interactions'. *Plant Direct* 8, no. 11 (November **2024**): e70017. https://doi.org/10.1002/pld3.70017. (Reproduced with permission under the license CC BY 4.0 https://creativecommons.org/licenses/by-nc-nd/4.0/)

Manuscripts

3. **Ruf**, Alessa, Elif Olkun, Jingli Lao, Vincent Ohlhauser, Neysa Rodriguez, Mara Martin-Rivero, Patrick Blumenkamp, Anne Lippegaus, Alexander Goesmann, Karina Brinkrol, Andreas Klingl, Blanca Landa, Kai Papenfort, Silke Robatzek, 'Hfq is integrated into transcriptional network in *Xylella fastidiosa* supporting lifestyle transition and systemic infection in plants', *awaits submission, anticipated submission date: end of 2025*

List of publications

Published Reviews, Opinions and Previews

1. **Ruf,** Alessa*, Lorenz Oberkofler*, Silke Robatzek, and Arne Weiberg. 'Spotlight on Plant RNA-Containing Extracellular Vesicles'. *Current Opinion in Plant Biology* 69 (1 October **2022**): 102272. https://doi.org/10.1016/j.pbi.2022.102272. (https://doi.org/10.1002/jev2.70022. (Reproduced with permission under the license CC BY 4.0 https://creativecommons.org/licenses/by/4.0/)

2. **Ruf,** Alessa, and Silke Robatzek. "Messenger RNA Just Entered the Chat": The next Layer of Cross-Kingdom RNA Transfer'. *Cell Host & Microbe* 32, no. 1 (10 January **2024**): 7–8. https://doi.org/10.1016/j.chom.2023.12.002. (Reproduced with permission under https://www.elsevier.com/about/policies-and-standards/copyright)

3. Thieron, Hannah*, Laura Krassini*, Seomun Kwon*, Sebastian Fricke, Sabrine Nasfi, Lorenz Oberkofler, Alessa **Ruf**, Julia Kehr, Karl-Heinz Kogel, Arne Weiberg, Michael Feldrbügge, Silke Robatzek, Ralph Panstruga. 'Practical Advice for Extracellular Vesicle Isolation in Plant-Microbe Interactions: Concerns, Considerations, and Conclusions'. *Journal of Extracellular Vesicles* 13, no. 12 (December **2024**): e70022. https://doi.org/10.1002/jev2.70022. (Reproduced with permission under the license CC BY 4.0 https://creativecommons.org/licenses/by-nc-nd/4.0/)

Summary

A hallmark of plant infections with microbes is the extensive shuttle of molecules between the interaction partners. Extracellular vesicles (EVs) have emerged as important players in the transfer of protein and nucleic acid signals between microbes and their plant hosts[1–3]. The bacterial plant pathogen *Xylella fastidiosa* (*Xf*) colonizes the xylem of a wide array of host plants leading to devastating diseases in agriculturally important crops such as olive, grapevine and almond[4]. To infect systemically, *Xf* relies on the shift between planktonic and biofilm lifestyle, a quorum-sensing dependent process mediated by the release of *Xf*-EVs[5]. We aimed to understand if *Xf*-EVs also play a role in delivering molecules to recipient cells. For this, we catalogued the protein, DNA and RNA cargo of *Xf*-EVs[6], which positions EVs as mediators of horizontal gene transfer in *Xf*. A major EV-associated genomic island encodes a class of small non-coding RNA, coined *sXF*s. First functional analysis of EV-delivered *sXF*s proposes cross-kingdom RNA interference-mediated regulation of plant immune receptors.

Given the presence of conserved Hfq-binding motifs at one of the *sXFs* loops, we further characterized the role of the EV-associated RNA chaperone Hfq and its bound sRNAs, revealing RNA-based regulation as a major contributor for cell-to-cell communication and lifestyle switches in *Xf*, which in turn mediates the bacterium's virulence[7]. On the plant side, we identify Argonaute 1 as a negative regulator of *Xf* infection in Arabidopsis revealing the involvement of RNA interference in plant resistance to infections with *Xf* [8].

Taken together, this work extends knowledge on how *Xf*-EVs act as extracellular communication tools for *Xylella fastidiosa* by (i) spreading genomic islands, (ii) silencing plant immunity receptors, potentially mediated by the delivery of *sXFs*, and (iii) facilitating the delivery of Hfq-bound sRNAs to mediate colony-wide lifestyle switches. It further highlights the importance of RNA-mediated regulation in plant infections with *Xf*, both on the plant and on the bacterial site. This adds a new molecular layer to our understanding of the virulence of this economically important plant pathogen.

Introduction

Plants under threat – infections with microbes on the rise

Plants are the base of all human nutrition, with a global agriculture value of 4 trillion US dollars in 2023[9]. Aside from abiotic stresses and poor waste management, biotic stress is a main threat resulting in an estimated loss of 40% of global crop production, costing the global economy an estimate of 220 billion US dollars losses per year[10]. An increasing global plant trade together with changing climate conditions, results in the (re-) emergence of many pathogens[11,12]. One example is the appearance of the Olive Quick Decline Syndrome (OQDS) in the Southern Italian region of Apulia resulting in the death of century-old olive trees with devastating socio-cultural and economical effects for the region[13]. The causal agent of this disease is the bacterial pathogen *Xylella fastidiosa* (*Xf*), which had previously been confined to the Americas, impacting *e.g.* the grapevine, almond and orange production. Its quick spread in the Mediterranean basin, there infecting grapevine, almonds, plum, cherry, oleander and ornamental plants, now also threatens major European agriculture branches[14]. The bacterium is transmitted by insects of the cicada family and is predicted to spread further, facilitated by the anthropogenic climate change providing optimal conditions for the insect vectors and the endurance of *Xf* in infected plants during mild winters[15].

Another recently emerging insect vector-born disease, the Syndrome Basses Richesses (SBR) is caused by the bacteria *Candidatus Arsenophonus phytopathogenicus* and *Candidatus Phytoplasma solani* which results in high yield losses in sugar beet and potato production in Middle Europe[16], highlights the importance of (re-)emergence of bacterial plant diseases. Both *Xf* and SBR-causing bacteria are transmitted by sap-feeding cicadas and infect different parts of the vasculature of their host plants: *Xf* is limited to the xylem and SBR-causing bacteria are phloem-restricted[4,17]. The important transport function of water and nutrients in the highly specialised vasculature tissue can be compromised by the presence of infecting microbes or by plant responses to the infection[18]. Their restriction to the vasculature and vector-based transmission sets them apart from better studied plant pathogenic bacterial model organisms, such as apoplast infecting *Pseudomonas syringae* (*Ps*), and makes their study technically very challenging[15,18,19]. Nevertheless, studying model bacterial pathogens of both plants and humans, together with established plant model systems such as *Arabidopsis thaliana* and tobacco, has brought forward valuable tools to gain mechanistic insights into how bacterial non-model pathogens interact with and infect their hosts[20,21]. This can help to develop strategies and cures which restrict the spread of pathogens and ultimately ensuring food security.

Xylella fastidiosa – *a threat to many*

At the species level, the Gram-negative bacterium *X. fastidiosa* can colonize more than 700 plant species, a number increasing with more plants tested for *Xf* presence[22]. While it persists in most plants as a commensal with no or very little symptoms, it causes devastating disease in others[23]. The cause of this differential response across hosts remains poorly understood. *Xf* is the causal agent of *e.g.* Citrus-Variegated Chlorosis (CVC), Pierce's Disease (PD) in grapevine, OQDS in olives, Almond Leaf Scorch (ALS), and Coffee Leaf Scorch (CLS)[4]. The establishment of *Xf* in different host plants is subspecies-dependent[4,24]. It has been speculated that the generation of subspecies in *Xf* is driven by Horizontal Gene Transfer (HGT)[25–31]. Subspecies of *Xf* differ in their natural DNA uptake rate with increased rate of competence when grown under natural growth conditions of liquid flow[32–34]. Most members of the subspecies *fastidiosa* (*Xff*) and readily uptake Environmental DNA (eDNA), resulting in intersubspecific recombination between both subspecies[33]. Although the subspecies *pauca* (*Xfp*) is the result of recent recombination events between *Xf* lineages and other bacteria[25], it lacks the ability to uptake eDNA under laboratory conditions, likely hindered by the activity of Restriction-Modification Systems (RMS)[35]. In *Xff*, growth stage, nutritional signals and methylation state of the transforming DNA influences recombination efficiency[34]. *Xf*'s Type-IV (T4) pili are indispensable for recombination in *Xf*, with minor pilin Fimbrial protein T3 (FimT3) functioning as the DNA receptor[36]. Integration of taken-up DNA into the genome is mediated by Competence (Com) proteins and Recombinase A (RecA)-mediated recombination[34]. Less than 80% of *Xf*'s pangenome has homologues in its clade of Xanthomonadales, while closely related species such as *Xanthomonas vasicola* and *Xanthmonas albilineans* share 99% and 95% with the Xanthomonadales clade, respectively[37]. This is indicative for a high rate of recombination in *Xf* with phylogenetically more distant species. Increased rate of eDNA uptake in *Xf* is speculated to be related to the loss of RecX, a suppressor of RecA activity[37–39]. Despite these genetic indications of elevated HGT potential in *Xf*, the mechanisms by which HGT occurs in the high-pressure watery xylem environment remain poorly understood.

The bacterium is transmitted from infected to healthy plants by xylem-feeding insects of the family of cicadas (*Cicadellidae*) and spittle bugs (*Aphrophoridae*), where *Xf* forms biofilms to persist in the foregut of the insect for weeks[40] (**Figure 1**a). In the plant, *Xf* is restricted to the

xylem, where it first also establishes biofilms before moving on to a more exploratory lifestyle growing in planktonic state[41].

The xylem, composed primarily of dead tracheary elements, forms a highly specialized vascular network that transports water and minerals from roots to leaves via transpiration-driven flow[42,43]. These hollow conduits originate from meristematic cells that undergo programmed cell death and are reinforced by a Primary Cell Wall (PCW) made of cellulose, hemicellulose and pectin, as well as a lignin-fortified Secondary Cell Wall (SCW) that provides the rigidity and hydrophobicity required to sustain water transport under tension[44,45] (**Figure 1**b). The pits, thin regions composed solely of PCW, enable lateral movement of xylem sap while serving as selective barriers against embolisms and pathogens[46,47]. This lignified, pit-perforated network generates and maintains substantial negative pressures (-4 to -80 atm) during transpiration[48,49], resulting in a mechanically and chemically challenging environment for microbial colonizers[50,51].

To thrive under these conditions, *Xf* requires strong adhesion to xylem surfaces, a property demonstrated in microfluidic assays where *Xf* cells withstand shear stresses up to 360 dyne/cm² [52]. Surface attachment and cell-to-cell aggregation is mediated by fimbrial and afimbrial adhesins and components of the Type-I and T4 pili[53–56]. A protective extracellular matrix rich in exopolysaccharides (EPS) further allows *Xf* to establish robust biofilms[57]. Filamentous cell morphologies bridging between microcolonies facilitate the communication in large-scale biofilms[58].

The switch between biofilm and planktonic growth are determinants for successful host infection and transmission of *Xf*[5]. This process is controlled by Diffusible Signal Factor (DSF)-mediated Quorum Sensing (QS) which also controls the release of extracellular vesicles (EVs), membrane surrounded nano-sized particles, functioning as anti-adhesive factors[4,5] (**Figure 1**b). This shifts *Xf* towards planktonic growth where twitching motility mediated by the T4 pili allow the bacteria to crawl along the vessel against the xylem sap flow[36,59]. Cell Wall Degrading Enzymes (CWDE) released by the Type-II Secretion System (T2SS) and EVs degrade pit membranes, which facilitates *Xf* systemic colonization of the xylem vessels across the whole tissue (**Figure 1**b). The molecular mechanisms underlying the onset of the switch between planktonic and biofilm growth remain poorly understood and the involvement of plant signals remains elusive. Infection with *Xf* results in changes in the ion-concentration in the leaf, with increased concentration of calcium (Ca^{2+})[60,61] and is speculated to influence *Xf* attachment[62]. Ca^{2+} acts as an environmental cue for *Xf* by directly binding to one Pilus Y1 (PilY1) adhesin

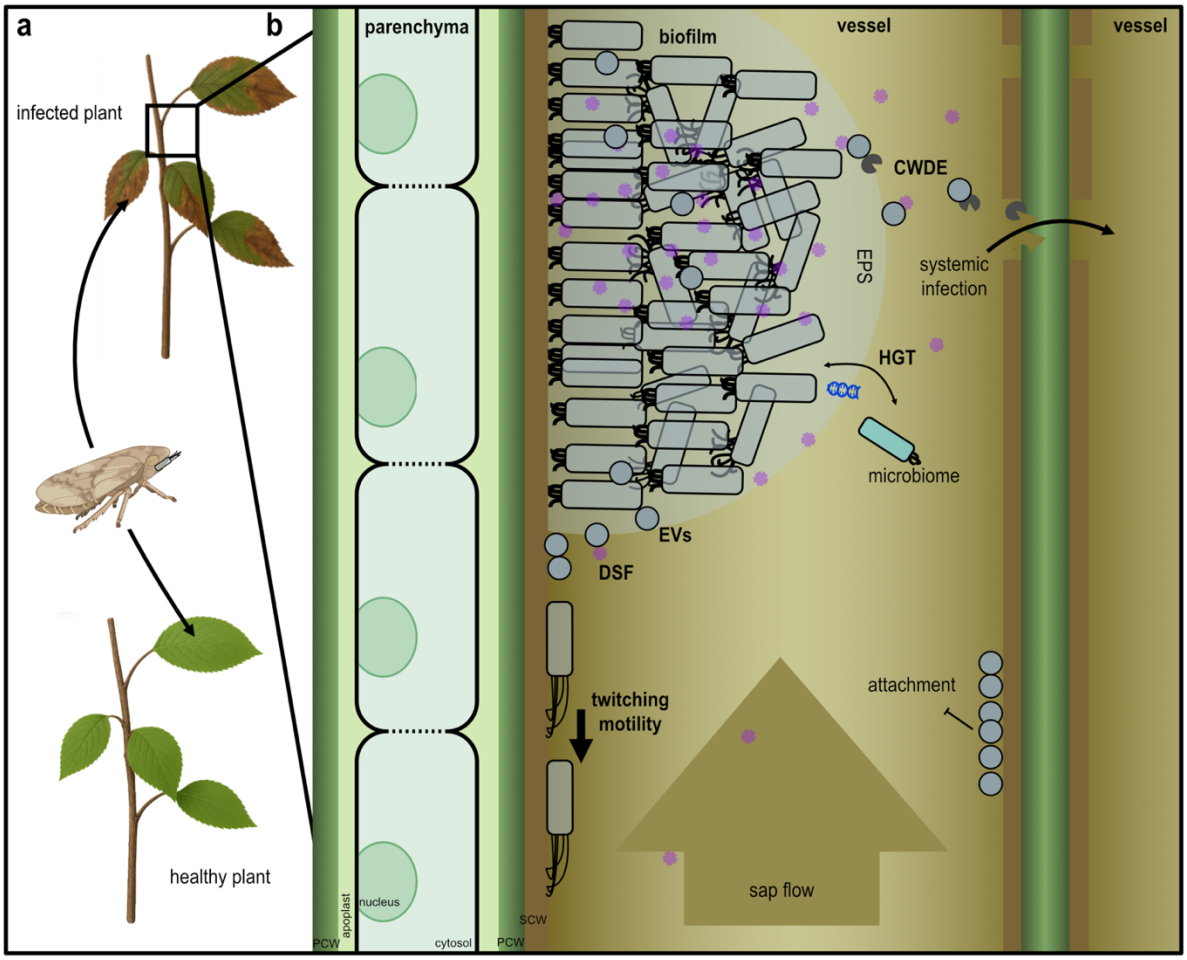

Figure 1: *X. fastidiosa* 's mode of infection.

Xf is transmitted from infected to healthy plants by xylem-feeding insects where it persists in the foregut in biofilms (**a**). In the plant, *Xf* exclusively colonizes the xylem vessels (**b**). Horizontal Gene Transfer (HGT) mediated by the uptake of extracellular DNA (blue helix) from *Xf* and microbiome cells, is speculated to facilitate *Xf*'s adjustment to new hosts. In the xylem, *Xf* attaches strongly to the vessel forming biofilms protected by a matrix of exopolysaccharides (EPS). Increasing colonization leads to high levels of QS-signals of the Diffusible Signal Factor (DSF) family in the vessel, enhancing the production of Extracellular Vesicles (EVs). Carrying adhesins, EVs block attachment sites which results in a shift to planktonic growth of the bacteria. To systemically colonize the plant, *Xf* moves against the sap flow using a Type-IV pilus-mediated twitching motility and the production of Cell-Wall Degrading Enzymes (CWDEs) facilitates the passage through xylem pit membranes. When colonizing new xylem vessels, DSF levels are low resulting in the establishment of new biofilms, which facilitates the uptake of *Xf* by insects, completing *Xf*'s lifecycle.
Image of insect and plants generated with BioRender©.

PCW - Primary Cell Wall; **SCW** - Secondary Cell Wall

homologue which results in increased twitching motility[54,63]. Ca^{2+} also leads to the activation of transcriptional responses regulating the biofilm machinery[64]. Given the central role of Ca^{2+} signalling in both bacterial and plant systems, it is conceivable that Ca^{2+} fluxes during infection act as a point of cross-communication. However, the molecular mechanisms underlying plant

responses to xylem colonization by *Xf*, and their potential impact on bacterial growth, remain poorly understood.

Plants can defend themselves - the plant immune system

Generally, plants detect the presence of microbes by conserved microbial molecules, referred to as Microbe-Associated Molecular Patterns (MAMPs) (**Figure 2**). Examples for well-characterized MAMPs are bacterial flagellin, bacterial Elongation Factor Tu (EF-Tu) and fungal chitin[65]. Mechanical disruption of protective layers by infecting microbes leads to the release of Damage-Associated Molecular Patterns (DAMPs), including oligomeric fragments of plant cell wall polysaccharides generated by microbial CWDEs, as well as phytocytokines, which are small secreted peptides or proteins released by the plant to amplify immune signalling and coordinate defence responses in neighbouring cells[66]. MAMPs, DAMPs and phytocytokines are recognized by Pattern-Recognition Receptors (PRRs) and their co-receptors which reside in the plasma membrane of the plant. Upon detection of such danger signals, a signalling cascade is triggered, resulting in the phosphorylation of downstream players, such as the Mitogen-Activated Protein Kinases (MAPKs), Receptor-Like Cytoplasmic Kinases (RLCKs), Calcium-dependent Protein Kinases (CPKs) and G-proteins[67]. As an example, the perception of the flagellin-derived immunogenic epitope flg22 by the Flagellin-Sensing 2 (FLS2) PRR and its co-receptor BRassinosteroid Insensitive 1-(BRI1)-Associated receptor Kinase 1 (BAK1) leads to the trans-phosphorylation of FLS2 and BAK1, and the RLCK Botrytis-Induced Kinase 1 (BIK1)[68]. Phosphorylated substrates downstream of PRR signalling trigger influx of Ca^{2+} across the plasma membrane via calcium channels, the production of Reactive Oxygen Species (ROS; O^{2-}) by oxidases and transcriptional reprogramming of defence genes in the nucleus[69]. This layer of plant immunity is referred to as Pattern-Triggered Immunity (PTI).

Microbes have evolved specialized molecules, effectors, which they deliver into the cell to counteract and overcome this first layer of defences. Most studied effectors are small, secreted proteins[70] but also secondary metabolites, toxins, phytohormones[71] and small RNAs (sRNA)[72] can act as effectors, interfering with plant physiology or supress immune responses[73].

In response to the detection of effectors or their activity on host proteins, plants mount a robust defence response termed Effector-Triggered Immunity (ETI), mediated by Resistance (R) proteins[74]. Most R proteins belong to the family of intracellular Nucleotide Binding Site-Leucine Rich Repeat (NBS-LRR) Receptors (NLR). Based on their N-terminal domains, they

can be further divided into Toll/Interleukin-1 Receptor (TIR) domain-NLRs (TNLs) and Coiled Coil (CC) domain-NLRs (CNLs)[75]. Interactions of effectors or effector-modulated host proteins with sensor NLRs lead to the downstream activation of helper NLRs[76]. Activated NLRs undergo conformational changes and multimerize, forming resistosomes[76]. Activation of CNLs results in their multimerization to membrane-associated pentamers which, in the example of the Arabidopsis CNL HopZ-activated resistance 1 (ZAR1), has Ca^{2+}-channel activity[77,78]. The N-terminal alpha-helices responsible for the pore-forming structure are conserved in CNLs of many plant species[79] and similar functions have been shown for other CNLs, including their assembly at organelle membranes[76,80,81].

Hydrolysis activity of TIR-domains of tetrameric TNLs and TIR-only proteins lead to the cleavage of signalling molecule Nicotinamide Adenine Dinucleotide (NAD+)[82,83], which in turn activates further downstream players. Up until now, all described downstream signalling of TNLs involves the lipase-like protein Enhanced Disease Susceptibility 1 (EDS1)**,** which forms exclusive dimers with PhytoAlexin Deficient 4 (PAD4) and Senescence-Associated Gene 101 (SAG101) to mediate further downstream signalling[76]. The downstream signalling of activated NLRs lead to a form of controlled cell death, referred to as the Hypersensitive Response (HR), restricting the spread of infection. Signalling pathways of PTI and ETI have synergistic effects, with ETI often being primed by PTI, resulting in a robust defence response together[84,85] (**Figure 2**).

(Post-) Transcriptional regulation of plant defences

The complexity of defence responses requires quick transcriptional reprogramming governed by a tight control of all players. Central to this is the mediation of transcriptional coordination by Transcription Factors (TFs) and their regulatory networks[86]. Activated signalling pathways modify phosphorylation state, subcellular localization and protein stability of TFs, which in turn regulate TF activity[86]. For example, the activation of MAPKs by PRRs or NLRs leads to the phosphorylation of WRKY class TFs. Their activity is considered a master regulator of (biotic) stress responses, activating *e.g.* the biosynthesis of plant defence hormones such as Salicylic Acid (SA)[87].

In addition, the immune transcriptional network is also regulated post-transcriptionally[86]. RNA interference (RNAi) evolved as an antiviral defence mechanism to degrade invading nucleic acids and has been co-opted to regulate endogenous gene expression. Depending on their mode

of biogenesis and action, two types of small (s) RNAs modulate messenger (m) RNA stability and thus exerts crucial post-transcriptional control[88]. MicroRNAs (miRNAs) are generally 20-22 nucleotides (nt) in length and are processed from endogenous primary transcripts of miRNAs (pri-miRNAs) with imperfectly paired hairpin conformations[89]. Perfectly complementary long double-stranded RNA (dsRNAs) of exogenous or endogenous origin give rise to small interfering RNAs (siRNAs)[90]. Both types of sRNAs are processed from longer precursors (pri-miRNAs or dsRNAs) by Dicer-Like (DCL) endonucleases into sRNA duplexes, methylated by Hua ENhancer 1 (HEN1) and incorporated into the RNA-Induced Silencing Complex (RISC) [90]. The RISC facilitates the pairing of loaded sRNAs with their target mRNA, guided by their main components, Argonaute (AGO) proteins[90,91]. Downregulation of target mRNAs occurs then by mRNA cleavage or translational inhibition[90]. RNAi signals can be amplified by RNA-Dependent RNA polymerases (RDRs), generating long dsRNAs from sRNAs which are being processed by members of DCLs into secondary phased siRNAs (phasiRNAs), a process mediated by DCL2/DCL4 in Arabidopsis[90,92]. These siRNA-based signals can travel in the plant systemically via the vasculature, spreading their signal[93].

The post-transcriptional regulation mediated by sRNAs includes key immunity players such as the expression of *FLS2*. The TFs Target Of Eat 1 (TOE1) and TOE2 negatively regulate *FLS2* expression and are both targets of the endogenous miRNA *miR172b* in Arabidopsis[94]. After flg22-treatment, the expression of *miR172b* increases, which releases TOE1/E2 repression of *FLS2* and activates FLS2-mediated immunity[94].

The expression of immunity receptors, particularly *NLRs*, poses an extensive fitness cost on plants[95,96]. The sRNA-mediated regulation of *NLR* expression has emerged as an important mechanism which allows to keep large genomic repertoires of *NLRs* while reducing the metabolic cost of their expression[97]. The sRNA-based regulation of *NLRs* is a very conserved mechanism across many plant species[98–100]. PhasiRNA production from *NLR*-targeting is widespread across different plant lineages[101,102] and further reduces the metabolic cost of *NLR* expression [102,103]. In tobacco and tomato, almost all *NLR* genes targeted by sRNAs give rise to secondary siRNAs (98% and 96% respectively)[97]. To give an instance, the conserved miRNA superfamily of *miR482/2118* targets the sequence of the conserved P-loop, the ATP-binding pocket of NLRs, which allows the post-transcriptional control of many *NLRs* at once[100,104]. Additionally, *miR482/2118*-targeting of *NLRs* also results in the production of phasiRNAs which enhances the silencing effect of *miR482/2118* further[105,106].

Moreover, PTI signalling alters miRNA expression which in turn leads to increased expression of *NLRs*, resulting in a priming effect of PTI over *NLR* expression[102,107]. For example, the

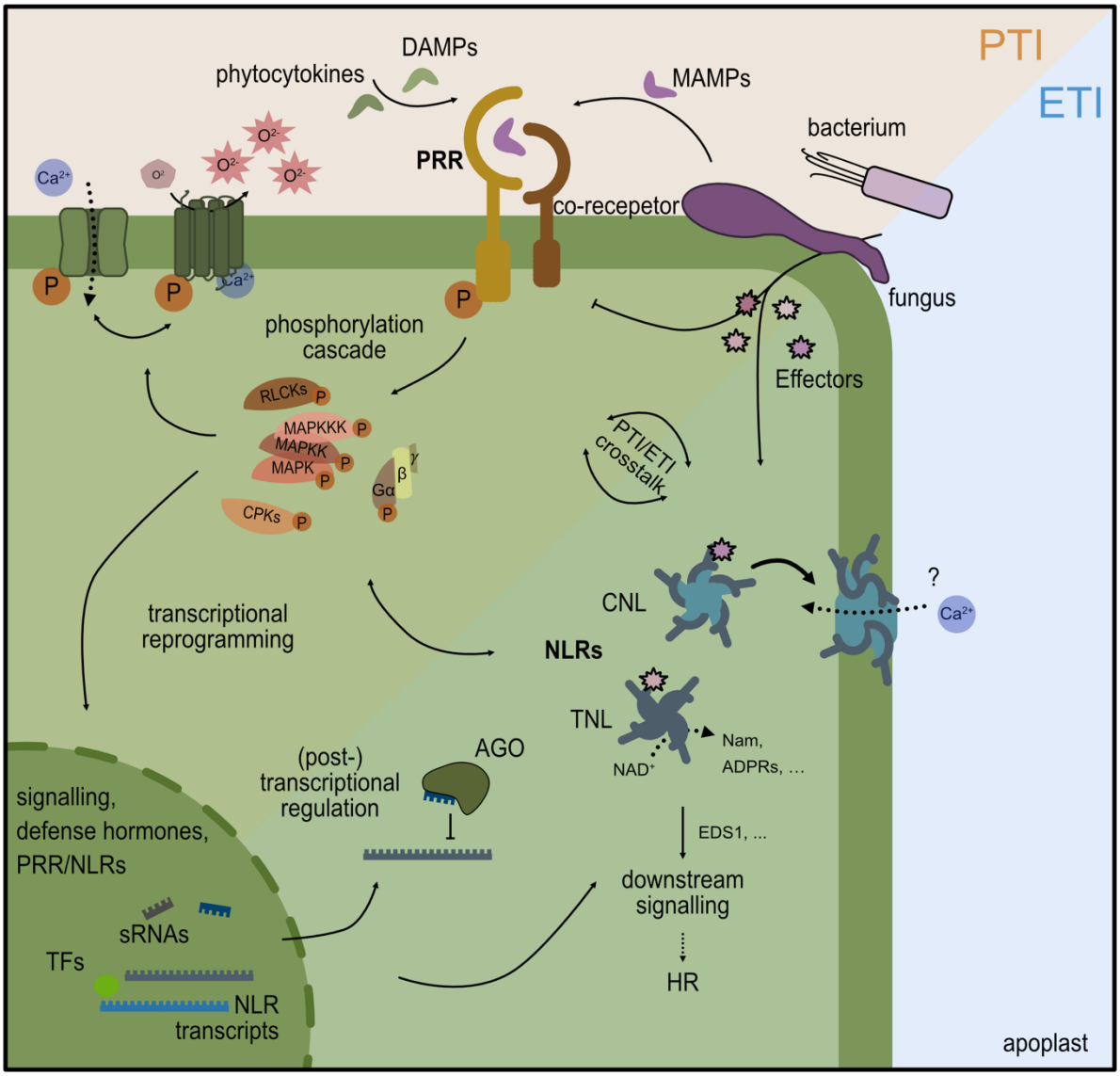

Figure 2: The plant immune system.

The plant immune system consists of two major immunity pathways: Pattern-Triggered Immunity (PTI) and Effector-Triggered immunity (ETI). PTI is triggered when MAMPs are being recognized by PRRs, which can also detect immunogenic plant signals such as DAMPs or phytocytokines. Dimerization of PRRs leads to their auto-phosphorylation which in turn will activate a downstream phosphorylation cascade mediated by intracellular kinases, including RLCKs, CPKs, MAPKs and G-proteins. Their activation triggers influx of calcium (Ca^{2+}) across the plasma membrane via calcium channels, the production of reactive oxygen species (O^{2-}) and transcriptional reprogramming of defence genes in the nucleus. Many pathogens deliver effectors into the plant cells which are being recognized by intracellular NLRs. Depending on their N-terminal domain, they are classified into CNLs or TNLs. Sensor NLRs recognises effectors or effector-induced changes at host proteins, resulting in conformational changes. NLR-triggered immunity results in complex downstream signalling, often involving lipase-like protein EDS1 and induces a hypersensitive response (HR), programmed cell death. Crosstalk between PTI and ETI include shared phospho-patterns and results in the potentiation of the immunity response. Expression of immunity players are regulated by multiple layers, including sRNA-mediated gene regulation and transcription factors.

MAMPs - Microbe-Associated Molecular Patterns; **PRRs** - Pattern-Recognition Receptors; **DAMPs** - Danger-associated Molecular Patterns; **RLCKs** - Receptor-Like Cytoplasmic Kinases; **CPKs** - Calcium-dependent Protein Kinases; **MAPK** - Mitogen-Activated Protein Kinase; **NLRs** - Nucleotide binding site-Leucine rich repeat-Receptors; **CNLs** - coiled coil domain NLRs; **TNLs** -Toll/Interleukin-1 Receptor (TIR)-domain NLRs; **ADPRs** -ADP Ribose; **NAM** - Nicotinamide.

Arabidopsis miRNA *miR472* and its RDR6-derived secondary siRNAs target a subset of *CNL* transcripts, including *Resistance to Pseudomonas Syringae 5* (*RPS5*)[107]. After PTI induction, *RDR6* expression decreases, resulting in increased expression of *RPS5* mediating ETI in responses to the Avirulence protein of *Pseudomonas syringae* pv. *Phaseolicola* B(AvrPphB)[107].
A miRNA-based priming effect is also associated with the effects of beneficial microbes, such as *Bacillus cereus* which can induce systemic resistance in Arabidopsis by modulating specific miRNAs[108–110]. This enhances basal immunity against the bacterial pathogen *Ps* pv. *tomato* strain DC3000 (*Pto* DC3000) and the fungal pathogen *Botrytis cinerea* (*Bc*), thereby priming the plant immune responses.
For example, beneficial microbes such as *Bacillus cereus* prime systemic resistance in Arabidopsis by modulating specific miRNAs, which enhance basal immunity against bacterial pathogen *Ps* pv. *tomato* strain DC3000 (*Pto* DC3000) and the fungal pathogen *Botrytis cinerea* (*Bc*) thereby preparing the plant for faster and stronger responses to subsequent pathogen attacks.
Lastly, cell non-autonomous functions of miRNAs and phasiRNAs help spread immunity signals, resulting in systemic resistance throughout the plant[102,111].
Taken together, in addition to their role in antiviral immunity, RNAi has broad functions in the regulation of immunity against cellular microbes. The genome of the experimental model plant *Arabidopsis thaliana* (*At*) encodes four DCLs and 10 AGOs[112] and the involvement of DCL and AGOs in response to infection vary depending on the microbe in question. For example, the loss-of-function mutant *dcl1*, which is required for producing miRNAs in *At,* show enhanced susceptibility to *Pto* DC3000[113] and *Bc*[72]. Similarly, *dcl4* mutants, which lack efficient production of secondary siRNAs in Arabidopsis, show enhanced susceptibility to the fungal pathogen *Verticillium dahlia* (*Vd*)[114]. Infection assays of Arabidopsis *ago1* mutants with bacterium *Pto* DC3000 and fungi *Sclerotinia sclerotiorum* suggests that AGO1 functions as a positive regulator of immunity[115,116], while infection assays with the fungal pathogens *Bc, Vd, Verticilium longisporum,* and *Botryosphaeria dothidea* and the oomycete *Hyaloperonospora arabidopsidis* propose negative regulation of immunity[72,114,117–119]. While early immune responses consist of a conserved core transcriptional response independent of the interacting microbe[120,121], later immune responses, including the ones regulated by RNAi, are driven by the recognition of MAMPs and effectors which vary between different microbes[85]. Specificity of RNAi is driven by RISC-loaded sRNAs which might further explain the differential role of RNAi in response to different microbes[122,123].

Effectors interfere with plant immunity regulation

Microbes have evolved effector molecules which can interfere with plant immunity on all conceivable levels[70,124]. This also includes effectors targeting the regulation of immunity gene expression. For example, Transcription Activator-Like Effectors (TALE) of the bacterial plant pathogens of *Xanthomonas* spp. are being delivered into the plant cell nucleus where they can directly interfere with gene expression by binding to conserved DNA motifs[125]. Interestingly, the effector Hrp Outer Protein T1-1 (HopT1-1) released by bacterial plant pathogen *Pto* DC3000 can hinder miRNA-based regulation of PTI[126,127], which is proposed to be mediated by a direct interaction of the effector with the plant AGO1 hindering its association with miRNAs[128].

Because RNAi is conserved across eukaryotes, sRNAs can also be employed as effector-like molecules. Plants and eukaryotic microbes can exchange sRNAs that are incorporated into each other's RNAi machinery, thereby enabling bi-directional cross-kingdom gene regulation, coined cross-kingdom RNAi (ckRNAi)[66,72,117,129–131] (**Figure 3**). This RNA-based warfare was first described in the interaction between the necrotrophic fungus *Bc* and its host plants *At* and tomato[72]. Secreted *Bc*-sRNAs are being integrated into the plants AGO1-RISC to silence important immunity transcripts such as *MAPK* [72]. This microbial strategy to interfere with plant immunity has been extended to other microbes since, including the oomycete *Hyaloperonospora arabidopsidis* and symbiotic nitrogen-fixing rhizobia [117,132–134] (**Figure 3**). The secretion of sRNAs by plants to silence the expression of important virulence factors in the microbes adds another layer of complexity to plant immunity and results in bi-directional ckRNAi[129,131]. For example, during the infection with *Vd*, cotton plants secrete sRNAs which target fungal virulence genes, supporting the plant's defences[130].

Defences mediated by dead tissue? - Vasculature infecting microbes

During the infection process, many microbes form intimate interaction sites with their hosts, such as appressorium structures formed by many pathogenic fungi, which facilitates the entry of the fungus and the exchange of effectors[135,136]. At interaction interfaces, microbial signals can be detected readily by membrane receptors activated by direct binding of microbial signal molecules[137]. However, a group of very specialized microbes is adapted to grow exclusively in the plant's water transporting tissue, the xylem, predominantly consisting of dead, lignified cells[138]. Xylem-colonizing pathogens are phylogenetically very diverse,

spanning fungal, oomycete and bacterial organisms[139,140]. To reach the xylem, some pathogens pass through other tissues first or use natural plant openings such as hydathodes, while others rely on insect vectors to be directly delivered into xylem[18]. Plant immune responses to xylem-colonizing pathogens include the formation of mechanical barriers by increased lignin deposition, the outgrowth of parenchyma cells, called tyloses, or the release of phenolic compounds to block the spread of the pathogen[139].

However, where and how the perception of xylem-colonizing microbes occurs remains still unknown. The most probable site for elicitor perception and immune response activation in the xylem is its only living cell type: the xylem parenchyma. In particular, parenchyma cells in direct contact with vessels, referred to as Vessel-Associated parenchyma Cells (VACs), may serve as the first responders capable of detecting immunogenic elicitors, as expression of PRRs such as *FLS2* and *EF-Tu Receptor* (*EFR*) has been detected in the xylem parenchyma[141,142]. Supporting this, PTI initiated in the xylem parenchyma through expression of the PRR *Xa3*/*Xa26* restricts infection by the xylem-colonizing *Xanthomonas oryzae* pv. *oryzicola* (*Xoo*) in rice[143,144], demonstrating the immune competence of this tissue. The systemic spread of MAMPs and DAMPs, free or in association with EVs[145,146], through the xylem sap could further immune prime distal with neighbouring tissue most likely also involved in the perception of xylem-limited microbes and the transmission of immune signals[139,147].

Plant responses to infection with Xylella fastidiosa

Although the mechanisms by which xylem-limited pathogens are detected remain unclear, several studies indicate that plants can sense the presence of *Xf* during infection. *Xf* lacks canonical effectors which is why most studies have focused on PTI-typical responses[41,148]. In response to infection with *Xf* several prototypic immune responses are activated. These include ROS bursts[149–151], callose and tylose formation, lignification[150,152,153], and the release of phenolic compounds[154–156]. Since *Xf's* EF-Tu-derived immunogenic epitope elf26 can be recognized by the Brassicaceae-restricted PRR EFR, its transfer and ectopic expression in sweet orange confers enhanced resistance to *Xfp*[149]. Of note, the EFR-mediated resistance in sweet orange mainly restricted the systemic spread of *Xfp* and it has been speculated that this could be correlated with the release of EVs, which carry EF-Tu[6,149,157].

Perception of *Xf* is also conferred by the recognition the immunogenic epitopes of the Cold Shock Proteins (CSP)[151] and lipopolysaccharides (LPS), structural components of the bacterial cell envelope[150]. *Xf* modifies its LPS with the O-antigen polymerase Wzy, shielding it from

recognition and thereby delaying and reducing the plant immune response[150]. To spread across the whole xylem, *Xf* degrades xylem pit membranes using CWDE[158–160]. This enzymatic activity most likely results in DAMPs which might also be perceived by infected plants[4]. Transgenic expression of small *Xf* proteins secreted via the T2SS induced "HR-like" symptoms in *Nicotiana tabacum*, indicative of a triggered ETI response[161] and similarly, infection of alfalfa with *Xfp* also resulted in "HR-like" responses[162]. The upregulation of putative *NLRs* in response to *Xf* suggests that effector recognition may play a role in host immune responses during pathogenesis[163,164]. However, an active interference or suppression of immune responses as often observed by effectors, has not (yet) been reported for *Xf*.

Taken together, these results indicate that the presence and activities of *Xf* in the xylem can be recognized by the plant despite *Xf*'s restriction to a predominantly dead tissue. However, molecular mechanisms and what players mediate this perception, especially in non-model plant hosts, is currently not understood. It is also not known in which tissue or what cells the perception occurs and if *Xf* signals can result in a response gradient across tissues away from xylem vessels.

Release of molecules into the extracellular space

Interaction between plants and microbes requires extensive exchange of signals, including the shuttling of molecules between hosts and microbes[165]. Plants actively remodel the pathogen's niche to create a hostile environment for the infecting microbe by releasing *e.g.* anti-microbial peptides and toxic compounds such as ROS, or by modulating pH levels and nutrient availability which aims to reduce infection success of the pathogen[166]. At the same time, microbes release effectors to counter-act the plants immune response or CWDE, aiming to facilitate their establishment in the host[166]. On both sides, this requires the release of molecules into the extracellular space.

Secretion systems

For the delivery of small molecules, proteins and nucleic acids, microbes have dedicated secretion systems (SS) facilitating the export into the extracellular space and hosts to establish their niche. To do so, Gram-negative bacteria need to export molecules across two membranes for which they have evolved sophisticated, multi-subunit complexes which either span one or both membranes[167]. Interestingly, *Xf* has a reduced arsenal of SS with Type-III SS (T3SS) and

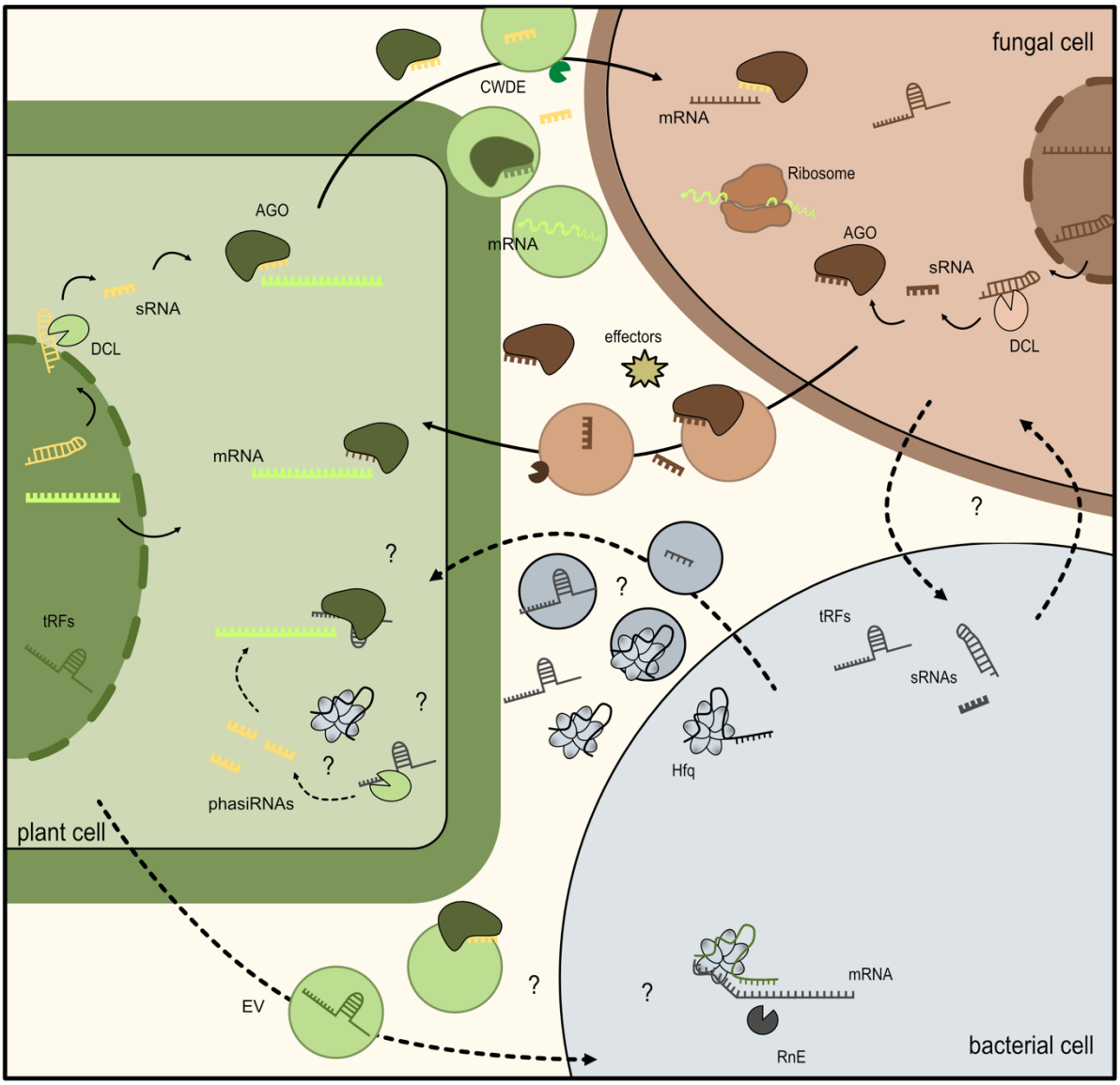

Figure 3: Cross-kingdom RNA interference.
CkRNAi between plants (green) and their interacting microbes mediated by extracellular vesicles (EVs). Eukaryotic organisms, such as plants and fungi (brown), encode canonical RNAi machineries, consisting of Argonaute (AGO) and sRNAs which are generated from longer, precursor RNA by Dicer-like endonucleases (DCL). In addition to endogenous post-transcriptional control, sRNAs are shuttled between plant and fungal cells, targeting messenger (m)RNAs of their counterpart. This transport occurs in part via EVs, but protein-complexes or naked sRNAs might also be shuttled between cells. Shuttle of plant mRNAs to the fungus results in expression of plant proteins by the fungal ribosomes. Small RNA-based regulation in Gram-negative bacteria (grey) often involves the conserved RNA chaperone Hfq which stabilizes bacterial sRNAs and facilitates base pairing between sRNAs and mRNA targets. Hfq-based regulation acts together with Ribonuclease E (RnE) which degrades targeted mRNAs. Several occurrences of ckRNAi between eukaryotic and bacterial cells have been reported, however large mechanistic parts are not understood. Transfer-RNAs (tRNAs) and derived tRNA-fragments (tRFs) are prime candidates to perform such interactions, as they are conserved across kingdoms. Processing of longer bacterial sRNAs by DCLs and integration into amplifications cycles similar as for phasiRNA, would allow integration and amplification of bacterial sRNAs into the RNAi pathways.

T6SS missing[168]. They are both important virulence determinants in many other pathogenic bacteria to directly inject effectors into hosts or microbial competitors[167].
For its virulence, *Xf* largely relies on the T2SS which transports periplasmic proteins across the outer membrane (OM) or facilitates their association with the OM [169]. Its pseudo pilus does not extend into the extracellular space and proteins released via the T2SS degrade plant cell walls[170], help the formation of biofilm[171] and aid virulence[172]. The T4SS is structurally related to the T2SS, with a pilus that extends through the OM[167]. Members of the T4SS superfamily are very diverse and have evolved to fulfil a broad range of functions[173], important for the pathogenicity of plant bacterial pathogens[174]. The T4-pilus can facilitate the capture and release of eDNA, mediating interbacterial DNA transfer and conjugation[175], also observed in *Xf* [36]. In some bacteria, including *Xf*, the T4-pilus is also used for twitching motility, pulling the bacteria forward by adhering to surfaces and retracting[36,59,176–178].

Extracellular vesicles as shuttle agents

In addition to membrane-spanning transporter complexes, all cells release forms of EVs, sometimes referred to as the "Type-0 secretion system"[179–181]. Depending on their cell of origin, these membrane-surrounded particles are between 10 - 1'000 nm in size and carry cargo in their lumen and corona and also include membrane-associated cargo[179–181]. The first reports of EVs dates to the late 1950s[182] and for a long time were thought of as artefacts or "garbage bags" of cells[183–186]. In the meantime, important functions of EVs in cellular homeostasis and communication have emerged[179–181].

Depending on their biogenesis path, EVs released by Gram-negative bacteria are coined outer-membrane vesicles (OMV) and outer-inner membrane vesicles (OIMV)[187]. OMVs are generated by blebbing off from the OM, releasing periplasmic and OM cargo but also cytosolic proteins, DNA, RNA, and virulence factors[187,188]. This process is influenced by the connection between the outer and inner membrane, and the linkage with the peptidoglycan layer[189,190]. OIMVs are generated by explosive cell lysis or when the peptidoglycan layer is transiently broken by autolysins[190–193]. OIMVs can also contain cytoplasmic cargo, including DNA[192]. As there is no clear marker distinguishing the types of EVs in bacteria based on their biogenesis path, they will collectively be referred to as EVs hereinafter.

Cellular functions and inter-bacterial communication mediated by bacterial EVs

The importance of EVs for bacterial cellular functions becomes apparent from the fact that, to this day, a "non-vesiculating" mutant could not be generated. Stressed cells show increased vesiculation, highlighting one function of EVs in releasing misfolded proteins and relieving membrane stress[194,195]. EVs also support regular growth of bacterial cells by taking up and scavenging toxins, antimicrobial compounds, ROS, and phages from the environment[196,197]. Their protein cargo also reveals nutrient-binding proteins and siderophores, which might facilitate nutrient acquisition in scarce environment or hostile host environments[196,198–200].

Bacteria live in communities. As unicellular organisms, many bacteria coordinate social activities via the release of diffusible QS-molecules to detect their growth density in the surroundings. EVs play an essential role in packaging and delivering the often hydrophobic QS-molecules in aqueous environments, both solubilising and protecting them[201–204], which in turn facilitates communication with more distant cells[205].

Bacterial cooperation and competition is also driven by exchange of genetic material across different species, which increases microbial adaptability to (new) environments[206]. DNA-carrying bacterial EVs shape the mobile gene pool in the environment by protecting DNA from degradation[207,208]. EVs can facilitate the delivery of genetic material to recipient cells, including plasmids and genes conferring antibiotic resistance[209–212]. This process, coined vesiduction, enables HGT among bacteria by encapsulating genetic material within EVs, which can be taken up by recipient cells and integrated into their genomes, resulting in genetic transformation[213].

Membrane-binding molecules can affect the formation and uptake of EVs in bacterial communities, modulating the dynamics of EV-mediated communication[214]. For example, EVs released by the soil bacterium *Buttiauxella agrestis* preferentially fuse with their parent cells and less with cells of another genera, indicating a specificity of EV uptake[215]. Another soil bacterium, *Cupriavidus necator*, can recruit EVs to recipient cells by employing the T4SS, which tethers EVs, helping with iron acquisition, interbacterial competition and HGT[216].

Compared to *Xanthomonas citri*, a close relative to *Xf* in the *Xanthomonadaceae* family, *Xf* releases high amounts of EVs, and their release is QS-dependent[5]. EVs carry adhesins, which hinder the attachment of *Xf* cells to surfaces and with that facilitates the shift from biofilm to planktonic growth, supporting systemic plant colonization and virulence[5]. Additionally, *Xf*-EVs

contain virulence factors, including the lipase/esterase LesA, a homologue of the CWDE LipA in Xanthomonas, and anti-toxins which aid the bacterium's virulence[217,218]. Whether EVs have additional roles in delivering molecules to neighbouring *Xf* cells or are also employed to deliver molecules to the host cells is not yet known.

EVs as molecular messengers to eukaryotic hosts

The uptake of bacterial EVs into host plant cells first requires a passing through the plant cell wall. CWDEs are part of many pathogenic bacteria's effector arsenal and can be secreted via EVs which, in turn, might facilitate their entry[1,217,219–223]. Increased cell wall plasticity at sites of cell wall genesis or plant infection might also be preferential entry points for EVs[1,224,225].

Uptake of bacterial EVs into mammalian cells include canonical uptake routes of Clathrin-Mediated Endocytosis (CME) and membrane fusion, similar to entry routes of viral particles[226–228]. Preferential uptake of EVs by specific cell types has been observed for mammalian EVs[229] and more transient interactions to deliver EV cargo ("Kiss-and-run-mechanism") have also been proposed[230] but remain to be further studied.
In plants, co-localisation of plant EV-marker Tetraspanin-8 (Tet8) with the Multivesicular Body (MVB)-marker Arabidopsis Rab5-like GTPase ARA6 suggests integration of plant EVs into the endomembrane pathway[1,131]. Indeed, uptake of labelled plant EVs by plant roots showed labelling of membranes as well as cytoplasmic signals, proposing uptake by membrane fusion as well as CME[231]. The insertion of EVs from plant pathogenic bacteria *Xanthomonas campestris* pv. *campestris* (*Xcc*) into the plant cell membrane suggests a delivery of bacterial EVs and their cargo via membrane-fusion[232]. Integration of bacterial EVs modifies the plant membrane and its trafficking dynamics, resulting in enhanced CME rates[232]. The insertion occurs at nano-domains and is Remorin-dependent, a scaffold protein organizing membrane lipids and proteins functioning as a signalling hub[232,233]. Nano-domains are also important for clathrin-independent endocytosis pathways, which are less well understood in plants[234] but might play a role in the uptake of EVs. Generally, it should be noted that the assessment of EV-uptake using labelled EVs with lipid dyes, as employed in most studies so far, has some pitfalls including secondary unspecific labelling of membranes and requires further validation[235].

Despite the incomplete mechanistic understanding, proof for successful delivery of vesicle-borne bacterial molecules into eukaryotic cells is supported by observed functional

consequences[236]. Importance of EVs in the interaction between plant and interaction microbes has been recognized[3,237,238]. Plant pathogenic bacteria also secrete toxins and virulence factors via EVs, actively aiding the infection process by granting protection in adverse environments [239,240]. In human bacterial pathogens, the packaging of virulence factors in EVs has been shown to help targeted delivery to specific host tissue[241–243]. Whether such a targeted delivery occurs in plants is not known.

The role of EVs in protecting and delivering sRNA[1,131,244,245] (**Figure 3**) is exemplified during the infection of Arabidopsis with the necrotrophic fungus *Bc*, where the plant and the fungus exchange sRNAs packaged in EVs, mediating the RNA-based bi-directional warfare[131,244]. Since then, association of RNAs with EVs has been shown for many other plant-microbe associations with functions extending ckRNAi[237,246–248]. For example, infected Arabidopsis plants send mRNAs to *Bc,* resulting in their translation by the fungal ribosomes interfering with the fungus's homeostasis[2,248]. EVs protect extracellular (ex)RNA from degradation which is especially important in protease-rich environments such as the apoplast of host plants[249,250] and unlike RNA-Binding Proteins (RBPs) alone, EVs can protect several RNAs at once[236]. Loading of RNAs into EVs seems to be specific, as RNA cargo of EVs differs from that of cells[251]. For eukaryotic vesicles, including plants, this specificity has partly been explained by association with specific RBPs and RNA-motifs[244,249,252–254].

Bacteria also send RNA molecules in EVs to interfere with host (immune) responses. For human pathogens, silencing of host immune responses by bacterial sRNAs loaded in EVs has been shown for several periodontal pathogens and the opportunistic bacterial pathogen *Pseudomonas aeruginosa*[255,256].

In the plant-pathogenic bacteria *Xoo,* the sRNA *Xosr001* associates with EVs to regulate the expression of a jasmonic acid methyl transferase in rice, which impairs host stomatal immunity[257]. Symbiotic nitrogen-fixing rhizobia bacteria send Transfer-RNA Fragments (tRFs) into their soybean host to regulate key host genes, facilitating the establishment of symbiosis[133]. While the latter study did not assess their association with EVs, tRNAs are frequently found as cargo of bacterial EVs[251,258,259] and might facilitate the compatibility of prokaryotic and eukaryotic interactions.

Despite the lack of canonical RNAi pathways in bacteria, RNA-based gene silencing has been expanded to bacterial microbes. A recent proof-of-concept study generated transgenic Arabidopsis lines expressing sRNAs targeting virulence factors of *Pto*DC300, which enhanced

resistance to infection with *Pto*DC3000, mediated in parts by sRNA associated with EVs[260]. With this, bacteria also join the battleground of bi-directional ckRNAi warfare but mechanistic details on how RNA-based communication between procaryotic and eukaryotic cells occur, are missing. This reflects both the limited understanding of RNA signalling in prokaryotes and the complexity of cross-kingdom RNA trafficking.

Bacterial small RNAs and their matchmaker Hfq

One major challenge in studying intracellular and extracellular roles of sRNAs in bacteria is the limited identification of novel bacterial sRNAs[261]. Heterogeneity of bacterial sRNAs in size, origin and function compared to well-described eukaryotic sRNAs, as well as their very small pairing region of < 10 nt with targets, makes identification of novel sRNAs and prediction of interactions very challenging[262–264]. Bacteria have a diverse set of sRNAs, heterogeneous in size, ranging from 50 to 500 nt and often deriving from intergenic regions in the genome[262]. Endogenously, sRNAs can fine-tune bacterial gene expression through base-pairing with translation initiation regions or coding sequence of target mRNAs, or act as sRNA sponges, sequestering other sRNAs to prevent them from binding their targets[262]. By blocking Ribosome Binding Sites (RBS), they effectively hinder translation initiation. Base pairing between sRNAs and mRNAs can either mark transcripts for degradation via endonucleases, such as the main mRNA decay Ribonuclease E (RnE), or stabilize mRNAs, resulting in increased translation[265,266].

Functionally, sRNAs are often divided into Host Factor for phage Qβ replication (Hfq)-dependant and Hfq-independent sRNAs. Hfq is a conserved RNA chaperone of the Sm/Lsm family which forms homo-hexameric rings[267] (**Figure 3**). Beside RNA metabolic functions, Hfq also stabilizes and delivers sRNAs to their mRNA target sides[268]. Hfq displays four surface sites which can bind and interact with RNA[269]. The proximal face recognizes sRNAs with U-rich regions, helping to display the "seed-region" of sRNAs binding their targets[270]. Initial work in the bacterial model organism *Escherichia coli* (*E. coli*) defined the Hfq-binding motif A-R-N for oligonucleotides binding to the distal face with one triplet of A-R-N binding to one subunit of Hfq with adenosine (A), purine nucleotide (R) and any third nucleotide (N)[271]. Binding of RNA to Hfq at the distal site has been extended to other A-rich motifs since[272–275], revealing a higher flexibility for RNA-binding to the distal site. Binding to both sites will result in further wrapping of the oligonucleotides around Hfq and interactions with the rim and C-

terminal tail of the protein contribute to the proper function of Hfq[269]. The largely unstructured C-terminal tail forms amyloid-like filaments which can integrate into membranes and disrupt membrane integrity[276,277].

Knockout mutants of Hfq in pathogenic bacteria often display increased stress sensitivity and reduced virulence linked to the loss in sRNA-based regulation in response to environmental triggers[278]. The expression of sRNAs in bacteria is very dynamic and adjusts swiftly to changing conditions[279,280]. This rapid and reversible post-transcriptional modulation of gene expression in response to environmental changes allows bacteria to rapidly adapt to stressors such as nutrient deprivation or host immune defences[261,281]. For example, in plant-pathogenic bacteria *Xoo,* the Hfq-dependent sRNA *Xonc3711* influences oxidative stress responses, biofilm formation and represses transcription of effector XopC2[282].

Hfq has been identified in several proteomic studies of bacterial EVs[200,283,284]. The integration of Hfq into bacterial membranes via its C-terminal domain, includes membranes of EVs[276,285,286]. Intriguingly, membrane-associated Hfq retains its RNA-binding capacity which might facilitate the accessibility and delivery of sRNAs via EVs[277,286–288]. In *E. coli*, the abundance of Hfq at EVs varies depending on growth state of the bacteria[283] and a selective loading of Hfq to EVs might explain differential loading of RNAs into bacterial EVs compared to cells[251], similar to the function of RBPs in eukaryotes[244,249,252].

Functionally, RNAs shuttled between organisms to perform ckRNAi rely on the conserved, eukaryotic RNAi-pathways[72,129,289], which are not found in prokaryotes. Fragments of evolutionary highly conserved tRNAs, tRFs, have been identified as prokaryotic regulators of eukaryotic transcription[133,290,291]. Association of tRFs with Hfq[292] and AGOs[293], might represent one way how prokaryotic RNAs are being integrated into eukaryotic post-transcriptional pathways[294]. The membrane association of Hfq and AGOs, particularly AGO1 and AGO7 in Arabidopsis[295–297], might further facilitate the exchange of RNAs via EVs.

… and what does this mean for Xylella fastidiosa*?*

Despite the lack of several functional secretion systems which can deliver effectors into the plant (T3SS, T4SS, T6SS), infection with *Xf* result in devastating disease outcomes in economically important crops[4]. Given the high production of EVs in *Xf*[5], it is intriguing to

speculate a role for EVs in delivering molecules to interacting microbes and host plants. So far, *Xf*-EVs have only been indirectly linked to *Xf*'s virulence by blocking attachment sites to facilitate the lifestyle switch between biofilm and planktonic[5]. With its reduced genome[298], *Xf* requires a very tight control of gene expression to enable the growth in the two very distinct states. However, underlying molecular mechanisms mediating this switch are not yet understood. In other bacteria, rapid switches between distinct states have been linked to sRNA-based regulation[299], a mechanism that remains entirely unexplored in *Xf*. Generally, knowledge and tools acquired in recent years in sRNA-based regulation in human pathogenic bacteria[300–302] have barely been extended to the plant microbe field, let alone for non-model organisms such as *Xf*.

By employing techniques from bacterial model organisms and making use of the experimental plant models *At* and tobacco, I first identified protein, RNA and DNA cargo of *Xf*-EV, and could then, second, reveal Hfq and sRNAs as important regulators for lifestyle transitions and virulence in *Xf*. Third, given the identified negative regulatory function of AGO1 in *Xf* infection in Arabidopsis, this work makes a first step in understanding how plant and bacteria RNAs and the shuttle of RNA between them, contribute to *Xf*'s virulence.

PUBLICATION 1 - Ruf et al., 2025 *JEV*

Journal of EXTRACELLULAR VESICLES Open Access ISEV

RESEARCH ARTICLE | Open Access

Extracellular Vesicles From *Xylella fastidiosa* Carry sRNAs and Genomic Islands, Suggesting Roles in Recipient Cells

Alessa Ruf, Patrick Blumenkamp, Christina Ludwig, Anne Lippegaus, Andreas Brachmann, Andreas Klingl, Alexander Goesmann, Karina Brinkrolf, Kai Papenfort, Silke Robatzek

First published: 25 June 2025 | https://doi.org/10.1002/jev2.70102

Summary

Here we show that extracellular vesicles (EVs) released by phytopathogenic bacterium *Xylella fastidiosa* (*Xf*) carries distinct molecular cargo compared to whole-cell lysates. *Xf*-EVs of subspecies *fastidiosa* are enriched in specific non-coding small RNAs (sRNAs), DNA sequences from genomic islands (GIs) and DNA- and RNA-binding proteins. Using size-exclusion chromatography and ultracentrifugation, the *Xf*-EVs were purified from *in vitro* cultures, and their cargo characterised by proteomics, DNA-sequencing (seq) and RNA-seq. We identified a family of genomic island-encoded sRNAs, designated *sXF*s, that is predicted to target four plant immune receptors in model host *Arabidopsis thaliana*. Of these, three are down-regulated after infection with *Xf* and one, a coiled coil domain-nucleotide binding site-leucine rich repeat (CNL) receptor, is also down-regulated in response to infiltration with *Xf*-EVs. This suggests, that *Xf*-EVs may function to suppress plant immunity by delivering sRNAs into the host to modulate the gene expression of immunity receptors. Moreover, the presence of GI-derived DNA in the EVs - encoding *sXF*s - suggests that *Xf* uses EVs also for horizontal gene transfer of pathogenicity-related GIs. Thus, we propose *Xf*-EVs as vehicles with a dual role: (i) delivering sRNA-based effectors to modulate gene expression in bacterial and plant recipient cells and (ii) mediating DNA transfer of GIs. These findings provide a molecular framework for understanding how *Xf* deploys EVs as "contact-independent" secretion mechanisms.

Contributions

Alessa Ruf: conceptualizing and design of experiments, establishing of EV-isolation pipeline, nucleic acid and protein analysis of EVs, scientific discussion, figure preparation, writing original draft of manuscript.

Patrick Blumenkamp: analysis of DNA-seq and RNA-seq data, establishing of target prediction pipeline, figure preparation (DNAseq plot; Figure 3a, b), scientific discussion, review and editing of manuscript.

Christina Ludwig: generation and first analysis of proteomics data, scientific discussion, review and editing of manuscript.

Anne Lippegaus: Preparation of RNA-seq libraries and sequencing, review and editing of manuscript.

Andreas Brachmann: Preparation of DNA-seq libraries and sequencing, review and editing of manuscript.

Andreas Klingl: Electron microscopy, funding acquisition, review and editing of manuscript.

Alexander Goesmann, Karina Brinkrolf: Bioinformatic support, funding acquisition, review and editing of manuscript.

Kai Papenfort: Funding acquisition, scientific discussion, review and editing of manuscript.

Silke Robatzek: Funding acquisition, conceptualizing and design of experiments, scientific discussion, writing original draft of manuscript.

I hereby confirm that the contributions to the research article “Extracellular Vesicles From *Xylella fastidiosa* Carry sRNAs and Genomic Islands, Suggesting Roles in Recipient Cells” published in *Journal of Extracellular Vesicles* Vol. 14, Issue 6 (June 25th, 2025) (https://isevjournals.onlinelibrary.wiley.com/doi/10.1002/jev2.70102) are correct.

Alessa Ruf (1st author)

Silke Robatzek (Last author)

Journal of Extracellular Vesicles

ISEV

RESEARCH ARTICLE OPEN ACCESS

Extracellular Vesicles From *Xylella fastidiosa* Carry sRNAs and Genomic Islands, Suggesting Roles in Recipient Cells

Alessa Ruf[1] | Patrick Blumenkamp[2] | Christina Ludwig[3] | Anne Lippegaus[4] | Andreas Brachmann[1] | Andreas Klingl[1] | Alexander Goesmann[2] | Karina Brinkrolf[2] | Kai Papenfort[4,5] | Silke Robatzek[1]

[1]LMU Munich Biocenter, Ludwig-Maximilian-University of Munich, Martinsried, Germany | [2]Bioinformatics and Systems Biology, Justus Liebig University Giessen, Giessen, Germany | [3]Bavarian Center for Biomolecular Mass Spectrometry (BayBioMS), TUM School of Life Sciences, Freising, Germany | [4]Bioinstrumentezentrum Friedrich- Schiller University, Institute of Microbiology, Jena, Germany | [5]Microverse Cluster, Friedrich Schiller University, Jena, Germany

Correspondence: Silke Robatzek (robatzek@bio.lmu.de)

Received: 24 October 2024 | **Revised:** 31 March 2025 | **Accepted:** 8 May 2025

Funding: This study was supported by the Deutsche Forschungsgemeinschaft provided to S.R. (Heisenberg funding RO 3550/17-1 and RO 3550/18-1) and to A.R. (RU5116 'exRNA' RO 3550/16-1). Research in the S.R. lab is further supported by the European Research Council (ERC Adv Grant 884235 'MultiX'). The Q Exactive HFX mass spectrometer was funded in part by the German Research Foundation (INST 95/1435-1 FUGG). K.P. acknowledges funding by the DFG (CRC1127-3 – Project-ID 239748522 and EXC 2051 – Project-ID 390713860) and the European Research Council (CoG-101088027).

Keywords: EVs | genomic islands | Hfq | horizontal gene transfer | small noncoding RNAs

ABSTRACT

Xylella fastidiosa (*Xf*) is a Gram-negative bacterial plant pathogen responsible for severe diseases in a variety of economically important crops. A critical aspect of its virulence is the production of extracellular vesicles (EVs). In this study, we discovered that DNA-binding proteins and nonribosomal RNA-binding proteins are abundant in the corona of *Xf*-EVs. DNA-seq revealed enrichment of three genomic islands (GIs) in EVs, which carry molecular signatures indicative of horizontal gene transfer (HGT). The most abundant GI encodes five homologous small RNAs designated *sXFs*. RNA sequencing revealed a distinct pattern of noncoding RNAs enriched in EVs, including four island-encoded *sXFs*. One of the *sXF*'s stem-loops contains motifs for binding the RNA chaperone Hfq, which is also abundant in EVs. Predicted target analysis suggests that *sXFs* play a role in regulation of natural competence in bacteria. Additionally, *sXF* plant target prediction identifies a coiled-coil nucleotide-binding domain leucine-rich repeat receptor (*CNL*) immune gene that is downregulated following *Xf* infection and *Xf*-EV treatment. We propose a model where *Xf* releases nucleic acid carrying EVs with two functions: one to deliver RNA-related cargo that regulates gene expression in both bacterial and plant cells, and another to deliver DNA-related cargo for the genetic transfer of genomic islands. We highlight island-encoded *sXFs* as potential virulence factors and vesiduction as a mechanism of HGT of *sXFs* in *Xf*. Taken together, our data on *Xf*-EV cargoes provide a molecular framework for understanding the virulence of *Xf*.

1 | Introduction

Pathogenic bacteria must adapt to and modulate their host's environment to ensure their survival and the establishment of infection within the host. Gram-negative bacteria release extracellular vesicles (EVs) to facilitate their proliferation, for example, by detoxifying host defences, immune suppression and nutrient acquisition as well as competing and cooperating with strains of host-associated bacterial communities (Rybak and Robatzek 2019; McMillan and Kuehn 2021; Toyofuku et al. 2023). EVs are mobile cytosol-derived cargo containing nanosized membrane spheres that are produced by bacteria in the form

of outer membrane vesicles (OMVs) and outer inner membrane vesicles (OIMVs) (Toyofuku et al. 2023). Different biogenesis routes of EVs indicate the release of heterogenic subpopulations of EVs with different types of cargo (Toyofuku et al. 2023). As long as biomarkers are not available to convincingly probe their origin, we will collectively refer to these vesicles as EVs.

EVs are classified as a bacterial Type-0 secretion system, selectively delivering bacterial cargoes into the environment. The cargoes include proteins, and nucleic acids present at the vesicle corona, a layer of biomolecules adsorbed onto the vesicle surface—as well as the membrane or the lumen, which provides protection against degradation. Since the EV cargo composition responds to developmental and environmental conditions, vesiculation enhances bacterial adaptability (Xiu et al. 2024). For example, EVs can carry toxins and enzymes that attack and degrade the cell walls of competitor strains or hosts, thus providing an advantage to the vesiculating bacteria (Toyofuku et al. 2023; Macion et al. 2021; De La Fuente et al. 2022). Moreover, EVs interact with recipient cells by delivering cargo to surface receptors or into the cytoplasm, leading to altered cellular processes in the recipient cells. This includes the modulation of host immune signalling by EV-packaged small (s)RNAs, which aids the bacterial infection process (Koeppen et al. 2016; Wu et al. 2024; Xie et al. 2024).

EVs are relevant for interbacterial competition and cooperation and facilitate the transfer of genetic material, including plasmids and antibiotic resistance genes, thereby enhancing genetic diversity and adaptability within microbial communities. EVs also enable horizontal gene transfer (HGT) among bacteria through a process known as vesiduction (Marinacci et al. 2023; Soler and Forterre 2020; Dell'Annunziata et al. 2021). In this process, genetic material is encapsulated within EVs, and upon delivery to recipient cells, it can integrate into the recipient's genome, leading to genetic transformation. Vesiduction is a crucial mechanism for the spread of antibiotic resistance and virulence traits, as it promotes the rapid dissemination of genetic information across bacterial populations and even across species barriers (Marinacci et al. 2023; Soler and Forterre 2020; Li et al. 2022; Johnston et al. 2023; Wang et al. 2022; Qiao et al. 2021). Since EVs protect DNA from degradation during transfer, vesiduction increases the efficiency of HGT, aiding bacterial evolution and adaptation (Marinacci et al. 2023). Canonical secretion systems, such as the Type-VI secretion system in *Cupriavidus necator*, function together with EVs in HGT by secreting molecules, which bind to lipopolysaccharides (LPSs) on EVs and tethers them to recipient cells (Li et al. 2022).

Xylella fastidiosa (*Xf*), a Gram-negative bacterium in the Xanthomonadaceae family, is a plant pathogen listed as a 'priority pest' in Europe. *Xf* exclusively colonizes two habitats: the plant xylem vessels and the foregut of insect vectors, such as sharpshooter leafhoppers and spittlebugs (Castro et al. 2021). Transmitted by these xylem sap-feeding insects, the bacterium infects around 700 plant species (EFSA 2023), causing severe agricultural diseases. These include Pierce's disease (PD) in grapevines caused by *X. fastidiosa* subsp. *fastidiosa* (*Xff*), as well as Citrus Variegation Chlorosis (CVC) in citrus trees and the Olive Quick Decline Syndrome (OQDS) in olives triggered by *X. fastidiosa* subsp. *pauca* (*Xfp*) (Landa et al. 2022). With its genome sequence serving as a reference and its genetic tractability, *Xff* strain Temecula1 (*Xff* Tem1) has provided most molecular mechanistic insights into *Xf* (Landa et al. 2022). The *Xfp* strain De Donno (*Xfp* DD) has a significant agricultural impact and is responsible for the recent outbreak of OQDS in Southern Europe (Landa et al. 2022). Because these two strains are adapted to different hosts, they offer a valuable opportunity to address the immune evasion modes of *Xf*.

The nonflagellated *Xf* bacteria spread through the xylem via both passive flow and twitching motility (Rapicavoli et al. 2018). As bacterial density increases, biofilm formation is initiated. The shift from planktonic to sessile states is regulated by quorum sensing (QS) and is driven by EVs, which promote bacterial detachment from surfaces (Ionescu et al. 2014). The link between vesiculation and surface detachment is evident from the genetic deletion of a diffusible signal factor (DSF) synthase, *rpfF*, in *Xff* Tem1, which led to hypervesiculation. This increased vesicle production reduced the bacterium's ability to attach to surfaces, thereby enhancing its ability to spread systemically (Ionescu et al. 2014). Previous proteomic analyses of EV-enriched fractions from cultured *Xf* revealed adhesins as cargoes, further supporting this phenotypic observation (Feitosa-Junior et al. 2019). Comparative analysis of EVs from *Xff* Tem1 and *Xff* DD provides insights into shared cargo that could influence their ability to colonize hosts.

The presence of cell wall-degrading enzymes suggests that *Xf* EVs contribute to the bacterium's virulence by promoting its systemic colonization, likely access to the living cells within the xylem tissue (Nascimento et al. 2016; Roper et al. 2007). Since cell wall degradation can release damage-associated molecular patterns (DAMPs), it is likely that this process triggers immune signalling (Lorrai and Ferrari 2021). Moreover, *Xf*-EVs carry the translation elongation factor EF-Tu, which induces plant immunity (Feitosa-Junior et al. 2019; Mitre et al. 2021; Nascimento et al. 2016). To evade host immunity, *Xff* Tem1 has been shown to shield its LPS (Rapicavoli et al. 2018). However, *Xf* lacks a Type-III secretion system, by which Gram-negative bacteria typically deliver Type-III-secreted effectors to suppress host defences and reprogram plant physiology (Macho and Zipfel 2015). This raises the question of how *Xf* overcomes plant immune responses induced by EF-Tu, the cold shock protein peptide csp22 and cell wall damage, for example, vessel lignification (Sabella et al. 2018; Burbank and Ochoa 2022).

Given the role of EVs in bacterial pathogenesis and as a Type-0 secretion system (Guerrero-Mandujano et al. 2017), we speculate that *Xf* utilizes EVs as a mechanism for delivering effectors in a contact-independent manner. To address this hypothesis, we profiled size-exclusion chromatography (SEC)-purified *Xf*-EV cargoes by proteomics, DNA sequencing (DNA-seq) and RNA sequencing (RNA-seq). Our analysis revealed that EVs have distinct protein, DNA and RNA profiles compared to whole-cell lysates (WCLs). EVs were enriched with noncoding (nc)RNAs, including four homologous small (s)RNAs, designated *sXFs*, which are encoded on a genomic island (GI) that is also enriched in EVs as DNA. Notably, a *sXF* predicted plant target is downregulated in *Xff*-infected and *Xff*-EV-treated plants.

2 | Material and Methods

2.1 | Culturing of *Xylella fastidiosa*

Xff Tem1 and *Xfp* DD were routinely grown for 5–10 days on Pierce's disease 3 (PD3) plates (Davis 1980). For liquid cultures, 200 mL PD2 (Davis 1980) was inoculated with resuspended *Xf* inoculum in phosphate buffered saline (PBS), and cultures were grown for approx. 4–7 days in PD2 (+50 µg/mL for Temecula1-GFP) at 28°C and 140 revolutions per minute (rpm), reaching an OD_{600}> 0.2.

2.2 | EV Isolation and Purification

Before harvesting cells, cultures were shaken to collect all cells from the cultures, including biofilm and planktonic cells in suspension. For WCL samples, 2 mL cultures were centrifuged for 15 min, 4000 × *g*. Supernatants were removed, and pellets were flash-frozen and kept at −80°C until further use. For *Xf*-EV isolation, 200 mL cultures were centrifuged at 4000 × *g* for 15 min, supernatants were filtered through 0.22 µm filters (Milipore, SEGTPT0045). Filtered supernatants were centrifuged at 38,000 × *g* for 1 h to remove cellular debris and then further centrifuged at 150,000 × *g* for 4 h. Then, pellets were resuspended in 2 mL filtered 1× PBS (pH 7.4) and further purified using qEV2 iZON SEC-columns (iZon qEV2 columns, 70 nm series, IC2-70, France). Fractions containing *Xf*-EVs were collected and either enriched using the qEV Concentration Kit (iZon; RCT02, France), qEV Magnetic Concentration Kit (iZon; RCT03, France) or Amicon centrifugal columns 30 kDa (Milipore, UFC9030), depending on further usage. An overview of the *Xf*-EV isolation workflow can be found in Figure S1A. For nucleic acid analysis, *Xff* Tem1-EVs were isolated from 1× 200 mL (DNA) or 2× 200 mL (RNA) cultures and concentrated using iZon concentrator beads (for DNA) or iZon magnetic concentrator beads (for RNA).

2.3 | EV Enzyme Treatments and Disruption

For enzyme treatments, SEC-purified *Xff* Tem1-EV samples (8 mL) were split into five fractions. Fraction 1 (untreated) was kept at 4°C while Fractions 2 and 3 were treated with 100 µg/mL Proteinase K (ProtK, 800U, NEB, P81075) for 30 min at 37°C. The reaction was stopped by addition of 6.6 µL of 100 mM PMSF and incubation at RT for 5 min. Then, Fraction 3 was treated with 10,000 U Micrococcal Nuclease (MNase, NEB M0247S) for 30 min at 37°C.

Fraction 4 was used for disruption assays of EVs with 1% Triton were performed according to (Huang et al. 2021). Fraction 5 was used for EV-burst assays SEC-purified EVs were washed twice with hypotonic buffer (2 mM Tris-HCl, 1 mM $MgCl_2$, 1 mM KCl) (Cheng et al. 2018) in Amicon centrifugal columns 30 kDa (Milipore, UFC5003), followed by ProtK and MNase treatments as described in 2.3. All fractions were incubated with 100 µL of qEV Magnetic concentrator beads (iZon; RCT03, France) at RT for 10 min and put on a magnetic stand to remove supernatant, following manufacture's description. Next, concentrated *Xff* Tem1-EV pellets were used for DNA or RNA extraction as described in 2.11 and 2.13.

2.4 | SEM and TEM Analysis

For scanning electron microscopy (SEM), samples were prepared as described previously (Janda et al. 2023). Microscopy was carried out on a Zeiss Auriga Crossbeam workstation (Zeiss, Oberkochen, Germany) at an acceleration voltage of 1.5 kV and a working distance of approximately 5 mm and by using the secondary electron (SE) detector. For transmission electron microscopy (TEM), isolated EVs were negatively stained with 1% uranyl acetate. Microscopy was carried out at 200 kV using a JEOL F200 (JEOL, Japan), equipped with a 20 mega pixel CMOS camera.

2.5 | Nanoparticle Tracking Analysis (NTA)

For EV characterization using a nanoparticle tracking analyser (ZetaView, Particle Metrix, Germany), appr. 10 µL of SEC-purified *Xf*-EVs were kept before further concentration with iZon concentrator beads. *Xf*-EVs were diluted to a concentration which resulted in approx. 200–300 particles per window; vesicle size and charge (zeta [ζ] potential) were determined with three measurements per sample.

2.6 | Labelling of *Xf*-EVs

For labelling of *Xf*-EVs, 100 µL of isolated vesicles were incubated with 1 mM FM4-64 (Invitrogen, T13320) and 1 mM SYTO RNAselect (Invitrogen, S32703) at room temperature (RT) for approx. 20 min. Then, any unincorporated dye was removed using Amicon centrifugal columns 30 kDa (Milipore, UFC5003), and columns were washed with 3× 100 µL 1× PBS. Signals were imaged using Leica Thunder imager with 100×/1.44 OIL UV objective. FM4-64 was excited at 390 nm and signal was collected over the whole spectrum. RNAselect was excited at 510 nm and the signal was collected at an emission wavelength 535 nm.

2.7 | Coomassie Staining

To estimate protein concentrations, Bradford assays were performed following the microassays (Sigma–Aldrich, B6916) according to the manufacturer's guidelines (Figure S2a, b). 30 µL of prepared samples were loaded onto 12% sodium dodecyl sulphate (SDS)-polyacrylamide gel electrophoresis and protein profiles were checked by colloidal Coomassie staining overnight.

2.8 | Sample Preparation for Proteomics

SEC-purified *Xf*-EV samples (8 mL) were split into two fractions. Fraction 1 (untreated) was kept at 4°C while Fraction 2 (ProtK treated) was treated with 100 µg/mL ProtK (800U, NEB, P81075) for 30 min at 37°C. The reaction was stopped by the addition of 6.6 µL of 100 mM PMSF and incubation at RT for 5 min. Then, both samples were incubated with 100 µL of iZon concentrator beads at RT for 1 h and pelleted at 16,800 × *g* for 10 min. Pellets were resuspended in 100 µL 1× PBS (pH 7.4). After the addition of 20 µL 6× Lämmli buffer 9.5 µL 50 mM dithiothreitol (DTT),

samples were boiled for 10 min at 98°C and then stored at −80°C until further use.

Four biological replicates of WCL, *Xf*-EV and *Xf*-EV + ProtK samples from *Xff* Tem1 as well as *Xfp* DD were denatured by the addition of 1× SDS loading buffer and heated for 10 min at 70°C. In-gel trypsin digestion was performed according to standard procedures (Shevchenko et al. 2006). In order to ensure equal protein concentrations across all analysed samples, a consistent protein amount of 10 µg per sample was run on a Nu-PAGE 4%–12% Bis-Tris protein gel (ThermoFisher Scientific) for about 1 cm. Subsequently, the still not size-separated single protein band per sample was cut, reduced (50 mM DTT), alkylated (55 mM chloroacetamide) and digested overnight with trypsin (Trypsin Gold, mass spectrometry grade, Promega). The obtained peptides were dried to completeness and resuspended in 24 µL (WCL) or 12 µL (*Xf*-EV and *Xf*-EV + ProtK) of 2% acetonitrile, 0.1% formic acid (FA) in HPLC grade water. Finally, 2 µL (WCL) or 5 µL (*Xf*-EV and *Xf*-EV + ProtK) of the sample was injected per mass spectrometric (MS) measurement.

2.9 | Liquid Chromatography-Mass Spectrometry (LC-MS/MS) Data Acquisition

LC-MS/MS data acquisition was carried out on a Dionex Ultimate 3000 RSLCnano system coupled to a Q-Exactive HF-X mass spectrometer (ThermoFisher Scientific, Bremen). Injected peptides were delivered to a trap column (ReproSil-pur C18-AQ, 5 µm, Dr. Maisch, 20 mm × 75 µm, self-packed) at a flow rate of 5 µL/min in 0.1% FA in HPLC grade water. After 10 min of loading, peptides were transferred to an analytical column (ReproSil Gold C18-AQ, 3 µm, Dr. Maisch, 450 mm × 75 µm, self-packed) and separated using a 50 min gradient from 4% to 32% of Solvent B (0.1% FA, 5% DMSO in acetonitrile) in Solvent A (0.1% FA, 5% dimethyl sulphoxide [DMSO] in HPLC grade water) at 300 nL/min flow rate. The Q-Exactive HF-X mass spectrometer was operated in data-dependent acquisition (DDA) and positive ionization mode. MS1 spectra (360–1300 m/z) were recorded at a resolution of 60,000 using an automatic gain control (AGC) target value of 3e6 and a maximum injection time (maxIT) of 45 ms. Up to 18 peptide precursors were selected for fragmentation. Only precursors with a charge state of 2–6 were selected, and dynamic exclusion of 25 s was enabled. Peptide fragmentation was performed using higher energy collision-induced dissociation (HCD) and a normalized collision energy (NCE) of 26%. The precursor isolation window width was set to 1.3 m/z. MS2 Resolution was 15,000 with AGC target value of 1e5 and maxIT of 25 ms.

2.10 | LC-MS/MS Data Analysis

Peptide identification and quantification was performed using the software MaxQuant (version 1.6.3.4) (Tyanova et al. 2016) with its built-in search engine Andromeda (Cox et al. 2011). MS2 spectra were searched against either the Uniprot protein database of *Xf* strain Temecula1 (ATCC 700964, UP000002516, 2007 protein entries, downloaded August 2023) or the Uniprot protein database of *Xfp* (UP000194146, 2059 protein entries, downloaded August 2023), respectively. The databases were further supplemented with the amino acid sequence of ProtK from *Parengyodontium album* (P06873) as well as common contaminants (built-in option in MaxQuant). Trypsin/P was specified as proteolytic enzyme. Carbamidomethylated cysteine was set as a fixed modification. Oxidation of methionine and acetylation at the protein N-terminus was specified as variable modifications. Results were adjusted to 1% false discovery rate (FDR) on the peptide spectrum match (PSM) level and protein level employing a target-decoy approach using reversed protein sequences. Label-free quantification (LFQ) (Cox et al. 2014) intensities were used for protein quantification with at least two peptides per protein identified. The minimal peptide length was defined as seven amino acids, and the 'match-between-runs' functionality was disabled. Only proteins for which LFQ values in at least three out of four replicates in at least one of the sample types were considered for further analysis. Missing values were imputed by a protein-specific constant value, which was defined as the lowest detected protein-specific LFQ-value over all samples divided by two. Additionally, a maximal imputed LFQ value was defined as the 15% quantile of the protein distribution from the complete dataset.

To identify proteins with a significantly higher abundance in EV samples compared to WCL samples, a Welch's t test was conducted. The resulting p values were corrected using the Benjamini–Hochberg method to control the FDR. Proteins with FDR < 0.05 and a fold-change > 1 in *Xf*-EVs compared to WCL were categorized as 'EV-enriched proteins'. All other proteins detected in the *Xf*-EV (or *Xf*-EV + ProtK) samples in at least three out of four replicates were categorized as 'present in EVs'. For functional categorization, identified EV proteins were manually sorted. Gene ontology (GO)-term enrichment was performed on all identified EV proteins, using an adjusted p value cutoff < 0.05. For rank analysis, (imputed) expression values for all EV proteins were averaged over the four replicates and ranked from highest to lowest. To compare the proteomes of both *Xf* subspecies, we reanalysed the *Xfp* DD data files against the *Xff* Tem1 reference database (*Xf strain* Temecula1, ATCC 700964, UP000002516). Proteins identified in both subspecies in at least three out of four replicates were defined as 'core EV cargo'. Functional categorization was also achieved through manual sorting. For comparison of identified EV proteins with previous publications (Feitosa-Junior et al. 2019; Nascimento et al. 2016), the presence of EV-protein content was compared using GeneID or ProteinIDs, respectively.

2.11 | DNA Isolation and DNA Sequencing

DNA isolation was performed using phenol/chloroform extraction as published in Spada et al. (2020). EV pellets were resuspended in DNA extraction buffer (SDS 0.5%, Tris-HCL 50 mM pH 8, EDTA 0.1 M) and 0.1 mg/mL of ProtK and incubated at 56°C overnight. Then, exosomal DNA was isolated using phenol/chloroform. DNA was pelleted for 2 h at −80°C and precipitation was facilitated by the addition of 1 µL glycogen (Thermo Scientific, FERR0051). DNA of untreated *Xff* Tem1-EVs was then used to perform DNA sequencing. The size and concentration of DNA were analysed using DNA high-sensitivity bioanalyzer chips. Sequencing libraries were constructed from 1 ng of DNA with the Nextera XT DNA Sample Preparation Kit (Illumina, Germany) according to the manufacturer's protocol. The library was quality controlled by analysis on an Agilent 2000 Bioanalyzer with the Agilent High Sensitivity DNA Kit (Agilent

Technologies, Germany) for fragment sizes of ca. 500–800 bp. Sequencing on a MiSeq sequencer (Illumina; 2× 300 bp paired-end sequencing, v3 chemistry) was performed in the Genomics Service Unit (LMU Biocenter, Martinsried, Germany). For PCR amplification of GI genes, EV pellets from Fractions 1–5 were used for DNA extraction, followed by regular PCR amplification using gene-specific primers and GoTaq (Promega, M7122) with 45× amplification cycles.

2.12 | DNA Analysis

The DNA sequences were adapter and quality trimmed with fastp v.0.23.4 (Chen et al. 2018) using default settings without length filtering ('–disable_length_filtering'). Due to a larger region of badly aligned reads in rRNA regions, DNA reads of rRNAs were filtered out with SortMeRNA v.4.3.6 (Kopylova et al. 2012) using 'smr_v4.3_default_db.fasta' from https://github.com/biocore/sortmerna/releases/download/v4.3.4/database.tar.gz. Afterwards, the reads were aligned to NCBI accession GCF_000007245.1 with Bowtie 2 v.2.5.3 (Langmead and Salzberg 2012) in '–very-sensitive' mode and a maximal insert size of 1000 bp (−X 1000). Conversion, sorting and filtering (unmapped reads) of SAM/BAM files were done with samtools v.1.19 (Li et al. 2009). Bedtools v.2.31.1 (Quinlan and Hall 2010) was used for binning aligned reads by alignment position. Coverage visualizations were created with Circos v.0.69.9 (Krzywinski et al. 2009) and Sushi v.1.31 (Phanstiel et al. 2014).

2.13 | RNA Isolation and RNA Sequencing

Total RNA was isolated from WCL and EV samples using Trizol, and RNA was purified using RNA Clean & Concentrator Kit with DNase treatment (ZymoResearch, R1013). Total RNA was isolated following Trizol procedure and purified using RNA Clean & Concentrator Kit (ZymoResearch, R1013) following the manufacturer's description. The RNA integrity was confirmed using a Bioanalyzer (Agilent). For total RNA-seq of WCL samples, rRNA was depleted using an Illumina Ribo-Zero Plus rRNA Depletion Kit (Illumina, #20040526). All cDNA libraries were prepared using the NEBNext Ultra II Directional RNA Library Prep Kit for Illumina (NEB; #E7760). cDNA libraries were sequenced using the Illumina NextSeq1000 system with 100-nt read length in paired-read mode. For RT-PCR amplification of ncRNAs, EV pellets were directly resuspended in 1 mL Trizol after purification and processed as described above. Extracted total RNA was used as a template to perform gene-specific RT using SuperScript III (ThermoFisher Scientific, 18080093). cDNA was then used as a template for regular PCR amplification using gene-specific primers and GoTaq (Promega, M7122) with 45× amplification cycles.

2.14 | RNA Analysis

The data was preprocessed, mapped and counted with Curare v.0.6.0 (Blumenkamp et al. 2024). This workflow used Trim Galore v.0.6.10 (https://www.bioinformatics.babraham.ac.uk/projects/trim_galore/) for quality control and adapter trimming with default settings. Mapping was performed with Bowtie 2 v.2.5.2 in '–very-sensitive' mode (Langmead and Salzberg 2012). Mapping results in SAM format were converted with samtools v.1.18 (Li et al. 2009). Features (CDS, ncRNA, tRNA and rRNA) were counted with featureCounts v.2.0.6 (Liao et al. 2014) with '-p –countReadPairs -s 2'. The genome GCF_000007245.1 and the new reannotation were used for the alignment and feature assignment, respectively.

2.15 | NcRNA Analysis

Sequences of *sXFs* were retrieved to perform sequence and secondary structure alignments using Copra-Tool (http://rna.informatik.uni-freiburg.de; version 5.0.10) (Wright et al. 2013; Wright et al. 2014; Raden et al. 2018).

2.16 | sRNA Target Prediction in *X. fastidiosa*

To predict targets in *Xff* Tem1, the intaRNA tool (http://rna.informatik.uni-freiburg.de; version 5.0.10) (Wright et al. 2014; Raden et al. 2018, Mann et al. 2017; Busch et al. 2008) was run locally against the newly annotated *Xff* Temecula1 genome with high-confidence interactions when p value < 0.05.

2.17 | sRNA Target Prediction in Host Plants

For target prediction in host plants of *Xf*, *sXF* fragments were generated employing a sliding-window approach. Target prediction was performed using psRNATarget (https://www.zhaolab.org/psRNATarget) (Dai et al. 2011; Dai and Zhao 2011; Dai et al. 2018) using the *Arabidopsis thaliana* Col-0 Reference genome TAIR 10 (JGI genomic project, Phytozome 13, 447_Araport11) and the *Vitis vinifera* genome PN40024.v4. PsRNATarget uses a mismatch-sensitive 'seed' region (Nucleotides 2–7) and mRNA target accessibility to identify and classify target genes. To increase prediction precision and reduce predicted candidates, we focussed our analysis on targets of 24-nt fragments. Interactions were classified high-confidence when E value ≤ 3. For overrepresentation (OR) analysis in *Arabidopsis* targets, Panther online tool was used (Panther19; https://pantherdb.org/) (Mi et al. 2019; Thomas et al. 2022). OR on *V. vinifera* targets and *Xf* transcripts were performed with the packages clusterProfiler and enrichplot in R.

2.18 | Plant Infection Assays

Fourteen-days-old sterile-grown *A. thaliana* Col-0 seedlings were infected with 5 µL *Xff* Tem1 inoculum (OD_{600} = 0.2 in 1× PBS, pH 7.4) or 5 µL 1× PBS (mock) by pricking with 27G needles. Seedlings were harvested 3 days postinoculation and snap-frozen until further use.

2.19 | EV Infiltration Assays

Fourteen-days-old sterile-grown *A. thaliana* Col-0 seedlings were transferred into 500 µL liquid ½ Murashige and Skoog media overnight. Then, media was removed and seedlings were flooded in either 500 µL 1× PBS pH 7.4 (mock) or 500 µL EVs collected from supernatants of 400 mL *Xff* Tem1 cultures after 0.22 µm

filtering, centrifugation at 38,000 × *g* for 1 h to remove cellular debris and then further centrifugation at 150,000 × *g* for 4 h. Vacuum was applied twice for 30 s. Seedlings were harvested 4 h later and snap-frozen until further use.

2.20 | Seedling Gene Expression Assays (RT-qPCRs)

Total RNA of seedlings was extracted using the CTAB-Method (Bemm et al. 2016) and DNase treated using Turbo DNase (Invitrogen, AM2238). qRT-PCRs were performed with 10 ng RNA using the NEB Luna Universal One-Step RT-qPCR Kit (E3005), in 10 µL reactions according to manufacturer guidelines (55°C 10 min, 95°C 1 min, 95°C 10 s, 60°C 30 s, 45 cycles and subsequent melting curve analysis) using primers according to Data S4. *CDKA* was used as a housekeeping gene, and expression values were analysed using the $2^{(-\Delta\Delta ct)}$ method (Livak and Schmittgen 2001) comparing treated samples (*Xff* Tem1 or *Xff* Tem1-EVs) to an average of respective mock samples. Significance was assessed by two-sided Student's *t* test ($\alpha = 0.05$, *p* values *< 0.05, ** < 0.01) using the stats-package in R.

2.21 | Genome Annotation

The genome of *Xff* Tem1 (NCBI accession GCF_000007245.1) was reannotated using the Bakta pipeline (Schwengers et al. 2021). The full annotation can be found in the Zenodo repository DOI 10.5281/zenodo.13970767.

2.22 | Statistical Analysis

All downstream analyses were performed using R version 2024.04.2+764.

3 | Results

3.1 | EVs Contain 301 Proteins in *Xff* Tem1 and 140 Proteins in *Xfp* DD

To identify potential effectors secreted by EVs, we determined the proteomes of purified EVs following MISEV guidelines (Lötvall et al. 2014; Théry et al. 2018; Witwer et al. 2021; Welsh et al. 2024). EVs were isolated from bacterial culture filtrates using differential ultracentrifugation followed by SEC (Figure S1a). SEM confirmed the characteristic vesicular structures (Figure S1b), with no apparent contamination from pili, ribosomes or phage particles. The vesicle diameters ranged from 70 to 300 nm, with a median of 136 nm (Figure S1c). The ζ-potential measurement showed an initial charge of −32.5 mV, which became less negative upon Proteinase (Prot)K treatment alone (−8 mV) and cotreatment with MNase (−20 mV) (Figure S1d). This indicates that the EV corona's protein and nucleic acid composition significantly influence vesicle charge. The more negative charge observed in cotreated EVs may be due to cell wall components like LPS (Rapicavoli et al. 2018; Sabra et al. 2003). Enzymatic removal of the EV corona did not affect median particle concentration but changed particle charge (Figure S1c–e), suggesting that the EV corona composition can influence vesicle biophysical parameters.

To determine the protein composition of *Xf*-EVs, we characterized purified vesicles using liquid chromatography-tandem mass spectrometry (LC-MS/MS) and compared it with proteomes from ProtK-treated EVs and WCL. A total of 1'105 proteins were identified in *Xff* Tem1 and 1'114 in *Xfp* DD across at least three replicates per sample type (Data S1). Principal component analysis (PCA) revealed systematic differences between the proteomes of the two sample types (WCL and EVs), with *Xff* Tem1 showing PC1 at 74.1% and PC2 at 10.5%, and *Xfp* DD showing PC1 at 88.4% and PC2 at 6.8% (Figure S2c, d). We identified 301 proteins in *Xff* Tem1-EVs, representing 27% of all *Xff* Tem1 proteins, while *Xfp* DD-EVs contained 140 proteins, approximately 13% of all *Xfp* DD proteins (Figure 1a, b, Data S1). Previous proteomics studies reported 99 and 123 proteins in crude *Xff* Tem1 vesicle samples (Feitosa-Junior et al. 2019; Nascimento et al. 2016), of which 13.6% and 32% were among the 301 *Xff* Tem1-EV proteins, respectively (Data S1).

Approximately two-thirds of the identified vesicle-associated proteins are sensitive to ProtK treatment, with 74.42% in *Xff* Tem1-EVs and 71.43% in *Xfp* DD-EVs (Figure 1a, b). The proteins detected in EVs were classified into two categories: (i) those enriched in EVs compared to WCL and (ii) those present in EVs (Figure 1c, d). Since EV proteomes differ significantly from those of WCL, this supports the existence of a selective mechanism for the delivery of protein cargoes to EVs (Toyofuku et al. 2023; Haurat et al. 2011).

We conducted GO analysis on all EV-associated proteins to investigate the cellular components (CCs), molecular functions (MFs) and biological processes (BPs) in which these proteins are involved. For *Xff* Tem1-EVs, 11 significantly enriched GO-terms were identified, primarily associated with the outer membrane (OM) compartment (for CC), peptidase activity (for MF), proteolysis and protein metabolic processes (for BP) (Figure S3a). In *Xfp*-EVs, 22 GO-terms were revealed, including additional terms related to ribosomal proteins (for CC), tRNA binding, rRNA binding, unfolded protein binding, protein folding chaperones and antioxidant activity (for MF). These terms also encompassed responses to toxic substances and oxidative stress, protein maturation and folding, detoxification and responses to chemical stimuli (for BP) (Figure S3b). Based on their functions, we further classified the EV proteins into eight categories: OM proteins, proteases, toxins, phage-related proteins, virulence factors, tRNA ligases, as well as DNA-binding proteins (DBPs) and RNA-binding proteins (RBPs); ribosomal proteins and proteins not fitting in any apparent category were not included (Figure 1e, f).

In both subspecies, the OM class contained the largest number of EV proteins (36 in *Xff* Tem1-EVs and 24 in *Xfp* DD-EVs), including TonB-dependent receptors, porins and fimbrial proteins (Data S1). The detection of OM proteins in our vesicle samples aligns with the hypothesis that *Xf* releases a significant proportion of EVs as OMVs through budding from the OM (Avila-Calderón et al. 2021). A rank analysis of all EV proteins revealed that EF-Tu is one of the most highly abundant protein cargoes in EVs for both subspecies (Figure 1g, h), highlighting the immunomodulatory capacity of *Xf* EVs (Mitre et al. 2021). Moreover, proteases were prevalent in EV samples from both *Xff* Tem1 (20 proteins) and *Xfp*

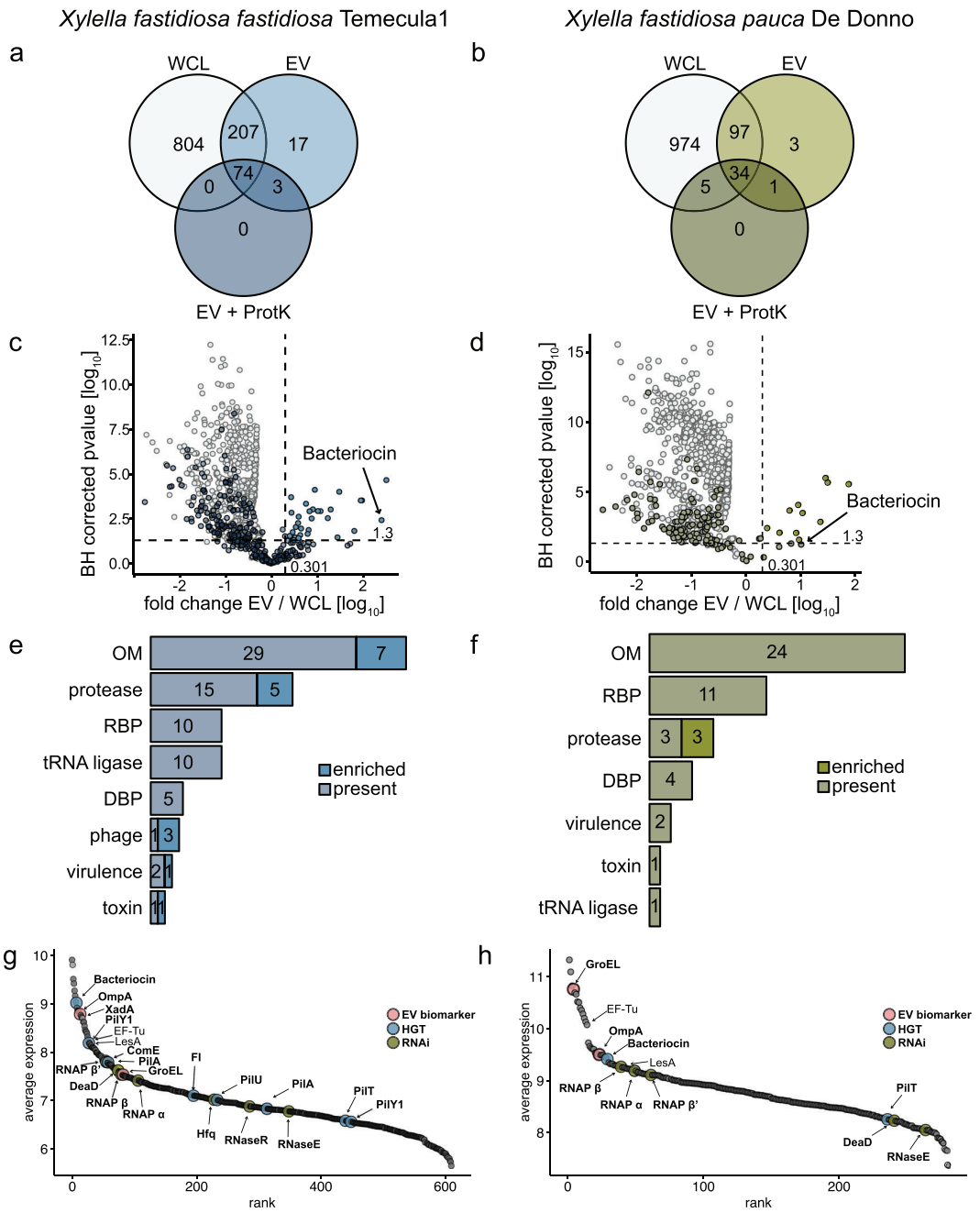

FIGURE 1 | Proteomic analysis identifies 301 and 140 proteins enriched in *Xff* Tem1- and *Xfp* DD-EVs, respectively. Comparison of proteins detected in whole-cell lysate (WCL), untreated EVs and EVs treated with Proteinase (Prot) K of *Xff* Tem1 (a, c, e, g) and *Xfp* DD (b, d, f, h). (a, b) Proteomic analysis on four biologically independent samples; proteins were considered when identified in $n \geqq 3$ replicates. (c, d) Volcano plots comparing WCL and EVs. EV proteins were categorized as enriched in EVs compared to WCL when fold change EV/WCL > 2 and BH corrected p value < 0.05 or present in EVs when identified in $n \geqq 3$ replicates; bacteriocin is highlighted as highly enriched EV protein. (e, f) EV proteins were manually categorized in DBP, RBP, tRNA ligases, virulence, phage, toxins, proteases and outer membrane (OM) proteins depending on their described function and number of identified proteins per category are displayed. (g, h) Rank plot analysis of highly abundant EV proteins; proteins potentially suitable as EV biomarker or proteins involved in horizontal gene transfer (HGT) or RNA interference (RNAi) are highlighted. EV, extracellular vesicle; *Xff*, *X. fastidiosa* subsp. *fastidiosa*; *Xff* Tem1, *Xff* strain Temecula1; *Xfp*, *X. fastidiosa* subsp. *pauca*; *Xfp* DD, *Xfp* strain De Donno.

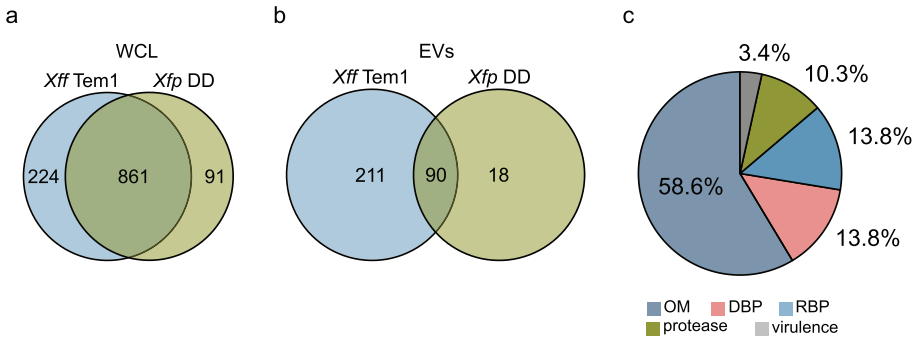

FIGURE 2 | *Xff* Tem1- and *Xfp* DD-EVs share many DNA- and RNA-binding proteins. (a) Overlap of *Xff* Tem1-EV and *Xfp* DD-WCL proteins. (b) Overlap of *Xff* Tem1-EV and *Xfp* DD-EV proteins. (c) Pie chart representing functional categories of the 90 shared proteins between *Xff* Tem1- and *Xfp* DD-EVs. EV, extracellular vesicle; WCL, whole-cell lysate; *Xff*, *X. fastidiosa* subsp. *fastidiosa*; *Xff* Tem1, *Xff* strain Temecula1; *Xfp*, *X. fastidiosa* subsp. *pauca*; *Xfp* DD, *Xfp* strain De Donno.

DD (six proteins), including the putative lipase/esterase LesA. Given that LesA is crucial for *Xff* Tem1 virulence in grapevine (Nascimento et al. 2016), this suggests that EVs isolated from cultured bacteria may contain proteins pertinent to *Xf* infection. This is further supported by the identification of three *Xff* Tem1- and two *Xfp* DD-annotated virulence proteins in the EV samples (Figure 1e, f, Data S1), including two AcvB-like proteins (Q87AC4, Q879Z9), VirK-like family proteins (Q87D31, UPI0003D31AC0) and a nucleoid structuring protein (H-NS histone family, virulence regulator; UPI00000C274D). Additionally, we identified 11 uncharacterized proteins in *Xff* Tem1-EVs (Data S1), which match parameters for computational prediction of candidate effectors such as a molecular mass of less than 30 kDa and the absence of transmembrane domains (Dalio et al. 2018).

3.2 | The Shared *Xf*-EV Proteome Includes Known EV Markers, DBPs and RBPs

Our next objective was to identify the EV proteome shared by both *Xf* subspecies. Utilizing the annotated reference proteome for *Xf* (*Xff* Tem1), we identified 861 proteins shared between the cellular sample of both subspecies (Figure 2b) and 90 proteins common to both *Xff* Tem1- and *Xfp* DD-EVs (Figure 2b, Data S1). More than half (58.6%) of the *Xf*-EV shared proteome consisted of proteins associated with the OM (Figure 2b). This includes the chaperonin GroEL (Q87BC0) as well as the OM proteins OmpW and OmpA (Q87AW4), a homologue of OM porin OprF in *Xf* (Table 1). GroEL was the third most abundant protein in *Xfp* DD-EV samples (Figure 1h). It is commonly found at EVs of various bacterial species and well-established as an EV biomarker (McCaig et al. 2013; Daleke-Schermerhorn et al. 2014; Yu et al. 2024). OmpW, abundantly present in OMVs and OprF, involved in OMV biogenesis, are recognized as biomarkers for OMVs from Gram-negative bacteria (Janda et al. 2023; Mathur et al. 2023; Ojima et al. 2018). The identification of shared EV proteins across *Xff* Tem1 and *Xfp* DD extends the known EV biomarkers for *Xf*, providing additional insights into conserved mechanisms of vesicle biogenesis.

Interestingly, while the cellular proteomes of *Xff* Tem1 and *Xff* DD exhibited a substantial overlap, their EV proteomes were distinctly different (Figure 2a, b). The cellular proteomes revealed an overlap of 861 proteins between the two subspecies, representing 79% of all cellular proteins in *Xff* Tem1 and 90% in *Xfp* DD (Figure 2a, b). Although 83% of the proteins found in *Xfp* DD-EVs (90/108) were also present in *Xff* Tem1-EVs, 70% of the proteins in *Xff* Tem1-EVs (211/301) were unique to this subspecies and absent in *Xfp* DD-EVs. Notably, we detected nearly three times more proteins in *Xff* Tem1-EVs compared to *Xfp* DD-EVs (301 vs. 108, Figure 2b). Given that the protein counts in the WCL samples were similar (1085 for *Xff* Tem1 and 952 for *Xfp* DD, Figure 2a), these findings suggest that each subspecies regulates protein sorting into EVs differently. Notably, we observed strain-specific differences, as *Xff* Tem1 released more EVs than *Xfp* DD when grown at similar ODs under the same culture conditions (Figure S2a), suggesting that *Xff* Tem1 has a more active vesiculation process.

The shared *Xf*-EV proteome was enriched for nonribosomal RBPs and DBPs, each comprising 13.8% of the proteome (Figure 2c, Figure 1e, f). Many of these proteins were sensitive to ProtK treatment (Data S1), indicating their likely presence at the vesicle corona. Among the identified RBPs is EF-Tu, which has been previously identified in crude vesicle samples and is known to contribute to vesicle immunogenicity (Feitosa-Junior et al. 2019; Mitre et al. 2021, Nascimento et al. 2016). We also found the RNA helicase DeaD and ribonuclease E, known to play roles in RNA metabolism, at EVs from both subspecies (Data S1) (Hussain 2024; Mackie 2013). By contrast, the RNA chaperone Hfq and Ribonuclease G were only detected in *Xff* Tem1-EVs. Additionally, *Xff* Tem1-EVs contain 11 tRNA ligases (Arg, Asp, Asn, Cys, His, Ile, Leu, Met, Phe, Thr and Val) (Data S1, Figure 1e), with one (Val) also present in *Xfp* DD-EVs (Data S1, Figure 1f). Most of these EV-associated tRNA ligases were sensitive to ProtK treatment, indicating their likely exposure on the vesicle corona.

We identified DBPs in EV samples from both subspecies (Data S1, Figure 1e–g), including DNA-directed RNA polymerase subunits (Table 2, Figure 1g, h). The DNA transport competence protein ComE (Q87BA0) was detected in *Xff* Tem1-EVs but not in *Xfp* DD-EVs (UPI0000007D60). ComE is located in the periplasm and plays a crucial role in facilitating the uptake of external DNA during natural transformation competence, a process well-documented in Gram-negative bacteria (Seitz and Blokesch 2013; Johnston et al. 2014). Since natural transformation competence has been described in *Xff* but not in *Xfp* (Kung and Almeida 2011; Kung et al. 2013; D'Attoma et al. 2020), we further explored

TABLE 1 | Shared EV proteins of *Xff* Tem1 and *Xfp* DD of category 'outer membrane' and known bacteria EV biomarkers found in EVs of both subspecies.

Uniprot	Gene	Locus tag	Description	Rank position in *Xff* Tem1 and *Xfp* DD
Q87AW4	ompA	PD_1924	Outer membrane porin	14/23
Q87BC0	groEL/ groL/ mopA	PD_1538	Chaperonin GroEL	81/4
Q879×4	cirA	PD_2065	TonB-dependent receptor	15/15
Q87AR6	bamD	PD_1756	Outer membrane proteiein assembly factor BamD	39/255
Q87C13		PD_1283	TonB-dependent receptor	7/12
Q87CZ4	pal	PD_0895	Peptidoglycan-associated protein	37/189
Q87CZ5	tolB	PD_0894	Tol-Pal system protein TolB	32/84
Q87EI1	oma	PD_0326	Outer membrane protein assembly factor BamA	24/140
Q87EI9		PD_0318	TonB-dependent receptor-like beta-barrel domain-containing protein	17/69
Q87EN9	oprO	PD_0264	Porin O	27/13
Q87AL6	ompW	PD_1807	Outer membrane protein	1/2
Q87DC8	pcp	PD_0757	Peptidoglycan-associated outer membrane lipoprotein	6/21

TABLE 2 | EV proteins of *Xff* Tem1 with reported roles in HGT.

Uniprot	Gene	Locus tag	Description	Role in HGT	Reference
Transformation pilus/competence proteins					
Q87AA4	pilA	PD_1924	Fimbrial protein	Major pilin subunit of (pseudo-) pilus structures	(Mackie 2013)
Q87AX2	pilQ	PD_1691	Fimbrial assembly protein	DNA transport across outer membrane	(Shenkutie et al. 2023)
Q87CD3, Q87CD4	pilU/T	PD_1148/ PD_1147	Twitching motility protein	Pilus retraction proteins (ATPases), DNA pulling, indispensable for competence	(Moriano-Gutierrez et al. 2020)
Q87BA0	comE	PD_1558	DNA transport competence protein	DNA import	(Johnston et al. 2014)
Q87E25, Q87FA5	pilY1	PD_0502/PD_0023	Type IV pilus biogenesis factor PilY1 homologue	Pilus assembly, twitching mobility, adhesion to host cell, antiretraction factor, tip of T4P, 'binds' to DNA (?)	(Touzdjian Pinheiro Kohlrausch Távora et al. 2022)
Toxin					
Q87BM1	frpC	PD_1427	Bacteriocin, toxin	Increases available DNA-pool	(Wholey et al. 2016; Kjos et al. 2016)
Other					
Q87CH6	FI	PD_1094	Phage-related contractile tail sheath protein	DNA packaging protein, structural component of bacteriophage tail (sheath)	

Xff Tem1-EV proteins potentially involved in HGT. These include key components of the Type-IV pilus (transformation pilus) consisting of PilA (Q87AA4), PilQ (Q87AX2), PilU/T (Q87CD3/Q87CD4) and PilY1 (Q87E25/Q87FA5). We also identified a phage protein with DNA-binding function (Q877CH6) (Table 2). Components of the transformation pilus were not identified in *Xfp* DD-EVs (Data S1, Figure 1e–g).

Pilus structures, composed primarily of the major pilin subunit PilA, bind extracellular double-stranded (ds)DNA and internalize it through the secretion pore PilQ, driven by pilus retraction. This process is powered by retraction ATPase such as PilU and PilT (Q87CD3, Q87CD4), which were also found in *Xff* Tem1-EVs. Together, these proteins and ComE are essential for natural transformation competence in bacteria (Seitz and Blokesch 2013; Johnston et al. 2014). Thus, we speculate that EVs may play a role in facilitating HGT in *Xff* Tem1, as documented in other bacteria (Tran and Boedicker 2017; Marinacci et al. 2023; Dell'Annunziata et al. 2021).

Interestingly, bacteriocin was one of the most abundant proteins in EVs of both strains of *Xf*-EVs, with its levels significantly enriched compared to WCL samples (Figure 1c, d, g, h). Bacteriocin has antimicrobial properties, inhibiting the growth of bacterial strains or species (Sugrue et al. 2024). In *Streptococcus pneumoniae*, bacteriocin expression has been linked to genetic adaptation through the predation of neighbouring cells (Wholey et al. 2016). By eliminating or inhibiting competitors, bacteriocin may help *Xf* to establish its niche dominance (Lacava et al. 2004; Deyett et al. 2017; Giampetruzzi et al. 2020; Vergine et al. 2020; Zicca et al. 2020; Anguita-Maeso et al. 2022).

3.3 | *Xff* Tem1-EVs Are Enriched in Genomic Islands (GIs)

Due to the higher vesicle production activity of *Xff* Tem1 and the abundance of DBPs with roles in HGT identified in its EVs (Table 2), we focussed our subsequent experiments on this strain to investigate the presence of DNA cargo. DNA-seq of cellular DNA from *Xff* Tem1 revealed uniform coverage across the entire genome (Figure S4a). By contrast, DNA sequences from purified *Xff* Tem1-EVs showed enrichment in three specific genomic regions (Figure S4b). Using 100 nt bins and averaging coverage across four replicates, we identified three regions with significantly higher coverage (Figure 3a, b, Figure S4b): Region 1 (454,900–468,200; coverage of 855), Region 2 (1,287,800–1,331,700; coverage of 4701) and Region 3 (2,009,200–2,017,100; coverage of 820). These regions exhibited a higher GC content compared to the genome average (57%, 57% and 58% vs 52%, respectively). The sequences within these regions predominantly encoded phage-related genes and genes coding for proteins with unknown functions (Figure 3c, Figure S5c, d). Regions 1 and 2 also included genes for the Type-II toxin-antitoxin system, DNA polymerase (*DnaP*), a DEAD/DEAH box helicase, a tyrosine-type recombinase/integrase and various toxins (Figure 3c, Figure S5c, d, Data S2).

Given that Region 2 showed the highest read coverage, we focussed on this region for further analysis. PCR-based amplification confirmed the presence of genes from Region 2 in *Xff* Tem1-EVs (Figure 3d). These genes were resistant to treatments with ProtK alone and cotreatment with MNase, suggesting that they are not associated to the ProtK-sensitive EV corona. Additional cotreatment with 1% TritonX-100 did not remove these PCR signals (Figure 3d). To support this observation, we burst EVs with hypotonic buffer treatment. Notably, cotreatments with ProtK and MNase also did not eliminate the PCR signals (Figure 3d), indicating that the DNA cargo is not freely dispersed within the vesicle lumen. TEM confirmed that treatment with 1% Triton X-100 or hypotonic buffer led to the breakdown of EV structures, with hypotonic buffer treatments revealing longish membrane fragments (Figure S6a). It is possible that the GI-encoded genes are not freely enclosed within the EV lumen but could be directly associated with EV membranes and thereby be protected from MNase digestion.

The high GC content, presence of phage-related genes, genes encoding tyrosine-type recombinases/integrases and the insertion near the 3′-ends of tRNA-encoding genes suggest that these regions represent GIs (Juhas et al. 2009). Region 2 begins approximately 600 nt downstream of the tRNA-Arg gene (PD_RS05700) (Figure S7). The presence of GIs in all three regions was confirmed using Atollgen for GI classification (Audrey et al. 2023): Regions 1 and 2 were classified as integrated elements (IEs), containing mobility genes such as 'Integrase Tyrosine' with PFAM entries PF13495, PF13102 and PF00589 for phage integrases. Region 2 also includes a Type-IV mobility gene (*VirB8*) and an endoribonuclease *L-PSP* (PF01042). Region 3 is an 'uncharacterized GI' and includes a Type-III restriction enzyme (PF04851) and the CRISPR-associated protein Cse1 (PF09481), suggesting the potential for transferring bacterial immunity islands via this region (Data S2). Of note, all three regions contain genes encoding for VRR-NUC domain-containing proteins (Figure 3c, Figure S5). Although little is known regarding the function of this domain in bacteria yet, previous studies proposed an antibacterial effect by inducing double-strand breaks of genes encoding VRR-NUC domain-containing proteins, which could help to enlarge the available gene pool for HGT (Hespanhol et al. 2022).

3.4 | Genome Annotation Reveals Nine Novel sRNAs Including Island-Encoding *sXFs*

Since RBPs were present at *Xf*-EVs (Table 3), we shifted our focus to explore potential RNA-like effectors, focussing on sRNAs (Wang et al. 2015). First, we inspected the quality reference genome of *Xff* Tem1 (ASM724v1; GCF_000007245.1-RS_2024_05_05) for the annotation of ncRNAs. Previously, four sRNAs have been annotated: the signal recognition particle sRNA small type-*ffs* (PD_RS11435), *RNase P* (*RnP*, PD_RS11320), 6S/*SsrS* (PD_RS11670) and the transfer-messenger (tm)RNA *SsrA* (PD_RS12290) (Table 4). We next reannotated the *Xff* Tem1 genome using Bakta (Schwengers et al. 2021), which includes Infernal versus Rfam ncRNA covariance models, which revealed nine novel sRNAs (Table 4). These sRNAs are homologous to *sX13*, *asX1* and sRNA-*Xcc1*, which have been linked to virulence in *Xanthomonas campestris* pv. campestris (*Xcc*) and *Xcv* (Schmidtke et al. 2012; Chen et al. 2011). We identified seven homologues of sRNA-*Xcc1* in the *Xf* Tem1 genome, of which five are encoded by loci that are in close proximity in the genome (1,313,466–1,315,082), clustered within the EV-associated

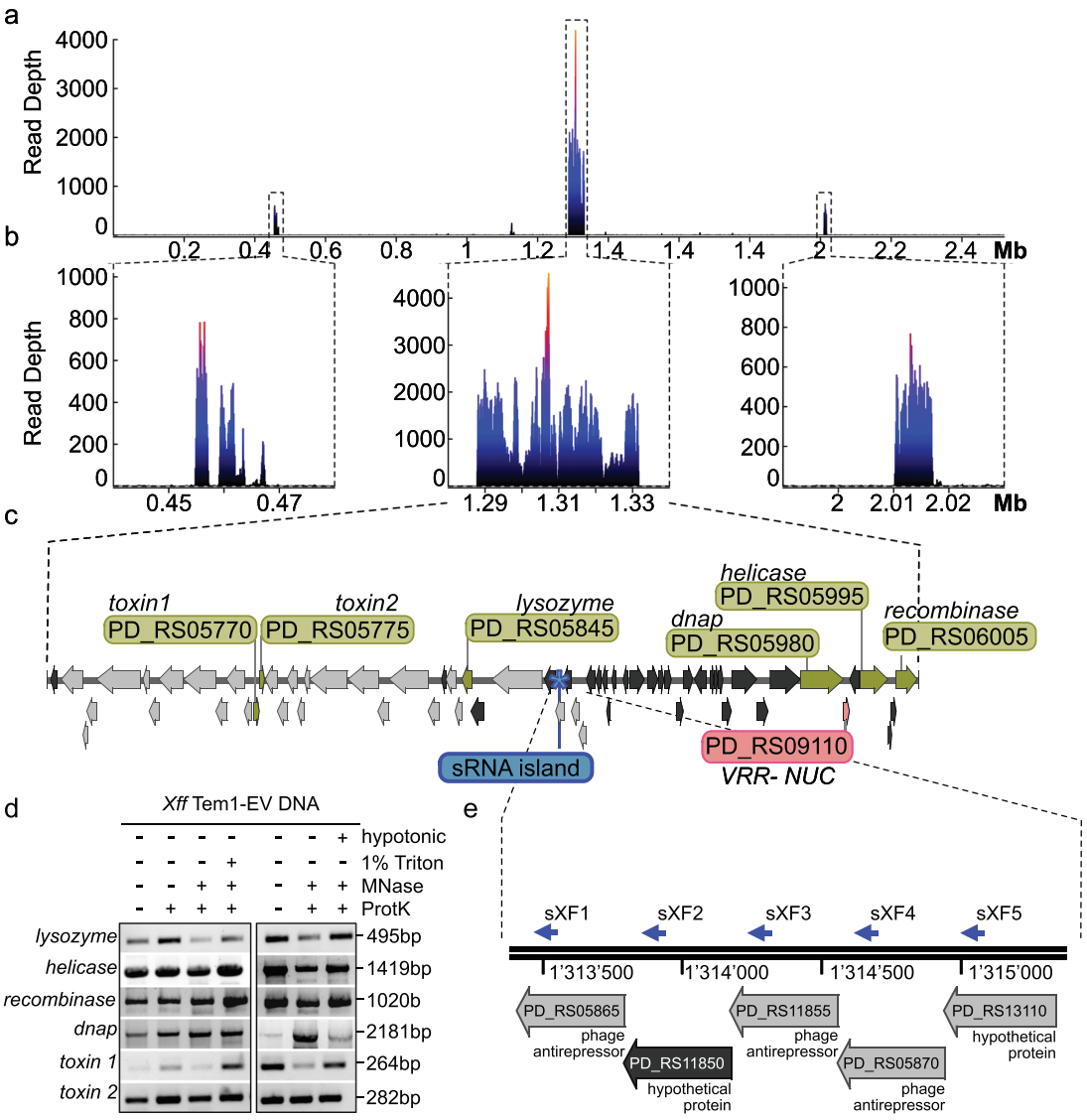

FIGURE 3 | DNA sequencing identifies three genomic islands enriched in *Xff* Tem1-EVs, including island-coding *sXF*s. (a, b) Mapping of sequencing reads to the reference chromosome sequence of *Xff* Tem1. Coverage plots show enrichment for three genomic regions: Region 1 from 454,900 to 468,200 bp with a length of 13.3 kb, Region 2 stretches from 1,287,800 to 1,331,700 bp (43.9 kb) and Region 3 from 2,009,200 to 2,017,100 bp (7.9 kb). (c) Region 2 contains many proteins of unknown function (dark grey) and phage proteins (light grey). It also contains genes encoding for two toxins (*toxin1* PD_RS05770; *toxin2* PD_RS05775), *lysozyme* (PD_RS05845), *DNA polymerase* (*DNAP*, PD_RS05980), *VRR-NUC domain-containing protein* (*VRR-NUC*, PD_RS09110), *DEAD/DEAH box helicase* (PD_RS05995) and *recombinase/integrase* (PD_RS06005). Visualization was done using SnapGene software (www.snapgene.com). (d) Genes encoding *toxin1, toxin2, lysozyme*, *helicase*, *recombinase* and *dnap* can be amplified from *Xff* Tem1-EVs untreated or treated with Proteinase K (ProtK) alone or in cotreatments with MNase, in EVs disrupted by 1% Triton-X-100 treatment or burst in hypotonic buffer. Similar results were observed in at least two independent experiments. (e) Region 2 also contains a sRNA-island of five homologous *sXF*s. EV, extracellular vesicle; *Xff*, *X. fastidiosa* subsp. *fastidiosa*; *Xff* Tem1, *Xff* strain Temecula1.

GI Region 2 (Figure 3e, Figure S7). These five homologues were designated as island-encoded *sXF1* to *sXF5* (Table 4).

3.5 | *Xff* Tem1-EVs Contain 826 Transcripts, Including *sXFs*

Prompted by the observation that purified *Xff* Tem1-EVs, labelled with the lipid dye FM4-64, stained positive for RNA (Figure S8), we further analysed their RNA content by RNA-seq. We defined EV-associated transcripts as those present in at least two out of three biological replicates, with an average of at least 10 transcripts per million (TPM). Using this criterion, we identified 826 transcripts in *Xff* Tem1-EVs and 2071 transcripts in WCL, indicating that approximately 40% of all cellular transcripts are also present in EVs (Data S3). Of the EV transcripts, about half (54%) correspond to coding sequences (CDS), compared to 63.7% in WCL samples (Figure 4a). Notably, there was a higher

TABLE 3 | EV proteins of *Xff* Tem1 with potential roles in RNAi.

Uniprot	Gene	Locus tag	Description	Role in RNAi	Reference
RNA binding					
Q87F71	hfq	PD_0066	Hfq	RNA chaperone, sRNA stability, facilitates base pairing sRNA–mRNA	(Santiago-Frangos and Woodson 2018)
Q87A48/ Q87D66	rne/vacB	PD_1983/PD_0820	Ribonuclease E/R	RNA processing/decay	(Mackie 2013)
Q87EU3	deaD	PD_0205	ATP-dependent RNA helicase DeaD	Unwinding of dsRNA, facilitate protein placement, posttranscriptional regulation	(Iost et al. 2013)
Transcription					
P66713, Q87A32, Q87A33	rpoA/B/C	PD_0461/PD_2001/ PD_2000	DNA-directed RNA polymerase (RNAP) subunits α, β, β'	Transcription of sRNAs/regulation of transcription via sRNAs?	(Wassarman and Storz 2000; Sukhodolets and Garges 2003)

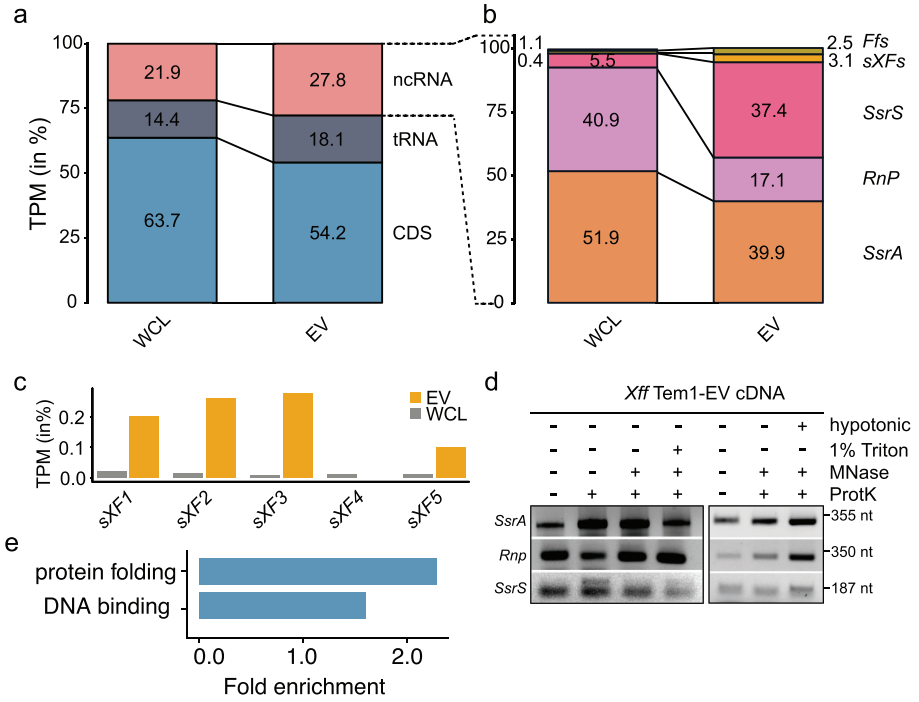

FIGURE 4 | RNA sequencing revealed 826 transcripts in *Xff* Tem1-EVs including island-encoded *sXFs*. (a) Proportions of coding-sequence (CDS), transfer (t)RNA and noncoding (nc) RNA in WCL and *Xff* Tem1-EV samples. (b) Types of ncRNAs found in WCL and *Xff* Tem1-EVs are *SsrA* encoding transfer-messenger (tm)RNA, RNaseP (*RnP*), *SsrS* (or 6S), island-encoded *sXFs* and signal-recognition particle (*SrP*, or *ffs*); fractions of ncRNA < 0.1% are not shown (only in WCL: *asX1* – 0.015%; TPP riboswitch – 0.027%; *sX13* – 0.040%. (c) Comparison of TPM of *sXFs* in *Xff* Tem1-WCL and EVs. (d) Amplification of ncRNAs *SsrA, SsrS* and *Rnp* from cDNA of *Xff* Tem1-EVs untreated or treated with ProtK alone or cotreated with ProtK and MNase, in EVs disrupted by 1% Triton-X-100 treatment or burst in hypotonic buffer. (e) Enriched GO-terms with adjusted *p* values < 0.05 of *Xff* Tem1-EV CDS transcripts contain protein folding (GO: 0006457) and DNA binding (GO:0003677). EV, extracellular vesicle; GO, gene ontology; ProtK, Proteinase K; TPM, transcripts per million; WCL, whole-cell lysate; *Xff*, *X. fastidiosa* subsp. *fastidiosa*; *Xff* Tem1, *Xff* strain Temecula1.

TABLE 4 | NcRNAs identified in *Xff* Tem1 (ASM724v1) and *Xfp* DeDonno (ASM211787v1) after annotation with Bakta.

Location	Strand	ncRNA	RFAM	RNA-seq
***Xylella fastidiosa* subsp. *fastidosa* Temecula1**				
397,674–397,770	+	Bacterial small signal recognition particle RNA (*SrP*)	RF00169	EV and cell
428,981–429,330	+	Bacterial RNase P class A (*RnP*)	RF00010	EV and cell
483,185–483,185	+	Xanthomonadaceae sRNA *sX13*	RF02232	Cellular only
956,107–956,224	+	Xanthomonadaceae sRNA *asX1*	RF02235	Cellular only
989,110–989,296	—	6S/*SsrS* RNA	RF00013	EV and cell
1,205,173–1,205,258	—	sRNA-*Xcc*1_1	RF02221	Cellular only
1,215,344–1,215,430	+	sRNA-*Xcc*1_2	RF02221	Cellular only
1,313,466–1,313,553	—	sRNA-*Xcc*1_3 (*sXF1*)	RF02221	EV and cell
1,313,852–1,313,937	—	sRNA-*Xcc*1_4 (*sXF2*)	RF02221	EV and cell
1,314,233–1,314,319	—	sRNA-*Xcc*1_5 (*sXF3*)	RF02221	EV and cell
1,314,614–1,314,702	—	sRNA-*Xcc*1_6 (*sXF4*)	RF02221	Cellular only
1,314,998–1,315,082	—	sRNA-*Xcc*1_7 (*sXF5*)	RF02221	EV and cell
2,447,459–2,447,813	+	Transfer-messenger RNA, *SsrA*	00013	EV and cell
Xylella fastidiosa subsp. *pauca* De Donno				
928,764–928,848	—	sRNA-*Xcc*1_1	RF02221	nd
949,862–949,978	+	Xanthomonadaceae sRNA *asX1*	RF02235	
998,907–999,092	—	6S / SsrS RNA	RF00013	
1,207,250–1,207,339	—	sRNA-*Xcc*1_2	RF02221	
1,323,982-1,324,064	—	C4 antisense RNA	RF01695	
1,324,110–1,324,191	—	*isrK* Hfq binding RNA	RF01394	
1,324,292–1,324,381	—	sRNA-*Xcc*1_3	RF02221	
1,334,999–1,335,093	+	C4 antisense RNA	RF01695	
1,878,802–1,878,919	—	Xanthomonadaceae sRNA *sX13*	RF02232	
1,918,731–1,919,080	—	Bacterial RNase P class A (*RnP*)	RF00010	
1,950,062–1,950,158	—	Bacterial small signal recognition particle RNA (*SrP*)	RF00169	
2,436,857–2,437,211	+	Transfer-messenger RNA, *SsrA*	00013	

Note: Highlighted in grey are ncRNAs that were previously annotated (GCF_000007245.1-RS_2024_05_05 and GCA_002117875.1- -RS_2024_05_05). Highlighted in blue are ncRNAs found in the EV-packaged GI identified in this paper. RFAM number refers to Database references (rfam.org) and RNA-seq results indicate if respective ncRNA was identified in cellular samples only or found in *Xff* Tem1-EVs.

proportion of tRNAs and ncRNAs in EVs compared to WCL, suggesting selective RNA loading into EVs. This specificity was further supported by the distinct distribution of ncRNA types between EVs and WCL. Although most ncRNAs in WCL samples are *SsrA* and *RnP* (51.9% and 40.9%, respectively), EVs showed a significantly larger proportion of *SsrS* (37.4%), island-encoded *sXFs* (3.1% compared to 0.4% in cells) and *Ffs* (2.5% compared to 1.1% in cells) (Figure 4b, c).

We confirmed the presence of most abundant ncRNAs at EVs by RT-PCR, which remained protected from degradation following treatment with ProtK alone or in combination with MNase (Figure 4d). This indicated that *SsrA*, *Rnp* and *SsrS* are not associated to the ProtK-sensitive EV corona. Combined ProtK, MNase and 1% Triton X-100 treatment did not eliminate the *SsrA*, *Rnp* and *SsrS* RT-PCR signals. Given that 1% Triton X-100 disrupts EV structures and ensuring enzyme activity in these conditions (Figure S6), this suggests that these ncRNAs are not freely enclosed within the EV lumen. Additionally, we burst EVs using hypotonic buffer followed by cotreatments with ProtK and MNase, but the *SsrA*, *Rnp* and *SsrS* RT-PCR signals persisted (Figure 4d). It is possible that the disruption of EVs by 1% Triton X-100 or hypotonic conditions generates membrane fragments to which ncRNAs may associate, either directly or indirectly via RBPs like Hfq, which can integrate into membranes (Turbant et al. 2024; Turbant et al. 2023; Mańka et al. 2025). This association could protect the ncRNAs from MNase degradation. Supporting this hypothesis, we consistently observed across independent experiments that the strongest RT-PCR signal occurred in hypotonic buffer-burst EVs cotreated with ProtK and MNase (Figure 4d).

To understand the potential functional roles of these vesicular transcripts, we performed GO-term enrichment analysis on all *Xff* Tem1-EV-associated CDS with an average of at least 100 TPM in EVs. This revealed that EV transcripts are enriched for processes such as DNA binding (GO:0003677) and protein folding (GO:0006457) (Figure 4e; Data S3). Notable DNA-binding transcripts include the phage recombination proteins *Bet* (Q87CQ1) and *FtsK* (Q87DL2), as well as the recombinase *XerD* (Q87DN0). *Xff* Tem1-EVs also contain transcripts encoding ComE, bacteriocin, four DBPs (H-NS and HU) and seven DNA-binding response regulators/transcriptional regulators as well as the transcription termination factor *Rho* and translation initiation factors *IF-1/-2/-3* and two transposases (Data S3). This suggests that EVs may influence DNA structures/chromosome organization and transcription to regulate HGT and stress response mechanisms in *Xf*.

3.6 | *sXFs* Have 212 Predicted *X. fastidiosa* Targets and Signatures for Hfq Binding

We then focussed on island-encoded *sXFs* because EVs showed a significantly larger proportion of these ncRNAs compared with cellular ncRNAs (Figure 4c) and exhibited homology to sRNA-*Xcc1*. In *Xcc*, sRNA-*Xcc1* is positively regulated by the virulence factors HrpG and HrpX (Chen et al. 2011), which indicates its potential role in bacterial virulence. This involvement might be through (i) regulating the bacterium's gene expression (Wu et al. 2021) or (ii) suppressing host defence mechanisms, as demonstrated in *X*anthomonas *oryzae* pv. *oryzicola* (*Xoc*) (Wu et al. 2024). To investigate this in *Xff* Tem1, we aimed to predict potential mRNA targets of the *sXFs*. We focussed on target predictions within *Xff* as well as in the host plant *V. vinifera* and the genetic model *A. thaliana*, both of which can be colonized by *Xff* (Mitre et al. 2021; Rogers 2012; Pereira et al. 2019).

Using IntaRNA (Mann et al. 2017) to predict RNA–RNA interactions between *sXFs*, which are around 90 nt in size (Figure 5a), and *Xff* Tem1 transcripts, we identified 212 potential mRNA targets of *sXFs* in *Xf* (Data S4). IntaRNA takes into account binding energies but also the accessibility of interacting subsequences (Mann et al. 2017). When analysing start and end points of interactions between *sXFs* with their targets, we observed four distinct patterns (Figure 5b): Category 1 includes interactions starting between 9 and 30 nt and ending after 55 nt; Category 2 is interactions starting between 46 and 60 nt and ending before 77 nt; full-length interactions are lengths greater than 74 nt; and end-binding starts after 50 nt and ends after 77 nt. We detected a peak in interactions between positions 10 and 20 nt (Category 1) and a second peak around position 50 nt (Category 2) (Figure 5c). For both categories, interactions commonly ended around 60–70 nt of *sXFs* (Figure 5c).

The consensus structure of all *sXFs* revealed three stem-loop domains (Figure 5d). Given that most interactions occurred between positions 10/50 and 70 nt of *sXFs*, we hypothesized that the first stem-loop does not directly interact with mRNA targets but may bind RBPs present at the EV corona (Figure 1g). Interestingly, the Hfq binding motif (ARN; Link et al. 2009) is present three times in this stem-loop (Figure 5a, d). Hfq was shown to interact with single-stranded RNAs but also binds to folded sRNAs and RNA folds of tRNAs (Link et al. 2009; Vogel and Luisi 2011; Antal et al. 2005). Therefore, we speculate that the ARN-motif-containing stem-loop might be involved in interactions with RBPs such as Hfq. Interactions with mRNAs in Category 1 might involve the remaining stem-loops, while Category 2 interactions likely involve only the third stem-loop (Figure 5d). An example for Category 1 is the high-confidence interaction of *sXF3* with the mRNA encoding bacteriocin (Figure 5e, p value < 0.001). The interaction of *sXF2* with the *comE* mRNA is an example for Category 2 (Figure 5f, g, p value < 0.01). *comE* is one of the 16 high-confidence *sXF* targets we identified as transcripts in EVs, following our analysis of the overlap between *sXF* targets and EV-associated CDS (Figure 5g; Data S4). The presence of both *sXF2* and Hfq in EVs suggests that *comE* transcript levels could be regulated through Hfq-mediated sRNA-mRNA pairing, highlighting a potential posttranscriptional control mechanism within *Xff* Tem1-EVs.

3.7 | *sXFs* Are Predicted to Target 366 and 632 Genes in Two Different Plant Hosts of *X. fastidiosa*

To mimic plant miRNA structures, we generated 24 nt-long fragments of all five homologous *sXFs* using a sliding-window approach. For target prediction in plants, we utilized 'seed'-sensitive psRNATarget (Dai et al. 2018), as previously described (Ren et al. 2019). This analysis initially predicted 2'858 targets in *A. thaliana* and 5'421 targets in *V. vinifera* (Data S4). GO-term enrichment analysis of the predicted targets revealed: (i) In *A. thaliana*, enriched MF-terms included responses to external stimuli and stress; and (ii) in *V. vinifera*, enriched MF-terms included trehalose metabolism in response to stress, mRNA *cis*-splicing and vesicle budding from membranes (Figure 6a, b).

Applying the same quality cutoff as in previous studies (Ren et al. 2019), we identified 366 high-confidence targets in *A. thaliana* and 632 in *V. vinifera* (Data S4). Notable high-confidence targets include: (i) In *A. thaliana*, four disease resistance proteins of the nucleotide-binding site (NBS) leucine-rich repeat (LRR) receptor (NLR) class (AT1G63350, AT5G11250, AT5G36930 and AT5G18370); and (ii) in *V. vinifera*, a putative LRR receptor kinase (Vitvi04g01426_t001) and the stress response factor *NAC Secondary Wall Thickening Promoting Factor 1* (*NST1*, Vitvi05g01129_t001), which is a putative target of an *sXF3* fragment (Table 5). NST1 has been associated with lignin biosynthesis and is regulated by xylem-specific transcription factors in *Arabidopsis* (Zhang et al. 2020; Liu et al. 2021). Increased lignification in the vasculature is a known response mechanism of host plants to *Xf* infections (Sabella et al. 2018). Several other transcription factors are potential targets of *sXFs*, indicating that these fragments may interfere with the regulation of immune responses (Data S4). Interestingly, the transcript of the lipid raft-associated protein Remorin (Vitvi15g01160_t001) is a putative target of an *sXF1* fragment (Table 5). The association of bacterial EVs with plant membranes involves Remorins, as shown for *Xcc*-EVs in *A. thaliana* (Tran et al. 2022).

Among the four predicted *sXF*-targeted *NLRs*, three were downregulated in response to infection with *Xff* Tem1 in *A.*

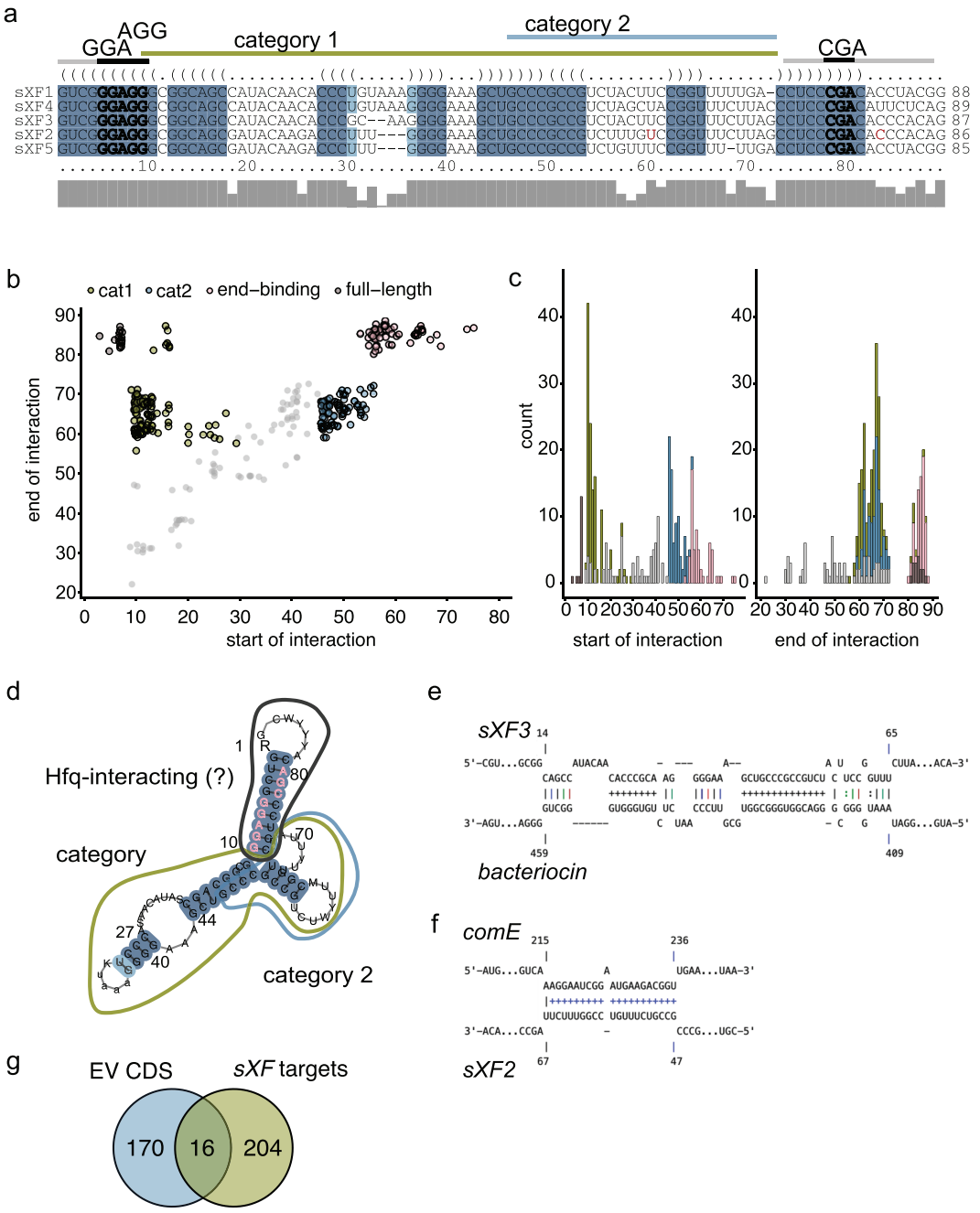

FIGURE 5 | *Xff* Tem1 encodes five sRNA homologues *sXFs*. (a) Five homologues of sRNA-*Xcc1* show high sequence conservation. (b) Predicted targets of *sXFs* are categorized as full-length binding (dark grey), end-binding (pink) or in two categories depending on their start and end of interaction with the target mRNA (Category 1 green, Category 2 blue). Unclassified interactions are depicted in light grey. (c) Most Category 1-interactions start at position 10 nt of sRNA and most Category 2-interactions around position 50 nt of the sRNA. (d) Secondary structure prediction of *sXFs*. (e) Interaction of *sXF3* and *bacteriocin* starting at position 14 nt of *sXF3* and ending at position 56 nt. (f) Interaction of *sXF2* and *ComE* starting at position 47 nt of *sXF3* and ending at position 67 nt. (g) Overlap of CDS in *Xff* Tem1-EVs and predicted *Xff* Tem1 targets of *sXF*s. EV, extracellular vesicle; *Xff*, *X. fastidiosa* subsp. *fastidiosa*; *Xff* Tem1, *Xff* strain Temecula1.

thaliana seedlings (Figure 6c). Downregulation of the coiled-coil-domain *NLR* (*CNL*) AT1G63350 was observed in seedlings following exogenous application of *Xff* Tem1-EVs, whereas the other three tested TIR-domain *NLRs* (*TNLs*) showed no such response (Figure 6d). Notably, the target site of the *CNL* AT1G63350 is located near the P-loop domain of the protein, unlike the three *TNLs* (Table 5, Figure 6e). The P-loop is a conserved sequence targeted by endogenous plant miRNAs from the miRNA482/2118 superfamily to regulate *NLR* expression (Zhang et al. 2022). These findings provide first insights that *Xf*-EVs could be involved in the interference with immune gene expression.

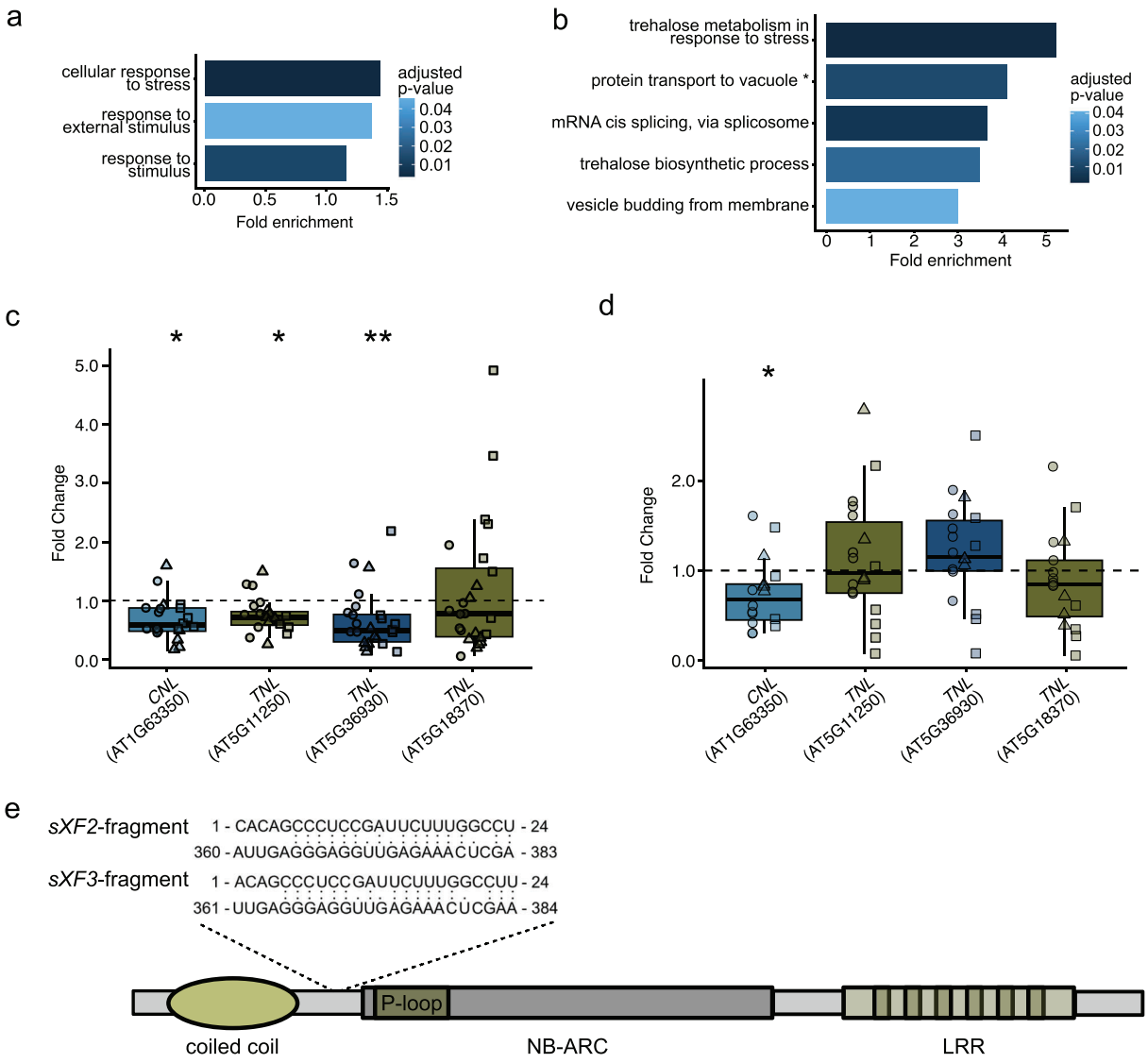

FIGURE 6 | Predicted *sXF*s targets are downregulated during infection and EV treatment. A GO-term analysis of predicted *in-planta* targets of *sXF*s are enriched in stress responses in (a) *Arabidopsis thaliana* and (b) the host *Vitis vinifera*. RT-qPCR results of the predicted target *NLRs* in *A. thaliana* seedlings 3 days postinfection with *Xff* Tem1 (c) and in response to infiltration with *Xff* Tem1-EVs after 4 h (d) Predicted target site of the *sXF2*/*sXF3* fragment in the *CNL* AT1G63350. *Full-term: protein transport to vacuole involved in ubiquitin-dependent protein catabolic process via the multivesicular body sorting pathway. EV, extracellular vesicle; GO, gene ontology; *Xff*, *X. fastidiosa* subsp. *fastidiosa*; *Xff* Tem1, *Xff* strain Temecula1.

4 | Discussion

4.1 | sRNA Delivery

The success of *Xf* infection has been linked to its ability to produce EVs, which facilitate detachment from surfaces and likely contribute to the delivery of cell wall-degrading enzymes, promoting systemic infection (Ionescu et al. 2014; Nascimento et al. 2016). Consistent with these roles and previous studies (Feitosa-Junior et al. 2019; Nascimento et al. 2016), we identified adhesins and the cell wall–degrading enzyme LesA in *Xf*-EVs (Figure 1g, h). Yet, EVs serve a broader function, as several bacterial pathogens use them to modulate plant immunity in a contact-independent manner. For example, EVs from the plant pathogens *P. syringae* pv. tomato (*Pto*) DC3000 and *Xcc* carry proteins related to plant immune activation as well as bacterial virulence and stress tolerance adaptation to the plant environment (Janda et al. 2023; Tran et al. 2022; McMillan et al. 2021; Bahar et al. 2016; Chalupowicz et al. 2023). Human bacterial pathogens also use EVs to secrete effectors, as seen in *Salmonella enterica* serovar Typhimurium, whose EVs contain virulence effectors that are encoded in a pathogenicity island (Kim et al. 2018).

EVs from *Xf* have been reported to carry the immune-activating protein EF-Tu (Mitre et al. 2021), yet it remained unknown whether they also contain effector-like molecules. While we identified eleven uncharacterized proteins in *Xff* Tem1-EVs that meet the criteria for bacterial effector candidates (Data S1; Dalio et al. 2018), this study focussed on the nucleic acid cargo of EVs,

TABLE 5 | Predicted plant targets of *sXF* fragments using psRNA-target.

Host	Target plant mRNA	sXF fragment	*E* value	Targeted subdomain	Interaction
A. thaliana	*CNL* (AT1G63350)	*sXF2*	3.0	Upstream of P-loop	1 - CACAGCCCUCCGAUUCUUUGGCCU - 24 360 - AUUGAGGGAGGUUGAGAAACUCGA - 383
		sXF3	3.0		1 - ACAGCCCUCCGAUUCUUUGGCCUU - 24 361 - UUGAGGGAGGUUGAGAAACUCGAA - 384
	TNL (AT5G11250)	*sXF2*	2.5	Intron	1 - CGAUUCUUUGGCCUGUUUCUGCCG - 24 73 - AUGCGGAAAUCGGACAAAGAGGGU - 96
	TNL (AT5G36930)	*sXF1*	2.5	TIR-domain	1 - CACAGCCCUCCAGUUUUUGGCCUU - 24 1171 - UGGGUGGGACAUCAAAAAUCGGAA - 1194
		sXF5	2.5		1 - CACAGCCCUCCAGUUUUUGGCCUU - 24 1171 - UGGGUGGGACAUCAAAAAUCGGAA - 1194
	TNL (AT5G18370)	*sXF2*	3.0	Downstream of LRR 9	1 - UUUCCCAGAACAUAGCGACGGCGG - 24 3052 - CCAUAAGCUUGUAUCGCUGCCGCA - 3075
		sXF5	3.0		1 - UUUCCCAGAACAUAGCGACGGCGG - 24 3052 - CCAUAAGCUUGUAUCGCUGCCGCA - 3075
V. vinifera	*NST1* (Vitvi05g01129_t001)	*sXF3*	3.0	No subdomain info	24 - UCCGAUUCUUUGGCCUUCAUCUGC - 1 453 - AGAUCAAGAAACCGGAAUUGGGUG - 476
	Remorin (Vitvi15g01160_t001)	*sXF1*	3.0	C-terminal	24 - CCCUCCAGUUUUUGGCCUUCAUCU - 1 386 - AGAAAGUGAAAAAUCGAAAGUAGA - 409

as our proteomics analysis revealed DBPs and RBPs at the *Xf*-EV corona (Figure 2c). Additionally, previous studies have reported sRNAs as effector-like molecules; for instance, genetic deletion of *sX13* reduced virulence in *Xcv* (Schmidtke et al. 2013), while overexpression of sRNAs in *Xcc* identified RsmU as a negative regulator of virulence and the hypersensitive response (Tang et al. 2020).

In this study, we identified the presence of major RNA types at *Xff* Tem1-EVs and revealed that approximately 30% of all EV-associated transcripts in *Xff* Tem1 encode ncRNAs, with proportions differing from those in WCL samples (Figure 4a, b). Similar enrichment of distinct ncRNAs in EVs has been reported for *X. oryzae*, *Pseudomonas aeruginosa*, *Vibrio fisheri* and *Escherichia coli* (Koeppen et al. 2016; Wu et al. 2024; Ghosal et al. 2015; Moriano-Gutierrez et al. 2020). Although transcripts for all seven homologues of sRNA-*Xcc1* were detected in WCL samples, the non-island encoded homologues were absent in EVs. By contrast, *Xff* Tem1-EVs contained transcripts for four out of the five island-encoded *sXFs* (Figure 4c). Homologues of *Xff* Tem1 *sXFs* are also present in the *Xfp* DD genome (Table 4); however, they are not clustered and are not encoded within a GI. Moreover, Hfq was detected exclusively in *Xff* Tem1-EVs and not in *Xfp* DD-EVs (Figure 1g, h). This suggests that *Xff* Tem1 utilizes EVs to deliver *sXFs* for Hfq-mediated RNA interference (RNAi), whereas *Xfp* DD may employ other EV-associated RBPs for RNAi.

The four EV-associated, island-encoded *sXFs* are homologous to sRNA-*Xcc1* (Figure 5a). In *Xanthomonas*, sRNA-*Xcc1* expression is controlled by HrpG and HrpX, key regulators of the Type-III secretion system (Teper et al. 2021). This suggests a role of sRNA-*Xcc1* in virulence, which could involve its transfer into plant cells and host immune modulation similar to the sRNA *Xosr001* from *Xoc* that targets *OsJMT1* in jasmonic acid signalling (Wu et al. 2024). To this end, the predicted high-confidence plant targets of *sXFs* include four *NLRs*, an *LRR* receptor kinase and *NST1* (Table 5), of which the *CNL* AT1G63350 and the two *TNLs* AT5G11250 and AT5G36930 were downregulated in seedlings infected with *Xff* Tem1 (Figure 6c).

Given that fragments of *sXF2* and *sXF3* are predicted to target an upstream region of the P-loop in the NB-ARC domain (Figure 6e, Table 5), a region of *CNLs* known to be targeted by (micro) miRNAs (Zhang et al. 2022; Shivaprasad et al. 2012), we propose that the phasiRNA pathway could integrate longer bacterial ncRNAs, such as *sXFs*, into the eukaryotic RNAi system. Thus, as an extension of cross-kingdom RNAi, bacterial sRNAs may engage with the phasiRNA pathway, allowing long bacterial sRNAs to be adapted for eukaryotic RNAi. This process could enhance signal amplification and facilitate the silencing of host targets.

ARGONAUTE (AGO) proteins play a key role in the phasiRNA pathway in plants, with AGO1 associating with endogenous sRNAs (Liu et al. 2020). AGO1 can also be hijacked by exogenous sRNAs from both pathogenic and mutualistic microbes, allowing them to suppress host defence genes and promote colonization sRNAs (Liu et al. 2021; Tran et al. 2022). *Bradyrhizobium japonicum* tRNA-derived sRNA fragments regulate soya bean genes associated with nodule symbiosis through AGO1 (Ren et al. 2019). We showed recently that AGO1 functions as a positive regulator of immunity against *Xff* Tem1 in leaf petioles from mature *A. thaliana* plants (Ruf et al. 2024), suggesting a role of the RNAi pathway in the interaction with *Xf*. Further investigation beyond the scope of this study is required to address how, when and where *sXFs* integrate into this pathway and thereby regulate host immune responses.

The observed downregulation of the *CNL* AT1G63350 in EV-treated seedlings suggests that *sXFs* may be delivered as virulence factors via EVs. RNA fold analysis predicted that the *sXFs* adopt a stable secondary structure with three stem-loop structures (Figure 5d). One stem-loop of *sXF* carries motifs for binding Hfq (Figure 5a, d), which is present at the corona of *Xff* Tem1-EVs (Figure 1g, Data S1). Hfq is inserted into EV membranes, potentially facilitating the interaction of sRNAs to EV membranes (Turbant et al. 2023). This is consistent with our observation that ncRNA cargo could associate with EV membranes (Figure 4d). Following the observation that *Xcc*-EVs interact with the plant cell plasma membrane (Tran et al. 2022), a similar scenario could be proposed for *Xf*-EVs, where ncRNA cargo, due to their association with the EV membrane, may also interact with plant plasma membranes.

Immunomodulation by EV-sRNAs has been reported across diverse bacteria–host interactions. EVs from *Xoc* contain sRNA Xosr001, which impairs stomatal immunity in rice by regulating OsJMT1 mRNA (Wu et al. 2024). Similarly, *P. aeruginosa* EVs carry sRNA52320 (a methionine tRNA fragment) along with sRNA4518698, sRNA2316613 and sRNA809738, all of which suppress host immune responses (Koeppen et al. 2016; Xie et al. 2024). In *Helicobacter pylori*, EV-enriched sR-2509025 and sR-989262 reduce LPS-triggered responses (Li et al. 2022). *Flavobacterium psychrophilum* EV-sRNAs interact with trout immune genes, promoting bacterial coldwater disease (Chapagain et al. 2024). In *E. coli*, the tRNA-derived fragment Ile-tRF-5X is released via EVs and transferred to human cells, where it enhances symbiosis by inducing MAP3K4 expression (Li et al. 2022).

The functions of many sRNAs require Hfq, which binds and stabilizes sRNAs and mediates the base-pairing with target mRNAs of host cells, leading to repression of translation or acceleration of mRNA decay (Chapagain et al. 2024; Diallo et al. 2022). Hfq has been described as a global posttranscriptional regulator, required, for example, for virulence, colonization, biofilm formation and QS (Waters and Storz 2009). In *Erwinia amylovora*, Hfq and two Hfq-regulated sRNAs, RprA and RyhA, are important for full virulence of this bacterial pathogen in pear and apple (Zeng et al. 2013). Further knowledge of Hfq-mediated RNAi could facilitate the development of RNA-based therapeutic approaches against *Xf*, such as exploiting Hfq for RNA-based antibacterial gene silencing (Good and Stach 2011).

4.2 | Vesiduction

sRNAs are also key regulators of various bacterial physiological processes, including stress response, metabolism, motility, QS and virulence gene regulation (Zhang et al. 2022; McMillan et al. 2021). In *Xcc*, RsmU regulates virulence and cell motility by antagonizing RsmA (Ren et al. 2019). Interestingly, possible competence regulatory elements in *Xff* Tem1 were predicted as *sXF* targets (Figure 5f). These included mRNAs coding for the competence proteins ComA and ComE, both involved in DNA binding and uptake (Johnston et al. 2014), the single-stranded (ss)DBP *SsbB* mRNA and mRNAs coding for Type-IV PilY/PilW/PlV proteins (Data S4). Generally, the Type-IV pilus interacts with DNA, conveying it to ComEA that binds dsDNA (Seitz and Blokesch 2013; Johnston et al. 2014). The captured dsDNA is converted into ssDNA and taken up across the membrane by ComEC (Johnston et al. 2014). The entering ssDNA is bound by SsbB and DrpA to integrate into the chromosome (Johnston et al. 2014).

Natural transformation occurs in *Xff* and has been observed under conditions of its natural growth environment of liquid flow (Kandel et al. 2016). Our data suggest that EV-associated *sXFs* are regulators of natural transformation. Neither ComE nor transformation pili components (Table 2) were detected in *Xfp* DD-EVs, whereas both are present in *Xff* Tem1-EVs. Interestingly, only the five island-encoded *sXFs* are absent from the *Xfp* DD genome, while the other four *sXFs* are present across its genome (Table 4). Taken together, this suggests that *Xff* Tem1-EVs may function as vesiduction agents, facilitating and regulating natural DNA uptake, a process observed in *Xff* strains but not in *Xfp* strains (Haurat et al. 2011; Avila-Calderón et al. 2021; Dalio et al. 2018; Chalupowicz et al. 2023; Kim et al. 2018).

Growing evidence suggests that horizontally acquired genes play a major role in shaping the genetic diversity of *Xf* and its virulence, with natural transformation likely being a key mechanism of HGT (Haurat et al. 2011; Schmidtke et al. 2013; Tang et al. 2020, Firrao et al. 2021; Jimenez et al. null). The DNA from the GI carrying the island coding for the five homologues *sXFs*, along with DNA from two other GIs, was enriched in the EVs (Figure 3a, b, Figures S4, S5). GIs are regions of bacterial genomes that are acquired through HGT (Fröhlich and Papenfort 2016). Their interaction with EV membranes suggests protection from adverse environments (Figure 3d), for example, during host infection, and the delivery of the DNA cargo upon association with the OM of surrounding recipient bacterial cells (Wen and Herman 2024), indicative of vesiduction (Soler and Forterre 2020). Studies have also demonstrated the importance of sRNAs in maintaining GIs within bacterial populations. A toxin–antitoxin system encoded by the multidrug resistance *Salmonella* Genomic Island 1 (SGI1) plays a critical role in the stable maintenance of SGI1 in the host chromosome (Huguet et al. 2016). This highlights an intricate relationship between sRNAs and GI in bacterial pathogens.

GIs can regulate biofilm formation and motility in bacteria, as shown in *Vibrio alginolyticus* (Cai et al. 2023). Biofilms are a form of cooperative, sessile lifestyle in bacteria and a persistent pathogenetic mechanisms of chronic infections (Muhammad et al. 2020). The ability to switch between planktonic and biofilm lifestyles is critical for *Xf*'s infection process and correlates with vesiculation (De La Fuente et al. 2022; Ionescu et al. 2014). QS regulates the release of EVs, which results in the detachment of *Xf* from surfaces and switch to planktonic life (Ionescu et al. 2014). Whether the regulation of biofilm formation in *Xf* involves the EV-enriched genomic regions or the island-encoded *sXFs*, as shown for various sRNAs in several bacteria (Cai et al. 2023; Van Puyvelde et al. 2013; Sass et al. 2017; Xiao et al. 2017; Shenkutie et al. 2023), remains to be addressed.

Our findings propose a model in which *Xf* cells release EVs with at least two functions (Figure 7): One functional type contains RBPs along with ncRNAs such as *sXFs* and *SsrA*, which are intended for delivery to recipient cells. These recipient cells could be plant cells, where they downregulate host immunity genes, or other *Xf* cells, where they influence natural transformation

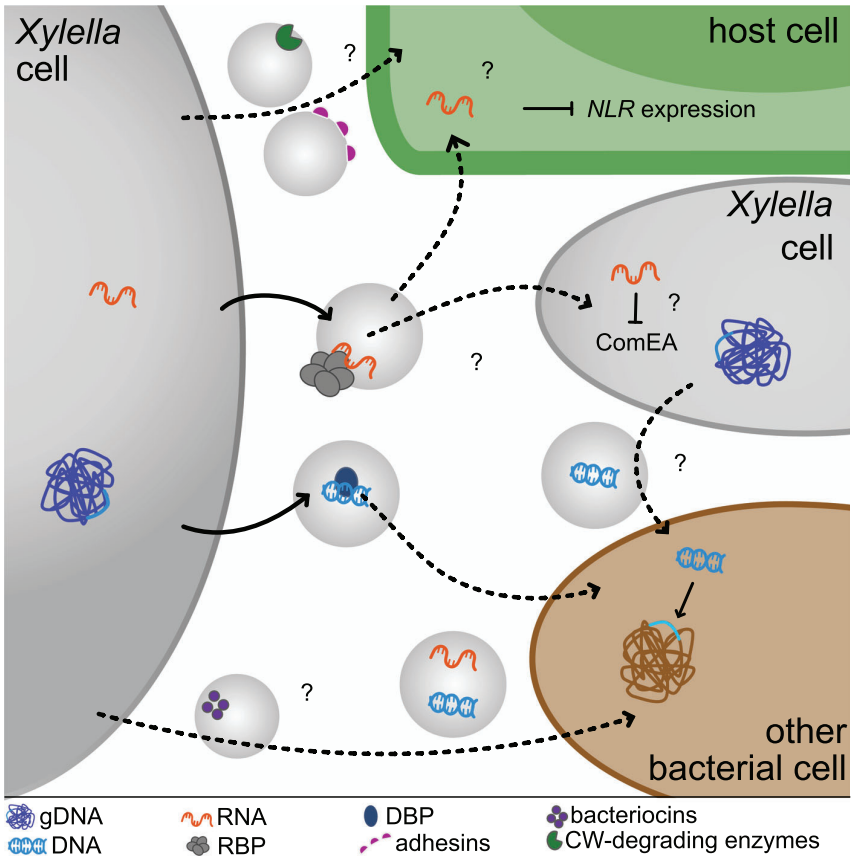

FIGURE 7 | Working model of how *Xff* Tem1uses EVs as a Type-0 secretion system in a contact-independent manner. A bacterial donor cell (left) releases EVs with different functional types, illustrated with different cargoes, in response to its physiological state. EVs containing nucleic acids are associated with either RNA or DNA and are decorated with RBPs and DBPs, respectively. The bacterium may utilize EVs for the delivery of *sXFs* and other ncRNAs to recipient host (plant) and bacterial cells, modulating, for example, plant immunity to aid infection, and natural competence in *Xff* Tem1 by influencing HGT. The secretion of GIs including the *sXFs*-encoding island in EVs as DNA suggests the transfer of this genetic material across the bacterial community and thereby its adaptability to the environment. Other functional types of EVs could be involved in the release of bacteriocin, potentially targeting other bacterial species to dominate the ecological niche as well as cell wall degrading enzymes for systemic plant infection and adhesins to promote the cell's detachment from surfaces. DBP, DNA-binding protein; EV, extracellular vesicle; GI, genomic island; HGT, horizontal gene transfer; RBP, RNA-binding protein; *Xff*, *X. fastidiosa* subsp. *fastidiosa*; *Xff* Tem1, *Xff* strain Temecula1.

capabilities. This is consistent with the finding that EV-packaged *SsrA* from *V. fischeri* regulates bacterial activity and contributes to maintaining homeostasis with its squid host *Euprymna scolopes* (Moriano-Gutierrez et al. 2020). The other functional type of EV contains DBPs and GIs, facilitating HGT of genetic material within the bacterial population. Consequently, the exchange of *sXFs* among bacterial cells could enable widespread regulation of host immunity and natural competence. Other functional types of EVs could deliver cell wall-degrading enzymes such as LesA and adhesins to regulate surface detachment (Ionescu et al. 2014; Nascimento et al. 2016).

Our data show that *Xff* Tem1 utilizes EVs as a Type-0 secretion system, enabling vesiduction and the delivery of sRNA to recipient cells without direct physical interaction. This contact-independent mechanism allows for the potential transmission of genetic information and effectors over longer distances. The absence of the EV-associated GI and island-encoded *sXFs* from the *Xfp* DD genome, along with the lack of Hfq and ComE in *Xfp* DD-EVs, suggests a distinct role for *Xfp* DD-EVs. Taken together, our proteomic analysis of *Xf*-EVs presents a putative list of EV markers and suggests strain-specific differences in their roles in RNAi and HGT. Additionally, our comprehensive data on *Xff* Tem1-EVs offer an essential molecular framework for understanding the virulence strategies of *Xf* and highlight potential target genes that could be engineered to evade targeting, thereby enhancing plant immunity (Touzdjian Pinheiro Kohlrausch Távora et al. 2022).

Author Contributions

Alessa Ruf: conceptualization (equal), data curation (equal), investigation (equal), methodology (equal), resources (equal), validation (equal), visualization (equal), writing – original draft (equal), writing – review and editing (equal). **Patrick Blumenkamp**: data curation (equal), investigation (equal), methodology (equal), resources (equal), software (equal), writing – review and editing (equal). **Christina**

Ludwig: conceptualization (equal), data curation (equal), funding acquisition (equal), investigation (equal), methodology (equal), resources (equal), writing – review and editing (equal). **Anne Lippegaus**: investigation (equal), methodology (equal), writing – review and editing (equal). **Andreas Brachmann**: investigation (equal), writing – review and editing (equal). **Andreas Klingl**: investigation (equal), writing – review and editing (equal). **Alexander Goesmann**: funding acquisition (equal), supervision (equal), writing – review and editing (equal). **Karina Brinkrolf**: supervision (equal), writing – review and editing (equal). **Kai Papenfort**: funding acquisition (equal), investigation (equal), methodology (equal), supervision (equal), writing – review and editing (equal). **Silke Robatzek**: conceptualization (equal), funding acquisition (equal), project administration (equal), supervision (equal), writing – original draft (equal), writing – original draft (equal), writing – review and editing (equal), writing – review and editing (equal).

Acknowledgements

The authors would like to thank members of the Robatzek laboratory for fruitful discussions. The authors acknowledge Niklas Schandry and Jin Yan Khoo for bioinformatics support, Marta Martin-Rivero, Vincent Ohlhauser, Elif Olkun for their laboratory assistance, and the computational and data resources provided by the Leibniz Supercomputing Centre (www.lrz.de). The authors thank Franziska Hackbarth for excellent technical assistance and maintenance of mass spectrometers at the Bavarian Center for Biomolecular Mass Spectrometry. The authors acknowledge technical assistance from the Bioinformatics Core Facility at the professorship of Systems Biology at JLU Giessen and the provision of computer resources and general support by the BiGi service center (BMBF grant 031A533) within the de.NBI network.

Open access funding enabled and organized by Projekt DEAL.

Conflicts of Interest

The authors declare no conflicts of interest.

Data Availability Statement

The mass spectrometric raw files as well as the MaxQuant output files have been deposited to the ProteomeXchange Consortium via the PRIDE partner repository and can be accessed using the identifier PXD056167. The raw data of sequencing can be accessed via EMBL-EBI (https://www.ebi.ac.uk/) with access code E-MTAB-14493 (DNAseq) and E-MTAB-14502 (RNAseq). Genome Annotation *Xff* Temecula1 (NCBI accession GCF_000007245.1) with Bakta has been deposited to Zenodo with DOI 10.5281/zenodo.13970767.

References

Anguita-Maeso, M., A. Ares-Yebra, C. Haro, et al. 2022. "*Xylella fastidiosa* Infection Reshapes Microbial Composition and Network Associations in the Xylem of Almond Trees." *Frontiers in Microbiology* 13: 866085. https://www.frontiersin.org/journals/microbiology/articles/10.3389/fmicb.2022.866085/full.

Antal, M., V. Bordeau, V. Douchin, and B. Felden. 2005. "A Small Bacterial RNA Regulates a Putative ABC Transporter*." *Journal of Biological Chemistry* 280, no. 9: 7901–7908.

Audrey, B., N. Cellier, F. White, P. É. Jacques, and V. Burrus. 2023. "A Systematic Approach to Classify and Characterize Genomic Islands Driven by Conjugative Mobility Using Protein Signatures." *Nucleic Acids Research* 51, no. 16: 8402–8412.

Avila-Calderón, E. D., M. D. S. Ruiz-Palma, and M. G. Aguilera-Arreola, et al. 2021. "Outer Membrane Vesicles of Gram-Negative Bacteria: An Outlook on Biogenesis." *Frontiers in Microbiology* 12: 557902. https://www.frontiersin.org/journals/microbiology/articles/10.3389/fmicb.2021.557902/full.

Bahar, O., G. Mordukhovich, D. D. Luu, et al. 2016. "Bacterial Outer Membrane Vesicles Induce Plant Immune Responses." *Molecular Plant-Microbe Interactions* 29, no. 5: 374–384.

Bemm, F., D. Becker, C. Larisch, et al. 2016. "Venus Flytrap Carnivorous Lifestyle Builds on Herbivore Defense Strategies." *Genome Research* 26, no. 6: 812–825.

Blumenkamp, P., M. Pfister, S. Diedrich, K. Brinkrolf, S. Jaenicke, and A. Goesmann. 2024. "Curare and GenExVis: A Versatile Toolkit for Analyzing and Visualizing RNA-Seq Data." *BMC Bioinformatics* 25, no. 1: 138.

Burbank, L. P., and J. Ochoa. 2022. "Evidence for Elicitation of an Oxidative Burst in *Vitis vinifera* by *Xylella fastidiosa* Cold Shock Protein Peptide csp20." *PhytoFrontiersTM* 2, no. 4: 339–341.

Busch, A., A. S. Richter, and R. Backofen. 2008. "IntaRNA: Efficient Prediction of Bacterial sRNA Targets Incorporating Target Site Accessibility and Seed Regions." *Bioinformatics* 24, no. 24: 2849–2856.

Cai, T., H. Tang, X. Du, et al. 2023. "Genomic Island-Encoded Diguanylate Cyclase From *Vibrio alginolyticus* Regulates Biofilm Formation and Motility in *Pseudoalteromonas*." *Microorganisms* 11, no. 11: 2725.

Castro, C., B. DiSalvo, and M. C. Roper. 2021. "*Xylella fastidiosa*: A Reemerging Plant Pathogen That Threatens Crops Globally." *PLoS Pathogens* 17, no. 9: e1009813.

Chalupowicz, L., G. Mordukhovich, N. Assoline, L. Katsir, N. Sela, and O. Bahar. 2023. "Bacterial Outer Membrane Vesicles Induce a Transcriptional Shift in *Arabidopsis* Towards Immune System Activation Leading to Suppression of Pathogen Growth in Planta." *Journal of Extracellular Vesicles* 12, no. 1: 12285.

Chapagain, P., A. Ali, D. T. Kidane, M. Farone, and M. Salem. 2024. "Characterisation of sRNAs Enriched in Outer Membrane Vesicles of Pathogenic Flavobacterium Psychrophilum Causing Bacterial Cold Water Disease in Rainbow Trout." *Journal of Extracellular Biology* 3, no. 6: e161.

Chen, S., Y. Zhou, Y. Chen, and J. Gu. 2018. "fastp: An Ultra-Fast All-in-One FASTQ Preprocessor." *Bioinformatics* 34, no. 17: i884–i890.

Chen, X. L., D. J. Tang, R. P. Jiang, et al. 2011. "sRNA-Xcc1, an Integron-Encoded Transposon- and Plasmid-Transferred Trans-Acting sRNA, Is Under the Positive Control of the Key Virulence Regulators HrpG and HrpX of *Xanthomonas campestris* Pathovar Campestris." *RNA Biology* 8, no. 6: 947–953.

Cheng, G., W. Li, L. Ha, et al. 2018. "Self-Assembly of Extracellular Vesicle-Like Metal–Organic Framework Nanoparticles for Protection and Intracellular Delivery of Biofunctional Proteins." *Journal of the American Chemical Society* 140, no. 23: 7282–7291.

Cox, J., M. Y. Hein, C. A. Luber, I. Paron, N. Nagaraj, and M. Mann. 2014. "Accurate Proteome-Wide Label-Free Quantification by Delayed Normalization and Maximal Peptide Ratio Extraction, Termed MaxLFQ." *Molecular & Cellular Proteomics* 13, no. 9: 2513–2526.

Cox, J., N. Neuhauser, A. Michalski, R. A. Scheltema, J. V. Olsen, and M. Mann. 2011. "Andromeda: A Peptide Search Engine Integrated Into the MaxQuant Environment." *Journal of Proteome Research* 10, no. 4: 1794–1805.

Dai, X., and P. X. Zhao. 2011. "psRNATarget: A Plant Small RNA Target Analysis Server." *Nucleic Acids Research* 39, no. Web Server issue: W155–W159.

Dai, X., Z. Zhuang, and P. X. Zhao. 2011. "Computational Analysis of miRNA Targets in Plants: Current Status and Challenges." *Briefings in Bioinformatics* 12, no. 2: 115–121.

Dai, X., Z. Zhuang, and P. X. Zhao. 2018. "psRNATarget: A Plant Small RNA Target Analysis Server (2017 Release)." *Nucleic Acids Research* 46, no. W1: W49–W54.

Daleke-Schermerhorn, M. H., T. Felix, Z. Soprova, et al. 2014. "Decoration of Outer Membrane Vesicles With Multiple Antigens by Using an Autotransporter Approach." *Applied and Environmental Microbiology* 80, no. 18: 5854–5865.

Dalio, R. J. D., J. Herlihy, T. S. Oliveira, J. M. McDowell, and M. Machado. 2018. "Effector Biology in Focus: A Primer for Computational Prediction and Functional Characterization." *Molecular Plant-Microbe Interactions* 31, no. 1: 22–33.

D'Attoma, G., M. Morelli, and L. De La Fuente, et al. 2020. "Phenotypic Characterization and Transformation Attempts Reveal Peculiar Traits of *Xylella fastidiosa* Subspecies *pauca* Strain De Donno." *Microorganisms* 8, no. 11: 1832.

Davis, M. J. 1980. "Isolation Media for the Pierce's Disease Bacterium." *Phytopathology* 70, no. 5: 425.

De La Fuente, L., M. V. Merfa, P. A. Cobine, and J. J Coleman. 2022. "Pathogen Adaptation to the Xylem Environment." *Annual Review of Phytopathology* 60, no. 1: 163–186.

Dell'Annunziata, F., V. Folliero, R. Giugliano, et al. 2021. "Gene Transfer Potential of Outer Membrane Vesicles of Gram-Negative Bacteria." *International Journal of Molecular Sciences* 22, no. 11: 5985.

Deyett, E., M. C. Roper, P. Ruegger, J. I. Yang, J. Borneman, and P. E Rolshausen. 2017. "Microbial Landscape of the Grapevine Endosphere in the Context of Pierce's Disease." *Phytobiomes Journal* 1, no. 3: 138–149.

Diallo, I., J. Ho, M. Lambert, et al. 2022. "A tRNA-Derived Fragment Present in *E. coli* OMVs Regulates Host Cell Gene Expression and Proliferation." *PLoS Pathogens* 18, no. 9: e1010827.

EFSA. 2023. "Update of the *Xylella* spp. Host Plant Database—Systematic Literature Search up to 30 June 2023." *EFSA Journal.* 21: e8477. https://www.efsa.europa.eu/en/efsajournal/pub/8477.

Feitosa-Junior, O. R., E. Stefanello, P. A. Zaini, et al. 2019. "Proteomic and Metabolomic Analyses of *Xylella fastidiosa* OMV-Enriched Fractions Reveal Association With Virulence Factors and Signaling Molecules of the DSF Family." *Phytopathology* 109, no. 8: 1344–1353.

Firrao, G., M. Scortichini, and L. Pagliari. 2021. "Orthology-Based Estimate of the Contribution of Horizontal Gene Transfer From Distantly Related Bacteria to the Intraspecific Diversity and Differentiation of *Xylella fastidiosa*." *Pathogens* 10, no. 1: 46.

Fröhlich, K. S., and K. Papenfort. 2016. "Interplay of Regulatory RNAs and Mobile Genetic Elements in Enteric Pathogens." *Molecular Microbiology* 101, no. 5: 701–713.

Ghosal, A., B. B. Upadhyaya, J. V. Fritz, et al. 2015. "The Extracellular RNA Complement of *Escherichia coli*." *MicrobiologyOpen* 4, no. 2: 252–266.

Giampetruzzi, A., P. Baptista, M. Morelli, et al. 2020. "Differences in the Endophytic Microbiome of Olive Cultivars Infected by *Xylella fastidiosa* Across Seasons." *Pathogens* 9, no. 9: 723.

Good, L., and J. E. M. Stach. 2011. "Synthetic RNA Silencing in Bacteria—Antimicrobial Discovery and Resistance Breaking." *Frontiers in Microbiology* 2: 185.

Guerrero-Mandujano, A., C. Hernández-Cortez, J. A. Ibarra, and G. Castro-Escarpulli. 2017. "The Outer Membrane Vesicles: Secretion System Type Zero." *Traffic (Copenhagen, Denmark)* 18, no. 7: 425–432.

Haurat, M. F., J. Aduse-Opoku, M. Rangarajan, et al. 2011. "Selective Sorting of Cargo Proteins Into Bacterial Membrane Vesicles*." *Journal of Biological Chemistry* 286, no. 2: 1269–1276.

Hespanhol, J. T., D. E. Sanchez-Limache, G. G. Nicastro, et al. 2022. "Antibacterial T6SS Effectors With a VRR-Nuc Domain Are Structure-Specific Nucleases." *eLife* 11: e82437.

Huang, Y., S. Wang, Q. Cai, and H. Jin. 2021. "Effective Methods for Isolation and Purification of Extracellular Vesicles From Plants." *Journal of Integrative Plant Biology* 63, no. 12: 2020–2030.

Huguet, K. T., M. Gonnet, B. Doublet, and A. Cloeckaert. 2016. "A Toxin Antitoxin System Promotes the Maintenance of the IncA/C-Mobilizable *Salmonella* Genomic Island 1." *Scientific Reports* 6: 32285.

Hussain, A. 2024. "DEAD Box RNA Helicases: Biochemical Properties, Role in RNA Processing and Ribosome Biogenesis." *Cell Biochemistry and Biophysics* 82, no. 2: 427–434.

Ionescu, M., P. A. Zaini, C. Baccari, S. Tran, A. M. Da Silva, and S. E Lindow. 2014. "*Xylella fastidiosa* Outer Membrane Vesicles Modulate Plant Colonization by Blocking Attachment to Surfaces." *Proceedings of the National Academy of Sciences of the United States of America* 111, no. 37: E3910–E3918. https://pnas.org/doi/full/10.1073/pnas.1414944111.

Iost, I., T. Bizebard, and M. Dreyfus. 2013. "Functions of DEAD-box Proteins in Bacteria: Current Knowledge and Pending Questions." *Biochimica et Biophysica Acta (BBA)—Gene Regulatory Mechanisms* 1829, no. 8: 866–877.

Janda, M., K. Rybak, L. Krassini, et al. 2023. "Biophysical and Proteomic Analyses of *Pseudomonas syringae* pv. *tomato* DC3000 Extracellular Vesicles Suggest Adaptive Functions During Plant Infection." *mBio* 14, no. 4: e0358922.

Jimenez, D., D. Beltran, and J. A. Castillo. "Mobile Genetic Elements of *Xylella fastidiosa* and Their Contribution to Pathogenicity." *Plant Pathology 2024;73:2490-2499*. https://onlinelibrary.wiley.com/doi/abs/10.1111/ppa.13992.

Johnston, C., B. Martin, G. Fichant, P. Polard, and J. P Claverys. 2014. "Bacterial Transformation: Distribution, Shared Mechanisms and Divergent Control." *Nature Reviews Microbiology* 12, no. 3: 181–196.

Johnston, E. L., L. Zavan, N. J. Bitto, S. Petrovski, A. F. Hill, and M. Kaparakis-Liaskos. 2023. "Planktonic and Biofilm-Derived Pseudomonas aeruginosa Outer Membrane Vesicles Facilitate Horizontal Gene Transfer of Plasmid DNA." *Microbiology Spectrum* 11, no. 2:e0517922.

Juhas, M., J. R. Van Der Meer, M. Gaillard, R. M. Harding, D. W. Hood, and D. W. Crook. 2009. "Genomic Islands: Tools of Bacterial Horizontal Gene Transfer and Evolution." *FEMS Microbiology Review* 33, no. 2: 376–393.

Kandel, P. P., S. M. Lopez, R. P. Almeida, and L. De La Fuente. 2016. "Natural Competence of *Xylella fastidiosa* Occurs at a High Frequency inside Microfluidic Chambers Mimicking the Bacterium's Natural Habitats." *Applied and Environmental Microbiology* 82, no. 17: 5269–5277.

Kim, S. I., S. Kim, E. Kim, S. Y. Hwang, and H. Yoon. 2018. "Secretion of *Salmonella* Pathogenicity Island 1-Encoded Type III Secretion System Effectors by Outer Membrane Vesicles in *Salmonella enterica* Serovar Typhimurium." *Frontiers in Microbiology* 9: 2810.

Kjos, M., E. Miller, J. Slager, et al. 2016. "Expression of *Streptococcus pneumoniae* Bacteriocins Is Induced by Antibiotics via Regulatory Interplay With the Competence System." *PLoS Pathogens* 12, no. 2: e1005422.

Koeppen, K., T. H. Hampton, M. Jarek, et al. 2016. "A Novel Mechanism of Host-Pathogen Interaction Through sRNA in Bacterial Outer Membrane Vesicles." *PLoS Pathogens* 12, no. 6: e1005672.

Kopylova, E., L. Noé, and H. Touzet. 2012. "SortMeRNA: Fast and Accurate Filtering of Ribosomal RNAs in Metatranscriptomic Data." *Bioinformatics* 28, no. 24: 3211–3217.

Krzywinski, M., J. Schein, İ. Birol, et al. 2009. "Circos: An Information Aesthetic for Comparative Genomics." *Genome Research* 19, no. 9: 1639–1645.

Kung, S. H., and R. P. P. Almeida. 2011. "Natural Competence and Recombination in the Plant Pathogen *Xylella fastidiosa*." *Applied and Environmental Microbiology* 77, no. 15: 5278–5284.

Kung, S. H., A. C. Retchless, J. Y. Kwan, and R. P. P. Almeida. 2013. "Effects of DNA Size on Transformation and Recombination Efficiencies in *Xylella fastidiosa*." *Applied and Environmental Microbiology* 79, no. 5: 1712–1717.

Lacava, P. T., W. L. Araújo, J. Marcon, W. Maccheroni Jr, and J. L. Azevedo. 2004. "Interaction Between Endophytic Bacteria From Citrus Plants and the Phytopathogenic Bacteria *Xylella fastidiosa*, Causal Agent of Citrus-Variegated Chlorosis." *Letters in Applied Microbiology* 39, no. 1: 55–59.

Landa, B. B., M. Saponari, O. R. Feitosa-Junior, et al. 2022. "*Xylella fastidiosa*'s Relationships: The Bacterium, the Host Plants, and the Plant Microbiome." *New Phytologist* 234, no. 5: 1598–1605.

Langmead, B., and S. L. Salzberg. 2012. "Fast Gapped-Read Alignment With Bowtie 2." *Nature Methods* 9, no. 4: 357–359.

Li, B., Y. Xu, T. Xu, et al. 2022. "Disruption of sncRNA Improves the Protective Efficacy of Outer Membrane Vesicles Against *Helicobacter pylori* Infection in a Mouse Model." *Infection and Immunity* 90, no. 8: e0026722.

Li, C., L. Zhu, D. Wang, et al. 2022. "T6SS Secretes an LPS-Binding Effector to Recruit OMVs for Exploitative Competition and Horizontal Gene Transfer." *The ISME Journal* 16, no. 2: 500–510.

Li, H., B. Handsaker, A. Wysoker, et al. 2009. "The Sequence Alignment/Map Format and SAMtools." *Bioinformatics* 25, no. 16: 2078–2079.

Li, P., W. Luo, T. X. Xiang, et al. 2022. "Horizontal Gene Transfer via OMVs Co-Carrying Virulence and Antimicrobial-Resistant Genes Is a Novel Way for the Dissemination of Carbapenem-Resistant Hypervirulent *Klebsiella pneumoniae*." *Frontiers in Microbiology* 13: 945972. https://www.frontiersin.org/journals/microbiology/articles/10.3389/fmicb.2022.945972/full.

Liao, Y., G. K. Smyth, and W. Shi. 2014. "featureCounts: An Efficient General Purpose Program for Assigning Sequence Reads to Genomic Features." *Bioinformatics* 30, no. 7: 923–930.

Link, T. M., P. Valentin-Hansen, and R. G. Brennan. 2009. "Structure of *Escherichia coli* Hfq Bound to Polyriboadenylate RNA." *Proceedings of the National Academy of Sciences of the United States of America* 106, no. 46: 19292–19297.

Liu, C., H. Yu, X. Rao, L. Li, and R. A. Dixon. 2021. "Abscisic Acid Regulates Secondary Cell-WALL Formation and Lignin Deposition in *Arabidopsis thaliana* Through Phosphorylation of NST1." *Proceedings of the National Academy of Sciences of the United States of America* 118, no. 5: e2010911118.

Liu, Y., C. Teng, R. Xia, and B. C. Meyers. 2020. "PhasiRNAs in Plants: Their Biogenesis, Genic Sources, and Roles in Stress Responses, Development, and Reproduction." *The Plant Cell* 32, no. 10: 3059–3080.

Livak, K. J., and T. D. Schmittgen. 2001. "Analysis of Relative Gene Expression Data Using Real-Time Quantitative PCR and the 2−ΔΔCT Method." *Methods (San Diego, Calif.)* 25, no. 4: 402–408.

Lorrai, R., and S. Ferrari. 2021. "Host Cell Wall Damage During Pathogen Infection: Mechanisms of Perception and Role in Plant-Pathogen Interactions." *Plants* 10, no. 2: 399. https://www.mdpi.com/2223-7747/10/2/399.

Lötvall, J., A. F. Hill, F. Hochberg, et al. 2014. "Minimal Experimental Requirements for Definition of Extracellular Vesicles and Their Functions: A Position Statement From the International Society for Extracellular Vesicles." *Journal of Extracellular Vesicles* 3: 00. 10.3402/jev.v3.26913.

Macho, A. P., and C. Zipfel. 2015. "Targeting of Plant Pattern Recognition Receptor-Triggered Immunity by Bacterial Type-III Secretion System Effectors." *Current Opinion in Microbiology* 23: 14–22.

Macion, A., A. Wyszyńska, and R. Godlewska. 2021. "Delivery of Toxins and Effectors by Bacterial Membrane Vesicles." *Toxins* 13, no. 12: 845.

Mackie, G. A. 2013. "RNase E: At the Interface of Bacterial RNA Processing and Decay." *Nature Reviews Microbiology* 11, no. 1: 45–57.

Mańka, R., K. Sapoń, J. Zaziąbło, T. Janas, A. Czogalla, and T. Janas. 2025. "The Role of RNA Structural Motifs in RNA-Lipid Raft Interaction." *Scientific Reports* 15, no. 1: 6777.

Mann, M., P. R. Wright, and R. Backofen. 2017. "IntaRNA 2.0: Enhanced and Customizable Prediction of RNA–RNA Interactions." *Nucleic Acids Research* 45, no. Web Server issue: W435–W439.

Marinacci, B., P. Krzyżek, B. Pellegrini, G. Turacchio, and R. Grande. 2023. "Latest Update on Outer Membrane Vesicles and Their Role in Horizontal Gene Transfer: A Mini-Review." *Membranes* 13, no. 11: 860.

Mathur, S., S. K. Erickson, L. R. Goldberg, S. Hills, A. G. B. Radin, and J. W. Schertzer. 2023. "OprF Functions as a Latch to Direct Outer Membrane Vesicle Release in *Pseudomonas aeruginosa*." *bioRxiv*.2023.11.12.566662.

McCaig, W. D., A. Koller, and D. G. Thanassi. 2013. "Production of Outer Membrane Vesicles and Outer Membrane Tubes by *Francisella novicida*." *Journal of Bacteriology* 195, no. 6: 1120–1132.

McMillan, H. M., and M. J Kuehn. 2021. "The Extracellular Vesicle Generation Paradox: A Bacterial Point of View." *The EMBO Journal* 40, no. 21: e108174.

McMillan, H. M., S. G. Zebell, J. B. Ristaino, X. Dong, and M. J Kuehn. 2021. "Protective Plant Immune Responses Are Elicited by Bacterial Outer Membrane Vesicles." *Cell Reports* 34, no. 3: 108645. https://www.cell.com/cell-reports/abstract/S2211-1247(20)31634-X.

Mi, H., A. Muruganujan, X. Huang, et al. 2019. "Protocol Update for Large-Scale Genome and Gene Function Analysis With the PANTHER Classification System (v.14.0)." *Nature Protocols* 14, no. 3: 703–721.

Mitre, L. K., N. S. Teixeira-Silva, K. Rybak, et al. 2021. "The *Arabidopsis* Immune Receptor EFR Increases Resistance to the Bacterial Pathogens *Xanthomonas* and Xylella in Transgenic Sweet Orange." *Plant Biotechnology Journal* 19, no. 7: 1294–1296.

Moriano-Gutierrez, S., C. Bongrand, T. Essock-Burns, L. Wu, M. J. McFall-Ngai, and E. G Ruby. 2020. "The Noncoding Small RNA SsrA Is Released by *Vibrio fischeri* and Modulates Critical Host Responses." *PLoS Biology* 18, no. 11: e3000934.

Muhammad, M. H., A. L. Idris, and X. Fan, et al. 2020. "Beyond Risk: Bacterial Biofilms and Their Regulating Approaches." *Frontiers in Microbiology* 11: 928. https://www.frontiersin.org/journals/microbiology/articles/10.3389/fmicb.2020.00928/full.

Nascimento, R., H. Gouran, and S. Chakraborty, et al. 2016. "The Type II Secreted Lipase/Esterase LesA Is a Key Virulence Factor Required for *Xylella fastidiosa* Pathogenesis in Grapevines." *Scientific Reports* 6, no. 1: 18598.

Ojima, Y., K. Yamaguchi, and M. Taya. 2018. "Quantitative Evaluation of Recombinant Protein Packaged Into Outer Membrane Vesicles of *Escherichia coli* Cells." *Biotechnology Progress* 34, no. 1: 51–57.

Pereira, W. E. L., C. B. Ferreira, R. Caserta, M. Melotto, and A. A. de Souza. 2019. "*Xylella fastidiosa* subsp. *pauca* and *fastidiosa* Colonize *Arabidopsis* Systemically and Induce Anthocyanin Accumulation in Infected Leaves." *Phytopathology* 109, no. 2: 225–232.

Phanstiel, D. H., A. P. Boyle, C. L. Araya, and M. P. Snyder. 2014. "Sushi.R: Flexible, Quantitative and Integrative Genomic Visualizations for Publication-Quality Multi-Panel Figures." *Bioinformatics* 30, no. 19: 2808–2810.

Qiao, W., L. Wang, Y. Luo, and J. Miao. 2021. "Outer Membrane Vesicles Mediated Horizontal Transfer of an Aerobic Denitrification Gene Between *Escherichia coli*." *Biodegradation* 32, no. 4: 435–448.

Quinlan, A. R., and I. M. Hall. 2010. "BEDTools: A Flexible Suite of Utilities for Comparing Genomic Features." *Bioinformatics* 26, no. 6: 841–842.

Raden, M., S. M. Ali, O. S. Alkhnbashi, et al. 2018. "Freiburg RNA Tools: A Central Online Resource for RNA-Focused Research and Teaching." *Nucleic Acids Research* 46, no. W1: W25–W29.

Rapicavoli, J. N., B. Blanco-Ulate, A. Muszyński, et al. 2018. "Lipopolysaccharide O-Antigen Delays Plant Innate Immune Recognition of *Xylella fastidiosa*." *Nature Communications* 9, no. 1: 390.

Ren, B., X. Wang, J. Duan, and J. Ma. 2019. "Rhizobial tRNA-Derived Small RNAs Are Signal Molecules Regulating Plant Nodulation." *Science* 365: 919–922.

Rogers, E. E. 2012. "Evaluation of *Arabidopsis thaliana* as a Model Host for *Xylella fastidiosa*." *Molecular Plant-Microbe Interactions* 25, no. 6: 747–754.

Roper, M. C., L. C. Greve, J. G. Warren, J. M. Labavitch, and B. C. Kirkpatrick. 2007. "*Xylella fastidiosa* Requires Polygalacturonase for Colonization and Pathogenicity in *Vitis vinifera* Grapevines." *Molecular Plant-Microbe Interactions* 20, no. 4: 411–419.

Ruf, A., H. Thieron, S. Nasfi, et al. 2024. "Broad-Scale Phenotyping in *Arabidopsis* Reveals Varied Involvement of RNA Interference Across Diverse Plant-Microbe Interactions." *Plant Direct* 8, no. 11: e70017.

Rybak, K., and S. Robatzek. 2019. "Functions of Extracellular Vesicles in Immunity and Virulence." *Plant Physiology* 179, no. 4: 1236–1247.

Sabella, E., A. Luvisi, A. Aprile, et al. 2018. "*Xylella fastidiosa* Induces Differential Expression of Lignification Related-Genes and Lignin Accumulation in Tolerant Olive Trees cv. Leccino." *Journal of Plant Physiology* 220: 60–68.

Sabra, W., H. Lünsdorf, and A. P. Zeng. 2003. "Alterations in the Formation of Lipopolysaccharide and Membrane Vesicles on the Surface of *Pseudomonas aeruginosa* PAO1 Under Oxygen Stress Conditions." *Microbiology (Reading)* 149, no. pt. 10: 2789–2795.

Santiago-Frangos, A., and S. A. Woodson. 2018. "Hfq Chaperone Brings Speed Dating to Bacterial sRNA." *WIREs RNA* 9, no. 4: e1475.

Sass, A., S. Kiekens, and T. Coenye. 2017. "Identification of Small RNAs Abundant in Burkholderia Cenocepacia Biofilms Reveal Putative Regulators With a Potential Role in Carbon and Iron Metabolism." *Scientific Reports* 7, no. 1: 15665.

Schmidtke, C., U. Abendroth, J. Brock, J. Serrania, A. Becker, and U. Bonas. 2013. "Small RNA sX13: A Multifaceted Regulator of Virulence in the Plant Pathogen *Xanthomonas*." *PLoS Pathogens* 9, no. 9: e1003626.

Schmidtke, C., S. Findeiß, C. M. Sharma, et al. 2012. "Genome-Wide Transcriptome Analysis of the Plant Pathogen *Xanthomonas* Identifies sRNAs With Putative Virulence Functions." *Nucleic Acids Research* 40, no. 5: 2020–2031.

Schwengers, O., L. Jelonek, M. A. Dieckmann, S. Beyvers, J. Blom, and A. Goesmann. 2021. "Bakta: Rapid and Standardized Annotation of Bacterial Genomes via Alignment-Free Sequence Identification." *Microbial Genomics* 7, no. 11: 000685.

Seitz, P., and M. Blokesch. 2013. "Cues and Regulatory Pathways Involved in Natural Competence and Transformation in Pathogenic and Environmental Gram-Negative Bacteria." *FEMS Microbiology Reviews* 37, no. 3: 336–363.

Shenkutie, A. M., D. Gebrelibanos, M. Yao, G. Bedada Hundie, F. W. N. Chow, and P. H. M. Leung. 2023. "Impairment of Novel Non-Coding Small RNA00203 Inhibits Biofilm Formation and Reduces Biofilm-Specific Antibiotic Resistance in *Acinetobacter baumannii*." *International Journal of Antimicrobial Agents* 62, no. 3: 106889.

Shevchenko, A., H. Tomas, J. Havli, J. V. Olsen, and M. Mann. 2006. "In-Gel Digestion for Mass Spectrometric Characterization of Proteins and Proteomes." *Nature Protocols* 1, no. 6: 2856–2860.

Shivaprasad, P. V., H. M. Chen, K. Patel, D. M. Bond, B. Santos, and D. C. Baulcombe. 2012. "A MicroRNA Superfamily Regulates Nucleotide Binding Site–Leucine-Rich Repeats and Other mRNAs." *Plant Cell* 24, no. 3: 859–874.

Soler, N., and P. Forterre. 2020. "Vesiduction: The Fourth Way of HGT." *Environmental Microbiology* 22, no. 7: 2457–2460.

Spada, S., N. P. Rudqvist, and E. Wennerberg. 2020. "Chapter Seven—Isolation of DNA From Exosomes." *Methods in Enzymology* Vol. 636: 173–183. https://www.sciencedirect.com/science/article/pii/S0076687920300343.

Sugrue, I., R. P. Ross, and C. Hill. 2024. "Bacteriocin Diversity, Function, Discovery and Application as Antimicrobials." *Nature Reviews Microbiology* 22, no. 9: 556–571.

Sukhodolets, M. V., and S. Garges. 2003. "Interaction of *Escherichia coli* RNA Polymerase With the Ribosomal Protein S1 and the Sm-Like ATPase Hfq." *Biochemistry* 42, no. 26: 8022–8034.

Tang, D., X. Chen, Y. Jia, et al. 2020. "Genome-Wide Screen and Functional Analysis in *Xanthomonas* Reveal a Large Number of mRNA-Derived sRNAs, Including the Novel RsmA-Sequester RsmU." *Molecular Plant Pathology* 21, no. 12: 1573–1590.

Teper, D., S. S. Pandey, and N. Wang. 2021. "The HrpG/HrpX Regulon of Xanthomonads—An Insight to the Complexity of Regulation of Virulence Traits in Phytopathogenic Bacteria." *Microorganisms* 9, no. 1: 187.

Théry, C., K. W. Witwer, E. Aikawa, et al. 2018. "Minimal Information for Studies of Extracellular Vesicles 2018 (MISEV2018): A Position Statement of the International Society for Extracellular Vesicles and Update of the MISEV2014 Guidelines." *Journal of Extracellular Vesicles* 7, no. 1: 1535750.

Thomas, P. D., D. Ebert, A. Muruganujan, T. Mushayahama, L. P. Albou, and H. Mi. 2022. "PANTHER: Making Genome-Scale Phylogenetics Accessible to All." *Protein Science* 31, no. 1: 8–22.

Touzdjian Pinheiro Kohlrausch Távora, F., F. de Assis dos Santos Diniz, C. de Moraes Rêgo-Machado, et al. 2022. "CRISPR/Cas- and Topical RNAi-Based Technologies for Crop Management and Improvement: Reviewing the Risk Assessment and Challenges towards a More Sustainable Agriculture." *Frontiers in Bioengineering and Biotechnology* 10: 913728.

Toyofuku, M., S. Schild, M. Kaparakis-Liaskos, and L. Eberl. 2023. "Composition and Functions of Bacterial Membrane Vesicles." *Nature Reviews Microbiology* 21, no. 7: 415–430.

Tran, F., and J. Q. Boedicker. 2017. "Genetic Cargo and Bacterial Species Set the Rate of Vesicle-Mediated Horizontal Gene Transfer." *Scientific Reports* 7: 8813.

Tran, T. M., C. P. Chng, X. Pu, et al. 2022. "Potentiation of Plant Defense by Bacterial Outer Membrane Vesicles Is Mediated by Membrane Nanodomains." *The Plant Cell* 34, no. 1: 395–417.

Turbant, F., Q. Machiels, J. Waeytens, F. Wien, and V. Arluison. 2024. "The Amyloid Assembly of the Bacterial Hfq Is Lipid-Driven and Lipid-Specific." *International Journal of Molecular Sciences* 25, no. 3: 1434.

Turbant, F., J. Waeytens, A. Blache, et al. 2023. "Interactions and Insertion of *Escherichia coli* Hfq Into Outer Membrane Vesicles as Revealed by Infrared and Orientated Circular Dichroism Spectroscopies." *International Journal of Molecular Sciences* 24, no. 14: 11424.

Tyanova, S., T. Temu, and J. Cox. 2016. "The MaxQuant Computational Platform for Mass Spectrometry-Based Shotgun Proteomics." *Nature Protocols* 11, no. 12: 2301–2319.

Van Puyvelde, S., H. P. Steenackers, and J. Vanderleyden. 2013. "Small RNAs Regulating Biofilm Formation and Outer Membrane Homeostasis." *RNA Biology* 10, no. 2: 185–191.

Vergine, M., J. B. Meyer, M. Cardinale, et al. 2020. "The *Xylella fastidiosa*-Resistant Olive Cultivar "Leccino" Has Stable Endophytic Microbiota During the Olive Quick Decline Syndrome (OQDS)." *Pathogens* 9, no. 1: 35.

Vogel, J., and B. F Luisi. 2011. "Hfq and Its Constellation of RNA." *Nature Reviews Microbiology* 9, no. 8: 578–589.

Wang, M., A. Weiberg, and H. Jin. 2015. "Pathogen Small RNAs: A New Class of Effectors for Pathogen Attacks." *Molecular Plant Pathology* 16, no. 3: 219–223.

Wang, Z., Z. Wen, M. Jiang, et al. 2022. "Dissemination of Virulence and Resistance Genes Among *Klebsiella pneumoniae* via Outer Membrane Vesicle: An Important Plasmid Transfer Mechanism to Promote the Emergence of Carbapenem-Resistant Hypervirulent *Klebsiella pneumoniae*." *Transboundary and Emerging Diseases* 69, no. 5: e2661–e2676.

Wassarman, K. M., and G. Storz. 2000. "6S RNA Regulates *E. coli* RNA Polymerase Activity." *Cell* 101, no. 6: 613–623.

Waters, L. S., and G. Storz. 2009. "Regulatory RNAs in Bacteria." *Cell* 136, no. 4: 615–628.

Welsh, J. A., D. C. I. Goberdhan, and L. O'Driscoll, et al. 2024. "Minimal Information for Studies of Extracellular Vesicles (MISEV2023): From Basic to Advanced Approaches." *Journal of Extracellular Vesicles* 13, no. 2: e12404.

Wen, A. X., and C. Herman. 2024. "Horizontal Gene Transfer and Beyond: the Delivery of Biological Matter by Bacterial Membrane Vesicles to Host and Bacterial Cells." *Current Opinion in Microbiology* 81: 102525.

Wholey, W. Y., T. J. Kochan, D. N. Storck, and S. Dawid. 2016. "Coordinated Bacteriocin Expression and Competence in *Streptococcus pneumoniae* Contributes to Genetic Adaptation Through Neighbor Predation." *PLoS Pathogens* 12, no. 2: e1005413.

Witwer, K. W., D. C. Goberdhan, and L. O'Driscoll, et al. 2021. "Updating MISEV: Evolving the Minimal Requirements for Studies of Extracellular Vesicles." *Journal of Extracellular Vesicles* 10, no. 14: e12182.

Wright, P. R., J. Georg, M. Mann, et al. 2014. "CopraRNA and IntaRNA: Predicting Small RNA Targets, Networks and Interaction Domains." *Nucleic Acids Research* 42, no. W1: W119–W123.

Wright, P. R., A. S. Richter, K. Papenfort, et al. 2013. "Comparative Genomics Boosts Target Prediction for Bacterial Small RNAs." *Proceedings of the National Academy of Sciences of the United States of America* 110, no. 37: E3487–E3496.

Wu, Y., S. Wang, W. Nie, et al. 2021. "A Key Antisense sRNA Modulates the Oxidative Stress Response and Virulence in *Xanthomonas oryzae* pv. *oryzicola*." *PLoS Pathogens* 17, no. 7: e1009762.

Wu, Y., S. Wang, P. Wang, et al. 2024. "Suppression of Host Plant Defense by Bacterial Small RNAs Packaged in Outer Membrane Vesicles." *Plant Communications* 5: 100817.

Xiao, G., H. Tang, S. Zhang, et al. 2017. "*Streptococcus suis* Small RNA rss04 Contributes to the Induction of Meningitis by Regulating Capsule Synthesis and by Inducing Biofilm Formation in a Mouse Infection Model." *Veterinary Microbiology* 199: 111–119.

Xie, Z., X. Wang, Y. Huang, et al. 2024. "*Pseudomonas aeruginosa* Outer Membrane Vesicle-Packed sRNAs Can Enter Host Cells and Regulate Innate Immune Responses." *Microbial Pathogenesis* 188: 106562.

Xiu, L., Y. Wu, G. Lin, Y. Zhang, and L. Huang. 2024. "Bacterial Membrane Vesicles: Orchestrators of Interkingdom Interactions in Microbial Communities for Environmental Adaptation and Pathogenic Dynamics." *Frontiers in Immunology* 15: 1371317. https://www.frontiersin.org/journals/immunology/articles/10.3389/fimmu.2024.1371317/full.

Yu, M. S. C., D. M. Chiang, M. Reithmair, et al. 2024. "The Proteome of Bacterial Membrane Vesicles in *Escherichia coli*—A Time Course Comparison Study in Two Different Media." *Frontiers in Microbiology* 15: 1361270. https://www.frontiersin.org/journals/microbiology/articles/10.3389/fmicb.2024.1361270/full.

Zeng, Q., R. R. McNally, and G. W. Sundin. 2013. "Global Small RNA Chaperone Hfq and Regulatory Small RNAs Are Important Virulence Regulators in *Erwinia amylovora*." *Journal of Bacteriology* 195, no. 8: 1706–1717.

Zhang, Q., F. Luo, Y. Zhong, J. He, and L. Li. 2020. "Modulation of NAC Transcription Factor NST1 Activity by XYLEM NAC DOMAIN1 Regulates Secondary Cell Wall Formation in *Arabidopsis*." *Journal of Experimental Botany* 71, no. 4: 1449–1458.

Zhang, Y., M. Waseem, Z. Zeng, et al. 2022. "MicroRNA482/2118, a miRNA Superfamily Essential for Both Disease Resistance and Plant Development." *New Phytologist* 233, no. 5: 2047–2057.

Zicca, S., P. De Bellis, M. Masiello, et al. 2020. "Antagonistic Activity of Olive Endophytic Bacteria and of *Bacillus* spp. Strains Against *Xylella fastidiosa*." *Microbiological Research* 236: 126467.

Supporting Information

Additional supporting information can be found online in the Supporting Information section.

Supporting Information Figures: S1–S8 **Supporting Information Data S1**: (a, b) List of identified proteins in EVs of *Xff* Tem1 and *Xfp* DD, (c) core EV proteins, c, (d) GO enrichments of *Xff* Tem1- and *Xfp* DD-EV proteins. **Supporting Information Data S2**: (a) Annotation of genes and (b) GI classification of Regions 1–3 identified in DNA-seq, (c) primers used to amplify genes of Region 2. **Supporting Information Data S3**: (a) TPM of RNA-seq, (b) GO enrichments of EV CDS, (c) RT primers used for amplification of ncRNAs. **Supporting Information Data S4**: (a) Target prediction of *sXFs* in *Xff* Tem1, (b) overlap of EV CDS and *Xff* Tem1 *sXFs*-targets, (c) target prediction of *sXFs* in *At* and (d) *Vv*, GO enrichments of predicted targets (e, f), (g) qRT-PCR primers used for gene expression study. **Supplementary Material**: jev270102-sup-0006-Sourcedata.xlsx

PUBLICATION 2 - Ruf, Thieron, Nasfi et al., 2024 *Plant Direct*

Plant Direct
Open Access

RESEARCH ARTICLE | Open Access

Broad-scale phenotyping in Arabidopsis reveals varied involvement of RNA interference across diverse plant-microbe interactions

Alessa Ruf, Hannah Thieron, Sabrine Nasfi, Bernhard Lederer, Sebastian Fricke, Trusha Adeshara, Johannes Postma, Patrick Blumenkamp, Seomun Kwon, Karina Brinkrolf, Michael Feldbrügge, Alexander Goesmann, Julia Kehr, Jens Steinbrenner, Ena Šečić, Vera Göhre, Arne Weiberg, Karl-Heinz Kogel, Ralph Panstruga, Silke Robatzek, on behalf of the exRNA consortium

First published: 15 November 2024 | https://doi-org.emedien.ub.uni-muenchen.de/10.1002/pld3.70017 | Citations: 1

Go here for SFX

Alessa Ruf, Hannah Thieron, and Sabrine Nasfi contributed equally to the study.

Summary

RNA interference (RNAi) is mediated by key players such as Dicer-Like (DCL) and Argonaute (AGO) proteins, which process and bind small RNAs (sRNAs) to regulate gene expression, which represents an important layer of plant immunity. In this study, we subjected a curated set of loss-of-function mutants of *AGO* genes (*AGO1*, *AGO2*, *AGO4*, *AGO10*) and a triple mutant of *DCL* (*DCL2/3/4*) in the model plant *Arabidopsis thaliana* to a diverse panel of microbes, including filamentous pathogens, bacterial pathogens and a fungal mutualist. Additionally, we assessed the expression dynamics of these RNAi components in response to the interactions with respective microbes. We find that the involvement of RNAi to plant immunity is context-dependent and shaped by the specific microbe, an effect most likely dependent on the specificity of involved sRNAs. In particular, in response to the vascular bacterial pathogen *Xylella fastidiosa*, loss of *AGO1* leads to increased bacterial colonisation, indicating that AGO1 contributes to the antibacterial defence against this pathogen. Notably, several interactions showed no phenotypic differences between infections in mutant and wild type suggesting considerable redundancy among RNAi components and that contribution of RNAi to plant immune responses is more nuanced than previously appreciated. Collectively, this research consortium-wide effort provides a basis for future mechanistic dissections of how specific AGOs and DCLs mediate plant immunity in response to diverse microbes.

Contribution

Alessa Ruf: Analysis of RT-qPCRs and microbe quantification, figure preparation, phenotyping of interaction with *Xylella fastidiosa*, *Xanthomonas campestris* and *Pseudomonas syringae*, coordination of experiments from all authors, scientific discussion, writing of manuscript

Hannah Thieron: Analysis of RT-qPCRs and microbe quantification, figure preparation, phenotyping of interaction with *Erysiphe cruciferarum*, coordination of experiments from all authors, scientific discussion, writing of manuscript.
Sabrine Nasfi: Analysis of RT-qPCRs and microbe quantification, figure preparation, phenotyping of interaction with *Serendipita indica*, coordination of experiments from all authors, scientific discussion, writing of manuscript
Bernhard Lederer: phenotyping of interaction with *Hyaloperonospora arabidopsidis,* phenotyping of mutants, scientific discussion, review and editing of manuscript.
Sebastian Fricke: phenotyping of interaction with *Verticilium longisporum*, scientific discussion, review and editing of manuscript.
Trusha Adeshara, Johannes Postma: phenotyping of interaction with *Tecaphora thlaspeos*, scientific discussion, review and editing of manuscript.
Patrick Blumenkamp: data mining and analysis of RNA-seq data; scientific discussion, review and editing of manuscript.
Seomun Kwon: scientific discussion, review and editing of manuscript.
Karina Brinkrolf, Michael Feldbrügge, Alexander Goesmann, Julia Kehr, Jens Steinbrenner Ena Secic, Vera Göhre, Arne Weiberg, Karl Heinz Kogel, Ralph Panstruga: conceptualization and design of experiments, scientific discussion, funding acquisition, review and editing of manuscript.
Silke Robatzek: conceptualization and design of experiments, scientific discussion, writing original draft of manuscript, funding acquisition.

I hereby confirm that all **three first authors have contributed substantially and equally** to the research article “Broad-scale phenotyping in Arabidopsis reveals varied involvement of RNA interference across diverse plant-microbe interactions” published in *Plant Direct* Vol. 8, Issue 11 (November 15th, 2024) (https://onlinelibrary.wiley.com/doi/10.1002/pld3.70017).

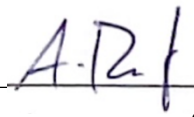

Alessa Ruf (Co-1st author)

Hannah Thieron (Co-1st author)

Sabrine Nasfi (Co-1st author)

Silke Robatzek (Last author)

Received: 25 June 2024 | Revised: 11 September 2024 | Accepted: 1 October 2024

DOI: 10.1002/pld3.70017

RESEARCH ARTICLE

Broad-scale phenotyping in Arabidopsis reveals varied involvement of RNA interference across diverse plant-microbe interactions

Alessa Ruf[1] | **Hannah Thieron**[2] | **Sabrine Nasfi**[3] | **Bernhard Lederer**[1] | **Sebastian Fricke**[4] | **Trusha Adeshara**[5] | **Johannes Postma**[5] | **Patrick Blumenkamp**[6] | **Seomun Kwon**[5] | **Karina Brinkrolf**[6] | **Michael Feldbrügge**[5] | **Alexander Goesmann**[6] | **Julia Kehr**[4] | **Jens Steinbrenner**[3] | **Ena Šečić**[3] | **Vera Göhre**[5,7] | **Arne Weiberg**[1] | **Karl-Heinz Kogel**[3,8] | **Ralph Panstruga**[2] | **Silke Robatzek**[1] | **on behalf of the exRNA consortium**

[1]LMU Munich Biocenter, Planegg, Germany

[2]Unit for Plant Molecular Cell Biology, Institute for Biology I, RWTH Aachen University, Aachen, Germany

[3]Institute of Phytopathology, Centre for BioSystems, Land Use and Nutrition, Justus Liebig University, Giessen, Germany

[4]Institute of Plant Science and Microbiology, Molecular Plant Genetics, Universität, Hamburg, Germany

[5]Institute for Microbiology, Cluster of Excellence on Plant Sciences, Heinrich-Heine University Düsseldorf, Düsseldorf, Germany

[6]Bioinformatics and Systems Biology, Justus Liebig University Giessen, Germany

[7]Hochschule Darmstadt, Darmstadt, Germany

[8]Institut de biologie moléculaire des plantes, CNRS, Université de Strasbourg, Strasbourg, France

Correspondence
Silke Robatzek, LMU Munich Biocenter, Großhadener Strasse 4, 82152 Planegg, Germany.
Email: robatzek@bio.lmu.de

Abstract

RNA interference (RNAi) is a crucial mechanism in immunity against infectious microbes through the action of DICER-LIKE (DCL) and ARGONAUTE (AGO) proteins. In the case of the taxonomically diverse fungal pathogen *Botrytis cinerea* and the oomycete *Hyaloperonospora arabidopsidis*, plant DCL and AGO proteins have proven roles as negative regulators of immunity, suggesting functional specialization of these proteins. To address this aspect in a broader taxonomic context, we characterized the colonization pattern of an informative set of *DCL* and *AGO* loss-of-function mutants in *Arabidopsis thaliana* upon infection with a panel of pathogenic microbes with different lifestyles, and a fungal mutualist. Our results revealed that, depending on the interacting pathogen, AGO1 acts as a positive or negative regulator of immunity, while AGO4 functions as a positive regulator. Additionally, AGO2 and AGO10 positively modulated the colonization by a fungal mutualist. Therefore, analyzing the role of RNAi across a broader range of plant-microbe interactions has identified previously unknown functions for AGO proteins. For some pathogen interactions, however, all tested mutants exhibited wild-type-like infection phenotypes, suggesting that the roles of AGO and DCL proteins in these interactions may be more complex to elucidate.

Alessa Ruf, Hannah Thieron, and Sabrine Nasfi contributed equally to the study.

Funding information
Deutsche Forschungsgemeinschaft (DFG), Grant/Award Numbers: FE448/15-1, GO 2037/8-1, GO 2064/4-1, KE 856/8-1, KO 1208/32-1, PA 861/22-1, RO 3550/16-1, WE 5707/2-1; Dr. Ernst-Leopold Klipstein Foundation

KEYWORDS
AGO, Argonaute, DCL, Dicer-like, RNAi

1 | INTRODUCTION

RNA interference (RNAi) is a conserved mechanism that regulates gene expression via small (s)RNAs (Huang et al., 2019; Tang et al., 2022), which can be classified into micro (mi)RNAs (20–22 nt) and small interfering (si)RNAs (21–24 nt). In the interaction with infectious agents, host sRNAs target foreign genes to mediate defense, e.g., against viruses (Obbard et al., 2008; Zhan & Meyers, 2023). Host sRNAs also fine-tune the expression of host immune-responsive genes, thereby orchestrating the outcome of infection against various pathogens (Šečić, Kogel, & Ladera-Carmona, 2021). For example, in the genetic model *Arabidopsis thaliana*, miRNA393 enhances resistance to *P. syringae pv. tomato* strain DC3000 (*Pto* DC3000) by regulating pattern-triggered immunity (PTI) through auxin signaling suppression (Navarro et al., 2006). During seedling development, miR172 inhibits the expression of FLAGELLIN SENSING2 (FLS2), a well-studied pattern recognition receptor (PRR) that confers PTI against flagellated bacteria (Zou et al., 2018). This suggests a role of miR172 in coordinating plant immunity and development.

The core mechanism of RNAi involves the production of dsRNAs, which are processed into sRNA duplexes by DICER-LIKE (DCL) proteins. These sRNAs are subsequently loaded into RNA-induced silencing complexes (RISCs) (Iwakawa & Tomari, 2022; Martín-Merchán et al., 2023). To amplify RNAi, RNA-dependent RNA polymerases use single-stranded sRNA to generate long dsRNAs, which are processed by DCL2/DCL4 into secondary-phased siRNAs (Curaba & Chen, 2008; Martín-Merchán et al., 2023). *A. thaliana* encodes four DCL proteins, each producing specifically sized sRNAs (Martín-Merchán et al., 2023), suggesting specific functions. A partial *DCL1* loss-of-function mutant in *A. thaliana* showed enhanced susceptibility to *Pto* DC3000 and *Botrytis cinerea* infection (Navarro et al., 2006; Weiberg et al., 2013), but also displayed developmental abnormalities. DCL2 and DCL4 mediate antiviral immunity (Taochy et al., 2017; Z. Wang et al., 2018) (Azevedo et al., 2010; Bouché et al., 2006; Deleris et al., 2006). DCL4 is also crucial for anti-fungal defense since *dcl4* mutants showed increased susceptibility to the vascular fungus *Verticillium dahliae* (Ellendorff et al., 2009).

ARGONAUTE (AGO) proteins are key components of RISCs, bind single-stranded sRNAs, and guide them to sequence-complementary RNA and DNA targets (Fang & Qi, 2016). Ten AGO proteins have been identified in *A. thaliana* that can be classified into three clades: i) AGO1/5/10 (clade I), ii) AGO2/3/7 (clade II), and iii) AGO4/6/8/9 (clade III) (Martín-Merchán et al., 2023). They feature different subcellular localization patterns and sRNA binding preferences. The expression patterns of *AGO* genes do not seem to correlate with their clade assignment and function. The members of clade I and clade III, *AGO1* and *AGO4*, are ubiquitously expressed across tissues and during various developmental stages of *A. thaliana* (Jullien et al., 2022). The expression of *AGO2* and *AGO3* is induced in response to diverse abiotic and biotic stresses (Martín-Merchán et al., 2023). For example, *AGO2* expression is upregulated during *Pto* DC3000 infection (Zhang et al., 2011).

Several studies have examined the roles of AGO proteins in plant immunity against eukaryotic and prokaryotic microbes. For example, specific partial loss-of-function mutants in *AGO1* are compromised in microbe-associated molecular pattern (MAMP)-induced immunity against *Pto* DC3000 (Li et al., 2010). Since infection with the fungal pathogen *Sclerotinia sclerotiorum* showed more severe necrotic disease symptoms in *ago1* mutants (Cao et al., 2020), the study suggests that AGO1 is a positive regulator of PTI and enhances resistance against *S. sclerotiorum*. However, AGO1 has also been described to negatively regulate plant immunity against the fungal pathogens *B. cinerea*, *V. dahliae*, *V. longisporum* and *Botryosphaeria dothidea*, as well as the oomycete *H. arabidopsidis* (Dunker et al., 2020; Ellendorff et al., 2009; Shen et al., 2014; Weiberg et al., 2013; Yu et al., 2017). Yet, AGO1 had no detectable role in the outcome of infection with the fungal and oomycete pathogens *Erysiphe cruciferarum* and *Albugo laibachii*, respectively (Dunker et al., 2020). Of the other clades, Arabidopsis *ago2* mutants are more susceptible to infection by *V. dahliae*, *S. sclerotiorum*, and species of the oomycete pathogen *Phytophthora* (Cao et al., 2020; Ellendorff et al., 2009; Guo et al., 2018). Furthermore, AGO4 contributes to resistance to *Pto* DC3000 and is required for both local and *Trichoderma*-induced systemic immunity against *B. cinerea* (Agorio & Vera, 2007; López et al., 2011; Rebolledo-Prudencio et al., 2022).

AGO proteins act together with their loaded sRNAs within the RISC complex, suggesting that the above-outlined examples of immunity regulation in *A. thaliana* likely depend on the specificity of the sRNAs. Beyond the evolution of pathogen-derived molecular suppressors that interfere with host RNAi (Hou et al., 2019; Navarro et al., 2006), infectious microbes can hijack host AGO1 and incorporate microbe-derived sRNAs to facilitate infection. This cross-kingdom (ck)RNAi has been demonstrated for the interaction of *A. thaliana* with the taxonomically diverse pathogens *B. cinerea* and *H. arabidopsidis* (Dunker et al., 2020; Weiberg et al., 2013). In both cases, it is mediated by fungal- or oomycete-derived sRNAs, respectively, which are loaded into host AGO1 and thereby interfere with host RNAi pathways. Supporting this, the *B. cinerea rdr1 and dcl1/dcl2* mutants were less virulent on both *A. thaliana* and *Solanum lycopersicum* hosts, since the production of sRNAs was nearly abolished in these fungal mutants (Cheng et al., 2023; Weiberg et al., 2013). Since plants also deliver sRNAs into *B. cinerea* (Cai et al., 2018), ckRNAi occurs in both directions of the interacting organisms.

Different *B. cinerea* genotypes exhibited varied infection phenotypes (Qin et al., 2023; Weiberg et al., 2013). Hence, the contribution of RNAi to the outcome of microbial infections tends to be more complex and possibly species- or even pathotype-dependent. Therefore, it cannot always be assumed with certainty that plant mutants in the RNAi pathway exhibit phenotypes at each time point when infected with any microbe. To address this aspect in a broader taxonomic context, we characterized the expression patterns and loss-of-function mutant phenotypes of an informative set of *DCL* and *AGO* genes upon infection with a panel of pathogenic filamentous microbes and bacteria, each with different lifestyles, including mutualistic colonization. We reproduced some previously investigated phenotypes and uncovered new roles for AGO1, AGO2, AGO4, and AGO10 in certain microbial interactions, specifically, the dual role of AGO1 as both a positive and negative regulator of plant immunity. This study provides a phenotypic framework for the context-dependent regulatory function of *DCL* and *AGO* genes in plant immunity, offering insights into how plants dynamically adjust their defense strategies to different types of microbial interactions.

2 | RESULTS

We selected a set of *A. thaliana* genes and their corresponding mutants that are informative for the siRNA pathway. These include *DCL2*, *DCL3*, *DCL4* and the triple *dcl2/3/4* mutant and members of the three AGO clades (*AGO1*, *AGO10*, the *ago1-27*, *ago1-46* and *ago10-1* mutants (clade I), *AGO2* and the *ago2-1* mutant (clade II), *AGO4* and the *ago4-2* mutant (clade III) (Table S1). Exploring publicly available transcriptome data of *A. thaliana* elicited with MAMPs from fungi (ch8, nlp20), oomycete (nlp20), and bacteria (flg22, elf16, LPS, nlp20) (Bjornson et al., 2021), we noted that all tested *AGO* but not the selected *DCL* genes were responsive to the immune stimuli (Figure S1). Of the *AGO* genes, *AGO2* showed upregulation in response to all MAMPs, while *AGO1*, *AGO4*, and *AGO10* were downregulated in response to bacterial MAMPs. This suggests that *AGO* genes across the three clades could be involved in PTI regulation. The strong MAMP-induced expression of *AGO2* is consistent with its documented role in immunity against the pathogenic fungus *S. sclerotiorum* and anti-bacterial immunity against *Pto* DC3000 and its AvrRpt2-avirulent derivative (Cao et al., 2020; Zhang et al., 2011).

Since *AGO* gene expression was responsive to MAMPs derived from different microbial taxa, we selected a panel of pathogenic fungi (*Thecaphora thlaspeos*, *E. cruciferarum*, *V. longisporum*), a symbiotic fungus (*Serendipita indica*), and bacterial pathogens (*Pto* DC3000, *X. campestris* pv. *campestris*, *Xylella fastidiosa* subsp. *fastidiosa*) to study the *DCL* and *AGO* expression profiles as well as the infection phenotypes of corresponding mutants in *A. thaliana* (Table S2). We also included an oomycete pathogen (*H. arabidopsidis*), given that AGO1-dependent ckRNAi has been demonstrated to play a role in its infection outcome in *A. thaliana* (Dunker et al., 2020). The selected microbes also differ in their lifestyles, with *H. arabidopsidis* and *Pto* DC3000 infecting leaf mesophyll tissue, *E. cruciferarum* invading leaf epidermal cells, *S. indica* colonizing roots, and *V. longisporum*, *X. campestris* pv. campestris and *X. fastidiosa* infecting the plant xylem, and *T. thlaspeos* growing systemically along the vasculature in both roots and aerial tissues (Table S2). Appreciating the diverse lifestyles, we performed the infection experiments tailored to the type of plant-microbe interaction and according to well-established protocols, yet mainly at the whole plant/organ scale with in vitro and soil-grown plants. Gene expression was analyzed at different time points in the early, middle, and late infection/colonization stages depending on the interacting microbe. The infection/colonization success was measured as the ability to invade host cells (number of penetration events), as microbial biomass (number of hyphae or microbial DNA/RNA), scoring of the infection progress, or as the capacity of the microbe to multiply within host tissue (number of colony-forming units [cfu]). To minimize the putative effect of seed batches, we used an age-matched seed collection of *A. thaliana* Col-0 and the selected *dcl2/3/4* and *ago* mutants for our experiments.

2.1 | AGO1 is a regulator of immunity against some but not all filamentous pathogens

We first tested our collection of plant lines and investigated the role of *DCL* and AGO proteins in the interaction with *H. arabidopsidis*. Expression of *DCL2*, *DCL4*, and *AGO2* was upregulated at middle (4 days post inoculation [dpi]) and late (6 dpi) stages of *H. arabidopsidis* infection, while *AGO4* was downregulated at these time points (Figure 1a). This is in agreement with the changes in the expression of *AGO2* and *AGO4* in response to the oomycete MAMP nlp20 (Figure S1). No drastic changes in gene expression were observed for *AGO1* and *AGO10* (Figure 1a). In the infection experiments, *ago1-27* and *ago1-46* mutants displayed enhanced resistance to *H. arabidopsidis* at 6 dpi (Figure 1b). No altered infection was observed in *ago2-1* and *ago4-2* mutants. This outcome is consistent with a previous report showing evidence for loading pathogen-derived sRNAs into *A. thaliana* AGO1, resulting in ckRNAi to support infection (Dunker et al., 2020). Collectively, the data suggests a specific role for AGO1 in the interaction with the oomycete pathogen.

AGO1 also negatively regulates immunity against fungal pathogens including, *B. cinerea* and *V. longisporum* but not *E. cruciferarum* (Dunker et al., 2020; Shen et al., 2014; Weiberg et al., 2013). Consistent with the fact that AGO1 negatively regulates immunity against *V. longisporum* (Shen et al., 2014), *AGO1* expression was downregulated in the course of infection with this fungal pathogen (Figure S2). By contrast, *DCL3* and *DCL4* were upregulated by *V. longisporum*, suggesting a different response to this pathogen.

Next, we explored the selected *DCL* and *AGO* genes for their expression profiles in response to the challenge with *E. cruciferarum*. We found reduced *AGO1*, *AGO4*, and *AGO10* expression and upregulation of the tested *DCL* genes across the time course (Figure 2a). Fungal entry rates were slightly, yet statistically significantly, increased in *ago1-27*, but no differences were observed in any of the other tested mutants, including the allelic *ago1-46* mutant (Figure 2b). This outcome

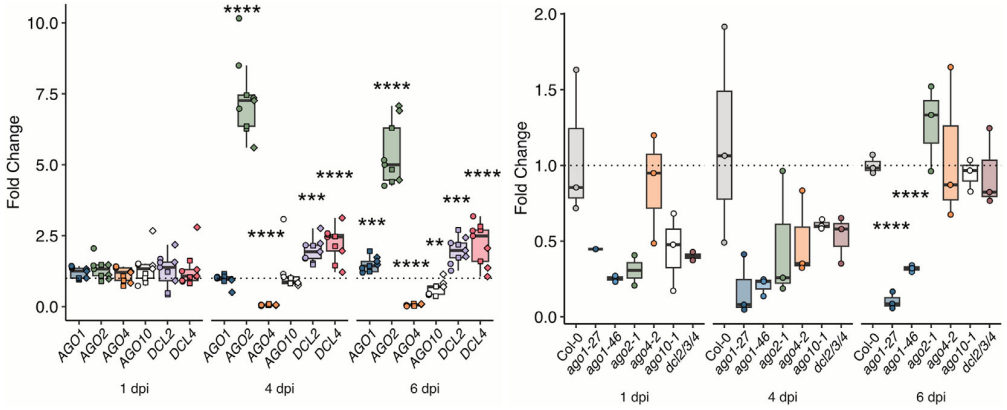

FIGURE 1 *DCL* and *AGO* gene expression patterns (a) and colonization in respective mutants (b) upon infection with *H. arabidopsidis* isolate Noco 2. (a) Samples were collected at 1 dpi (days post inoculation), 4 dpi, and 6 dpi. The RNA levels are relative to mock and normalized against *CDKA*. The results of three biological replicates are depicted. (b) Pathogen load on *ago* and *dcl* mutants was assessed by measuring relative *H. arabidopsidis* gDNA quantities with RT-qPCR at 1 dpi, 4 dpi, and 6 dpi. The result of one biological replicate is depicted. Error bars show standard deviation. Statistical significance was assessed by two-sided Welch's *t*-test ($\alpha = .05$, *p*-values * < .05, ** < .01, *** < .001, **** < .0001). Symbols indicate number of biological replicates. Circle = first, square = second, diamond = third. The dashed line indicates a fold change = 1.

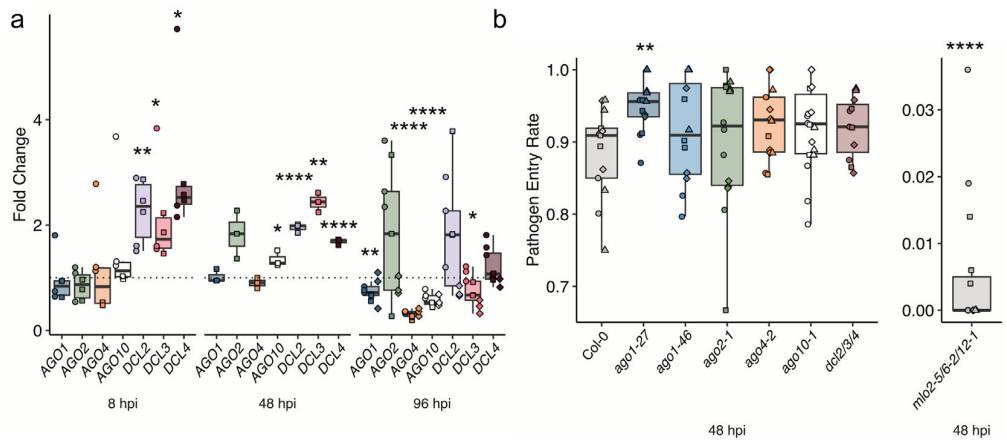

FIGURE 2 *DCL* and *AGO* gene expression patterns (a) and colonization in respective mutants (b) upon *E. cruciferarum* infection in a time course experiment. (a) Samples were collected at 8 hpi (hours post inoculation), 48 hpi, and 96 hpi. The RNA levels are relative to mock and normalized against *CDKA*. The results of three biological replicates are depicted. (b) Infection success on *ago* and *dcl* mutants was assessed by determining *E. cruciferarum* host cell entry rates at 48 hpi. The results of four biological replicates are depicted. Error bars show standard deviation. Statistical significance was assessed by two-sided Welch's *t*-test ($\alpha = .05$, *p*-values * < .05, ** < .01, *** < .001, **** < .0001). Symbols indicate number of biological replicates. Circle = first, square = second, diamond = third, triangle = fourth. The dashed line indicates a fold change = 1.

confirms previous data on unaltered *E. cruciferarum* infection in *ago1-46*. However, it contrasts the reported wild type-like phenotype in *ago1-27* (Dunker et al., 2020) possibly due to different scoring: the previous study evaluated leaf necrosis, while in our study, fungal penetration was scored. Furthermore, a clear regulation of *E. cruciferarum* penetration success by AGO1 cannot be established, since the two *ago1* mutants exhibited different infection phenotypes to this fungus (Figure 2b). We also investigated the role of AGO1 during infection with *T. thlaspeos* and observed wild-type-like colonization in *ago1-27* mutants (Figure 3). By contrast, *ago4-2* mutants showed significantly enhanced susceptibility, thereby revealing a previously unknown role for AGO4 as a positive regulator of immunity to this smut fungus.

2.2 | AGO1 is a regulator of certain but not all bacterial infections

Motivated by the previous reports on the roles of AGO1 and AGO2 in immunity against bacterial pathogens (Ren et al., 2019; Zhang et al., 2011), we examined the roles of the selected *DCL* and *AGO* genes in infection by three different bacterial pathogens. Interestingly, AGO1 might be required for immunity against *X. fastidiosa*, since it was upregulated at late infection stages (Figure 4a), and both *ago1-27* and *ago1-46* displayed enhanced susceptibility (Figure 4b). All other tested genes showed wild-type-like expression patterns, and the respective mutants supported wild-type-like infection success of *Pto* DC3000

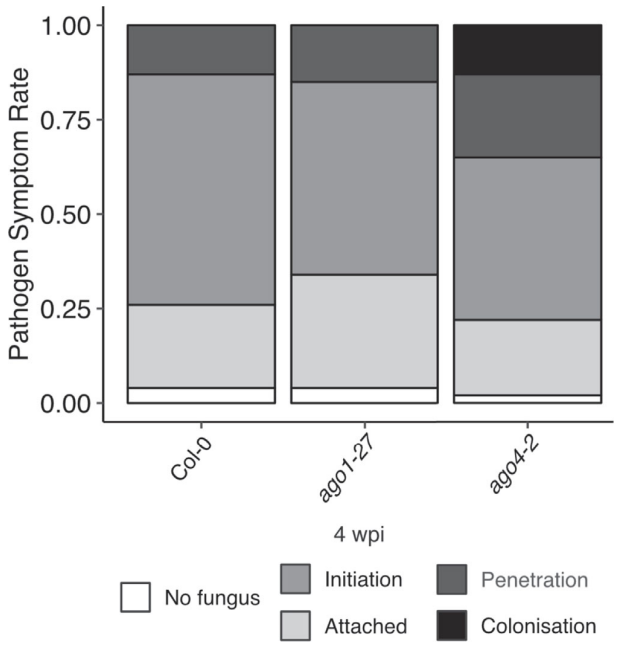

FIGURE 3 Colonization in *ago* mutants upon *T. Thlaspeos* infection. Colonization was visualized after four weeks by staining with wheat germ agglutinin (WGA, fungal hyphae) and propidium iodide (PI, plant background). In at least 150 seedlings per line, fungal progression was classified into (i) attachment of the fungus to plant tissue, (ii) initiation of penetration as indicated by bulging of the hyphal tip, (iii) penetration into the plant tissue, and (iv) colonization along the vasculature. Similar results were obtained in three independent experimental replicates.

(Figure S3A and S3B) and *X. campestris* pv. *campestris* (Figure S4A and S4B). The tested bacteria are Gram-negative γ-proteobacteria, including two belonging to the Xanthomonadaceae and colonizing xylem vessels (Table S3). However, the positive regulatory function of AGO1 appears to be specific to immunity against *X. fastidiosa*.

Previously, AGO2 and AGO4 were shown to positively regulate immunity against *Pto* DC3000 strains (Agorio & Vera, 2007; López et al., 2011; Zhang et al., 2011), which is not consistent with our findings. We neither detected any obvious induction of *AGO2* expression nor increased *Pto* DC3000 susceptibility in *ago2* and *ago4* mutants (Figure S3). It is possible that the different outcomes for these mutants might depend on the methods of bacterial inoculation, as in the previous studies, bacteria were applied by syringe-based leaf infiltration, while in this study, *Pto* DC3000 was sprayed onto the leaf surface. The two inoculation methods differ, as syringe inoculation bypasses stomatal immunity (Melotto et al., 2017).

2.3 | AGO2 and AGO10, but not AGO1, are potential regulators of fungal mutualism

Soybean AGO1 plays a positive role in the bacterial *Sinorhizobium* root-nodule symbiosis via ckRNAi (Ren et al., 2019). Furthermore, AGO1 has been speculated to regulate fungal symbiosis, supported by the prediction of plant mRNA targets of fungal sRNAs accumulating in the symbiosis between beneficial microorganisms and their hosts (Silvestri et al., 2019; Valdés-López et al., 2019; Wong-Bajracharya et al., 2022). Therefore, we next conducted colonization experiments with the mutualist basidiomycete *S. indica*, revealing *AGO4* downregulation at late time points (Figure 5a). The other tested *DCL* and *AGO* genes revealed no statistically significant changes in response to *S. indica* colonization at the investigated time points (Figure 5a). Interestingly, roots of *ago2-1* and *ago10-1* mutants showed reduced colonization by *S. indica*, whereas *ago1-27*, *ago4-2*, and *dcl2/3/4* exhibited wild type-like colonization (Figure 5b). It suggests that AGO2 and AGO10, but not AGO1, function as potential positive regulators during colonization in the mutualistic interaction of *A. thaliana* with *S. indica*, or negatively regulate immunity against this beneficial fungus. Moreover, although clade I AGO1 and AGO10 are phylogenetically related, AGO10 may have a specific function in fungal mutualism. Of note, miRNAs can be sequestered by different AGO proteins, leading to different outcomes, e.g., as shown for miRNA165/166 in flower development, which depends on their binding to AGO1 and AGO10 (Ji et al., 2011).

2.4 | AGO expression patterns do not seem to correlate with their function in immunity

We utilized heat maps to summarize our mutant infection and gene expression data. Overall, some of the most striking phenotypes were associated with *ago1*, *ago2*, and *ago10* mutants: *ago1* mutants were more susceptible to *X. fastidiosa* but more resistant to *H. arabidopsidis* while *ago2* and *ago10* were more resistant to *S. indica* (Figure 6a). Yet, despite these notable phenotypes, the overall gene expression patterns did not correlate with the mutant infection data (Figure 6b). The most striking changes in gene expression were observed for *AGO2* and *AGO4*, showing up- and down-regulation upon *H. arabidopsidis* infection, respectively (Figure 6b). *AGO4* and *AGO10* were also down-regulated in response to *E. cruciferarum*. This suggests distinct underlying mechanisms or pathways influencing the observed phenotypic outcomes.

3 | DISCUSSION

RNAi executed by DCL and AGO proteins is considered a conserved process regulating the outcome of plant-microbe interactions. Previous studies have described the roles of AGOs as positive and negative plant immunity regulators, likely linked to their binding of host or pathogen-derived sRNAs. Here, we i) confirm previous findings for AGO1 in negatively regulating immunity against *H. arabidopsidis* (Figure 1b) and ii) reveal a potential positive regulatory role of AGO1 in immunity against *X. fastidiosa* (Figure 4b). Moreover, iii) we identified clade I AGO10 and clade II AGO2 as positive modulators of *S. indica* root colonization (Figure 5b), and iv) revealed clade III AGO4

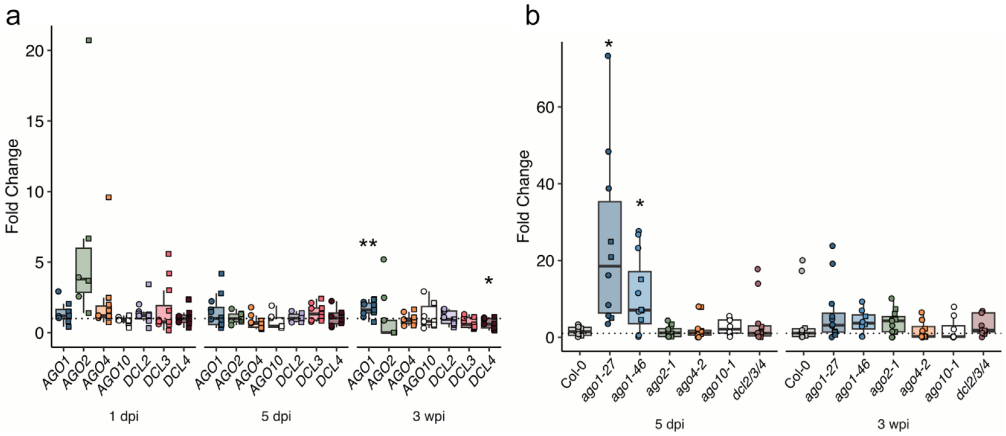

FIGURE 4 *DCL* and *AGO* gene expression patterns (a) and colonization in respective mutants (b) upon *Xylella fastidiosa subsp. fastidiosa* Temecula1 infection. (a) Samples were collected from petioles at 1 (day post-infection), 5 dpi, and 3 wpi (weeks post-infection). The RNA levels are relative to mock and normalized against *CDKA*. The results of two biological replicates are depicted. (b) Pathogen load on *ago* and *dcl* mutants was assessed by RT-qPCR at 5 dpi and 3 wpi. The results of two biological replicates are depicted. Error bars show standard deviation. Statistical significance was assessed by two-sided Welch's *t*-test ($\alpha = .05$, *p*-values * < .05, ** < .01, *** < .001, **** < .0001). Symbols indicate number of biological replicates. Circle = first, square = second, diamond = third. The dashed line indicates a fold change = 1.

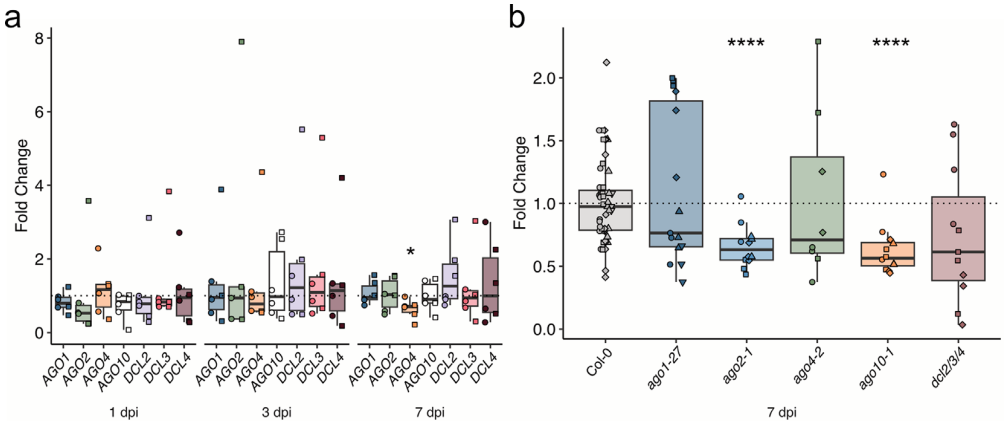

FIGURE 5 *DCL* and *AGO* expression patterns (a) and colonization in respective mutants (b) upon infection with *S. indica*. (a) Samples were collected from roots at 1 dpi (day post inoculation), 3 dpi, and 7 dpi. The RNA levels are relative to mock and normalized against *UBC21*. The results of two biological replicates are depicted. (b) Pathogen load on *ago* and *dcl* mutants was assessed by measuring relative *S. indica* gDNA quantities with RT-qPCR at 7 dpi. The results of at least three biological replicates are depicted. Error bars show standard deviation. Statistical significance was assessed by two-sided Welch's *t*-test ($\alpha = .05$, *p*-values * < .05, ** < .01, *** < .001, **** < .0001). Symbols indicate number of biological replicates. Circle = first, square = second, diamond = third. The dashed line indicates a fold change = 1.

as a positive control element of *T. thlaspeos* infection (Figure 3). Thus, our broad-scale phenotyping uncovered previously unknown positive and negative regulatory functions of different AGO proteins in the context of plant-microbe interactions (Figure 6c).

AGO1's negative adjustment of plant immunity is influenced by its role as a target for pathogen-derived sRNAs and its function in ckRNAi (Dunker et al., 2020; Weiberg et al., 2013). Therefore, it is possible that AGO1-related AGO10 and AGO2 might be hijacked by *S. indica*-secreted sRNAs, providing a possible molecular mechanism of their positive modulatory role in mutualism with this fungus. Indeed, the production of host and fungal-derived sRNAs has been revealed in the beneficial interaction of *Brachypodium distachyon* with *S. indica* (Šečić, Zanini, et al., 2021), which could result in post-transcriptional gene silencing (PTGS) of plant immunity genes and thereby facilitating *S. indica* colonization. This scenario is consistent with AGO1's role in bacterial symbiosis, binding rhizobial tRNA-derived sRNA fragments (tRFs) that promote host nodulation (Ren et al., 2019). Additionally, clade I AGOs could influence the host's transcriptional response to symbiosis, as reported for AGO5 in rhizobia-*Phaseolus vulgaris* symbiosis (del Sánchez-Correa et al., 2022).

A positive immune regulatory function of AGO proteins has been linked to its binding of host endogenous sRNAs. For example, miR393b* bound to AGO2 triggers *MEMB12* (encoding a Golgi-localized SNARE protein) cleavage, which results in increased

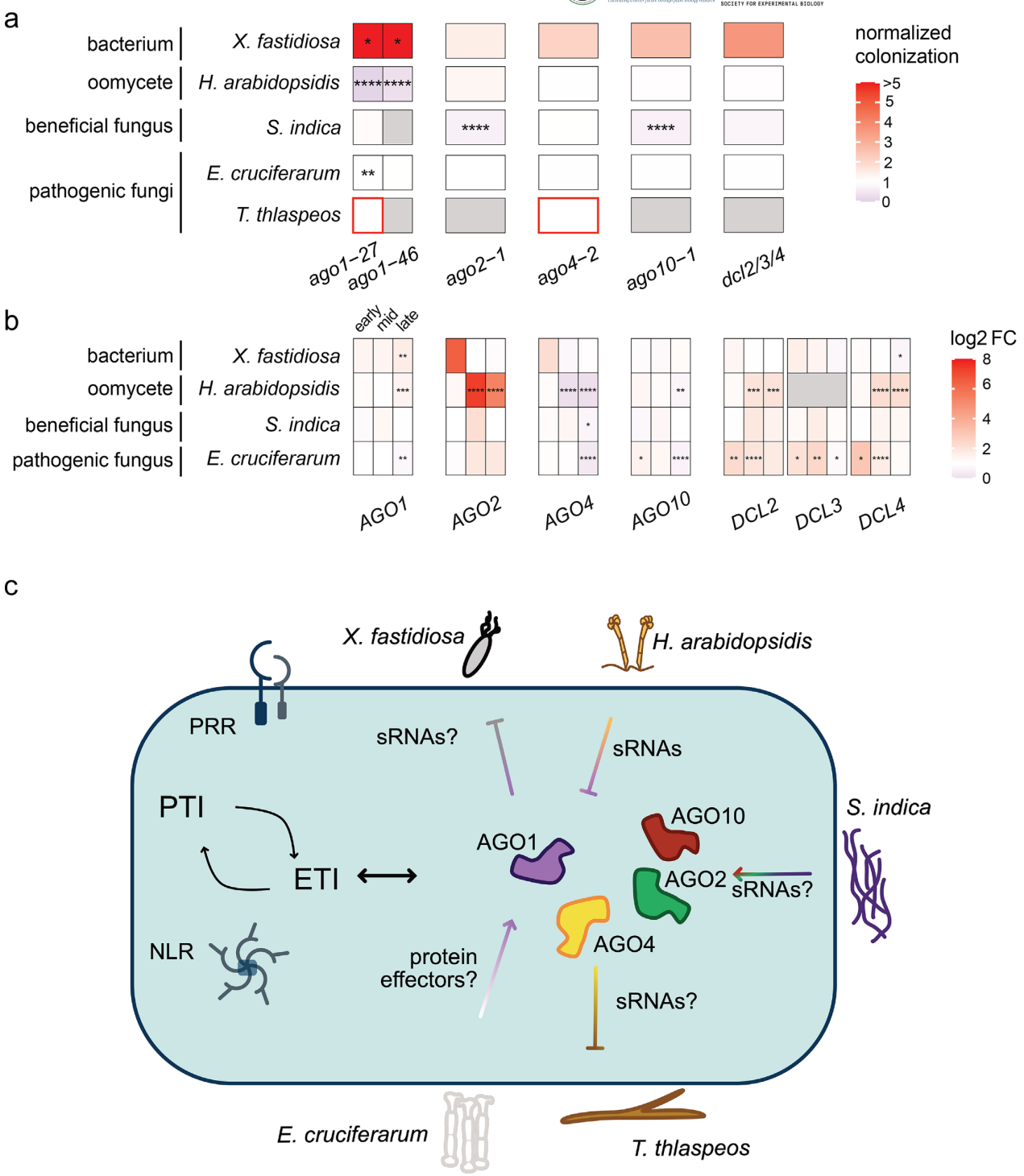

FIGURE 6 Legend on next page.

FIGURE 6 Overall results presented in heat maps and a graphical summary. (a) The heat map shows the colonization success of *S. indica*, *Xylella fastidiosa*, *T. thlaspeos*, *H. arabidopsidis*, and *E. cruciferarum* in the set of selected Arabidopsis mutants (*ago1*−27, *ago1*−46, *ago2*−1, *ago4*−2, *ago10*−1, *dcl2/3/4*) at 7 dpi, 5 dpi, 2 dpi, 6 dpi, and 2 dpi, respectively to the interacting microbe. Color intensity within each cell represents the degree of colonization success relative to wild-type Col-0 plants, with red indicating more colonization and blue indicating less colonization. Significant differences are marked with asterisks ($\alpha = .05$; adjusted *p*-values: * < .05, < .01, * < .001, **** < .0001). Non-quantifiable colonization success in *T. thlaspeos* is indicated as red boxes to indicated increased colonization. (b) Transcript abundance as log2 (fold change) of the genes of interest (*AGO1*, *AGO2*, *AGO4*, *AGO10*, *DCL2*, *DCL3*, *DCL4*) was assessed at an early, mid, or late infection stage in Col-0 for each microbe. Color intensity within each cell corresponds to the change in gene expression relative to non-inoculated samples, with red indicating upregulation and blue indicating downregulation. Significant differences are indicated with asterisks ($\alpha = .05$, adjusted *p*-values * < .05, < .01, * < .001, **** < .0001). Non-tested conditions are indicated as gray boxes. (c) Proposed model. Potential cross-talk between the plant immune system and the RNA interference pathway influenced by different microbes. Key components of the plant immune system include pattern recognition receptors (PRRs) mediating pattern-triggered immunity (PTI) and nucleotide-binding leucine-rich repeat receptors (NLRs) involved in effector-triggered immunity (ETI). Microbes such as *X. fastidiosa*, *Hyaloperonospora arabidopsidis*, *Serendipita indica*, *Tecaphora thlaspeos*, and *Erysiphe cruciferarum* may interact with the plant immune system indirectly via Argonaute (AGO) proteins. This modulation can occur bidirectionally and might be mediated by small RNAs (sRNAs) and/or effector proteins, depending on the specific microbe involved. The arrows indicate hypothesized relationships based on the presented data.

resistance due to the secretion and accumulation of the Pathogenesis-Related (PR) 1 protein (Zhang et al., 2011). A potential function of AGO1 in restricting *X. fastidiosa* infection may be related to endogenous host sRNAs associated with the control of PTI or its execution (Mitre et al., 2021; Navarro et al., 2006; Zhang et al., 2011). Given that ckRNAi functions in both directions (Cai et al., 2018), plants may also send AGO1-dependent sRNAs to alter *X. fastidiosa* growth, interfering with gene silencing in bacteria (Papenfort & Melamed, 2023).

The identification of AGO4 as a positive control element of resistance to *T. thlaspeos* expands the importance of this AGO protein beyond its requirement for immunity against *Pto* DC3000 and *B. cinerea* (Agorio & Vera, 2007; Rebolledo-Prudencio et al., 2022). Of note, upon infection with *Blumeria graminis* f.sp. *tritici*, *AGO4* was significantly downregulated in the wheat progenitor *Aegilops tauschii*, which was accompanied by a substantial reduction in AGO4a-sorted 24-nt siRNA levels, and enrichment for 'response to stress' gene functions, including receptor kinase, peroxidase, and pathogenesis-related genes, suggesting that AGO4 in some cases is a strong negative regulator of immunity (Geng et al., 2019). It further highlights the involvement of clade III AGOs-mediated TGS in the modulation of plant immunity. Interestingly, AGO1 was not required for *T. thlaspeos* infection at the early stages of colonization. Other AGOs of clade I and clade II need to be investigated to address the putative role of PTGS in this fungal interaction during the established biotrophic phase or during fungal sporulation.

The other tested interactions did not reveal obvious phenotypes. This was unexpected given the functional conservation of AGOs and the ubiquitous expression of key members like *AGO1* and *AGO4* in most tissues, including leaves, roots, and the vasculature (Martín-Merchán et al., 2023; Wook et al., 2011). The transcriptional response of *DCL* and *AGO* genes was mostly not correlated with infection phenotypes in respective mutants. Considering the different infection types, from epidermal (*E. cruciferarum*), leaf mesophyll (*H. arabidopsidis*,, *Pto* DC3000), root (*S. indica*) to vascular tissues (*V. longisporum*, *X. campestris* pv. *campestris*, *X. fastidiosa*, *T. thlaspeos*), a spatiotemporal resolution might be needed to observe changes in gene expression at the actual site of pathogen colonization (Dunker et al., 2020). We speculate that functional redundancy within the DCL and AGO family is likely accounting for wild-type-like phenotypes in some of the tested interactions. This includes the *dcl2/3/4* triple mutant, therefore suggesting potential further redundancy of these three encoded proteins with DCL1. Moreover, infection with *E. cruciferarum* and *X. campestris* pv. *campestris* did not reveal infection phenotypes in the tested mutants (Figure 2b and Figure S4B). This could suggest more functional redundancies among AGO proteins than expected.

To a large extent, the outcome of infection success is determined by the ability of the pathogen to suppress host immunity (Jones et al., 2024). This capacity is encoded in the pathogen's repertoire of diverse molecular effectors (Y. Wang et al., 2022). For example, the virulence of bacterial pathogens like *Pto* DC3000 and *X. campestris* pv. *campestris* mainly involves Type-3-secreted effector proteins (Y. Wang et al., 2022). *X. fastidiosa* lacks a Type-3 secretion system (Landa et al., 2022), and immune-suppressing protein effectors have not been described to date. Thus, the bacterium might not be able to overcome AGO1-mediated defenses. Effector proteins have also been demonstrated to improve infection of powdery mildew fungi such as *E. cruciferarum* (Bourras et al., 2018). It is, therefore, possible that protein effectors could be largely responsible for virulence in a given microbe, contrasting to the virulence mechanisms of *B. cinerea* and *H. arabidopsidis*, which at least in part rely on sRNA-like effectors (Dunker et al., 2020; Weiberg et al., 2013). Moreover, protein effectors could suppress host RNAi (Hou et al., 2019; Navarro et al., 2006). Since pathotypes of microbial subspecies encode different effector repertoires, their interaction with the host's RNAi machinery might differ (Qin et al., 2023; Weiberg et al., 2013).

To conclude, analyzing the role of RNAi in plant immunity across taxonomically diverse microbes may be more complex and might need refined experimental set-ups beyond whole plant phenotyping with improved spatiotemporal resolution. We consider three levels of functional redundancy, which complicate the phenotypic analysis: i) similar or overlapping functions of DCL and AGO clade members, ii) microbial virulence conferred by protein effectors, including iii) microbial protein effectors suppressing host RNAi. Therefore, experimental studies would benefit from using higher-order plant mutants (if not exhibiting severe

developmental phenotypes) and combinatorial analysis with different pathotypes of microbial (sub-)species, as well as microbial mutants compromised e.g. for selected protein effectors or their secretion. Taken together, this phenotypic framework will now make it possible to dissect the molecular mechanisms by which AGOs function, whether host sRNAs modulate the plant's immune system, are secreted to function in the microbe, or if microbe-derived sRNAs are delivered into the plant. Ultimately, this will allow improvement of plant protection.

4 | MATERIAL AND METHODS

4.1 | Plant materials

A. thaliana Col-0 mutants included published *ago1–27*, *ago1–46*, *ago2–1*, *ago4–2*, *ago10–1*, and *dcl2/3/4* (Table S1). Age-matched seeds were used for all experiments. The *eds1–2* mutant was used for propagation of the *E. cruciferarum* inoculum, and the *mlo2–5/6–2/12–1* mutant as an additional control for powdery mildew infection experiments (Bartsch et al., 2006; Consonni et al., 2006).

4.2 | Primers

All primers used in this study are listed in Table S3. The *CDKA* gene expression was used as a reference to assess the expression levels of the selected *AGO/DCL* genes and to quantify microbial growth *in planta* (*H. arabidopsidis*, *X. fastidiosa*) by (RT)-qPCR. For *S. indica* colonization, *UBC21* was used as a reference gene.

4.3 | Microbial infections

4.3.1 | *Hyaloperonospora arabidopsidis*

Plants for infection with *H. arabidopsidis* (GÄUM.) isolate Noco 2, *A. thaliana* plants were grown on soil under long day conditions (16 h light, 8 h dark, 60% relative humidity). Two weeks-old *A. thaliana* plants were inoculated with a final spore concentration of $2*10^4$ spores mL^{-1} as previously described (Ried et al., 2019). For biomass quantification, two leaves and two cotyledons were pooled for one technical replicate, followed by genomic DNA extraction with CTAB and RNase A treatment (Promega) (Chen & Ronald, 1999). The isolated DNAs were diluted to 5 ng/µl. *H. arabidopsidis* gDNA relative to *A. thaliana* was quantified by qPCR with Primaquant low ROX qPCR master mix (Steinbrenner Laborsysteme) according to the manufacturer's instructions (95 °C 3 min, 95 °C 20 s, 60 °C 30 s, 72 °C 40 s, 40 cycles, and subsequent melting curve analysis).

For RT-qPCR, four leaves were pooled for one technical replicate. The CTAB method was used for total RNA extraction (Bemm et al., 2016). Genomic DNA was removed by DNase I digestion (Sigma-Aldrich) following the manufacturer's instructions. For cDNA synthesis with the Maxima H Minus Reverse Transcriptase (Thermo Fisher Scientific) kit, 1 µg of total RNA from each sample was used. Relative gene expression was quantified by qPCR with the Primaquant low ROX qPCR master mix (Steinbrenner Laborsysteme), according to the manufacturer's instructions (95 °C 3 min, 95 °C 20 s, 60 °C 30 s, 72 °C 40 s, 40 cycles, melting curve analysis).

4.3.2 | *Erysiphe cruciferarum*

Plants for *E. cruciferarum* infection were grown on SoMi 513 soil (Hawita, Vechta, Germany) in 9*9 cm pots under short-day conditions with an 8-h photoperiod at 22 °C and 16 h darkness at 20 °C. *E. cruciferarum* (in-house isolate of RWTH Aachen) was cultivated selectively on *A. thaliana eds1–2* (Bartsch et al., 2006) at 20 °C with an 8-h photoperiod. Spores from three pots of plants, collected at 20–28 dpi, were used for the inoculation of 10 pots. For this, four weeks-old healthy Col-0 plants, the selected mutant lines, and the resistant *mlo2–5/6–2/12–1* triple mutant (negative control) were placed in an inoculation tower and heavily infected inoculum plants were gently agitated to release spores. To determine fungal entry rates, for one technical replicate leaves from one plant were harvested at 48 hours post inoculation (hpi) and collected in 80% EtOH for de-staining of leaf pigments. Fungal structures were stained with Coomassie staining solution (45% MeOH (v/v), 10% acetic acid (v/v), .05% Coomassie blue R-250 (w/v)). Samples were double-blinded and leaves were analyzed by light microscopy. The fungal entry rate was determined as the percentage of spores successfully developing secondary hyphae over all spores that attempted penetration, visible by the presence of an appressorium (Kusch et al., 2019). At least 100 interaction sites on leaves of three different plants per independent replicate were analyzed.

For RT-qPCR, total RNA was extracted from leaves of uninoculated Arabidopsis and leaves sampled at 8, 48, or 96 hpi with *E. cruciferarum* using TRI reagent ® (Sigma Aldrich). For one technical replicate, each one leaf of three different plants was pooled. The remaining DNA was digested using DNase I (Thermo Fisher Scientific, USA). For cDNA synthesis, 1 µg RNA was used with the High-Capacity cDNA Reverse Transcription Kit (Applied Biosystems). Relative expression of target genes was quantified by RT-qPCR (95 °C 3 min, 95 °C 10 s, 60 °C 60 s; 40 cycles; melting curve analysis) with the Takyon no ROX SYBR 2X master mix (Eurogentec).

4.3.3 | *Verticilium longisporum*

Arabidopsis mutants used for *V. longisporum (VL43)* (Zeise & Von Tiedemann, 2002)infection were grown directly on soil in a climate chamber with 22 °C/18 °C day/night cycle with 8 h of light. For infection of mutant lines, an inoculation suspension was used. This suspension was prepared by flooding a fully grown three weeks-old culture of *V. longisporum* grown on Potato Dextrose Agar (PDA) agar (Carl Roth, Art. No. X931.1) in a Petri dish at 22 °C, in the dark with 10 ml ddH_2O. The Petri dish was scraped with a small metal spatula to release conidia in suspension. The suspension was filtered through miracloth

(Calbiochem, 475,855) to exclude mycelium, and spore concentration was determined using a hemocytometer (Thoma counting chamber - Marienfeld). The final concentration of the spore suspension was adjusted to 10.000.000 spores/mL. Two weeks-old seedlings of *A. thaliana* (Col-0 and mutant lines) were infected by pipetting 1 ml of inoculation suspension directly in the soil. For one technical replicate, leaf material from one plant was harvested 1, 7, and 35 dpi and ground on liquid nitrogen. Total RNA extraction was done using TRIzol® (Invitrogen) and Zymo RNA Clean & Concentrator-25 Kit with in-column DNase I digestion. cDNA synthesis was generated using 200 ng/µL of the extracted total RNA using RevertAid Reverse transcriptase (Thermo Scientific) following manufacturer guidelines. For subsequent qPCR, the SYBR™ Green PCR Master Mix (Applied Biosystems) was used (Thermo Fisher Scientific 4,309,155). For this, 10 µl reactions were set up, consisting of 5 µl SYBR master mix, .5 µl of each primer, 3.5 µl H_20, and .5 µl cDNA, run with 3 min of 95 °C followed by 40 cycles of 95 °C for 10s, 60 °C for 1 min, and subsequent melting curve analysis, on a QuantStudio 6 Flex (Applied Biosystems).

4.3.4 | *Thecaphora thlaspeos*

One seed of an Arabidopsis line was co-germinated with 300 sterilized teliospores of *T. thlaspeos* (collection 2022, Frantzeskakis et al., 2017) in 300 µl liquid half-strength Murashige and Skoog with Nitrate (MSN) medium (Duchefa) containing 1% sucrose in a well of a 96-well plate. The infections were incubated for four weeks in a light chamber for *A. thaliana* at long-day conditions (120 µE, 12 h 21 °C light, 12 h 18 °C darkness). Seedlings were then stained with wheat germ agglutinin (WGA) and propidium iodide (PI) as previously described (Frantzeskakis et al., 2017) and scored microscopically for fungal infection stages (Zeiss Axio Immager M1). Up to 160 seedlings, each representing one biological replicate, were inspected per line and experiment.

4.3.5 | *Serendipita indica*

A. thaliana mutant lines were grown on vertical square Petri dishes on *A. thaliana* Salt medium (ATS) (Lincoln et al., 1990) without sucrose and supplemented with 4.5 g/l Gelrite (Duchefa #G1101) in a 22 °C day/18 °C night cycle (8 h of light). Spores of *S. indica* (IPAZ-11827, Institute of Phytopathology, Giessen, Germany) were freshly isolated from the plates by scraping the agar using water supplied with .002% Tween 20 added and then filtered through miracloth (Merck Millipore), centrifuged at 3.000 x g for 7 min, then resuspended in water supplied with .002% Tween 20 and adjusted to 500.000 spores mL^{-1}. Roots of 14 days-old plants were inoculated with 1 ml of a suspension of 500.000 chlamydospores mL^{-1} in water with .002% Tween 20 per Petri dish. Control plants were treated with water supplied with .002% Tween 20 (mock). Inoculated roots of different mutants are harvested after seven days, and ground for 1 min at 30 Hz with the pre-cooled Retsch Mill (Tissue Lyser II, Retsch, Qiagen). For one technical replicate, roots from one plate were pooled. For quantification of *S. indica* colonization, genomic DNA was extracted using a Qiagen DNA extraction kit (QIAGEN, 69504). Fungal colonization was quantified using internal transcribed spacer (ITS) primers (see Table S3) and SYBR Green JumpStart Taq ReadyMix (Sigma Aldrich, 1,003,444,642) with a QuantStudio5 Real-Time PCR System (Applied Biosystems). A total of 2 µl ROX (CRX reference dye, Promega, C5411) were added to 1 ml SybrGreen as a passive reference dye that allows fluorescent normalization for qPCR data. The PCR conditions were 95 °C for 5 min followed by 40 cycles of 95 °C for 15 s, 60 °C for 30 s, and 72 °C for 30 s, followed by melting curve analysis.

For *DCL* and *AGO* gene expression, Arabidopsis Col-0 plants were grown on ATS plates and inoculated with *S. indica* spores as previously described above. Control plants were treated with water containing .002% Tween 20 (mock). Inoculated roots were harvested at 1, 3, and 7 dpi, ground with the tissue lyser, and RNA was extracted using Trizol and Zymo kit (Zymo research R2070), with a subsequent in-column DNase digestion. cDNA was generated from 1 µg RNA using Revert Aid Reverse transcriptase. Gene transcription was quantified by qPCR using SYBR Green JumpStart Taq ReadyMix (Sigma Aldrich, 1,003,444,642) with QuantStudio5 Real-Time PCR System (Applied Biosystems). A total of 2 µl ROX (CRX reference dye, Promega, C5411) were added to 1 ml SybrGreen as a passive reference dye that allows fluorescent normalization for qPCR data. The PCR conditions were 95 °C for 5 min, followed by 40 cycles of 95 °C for 15 s, 60 °C for 30 s, and 72 °C for 30 s, followed by a melting curve analysis. *Ubiquitin* (*UBC21*, *AT5G25760*) was used as a housekeeping gene for all experiments. Roots from two ATS plates were harvested and considered as one technical replicate. The results of three or more biological replicates are included in the data analysis.

4.3.6 | *P. syringae* pv. *tomato* DC3000

Plants for *Pto* DC3000 infection were grown on soil with 10 h light and 55% humidity for four to five weeks. *Pto* DC3000 was routinely grown at 28 °C on King's B plates with 1% Agar. Overnight plate-grown *Pto* DC3000 cells were resuspended in 10 mM $MgCl_2$ and .04% Silwet L-77 and diluted to $OD_{600} = .02$. The *A. thaliana* plants were sprayed from below and on top with inoculum. Discs of the infected leaves (one disc per leaf, .6 cm diameter) were excised at 1 dpi and 3 dpi. For one technical replicate, four leaf discs from one plant were pooled and ground in 200 µl 10 mM $MgCl_2$. Serial dilutions were plated on King's B medium with rifampicin (50 µg mL^{-1}) and bacterial colonies were quantified after two days of incubation at 28 °C. At least four plants per genotype and time points were harvested and plated. Results of three independent rounds of infection are included.

For qRT-PCR, for one technical replicate, two inoculated or mock-treated (sprayed with buffer-only) leaves per plant were harvested at 6 hpi, 1 dpi, and 3 dpi. Leaf material was ground using a tissue lyser and RNA extractions performed with Trizol reagent

(Invitrogen, USA) according to the manufacturer's protocol and the Zymo RNA Clean & Concentrator Kit, including in-column DNase treatment. RT-qPCR was performed using the NEB Luna® Universal One-Step RT-qPCR Kit (E3005) according to the manufacturer's instructions (55 °C 10 min, 95 °C 1 min, 95 °C 10 s, 60 °C 30 s, 45 cycles, and subsequent melting curve analysis). Reactions were set-up in duplicates using 10 ng RNA in 10 µl reactions. At least four samples per time point and treatment were analyzed, two rounds of infection were included.

4.3.7 | *X. campestris* pv. *campestris*

Plants for *X. campestris* pv. *campestris* infection were grown on soil with 10 h light and 55% humidity for four to five weeks. *X. campestris* pv. campestris 8004 was routinely grown at 28 °C on NYG (Nutrient Yeast Glycerol Agar, Daniels et al., 1984) media with 1% agar. Inoculum was prepared freshly by scraping bacteria from plates and resuspended in 1x PBS for a final OD_{600} of .4. Four leaves per plant were inoculated by application of 5 µl drops of bacterial suspension onto the midvein of leaves prior to pricking with a .4 * 20 mm needle five times. Plants were covered in a plastic bag for the first two days to create optimal infection conditions with high humidity. Discs of the inoculated leaves (one disc per leaf, .6 cm diameter) were excised at 3 dpi and 5 dpi. For one technical replicate, two leaf discs of one plant were pooled and ground in 200 µl 10 mM $MgCl_2$. Serial dilutions were plated on King's B medium supplemented with rifampicin (50 µg mL^{-1}), and bacterial colonies were quantified at two days after incubation at 28 °C. Suspensions that resulted in no colonies were excluded from the analysis. At least four samples per genotype and time point were harvested and plated. Results of three independent rounds of infection are included.

For qRT-PCR, for one technical replicate, two inoculated or mock-treated leaves per plant were harvested at 1 dpi, 3 dpi, and 7 dpi. RNA extraction and qRT-PCR reactions were performed as described above for *Pto* DC3000.

4.3.8 | *X. fastidiosa* subsp. *fastidiosa*

Plants for *X. fastidiosa* subsp. *fastidiosa* infection were grown on soil with 10 h light and 55% humidity for four to five weeks. *X. fastidiosa* subsp. *fastidiosa* Temecula1 (ATCC 700964) was routinely grown at 28 °C on PD3 plates (Pierce's Disease 3, Davis, 1980) for approx. seven to ten days. The inoculum was prepared freshly by scraping bacteria from the plate and resuspending it in 1x PBS for a final OD_{600} of .5. Four leaves per plant were inoculated by application of 5 µl drops of bacterial suspension onto the midvein of leaves prior to pricking with a .4 * 20 mm needle 5 times. For one technical replicate, two petioles per plant were combined and harvested at 5 dpi and 3 weeks post-inoculation (wpi). RNA was extracted from two petioles of infected samples after disruption with a tissue lyser, using Trizol reagent (Invitrogen, USA) according to the manufacturer's protocol and Zymo RNA Clean & Concentrator Kit, including in-column DNase treatment. qRT- PCR was performed with 10 ng RNA using the NEB Luna® Universal One-Step RT-qPCR Kit (E3005), in 10 µl reactions according to manufacturer guidelines (55 °C 10 min, 95 °C 1 min, 95 °C 10 s, 60 °C 30 s, 45 cycles, and subsequent melting curve analysis) using primers for *Xf16S* and *CDKA* (see Table S3) to normalize for plant material. At least four samples per genotype and time points were analyzed. Results of two independent rounds of infections are included.

For qRT-PCR, for one technical replicate, two inoculated leaves or mock-treated leaves per plant were harvested at 1 dpi, 5 dpi, and 3 wpi. RNA extraction and qRT-PCR reactions were performed as described above for *Pto* DC3000.

4.4 | Statistical analysis

All data was analyzed using R (version 2023.06.0 + 421) and statistical analysis was performed using the stats-package (R: The R Project for Statistical Computing, n.d.). For infection data, mutant measurements were compared to respective measurements in Col-0. For RT-qPCR and qPCR data analysis, expression values were analyzed using the $2^{(-\Delta\Delta ct)}$ method (Livak & Schmittgen, 2001) and normalized against *CDKA* or *UBC21* (*S. indica*) as housekeeping genes and the average of respective mock samples. For *E. cruciferarum*, all time points were compared to T0. Significance was assessed by two-sided Welch's *t*-test ($\alpha = .05$, *p*-values * < .05, ** < .01, *** < .001, **** < .0001) using the stats-package in R. Heat maps were generated using geom_tile of the ggplot package in R depicting average of normalized colonization compared to Col-0 at selected time point or average of log2 foldchange of gene expression at early, mid or late time point. We considered tissue from independently inoculated plants as technical replicates, which were pooled in some instances. Independent biological replicates of the experiments were performed to confirm results at least twice.

4.5 | Use of public data

The heat map showing the differential expression of *DCL* and *AGO* genes (Figure S1) was generated using data from Bjornson et al., 2021 (Tables S1 and S2) with Python v3.11.4 (Van Rossum & Drake, 1995) and Seaborn v0.12.2 (Waskom, 2021).

4.6 | Accession numbers

Genes reported in this article can be found in the GenBank/RGAP databases under the following accession numbers: *AGO1 (AT1G48410), AGO2 (AT1G31280), AGO4 (AT2G27040), AGO10 (AT5G43810), DCL2 (AT3G03300), DCL3 (AT3G43920), and DCL4 (AT5G20320), CDKA (AT3G48750.1), UBC21 (AT5G25760).*

AUTHOR CONTRIBUTIONS

A.R., H.T., S.N., B.L., S.F., J.K., J.S., E.S., S.K., V.G., M.F., A.W., K.H.K., R.P., S.R. designed the methodology; A.R., H.T., S.N., B.L., S.F., T.A., J.P., E.S. performed research; A.R., H.T., S.N., B.L., S.F., V.G., P.B., K.B. analyzed data; A.G., J.K., V.G., A.W., K.H.K., R.P., S.R. conceived the project and supervised the research; A.R., H.T., S.N., S.R. wrote the manuscript with input from all authors.

ACKNOWLEDGMENTS

This work was enabled by grants within the research unit FOR5116 "exRNA" funded by the Deutsche Forschungsgemeinschaft (DFG). Individual grants of this research unit comprise DFG projects FE448/15-1 to M. F, GO 2037/8-1 to A. G, GO 2064/4-1 to V. G., KE 856/8-1 to J.K., KO 1208/32-1 to K.K., PA 861/22-1 to R. P, RO 3550/16-1 to S.R. and WE 5707/2-1 to A.W. S.N. was supported by a Dr. Ernst-Leopold Klipstein Foundation grant. We thank Elif Olkun for technical support. Open Access funding enabled and organized by Projekt DEAL.

CONFLICT OF INTEREST STATEMENT

The authors declare no conflict of interest.

PEER REVIEW

The peer review history forthis article is available in the Supporting Information for this article.

DATA AVAILABILITY STATEMENT

The data that support the findings of this study are available from the corresponding author upon reasonable request.

ORCID

Alessa Ruf https://orcid.org/0000-0003-0919-9717
Sabrine Nasfi https://orcid.org/0000-0001-5916-0824
Johannes Postma https://orcid.org/0009-0002-0565-4487
Patrick Blumenkamp https://orcid.org/0000-0002-7013-9601
Alexander Goesmann https://orcid.org/0000-0002-7086-2568
Julia Kehr https://orcid.org/0000-0003-3617-9981
Jens Steinbrenner https://orcid.org/0000-0003-1008-2268
Arne Weiberg https://orcid.org/0000-0003-4300-4864
Karl-Heinz Kogel https://orcid.org/0000-0003-1226-003X
Ralph Panstruga https://orcid.org/0000-0002-3756-8957
Silke Robatzek https://orcid.org/0000-0002-9788-322X

REFERENCES

Agorio, A., & Vera, P. (2007). ARGONAUTE4 is required for resistance to *Pseudomonas syringae* in Arabidopsis. *The Plant Cell*, *19*(11), 3778–3790. https://doi.org/10.1105/tpc.107.054494

Azevedo, J., Garcia, D., Pontier, D., Ohnesorge, S., Yu, A., Garcia, S., Braun, L., Bergdoll, M., Hakimi, M. A., Lagrange, T., & Voinnet, O. (2010). Argonaute quenching and global changes in Dicer homeostasis caused by a pathogen-encoded GW repeat protein. *Genes & Development*, *24*(9), 904–915. https://doi.org/10.1101/gad.1908710

Bartsch, M., Gobbato, E., Bednarek, P., Debey, S., Schultze, J. L., Bautor, J., & Parker, J. E. (2006). Salicylic acid–independent ENHANCED DISEASE SUSCEPTIBILITY1 signaling in Arabidopsis immunity and cell death is regulated by the monooxygenase FMO1 and the Nudix hydrolase NUDT7. *The Plant Cell*, *18*(4), 1038–1051. https://doi.org/10.1105/tpc.105.039982

Bemm, F., Becker, D., Larisch, C., Kreuzer, I., Escalante-Perez, M., Schulze, W. X., Ankenbrand, M., de Weyer, A.-L. V., Krol, E., Al-Rasheid, K. A., Mithöfer, A., Weber, A. P., Schultz, J., & Hedrich, R. (2016). Venus flytrap carnivorous lifestyle builds on herbivore defense strategies. *Genome Research*, *26*(6), 812–825. https://doi.org/10.1101/gr.202200.115

Bjornson, M., Pimprikar, P., Nürnberger, T., & Zipfel, C. (2021). The transcriptional landscape of *Arabidopsis thaliana* pattern-triggered immunity. *Nature Plants*, *7*(5), 579–586. https://doi.org/10.1038/s41477-021-00874-5

Bouché, N., Lauressergues, D., Gasciolli, V., & Vaucheret, H. (2006). An antagonistic function for Arabidopsis DCL2 in development and a new function for DCL4 in generating viral siRNAs. *The EMBO Journal*, *25*(14), 3347–3356. https://doi.org/10.1038/sj.emboj.7601217

Bourras, S., Praz, C. R., Spanu, P. D., & Keller, B. (2018). Cereal powdery mildew effectors: A complex toolbox for an obligate pathogen. *Current Opinion in Microbiology*, *46*, 26–33. https://doi.org/10.1016/j.mib.2018.01.018

Cai, Q., Qiao, L., Wang, M., He, B., Lin, F.-M., Palmquist, J., Huang, S.-D., & Jin, H. (2018). Plants send small RNAs in extracellular vesicles to fungal pathogen to silence virulence genes. *Science*, *360*(6393), 1126–1129. https://doi.org/10.1126/science.aar4142

Cao, J.-Y., Xu, Y.-P., & Cai, X.-Z. (2020). Integrated miRNAome and transcriptome analysis reveals Argonaute 2-mediated defense responses against the devastating Phytopathogen *Sclerotinia sclerotiorum*. *Frontiers in Plant Science*, *11*, 500. https://doi.org/10.3389/fpls.2020.00500

Chen, D.-H., & Ronald, P. C. (1999). A rapid DNA minipreparation method suitable for AFLP and other PCR applications. *Plant Molecular Biology Reporter*, *17*(1), 53–57. https://doi.org/10.1023/a:1007585532036

Cheng, A.-P., Lederer, B., Oberkofler, L., Huang, L., Johnson, N. R., Platten, F., Dunker, F., Tisserant, C., & Weiberg, A. (2023). A fungal RNA-dependent RNA polymerase is a novel player in plant infection and cross-kingdom RNA interference. *PLOS Pathogens*, *19*(12), e1011885. https://doi.org/10.1371/journal.ppat.1011885

Consonni, C., Humphry, M. E., Hartmann, H. A., Livaja, M., Durner, J., Westphal, L., Vogel, J., Lipka, V., Kemmerling, B., Schulze-Lefert, P., Somerville, S. C., & Panstruga, R. (2006). Conserved requirement for a plant host cell protein in powdery mildew pathogenesis. *Nature Genetics*, *38*(6), 716–720. https://doi.org/10.1038/ng1806

Curaba, J., & Chen, X. (2008). Biochemical activities of Arabidopsis RNA-dependent RNA polymerase 6 *. *Journal of Biological Chemistry*, *283*(6), 3059–3066. https://doi.org/10.1074/jbc.M708983200

Daniels, M. J., Barber, C. E., Turner, P. C., Cleary, W. G., & Sawczyc, M. K. (1984). Isolation of mutants of *Xanthomonas campestris* pv. Campestris showing altered pathogenicity. *Microbiology*, *130*(9), 2447–2455. https://doi.org/10.1099/00221287-130-9-2447

Davis, M. J. (1980). Isolation media for the Pierce's disease bacterium. *Phytopathology*, *70*(5), 425. https://doi.org/10.1094/Phyto-70-425

Deleris, A., Gallego-Bartolome, J., Bao, J., Kasschau, K. D., Carrington, J. C., & Voinnet, O. (2006). Hierarchical action and inhibition of plant Dicer-like proteins in antiviral defense. *Science*, *313*(5783), 68–71. https://doi.org/10.1126/science.1128214

Dunker, F., Trutzenberg, A., Rothenpieler, J. S., Kuhn, S., Pröls, R., Schreiber, T., Tissier, A., Kemen, A., Kemen, E., Hückelhoven, R., & Weiberg, A. (2020). Oomycete small RNAs bind to the plant RNA-induced silencing complex for virulence. *eLife*, *9*, e56096. https://doi.org/10.7554/eLife.56096

Ellendorff, U., Fradin, E. F., de Jonge, R., & Thomma, B. P. H. J. (2009). RNA silencing is required for Arabidopsis defence against Verticillium

wilt disease. *Journal of Experimental Botany*, *60*(2), 591–602. https://doi.org/10.1093/jxb/ern306

Fang, X., & Qi, Y. (2016). RNAi in plants: An Argonaute-centered view. *The Plant Cell*, *28*(2), 272–285. https://doi.org/10.1105/tpc.15.00920

Frantzeskakis, L., Courville, K. J., Plücker, L., Kellner, R., Kruse, J., Brachmann, A., Feldbrügge, M., & Göhre, V. (2017). The plant-dependent life cycle of *Thecaphora thlaspeos*: A smut fungus adapted to Brassicaceae. *Molecular Plant-Microbe Interactions*, *30*(4), 271–282. https://doi.org/10.1094/MPMI-08-16-0164-R

Geng, S., Kong, X., Song, G., Jia, M., Guan, J., Wang, F., Qin, Z., Wu, L., Lan, X., Li, A., & Mao, L. (2019). DNA methylation dynamics during the interaction of wheat progenitor *Aegilops tauschii* with the obligate biotrophic fungus *Blumeria graminis* f Sp. *tritici*. *New Phytologist*, *221*(2), 1023–1035. https://doi.org/10.1111/nph.15432

Guo, N., Zhao, J., Yan, Q., Huang, J., Ma, H., Rajput, N. A., Jiang, H., Xing, H., & Dou, D. (2018). Resistance to *Phytophthora* pathogens is dependent on gene silencing pathways in plants. *Journal of Phytopathology*, *166*(6), 379–385. https://doi.org/10.1111/jph.12695

Hou, Y., Zhai, Y., Feng, L., Karimi, H. Z., Rutter, B. D., Zeng, L., Choi, D. S., Zhang, B., Gu, W., Chen, X., Ye, W., Innes, R. W., Zhai, J., & Ma, W. (2019). A *Phytophthora* effector suppresses trans-kingdom RNAi to promote disease susceptibility. *Cell Host & Microbe*, *25*(1), 153–165. e5. https://doi.org/10.1016/j.chom.2018.11.007

Huang, C.-Y., Wang, H., Hu, P., Hamby, R., & Jin, H. (2019). Small RNAs – Big players in plant-microbe interactions. *Cell Host & Microbe*, *26*(2), 173–182. https://doi.org/10.1016/j.chom.2019.07.021

Iwakawa, H.-O., & Tomari, Y. (2022). Life of RISC: Formation, action, and degradation of RNA-induced silencing complex. *Molecular Cell*, *82*(1), 30–43. https://doi.org/10.1016/j.molcel.2021.11.026

Ji, L., Liu, X., Yan, J., Wang, W., Yumul, R. E., Kim, Y. J., Dinh, T. T., Liu, J., Cui, X., Zheng, B., Agarwal, M., Liu, C., Cao, X., Tang, G., & Chen, X. (2011). ARGONAUTE10 and ARGONAUTE1 regulate the termination of floral stem cells through two MicroRNAs in Arabidopsis. *PLoS Genetics*, *7*(3), e1001358. https://doi.org/10.1371/journal.pgen.1001358

Jones, J. D. G., Staskawicz, B. J., & Dangl, J. L. (2024). The plant immune system: From discovery to deployment. *Cell*, *187*(9), 2095–2116. https://doi.org/10.1016/j.cell.2024.03.045

Jullien, P. E., Schröder, J. A., Bonnet, D. M. V., Pumplin, N., & Voinnet, O. (2022). Asymmetric expression of Argonautes in reproductive tissues. *Plant Physiology*, *188*(1), 38–43. https://doi.org/10.1093/plphys/kiab474

Kusch, S., Thiery, S., Reinstädler, A., Gruner, K., Zienkiewicz, K., Feussner, I., & Panstruga, R. (2019). Arabidopsis mlo3 mutant plants exhibit spontaneous callose deposition and signs of early leaf senescence. *Plant Molecular Biology*, *101*(1), 21–40. https://doi.org/10.1007/s11103-019-00877-z

Landa, B. B., Saponari, M., Feitosa-Junior, O. R., Giampetruzzi, A., Vieira, F. J. D., Mor, E., & Robatzek, S. (2022). Xylella fastidiosa's relationships: The bacterium, the host plants, and the plant microbiome. *New Phytologist*, *234*(5), 1598–1605. https://doi.org/10.1111/nph.18089

Li, Y., Zhang, Q., Zhang, J., Wu, L., Qi, Y., & Zhou, J.-M. (2010). Identification of MicroRNAs involved in pathogen-associated molecular pattern-triggered plant innate immunity. *Plant Physiology*, *152*(4), 2222–2231. https://doi.org/10.1104/pp.109.151803

Lincoln, C., Britton, J. H., & Estelle, M. (1990). Growth and development of the axr1 mutants of Arabidopsis. *The Plant Cell*, *2*(11), 1071–1080.

Livak, K. J., & Schmittgen, T. D. (2001). Analysis of relative gene expression data using real-time quantitative PCR and the $2^{-\Delta\Delta CT}$ method. *Methods*, *25*(4), 402–408. https://doi.org/10.1006/meth.2001.1262

López, A., Ramírez, V., García-Andrade, J., Flors, V., & Vera, P. (2011). The RNA silencing enzyme RNA polymerase V is required for plant immunity. *PLoS Genetics*, *7*(12), e1002434. https://doi.org/10.1371/journal.pgen.1002434

Martín-Merchán, A., Moro, B., Bouet, A., & Bologna, N. G. (2023). Domain organization, expression, subcellular localization, and biological roles of ARGONAUTE proteins in Arabidopsis. *Journal of Experimental Botany*, *74*(7), 2374–2388. https://doi.org/10.1093/jxb/erad030

Melotto, M., Zhang, L., Oblessuc, P. R., & He, S. Y. (2017). Stomatal defense a decade later. *Plant Physiology*, *174*(2), 561–571. https://doi.org/10.1104/pp.16.01853

Mitre, L. K., Teixeira-Silva, N. S., Rybak, K., Magalhães, D. M., de Souza-Neto, R. R., Robatzek, S., Zipfel, C., & de Souza, A. A. (2021). The Arabidopsis immune receptor EFR increases resistance to the bacterial pathogens *Xanthomonas* and *Xylella* in transgenic sweet orange. *Plant Biotechnology Journal*, *19*(7), 1294–1296. https://doi.org/10.1111/pbi.13629

Navarro, L., Dunoyer, P., Jay, F., Arnold, B., Dharmasiri, N., Estelle, M., Voinnet, O., & Jones, J. D. G. (2006). A plant miRNA contributes to antibacterial resistance by repressing auxin signaling. *Science*, *312*(5772), 436–439. https://doi.org/10.1126/science.1126088

Obbard, D. J., Gordon, K. H. J., Buck, A. H., & Jiggins, F. M. (2008). The evolution of RNAi as a defence against viruses and transposable elements. *Philosophical Transactions of the Royal Society, B: Biological Sciences*, *364*(1513), 99–115. https://doi.org/10.1098/rstb.2008.0168

Papenfort, K., & Melamed, S. (2023). Small RNAs, large networks: Post-transcriptional regulons in gram-negative bacteria. *Annual Review of Microbiology*, *77*, 23–43. https://doi.org/10.1146/annurev-micro-041320-025836

Qin, S., Veloso, J., Baak, M., Boogmans, B., Bosman, T., Puccetti, G., Shi-Kunne, X., Smit, S., Grant-Downton, R., Leisen, T., Hahn, M., & van Kan, J. A. L. (2023). Molecular characterization reveals no functional evidence for naturally occurring cross-kingdom RNA interference in the early stages of *Botrytis cinerea*–tomato interaction. *Molecular Plant Pathology*, *24*(1), 3–15. https://doi.org/10.1111/mpp.13269

R: The R Project for Statistical Computing. (n.d.). Retrieved 21 June 2024, from https://www.r-project.org/

Rebolledo-Prudencio, O. G., Estrada-Rivera, M., Dautt-Castro, M., Arteaga-Vazquez, M. A., Arenas-Huertero, C., Rosendo-Vargas, M. M., Jin, H., & Casas-Flores, S. (2022). The small RNA-mediated gene silencing machinery is required in Arabidopsis for stimulation of growth, systemic disease resistance, and suppression of the nitrile-specifier gene NSP4 by Trichoderma atroviride. *The Plant Journal*, *109*(4), 873–890. https://doi.org/10.1111/tpj.15599

Ren, B., Wang, X., Duan, J., & Ma, J. (2019). Rhizobial tRNA-derived small RNAs are signal molecules regulating plant nodulation. *Science*, *365*, 919–922. https://doi.org/10.1126/science.aav8907

Ried, M. K., Banhara, A., Hwu, F.-Y., Binder, A., Gust, A. A., Höfle, C., Hückelhoven, R., Nürnberger, T., & Parniske, M. (2019). A set of Arabidopsis genes involved in the accommodation of the downy mildew pathogen *Hyaloperonospora arabidopsidis*. *PLoS Pathogens*, *15*(7), e1007747. https://doi.org/10.1371/journal.ppat.1007747

del Sánchez-Correa, M. S., Isidra-Arellano, M. C., Pozas-Rodríguez, E. A., del Rocio Reyero-Saavedra, M., Morales-Salazar, A., del Castillo, S. M. L.-C., Sanchez-Flores, A., Jiménez-Jacinto, V., Reyes, J. L., Formey, D., & Valdés-López, O. (2022). Argonaute5 and its associated small RNAs modulate the transcriptional response during the rhizobia-Phaseolus vulgaris symbiosis. *Frontiers in Plant Science*, *13*, 1034419. https://doi.org/10.3389/fpls.2022.1034419

Šečić, E., Kogel, K.-H., & Ladera-Carmona, M. J. (2021). Biotic stress-associated microRNA families in plants. *Journal of Plant Physiology*, *263*, 153451. https://doi.org/10.1016/j.jplph.2021.153451

Šečić, E., Zanini, S., Wibberg, D., Jelonek, L., Busche, T., Kalinowski, J., Nasfi, S., Thielmann, J., Imani, J., Steinbrenner, J., & Kogel, K.-H. (2021). A novel plant-fungal association reveals fundamental sRNA and gene expression reprogramming at the onset of symbiosis. *BMC Biology*, *19*(1), 171. https://doi.org/10.1186/s12915-021-01104-2

Shen, D., Suhrkamp, I., Wang, Y., Liu, S., Menkhaus, J., Verreet, J.-A., Fan, L., & Cai, D. (2014). Identification and characterization of microRNAs in oilseed rape (*Brassica napus*) responsive to infection with the pathogenic fungus *Verticillium longisporum* using brassica AA (*Brassica rapa*) and CC (*Brassica oleracea*) as reference genomes. *New Phytologist*, *204*(3), 577–594. https://doi.org/10.1111/nph.12934

Silvestri, A., Fiorilli, V., Miozzi, L., Accotto, G. P., Turina, M., & Lanfranco, L. (2019). In silico analysis of fungal small RNA accumulation reveals putative plant mRNA targets in the symbiosis between an arbuscular mycorrhizal fungus and its host plant. *BMC Genomics*, *20*(1), 169. https://doi.org/10.1186/s12864-019-5561-0

Tang, Y., Yan, X., Gu, C., & Yuan, X. (2022). Biogenesis, trafficking, and function of small RNAs in plants. *Frontiers in Plant Science*, *13*, 825477. https://doi.org/10.3389/fpls.2022.825477

Taochy, C., Gursanscky, N. R., Cao, J., Fletcher, S. J., Dressel, U., Mitter, N., Tucker, M. R., Koltunow, A. M. G., Bowman, J. L., Vaucheret, H., & Carroll, B. J. (2017). A genetic screen for impaired systemic RNAi highlights the crucial role of DICER-LIKE 2. *Plant Physiology*, *175*(3), 1424–1437. https://doi.org/10.1104/pp.17.01181

Valdés-López, O., Formey, D., Isidra-Arellano, M. C., del Rocio Reyero-Saavedra, M., Fernandez-Göbel, T. F., & del Socorro Sánchez-Correa, M. (2019). Argonaute proteins: Why are they so important for the legume–*Rhizobia* symbiosis? *Frontiers in Plant Science*, *10*, 1177. https://doi.org/10.3389/fpls.2019.01177

Van Rossum, G., & Drake, F. L. Jr. (1995). *Python reference manual*. Centrum voor Wiskunde en Informatica Amsterdam.

Wang, Z., Hardcastle, T. J., Pastor, A. C., Yip, W. H., Tang, S., & Baulcombe, D. C. (2018). A novel DCL2-dependent miRNA pathway in tomato affects susceptibility to RNA viruses. *Genes & Development*, *32*(17–18), 1155–1160. https://doi.org/10.1101/gad.313601.118

Wang, Y., Pruitt, R. N., Nürnberger, T., & Wang, Y. (2022). Evasion of plant immunity by microbial pathogens. *Nature Reviews Microbiology*, *20*(8), 449–464. https://doi.org/10.1038/s41579-022-00710-3

Waskom, M. L. (2021). seaborn: Statistical data visualization. *Journal of Open Source Software*, *6*(60), 3021. https://doi.org/10.21105/joss.03021

Weiberg, A., Wang, M., Lin, F.-M., Zhao, H., Zhang, Z., Kaloshian, I., Huang, H.-D., & Jin, H. (2013). Fungal small RNAs suppress plant immunity by hijacking host RNA interference pathways. *Science*, *342*(6154), 118–123. https://doi.org/10.1126/science.1239705

Wong-Bajracharya, J., Singan, V. R., Monti, R., Plett, K. L., Ng, V., Grigoriev, I. V., Martin, F. M., Anderson, I. C., & Plett, J. M. (2022). The ectomycorrhizal fungus *Pisolithus microcarpus* encodes a microRNA involved in cross-kingdom gene silencing during symbiosis. *Proceedings of the National Academy of Sciences*, *119*(3), e2103527119. https://doi.org/10.1073/pnas.2103527119

Wook, K., Eamans, A. L., & Waterhouse, P. M. (2011). RNA processing activities of the Arabidopsis Argonaute protein family. In P. Grabowski (Ed.), *RNA processing*. INTECH. https://doi.org/10.5772/22686

Yu, X., Hou, Y., Chen, W., Wang, S., Wang, P., & Qu, S. (2017). *Malus hupehensis* miR168 targets to ARGONAUTE1 and contributes to the resistance against *Botryosphaeria dothidea* infection by altering defense responses. *Plant and Cell Physiology*, *58*(9), 1541–1557. https://doi.org/10.1093/pcp/pcx080

Zeise, K., & Von Tiedemann, A. (2002). Host specialization among vegetative compatibility groups of *Verticillium dahliae* in relation to *Verticillium longisporum*. *Journal of Phytopathology*, *150*(3), 112–119. https://doi.org/10.1046/j.1439-0434.2002.00730.x

Zhan, J., & Meyers, B. C. (2023). Plant small RNAs: Their biogenesis, regulatory roles, and functions. *Annual Review of Plant Biology*, *74*, 21–51. https://doi.org/10.1146/annurev-arplant-070122-035226

Zhang, X., Zhao, H., Gao, S., Wang, W.-C., Katiyar-Agarwal, S., Huang, H.-D., Raikhel, N., & Jin, H. (2011). Arabidopsis Argonaute 2 regulates innate immunity via miRNA393*—mediated silencing of a Golgi-localized SNARE gene, MEMB12. *Molecular Cell*, *42*(3), 356–366. https://doi.org/10.1016/j.molcel.2011.04.010

Zou, Y., Wang, S., Zhou, Y., Bai, J., Huang, G., Liu, X., Zhang, Y., Tang, D., & Lu, D. (2018). Transcriptional regulation of the immune receptor FLS2 controls the ontogeny of plant innate immunity. *The Plant Cell*, *30*(11), 2779–2794. https://doi.org/10.1105/tpc.18.00297

SUPPORTING INFORMATION

Additional supporting information can be found online in the Supporting Information section at the end of this article.

How to cite this article: Ruf, A., Thieron, H., Nasfi, S., Lederer, B., Fricke, S., Adeshara, T., Postma, J., Blumenkamp, P., Kwon, S., Brinkrolf, K., Feldbrügge, M., Goesmann, A., Kehr, J., Steinbrenner, J., Šečić, E., Göhre, V., Weiberg, A., Kogel, K.-H., Panstruga, R., Robatzek, S., & on behalf of the exRNA consortium (2024). Broad-scale phenotyping in Arabidopsis reveals varied involvement of RNA interference across diverse plant-microbe interactions. *Plant Direct*, *8*(11), e70017. https://doi.org/10.1002/pld3.70017

MANUSCRIPT - Ruf et al., 2025 *tbs*

Hfq is integrated into transcriptional networks in *Xylella fastidiosa* supporting lifestyle transition and systemic infection in plants

Alessa Ruf[1], Elif Olkun[1], Jingli Lao[1], Vincent Ohlhauser[1], Neysa Rodriguez[1], Marta Martin-Rivero[1], Andreas Klingl[1], and Silke Robatzek[1, #]

Summary

An important virulence determinant of the phytopathogenic bacterium *Xylella fastidiosa* (*Xf*) is the shift between planktonic and biofilm growth state which is triggered by environmental changes. In this study, we revealed that the RNA chaperone Hfq plays a central role in the regulatory networks governing this process. As a result, generated Δ*hfq* mutants are disrupted in planktonic growth, twitching motility and systemic colonisation in plants, leading to reduced virulence. Transcriptomic profiling of *Xf* wildtype and Δ*hfq* cells suggest that Hfq functions within transcriptional networks of two-component regulatory systems, facilitating drastic transcriptional changes required for the change into a different growth state. By sequencing size-selected transcripts, we annotated *de novo* sRNAs in *Xf*. Target prediction revealed candidate sRNAs which might be involved in the Hfq-based regulation of growth state switches. Remarkably, Hfq and sRNAs localise to *Xf* extracellular vesicles, which could enable the regulation of synchronised colony-wide lifestyle switches. Taken together, these findings expand our understanding of bacterial regulatory networks and enlarges the molecular understanding on how *Xf* coordinates its virulence.

Contribution

Alessa Ruf: conceptualizing and planning of experiments, performing research and analysis, bioinformatic analysis, supervising, writing of original draft of manuscript.

Elif Olkun: conceptualizing and planning of experiments, performing research and analysis, review and editing of manuscript.

Jingli Lao: performing research and analysis (Arabidopsis infections, qPCR).

Vincent Ohlhauser: performing research and analysis (generation of constructs for homologous recombination, mutant phenotyping, nutrient downshifts, life/dead staining, sequencing, bioinformatic analysis), methodology writing.

Neysa Rodriguez: generation of mutant, technical support, *Xylella* culturing.

Marta Martin-Rivero: generation of mutant, tobacco infections, extraction of DNA, technical support, *Xylella* culturing, methodology writing.

Andreas Klingl: electron microscopy, scientific discussion, funding acquisition.

Silke Robatzek: Funding acquisition, conceptualizing and design of experiments, scientific discussion, writing original draft of manuscript.

I hereby confirm that the indicated contributions to the manuscript “Hfq is integrated into transcriptional networks in *Xylella fastidiosa* supporting lifestyle transition and systemic infection in plants” are correct.

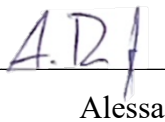

Alessa Ruf (1st author)

Silke Robatzek (Last author)

Hfq is integrated into transcriptional networks in *Xylella fastidiosa* supporting lifestyle transitions and systemic infection in plants

Alessa Ruf[1], Elif Olkun[1], Jingli Lao[1], Vincent Ohlhauser[1], Neysa Rodriguez[1], Marta Martin-Rivero[1], Andreas Klingl[1], and Silke Robatzek[1, #]

[1]LMU Munich Biocenter, Ludwig-Maximilian-University of Munich, Großhaderner Strasse 4, 82152 Martinsried, DE

[#]Correspondence: Silke Robatzek
LMU Munich Biocentre
Tel.: +49-2180-74124
Email: robatzek@bio.lmu.de

Manuscript information: Abstract (145 words), text excluding references (6'419 words).
Number of figures: 8 main figures; 8 supplemental figures.

Abstract

Xylella fastidiosa causes serious disease in many crops, yet how it coordinates virulence at the transcriptional level remains poorly understood. A hallmark of its infection strategy is the ability to switch between planktonic growth and biofilm formation in response to environmental cues such as nutrient availability. Here, we identify the RNA chaperone Hfq as a central regulator of these lifestyle transitions. Hfq is required for normal planktonic growth, early steps of biofilm formation including twitching motility, and efficient escape from local infection sites to enable systemic colonization in plants. Integrated transcriptomic analyses of mRNA and sRNAs revealed that Hfq controls the abundance of transcriptional regulators through sRNA-mRNA interactions, influencing broad regulatory networks. Strikingly, Hfq also associated with extracellular vesicles which might facilitate colony-wide coordinated lifestyle switches. Together, our findings position Hfq as a key regulatory hub coordinating environmental adaptation and plant virulence in *X. fastidiosa*.

Keywords: Hfq, small RNAs, extracellular vesicles, twitching motility, transcriptional regulators, biofilm, cell-cell aggregation

Introduction

Xylella fastidiosa (*Xf*) is a bacterial pathogen responsible for a rising number of economically devastating plant diseases worldwide, including Pierce's Disease (PD) in grapevine, Citrus Variegated Chlorosis (CVC), and the Olive Quick Decline Syndrome (OQDS) in southern Europe[1–3]. In grapevine, *Xylella fastidiosa* subsp. *fastidiosa* causes leaf scorch, stunted shoot growth, and progressive vine decline, ultimately leading to plant death if unmanaged[4,5]. *X. fastidiosa* is transmitted by xylem-feeding hemipteran vectors, such as sharpshooters and spittlebugs, which introduce the bacteria directly into the plant's xylem[6]. The bacterium then colonizes vessels, spreads systemically through the vasculature, and establishes persistent infections that disrupt water transport and induce desiccation stress in plants[3].

The virulence of *Xf* is closely linked to its capacity to switch between planktonic and biofilm-forming states[7]. This transition is triggered by environmental cues such as nutrient availability and Ca^{2+} levels[8–11], beginning with the attachment of planktonic cells via fimbrial and afimbrial adhesins[12]. This is followed by cell-cell aggregation mediated by Type I- and Type-IV pili[13] and the production of an extracellular matrix rich in exopolysaccharides (EPS)[14,15]. *Xf* biofilm

development is regulated by quorum sensing (QS), mediated by diffusible signalling factors (DSFs) such as *cis*-2-tetradecenoic acid[16]. DSF is synthesized by the Regulation of Pathogenicity Factor F (RpfF) enzyme in a cell density-dependent manner[17]. The two-component regulatory system consisting of the sensor kinase RpfC and regulator RpfG mediate DSF perception[18]. Another two-component system consisting of sensor kinase PhoQ and response regulator PhoP[19], along with the second messenger cyclic di-GMP (c-di-GMP)[20,21], respond to environmental cues such as low Mg^{2+} in the xylem, also regulating biofilm and cell-cell aggregation.

Xf's ability to attach to surfaces and form biofilms enhances its insect transmissibility[22,23]. In plants, surface attachment facilitates colonization of xylem vessels under continuous sap flow[12]. Cell-cell aggregation can reduce hydraulic conductivity, contributing to drought stress, while larger biofilm structures may block vessels, triggering disease symptoms[24]. Yet, *Xf* mutants defective in surface attachment or cell-cell aggregation are often hypervirulent in grapevine, as reduced adhesion facilitates their systemic spread[22,25,26].

The switch from biofilm to planktonic state in *Xf* is associated with increased production of extracellular vesicles (EVs), likely in the form of outer membrane vesicles (OMVs). *Xf*-EVs block bacterial interactions with vessel walls due to the presence of adhesins on the vesicle corona[27,28]. The release of *Xf*-EVs is regulated by the DSF-mediated QS[27]. EVs also facilitate the secretion of *Xf* virulence factors, including cell wall modulating enzymes such as the lipase/esterase LesA[29]. Alongside polygalacturonase PglA and the β-1,4-endoglucanases EngXCA1 and EngXCA2, which are secreted via the Type II secretion system, these enzymes are believed to facilitate bacterial migration within xylem vessels by degrading pit membranes[30–33]. This activity promotes systemic spread, enables colonization of new xylem vessels, and likely releases carbohydrates that support bacterial growth and survival. Moreover, twitching motility, which depends on Type IV-pili and is regulated by Ca^{2+}, is essential for *Xf*'s ability to migrate against the direction of the transpiration stream[9].

Additional virulence traits of *Xf* include the modulation of its lipopolysaccharide (LPS) composition, which helps shield the bacterium from recognition by the plant immune system[1], and the detoxification of reactive oxygen species (ROS), enabling *Xf* to withstand host-induced oxidative stress during colonizatio[34,35]. Interestingly, a mutant in the redox-sensing transcription factor OxyR was impaired in surface attachment, cell-cell aggregation, and

biofilm maturation, indicating that ROS may serve as environmental cue that stimulates biofilm development[36]. The redox switch Biofilm Growth-Associated Repressor (BigR) also facilitates biofilm growth in response to environmental sulphide levels[37–39].

We recently discovered that *Xf*-EVs carry small RNAs (sRNAs), designated *sXF*s, which are capable of targeting host immunity genes[28]. The tested target genes were significantly downregulated during *Xf* infection in *Arabidopsis thaliana,* with one of them also showing reduced expression following treatment with *Xf*-EVs, suggesting that *sXF*s may play a role in modulating host immune responses. Additionally, we found that the *Xf*-EV corona was decorated with RNA-binding proteins (RBPs), including Host Factor for Phage Q beta (Hfq)[28]. Hfq, a global RNA chaperone, forms homohexameric, ring-shaped structures that facilitates nucleic acid binding[40]. Hfq can control gene expression by stabilizing and protecting sRNAs from ribonucleolytic degradation and mediating their interactions with target mRNAs[41,42]. Notably, one of the stem loops of *sXF*s contains three conserved Hfq binding motifs, suggesting that Hfq may play a role in stabilizing *sXF*s and enhancing their impact on host immunity.

In the plant pathogens *Agrobacterium tumefaciens* and *Erwinia amylovora*, as well as in human pathogens including *Pseudomonas aeruginosa* and *Vibrio cholerae*, Hfq regulates virulence determinants and the transition between planktonic and biofilm lifestyles[43–47].
In *Xf*, the extent of Hfq's regulatory role and the identity of its associated sRNAs remain largely undefined. Here, we investigate the role of Hfq and sRNAs in regulating the transition from planktonic to biofilm states in *Xylella fastidiosa* subsp. *fastidiosa* Temecula1 (*Xff* Tem1), a highly virulent isolate linked to PD that can colonize the experimental model plants *Arabidopsis thaliana*[48] and *Nicotiana tabacum*[49]. Through targeted mutagenesis, transcriptomic profiling, and functional assays, we found that Hfq and sRNAs are integrated into *Xf*'s signal-response systems. These include QS- and environmental-sensing systems which control the motility of this bacterium and with that, also it's virulence.

Results

Xff *Tem1 Δ*hfq *bacteria are locked in biofilm state*

To investigate the role of Hfq in the lifestyle and virulence of *Xff* Tem1, we generated a Δ*hfq* mutant via homologous recombination, inserting a kanamycin resistance cassette into the *hfq* gene (Supplemental Figures S1a, S1b, S1c, S1d). When cultured in the rich PD2 medium, Δ*hfq*

bacteria showed impaired macroscopic planktonic growth and visibly reduced surface-attached biofilm compared to wild type (WT) *Xff* Tem1 (Figures 1a, 1b). Quantification of planktonic cells revealed a significant reduction in Δ*hfq* cell density relative to WT (Figure 1c). By contrast, biofilm formation was increased in the Δ*hfq* mutant (Figure 1d), resulting in an elevated biofilm-to-planktonic cell ratio (Figure 1e). This observation is also confirmed by elevated exopolysaccharide (EPS) levels in Δ*hfq* (1.6 µg/ml) compared to WT (0.5 µg/ml) (Figure 1f). Cells of Δ*hfq* aggregate more than WT cells, with approx. 30 % of cell aggregated in WT and 90 % aggregated in Δ*hfq* (Figure 1g). Fringe widths of *Xf* growing on agar plates supplemented with Ca^{2+} were reduced in Δ*hfq* compared to WT (Figures 1h, 1i), indicating reduced levels of twitching motility in Δ*hfq*. Electron microscopy revealed morphological differences between WT and Δ*hfq* mutant cells, with the Δ*hfq* mutant exhibiting a significant reduction in pili structures, particularly in planktonic cells (Figures 1i, 1j). These observations indicate that Hfq is involved in regulating cell-to-cell attachments and motility, ultimately influencing the planktonic and biofilm lifestyles of *Xff* Tem1.

Sudden nutrient downshift assay triggers cell growth change dependent on Hfq

Next, we examined how growth in the minimal medium 3G10-R, which more closely resembles conditions in xylem sap[50], affects *Xff* Tem1. Given the fastidious growth of *Xff* Tem1, we first pre-cultured the bacteria in PD2 medium and then conditioned them in either fresh PD2 or 3G10-R for 4, 8, 24, and 96 hrs (Supplemental Figures S2a-d). No significant impact on cell viability was observed either 4 hrs or 4 days post-medium shift (Supplemental Figures S3a, S3b). In WT, planktonic growth of *Xff* Tem1 increased over time in both media, but more planktonic cells were present in PD2 compared to 3G10-R (Supplemental Figure S2b). By contrast, biofilm formation was greater in 3G10-R between 4-24 hrs, but decreased at 96 hrs, reaching lower levels than in PD2 (Supplemental Figure S2c). Consequently, the biofilm-to-planktonic cell ratio increased between 4-24 hrs in 3G10-R, whereas in PD2, this ratio increased at 96 hrs (Supplemental Figure S2d). As a proxy to fluctuating conditions between insect vector and plant host xylem sap in *Xff* Tem1's life cycle, the sudden nutrient downshift induces rapid adaptive responses, such as biofilm formation and dispersal.

Hfq facilitates transcriptomic responses to sudden nutrient downshift

To dissect the Hfq-dependent networks that govern the transition between planktonic and biofilm lifestyles in *Xff* Tem1, we performed comparative RNA-seq on WT and Δ*hfq* bacteria

following the nutrient downshift. Using a recent re-annotation of the *Xff* Tem1 reference genome[51], a total of 2'383 coding sequences (CDS) were identified in *Xff* Tem1 WT and Δ*hfq* across four biological replicates per condition, representing 98.65% of all annotated CDS. The Principal Component Analysis (PCA) revealed clear transcriptomic separation among the four sample types (WT and Δ*hfq* strains grown in PD2 and 3G10-R media, respectively) (Figure 2a). PC1 accounted for 82% of the variance, distinguishing between bacterial genotypes, while PC2 captured 13% of the variance related to media conditions (Figure 2a). While both *Xff* Tem1 WT and Δ*hfq* cells respond transcriptomically to the sudden nutrient downshift, this response is significantly less pronounced in the absence of Hfq (Figures 2a, 2b, 2d, 2e). In response to the nutrient downshift, *Xff* Tem1 WT exhibited 446 differentially expressed genes (DEGs), representing 18% of all CDS, with 230 genes upregulated and 216 downregulated in 3G10-R compared to PD2 (Fold change >/< 1.5 and BH-corrected p-value < 0.05) (Figures 2b, 2d). By contrast, Δ*hfq* exhibited 251 DEGs, approximately 10% of CDS, with 148 upregulated and 103 downregulated genes in response to nutrient shift (Figures 2b, 2e). In both media conditions, the absence of Hfq has a strong influence on the cellular transcriptome (Figures 2a, 2c, 2f, 2g) with 626 genes differentially expressed in Δ*hfq* in PD2 (Figure 2 c, f) and 829 genes in 3G10-R compared to WT (Figures 2c, 2g).

In *Xf*, the Type IV-pilus is a very large multi-protein complex consisting of over 30 proteins mediating twitching motility[52]. Retraction ATPases PilT (PD_1147) and PilU (PD_1148) enable cell movement by readily degrading the pilus, resulting in pulling forward of the cell. Significant reduced expression of both retraction ATPases in 3G10-R in WT (Figures 2d, 3a) indicate reduced twitching motility, leading to increased biofilm formation as observed in response to the nutrient downshift in WT (Supplemental Figure S2c). Δ*hfq* cells are blocked in biofilm formation (Figure 1b, 1d, 1f, 1g, 1h) and retraction ATPases *pilT* and *pilU* are not significantly differently regulated in Δ*hfq* in response to the nutrient downshift (Figures 2e, 3a). One of the two homologous c-di-GMP receptors, *pilZ* (PD_1497), is significantly upregulated in response to the nutrient downshift only in WT, indicating an increased sensitivity to c-di-GMP resulting in the inhibition of pilus motor activity (Figures 2d, 2e, 3a). All three pilus component-encoding genes are differentially expressed when comparing WT and Δ*hfq* gene expression with increased levels of *pilU* and *pilT* and decreased levels of *pilZ* in PD2 conditions in Δ*hfq* (Figures 2f, 2g, 3b), indicating a role of Hfq in regulating the expression of these three pilus component-encoding genes in a sudden nutrient downshift. Most of the Type IV-pilus and (a)fimbrial adhesins encoding genes do not directly respond to the

nutrient downshift but are differentially expressed when comparing WT and Δ*hfq* cells (Figures 2d-g, Supplemental Figure S4a). In total, 22 pilus and (a)fimbrial genes were differentially regulated between WT and Δ*hfq* cells in both media conditions (Figures 2f, 2g, 3c, Supplemental Figure S4a) resulting in an drastically reduced twitching motility (Figure 1h, 1i) and increased cell-to-cell attachment (Figure 1g) as observed in *Xff* Tem1 Δ*hfq* compared to *Xff* WT. Taken together, the absence of Hfq reduces the responsiveness of *Xff* pilus motor activity to the nutrient downshift and leads to an overall dysregulation of attachment and motility in *Xff*.

Hfq modulates the expression of transcriptional regulators and quorum sensing system in response to nutrient downshift

To gain more insight into what biological processes were unique in response to the nutrient downshift in *Xff* Tem1 WT compared to Δ*hfq*, we performed Gene Ontology (GO) analysis on differentially expressed genes (DEGs) in response to the nutrient downshift in WT and in Δ*hfq* (Supplemental Figures S4b, S4c). Genes associated with metabolic and biosynthetic processes were most prominently affected by the nutrient downshift (Supplemental Figures S4b, S4c): In particular, genes related to methionine, threonine and histidine biosynthesis were upregulated in both genotypes, though the upregulation was less pronounced in Δ*hfq (*Supplemental Figure S5a). Interestingly, the two molecular functions “unfolded protein binding” and “DNA-binding transcription factor activity” were exclusively associated with DEGs in response to nutrient downshift in WT but not in Δ*hfq* (Figure 3d), indicating an upstream role of Hfq in regulating the expression of transcription factors in the adjustment to the sudden nutrient downshift.

Hence, we next focussed on transcriptional regulators, which responded to the nutrient downshift only in WT but not in Δ*hfq*. Of note, *ompA* (PD_1699), one of the first mRNAs identified to be regulated by Hfq in bacterial model organism *Escherichia coli*[53], was also differentially expressed in our set-up (Figure 4a). We identified seven transcriptional regulators with a differential response to nutrient downshift between WT and Δ*hfq* (Figure 4a). This includes the expression of transcription factors *biofilm-growth associated repressor* (*bigR*, PD_1891), the response regulator *popP/phoP* (PD_1679) and *tryptophan operon repressor* (*trpR*, PD_0871), of which all three were only responsive to the nutrient downshift in WT, but not in Δ*hfq*. BigR is a sulphite-sensing transcriptional repressor of plant-associated bacteria which regulates genes implicated in biofilm growth[37,39]. In *Xanthomonas citri* subsp. *citri,*

PhoP regulates a global signalling network coordinating the adjustment to host environment, including motility, biofilm formation and expression of virulence factors[54]. In *Xf*, PhoP is involved in the regulation of biofilm formation and cell-cell aggregation and is essential for *Xf*'s virulence in grapevine[55]. In *Xanthomonas oryzae* pv. *oryzae,* TrpR is involved in stress tolerance, motility and virulence by regulating the expression of sigma factor *rpoD*[56]. The attenuator sRNA *rnTrpl* regulates expression of tryptophane in an Hfq-dependent manner in *E. coli*[57,58]. Additionally, the negative regulator of sigma E activity *rseA* (PD_1285) is regulated by sRNAs *RyhB* and *FnrS* in *E. coli*[59] and *rseA* regulates its own operon. In *Xff* Tem1, the *rseA* operon also includes *algU* (PD_1284) which influences cell-cell aggregation, attachment, biofilm and virulence in *Xf* [60]. It also increases the expression of RNA polymerase sigma-H factor *algH* (PD_1276) in *Xf* [60], a transcriptional regulator also responsive to the nutrient downshift in WT but not in Δ*hfq* (Figure 4a). Additionally, we find 26 transcriptional regulators differentially expressed between WT and Δ*hfq* in at least one media condition, of which 11 are also responsive to the sudden nutrient downshift, indicating their potential regulation by Hfq (Supplemental Figure S5b, S5c). This includes *bolA* (PD_1468), which is a described transcriptional switch in *E. coli*, reducing motility for biofilm development[61] and three homologues of *marR/yyba* (PD_0175; PD_0595; PD_0707), a QS-controlled transcription factor regulating motility in *Pseudomonas syringae* pv. *tabaci*[62].

The DSF-mediated QS-system regulates biofilm formation and virulence in *Xf* [22,63]. To see if components of the QS-system are also responsive in our set-up, we checked their transcriptional response to the nutrient down-shift in WT and Δ*hfq*. Intriguingly, both homologues of response regulator1 *rpfG* (PD_0405; PD_2050), Glutamate methyltransferase *cheB* (PD_0849), Chemotaxis protein *cheW* (PD_0850), and histidine kinases *rpfC* and *cheY* (PD_0675; PD_0406) respond to nutrient downshift in WT but not in Δ*hfq* (Figure 4b). The DSF-synthase *rpfF* (PD_0407) and CoA-ligase *rpfB* (PD_0233) respond strongly to the sudden nutrient downshift, also in the absence of Hfq. Of note, genes of described virulence factors lipase/esterase *lesA* (PD_1703)[29] and O-antigen ligase *wzy* (PD_0814)[1] also show Hfq-dependent expression (Figure 4c). Taken together, our set-up identified several transcriptional regulators and parts of the QS-system which (i) regulate observed growth phenotypes in response to nutrient downshift and (ii) are dependent on Hfq.

Expression of sRNA adjusts in response to nutrient downshift

Hfq is commonly associated with sRNA-mediated regulation[40]. For a *de novo* annotation of sRNAs in *Xff* Tem1, we first performed sRNA sequencing of size-selected transcripts of WT bacteria following the nutrient downshift (Supplemental Figure 6a). To reduce false positives from degraded mRNA fragments, we skipped fragmentation in the library preparation. Paired-end sequencing and analysis with the sRNA detection pipeline APERO[64] revealed 726 (PD2) and 740 (3G10-R) high-confidence sRNA candidates in *Xff* Tem1 (size < 251; freq > 99). Depending on their genomic origin, APERO classifies sRNAs into CDS-spanning (sense and antisense) and intergenic sRNAs (intergenic, 5' or 3' untranslated regions) (Supplemental Figures S6b-e). To further reduce false-positive from mRNA degradation products, we excluded all sRNAs deriving from sense CDS regions, *i.e.* filtering for antisense and intergenic sRNAs. We identified 346 (336) antisense, 224 (232) intergenic and 24 (28) antisense/intergenic sRNAs in PD2 (3G10-R) (Supplemental Figure S6c, S6d). This means a total of 594 sRNAs in PD2 and 596 sRNAs in 3G10-R, of which 254 (27%) were shared in both conditions (Figure 5a). We also compared expression levels of shared sRNAs found in both media conditions using DESeq2 (Supplemental Figures S6a, S6e). We found 36 sRNAs upregulated in PD2 and 20 sRNAs upregulated in 3G10-R (Figure 5b) across two biological replicates per conditions. Taken together, we identified 376 sRNAs enriched or unique to rich media (PD2-sRNAs) and 362 sRNAs enriched or unique to xylem-mimicking conditions (3G10R-sRNAs).

sRNAs have predicted UTR targets including operons of rpfG, bigR *and* trpR

To gain insight into potential *cis* and *trans* interactions of sRNAs with bacterial transcripts, we performed target prediction of PD2- and 3G10-R-sRNAs using the IntaRNA tool with optimized parameters for genome-wide sRNA target prediction ("IntaRNAsTar")[65]. For this, we generated a manually curated annotation file, which contained CDS of *Xff* Tem1 as well as untranslated regions (UTRs). To identify Hfq-dependent sRNA interactions, we focused on 5'-UTRs of previously identified DEGs, whose response to the sudden nutrient downshift was Hfq-dependent (Figure 4). The PD2-sRNA *XF25802* derives from the 3'-UTR of *lysS* (PD_0404), reaching into the intergenic region between *lysS* and the *rpfG-rpfC* operon (PD_0405; PD_0406) (Figure 5c). *XF25802* forms a stable secondary structure (Figure 5d) and is exclusively found in PD2. *XF25802* also covers the ribosomal binding site (RBS) of *rpfG-rpfC*, which might be the reason for the Hfq-dependent downregulation of both genes observed in PD2 compared to 3G10-R media (Figure 4, Supplemental Figure S7). Interactions of sRNAs

in *trans*, include the PD2-sRNA *XF37402* which can bind to the RBS of the operon that contains *bigR* (PD_1891) and forms a stable secondary structure (Figures 5e, 5f). *XF37402* is encoded antisense to the sulfate ABC transporter permease subunit *cysT*/*cysU* (PD_0589), which is upregulated in PD2 only in WT. The stable 3G10R-sRNA *XF65031* can bind to the RBS of the open reading frame of *trpR* (PD_0871) in *trans* (Figures 5g, 5h), which might reduce the expression of the tryptophane repressor in response to the nutrient downshift (Figure 4). The expression of genes of all three selected operons shows Hfq-dependence in their response to the nutrient downshift (Supplemental Figure S7).

EV-delivered Hfq and sRNAs facilitate cell-to-cell communication

The transition between biofilm and planktonic states correlates with increased *Xff* Tem1 vesiculation[27]. Therefore, we examined whether a sudden nutrient downshift and Hfq influence EV production. The EV concentration from *Xff* Tem1 WT increased at 4 h after shifting to 3G10-R medium compared with PD2, which was also observed in Δ*hfq* mutants, albeit to a lesser extent (Figure 6a). In both media conditions, Δ*hfq* vesiculates less than WT cells. Moreover, Hfq is found at the corona of *Xff* Tem1 EVs[28]. We confirmed the presence of Hfq at the EV corona by immunogold labelling of untreated EVs, Proteinase K-treated and bursted (hypotonic buffer-treated) EVs (Figure 6b). Similar to DSFs, which are delivered by EVs[27,66], sRNAs associated with Hfq might regulate colony-wide transcriptional changes.

Hfq is required for systemic infection

We next examined how disruption of Hfq impacts the bacterium's virulence. As a model, we used *A. thaliana*, which is known to be colonized by *Xff* Tem1[48]. Interestingly, Δ*hfq* bacteria exhibited significantly higher loads in total tissue compared to WT (Figure 7a). Bacterial loads in distal tissues were reduced in WT and Δ*hfq* when normalized to the site of inoculation (petiole) (Figure 7b) with bacterial loads in distal tissues more reduced in Δ*hfq* than WT bacteria (Figure 7b). These findings suggest that although Δ*hfq* bacteria proliferate more robustly at the local infection site, they are impaired in systemic colonization. In *A. thaliana*, infection with *Xf* is mostly asymptomatic[67]. Hence, we performed infection assays in *Nicotiana tabacum* cultivar SR1[68]. Leaf scorching symptomsm, visible as browning, appeared 7 weeks post quadruple infection on locally infected leaves, to a much higher extend in WT-infected plants than Δ*hfq*-infected plants (Figure 7c). After 8 weeks, leaf scorching appeared in upper, newer leaves exclusively in WT-infected plants. Browning symptoms were absent in PBS-

infected control plants (Supplemental Figure 8). Taken together, Hfq-dependent expression of virulence factors *lesA* and *wzy* (Figure 4c) and reduced motility in Δ*hfq*, also reduces the systemic spread of *Xf* in plants.

Discussion

Hfq and associated sRNAs integrate environmental cues for changing conditions

Xff Tem1, like other bacteria, must constantly adjust its transcriptional program to respond to environmental changes, including shifts in nutrient availability. One of the major challenges is the transition between biofilm state and planktonic growth, which is a key determinant of its systemic spread in the plant and consequently, of virulence[23,27]. The transition is mediated by quorum sensing factors[21,63], two-component regulatory systems[19] and responses to sensed changing nutrient conditions, such as *e.g.* hypoxia[38,39]. Plant responses leading to differences in xylem ion composition such as Ca^{2+} or the presence of ROS molecules might also function as environmental cues for *Xff* Tem1[10,36]. In response, *Xff* Tem1 must rapidly reprogram its transcriptome to achieve increased motility and decreased cell-to-cell and surface attachment. We used a sudden nutrient downshift assay as a proxy for changing conditions *Xf* encounters in the plant. This set-up suggests that the RNA chaperone Hfq plays a critical role in regulating the transition between planktonic and biofilm states in *Xff* Tem1. In Δ*hfq*, *Xff* Tem1 fails to respond transcriptionally to changed conditions which locks cells in aggregated, non-motile states resulting in biofilm growth and only local infection.

These findings establish Hfq as a key regulatory hub controlling lifestyle transition in *Xff* Tem1, and consequently of systemic plant infection (Figure 8). A similar role for Hfq has been identified in plant-pathogenic bacteria *Erwinia amylovora*, where Hfq and associated sRNAs regulate motility and biofilm dispersal, resulting in reduced virulence in Hfq knock-out mutants[47,46,69,43]. Studies in potato and rice pathogens *Dickeya oryzae* and *Dickeya dadantii* also place Hfq as central role coordinating motility, biofilm formation and expression of virulence factors[70,71]. Collectively with our findings, this points to a conserved role of Hfq in synchronizing motility, biofilm behaviour, and virulence during host infection.

Regulation of targets via Hfq is predominantly mediated through associated sRNAs[40]. sRNA-based regulation is very dynamic and highly adjustable to changing conditions[72,73]. Our pipeline identified the expression of over 350 antisense and intergenic sRNA candidates enriched or unique to each media condition, indicating a very dynamic adjustment of sRNA repertoire in *Xff* Tem1 to the sudden nutrient downshift. Target predictions of these sRNAs,

suggest that Hfq-mediated regulation is integrated into broader regulatory systems facilitating lifestyle switches in *Xff* Tem1. Feed-forward loops integrating Hfq-bound sRNAs into transcriptional circuits mediated by transcription factors can amplify signals and rapidly reprogram transcription to support drastic lifestyle changes under shifting environmental conditions[74]. A well-characterized example of such an sRNA-integrated feed-forward loop is the FarS-FadR circuit in *Vibrio cholerae*, where transcription factors and sRNA-mediated regulation together regulate fatty acid metabolism[75]. Taken together, our results highlight the importance of sRNA-mediated regulation of lifestyle switches in *Xff* Tem1 and its virulence.

Extracellular delivery of Hfq and sRNAs might support colony-wide lifestyle changes

We confirmed the association of Hfq with EVs of *Xff* Tem1. In *E. coli*, association of Hfq with EVs depends on the growth state of the bacteria[76], indicating a dynamic adjustment of EV-association of Hfq. Through the integration of Hfq into membranes, Hfq is speculated to deliver sRNAs across cellular boarders while retaining sRNA-binding capacities[77,78]. In our previous work, we found virulence-related sRNAs associated with EVs[28]. Whether the here identified sRNAs that mediate colony-wide lifestyle changes are also being delivered to neighbouring cells via EV-associated Hfq, awaits validation. These findings would further implicate EVs in colony-wide QS, a process previously associated with the delivery of diffusible signal factors by EVs[27,66]. For example, in human bacterial pathogen *Pseudomonas aeruginosa* (*Pa*), biofilm and virulence are regulated by intracellular and extracellular functions of QS-signals and Hfq bound to specific sRNAs. QS-signals as well as Hfq and QS-regulating sRNAs are associated with *Pa* EVs, and collectively modulate the transcription of QS-regulatory genes of bacterial populations[79].

We therefore propose a model in which Hfq and its associated sRNAs are integrated into sensing and regulatory processes in response to changed environment conditions, mediating lifestyle switches and ultimately systemic colonization *in planta* (Figure 8).

Material & Method

Culturing of Xff *and growth curves*

Xylella fastidiosa subsp. *fastidiosa* strain Temecula1 (*Xff* Tem1) was routinely grown for 5-10 days on Pierce's Disease 3 (PD3) plates[80], for *Xff* Tem1-GFP supplemented with 50 µg/mL Kanamycin. For liquid cultures, 200 mL PD2[80] was inoculated with resuspended *Xff* inoculum in 1x phosphate buffered saline pH 7.4 (1x PBS) and cultures were grown for 4-7 days at 28 °C and 140 rpm reaching an $OD_{600} > 0.2$.

Generation of mutants in Xff

Xff knockout mutants were generated via homologous recombination as previously reported[81]. Briefly, linear fragments of around 800 nt starting 600 nt upstream and 560 nt downstream of Hfq were amplified from *Xff* genomic DNA with overlaps (Supplemental Figure S1). The Kanamycin-resistance cassette (KanR) was amplified from pDONR201 with matching overlaps and fragments were assembled into pGG-A-pJ23119-B using Gibson Assembly following NEBuilder standard protocol (NEB #E2621). Final constructs were confirmed via sequencing and knock-out cassette was amplified from the construct using Q5-polymerase (NEB #M0493) and purified. For transformation, *Xff* Tem1 was resuspended in 1x PBS to reach OD_{600} 0.5, plated as single droplets onto PD3 plates supplemented with 1 µM $CaCl_2$ and covered with a droplet of 1 ng of linear PCR-fragment. After three days, mixture was plated onto fresh PD3 plates, supplemented with 1 µM $CaCl_2$ and 50 µg/mL Kanamycin. After 2 weeks, single colonies were resuspended in 1x PBS and transferred onto new PD3 plates with 50 µg/mL Kanamycin. Successful integration of KanR was confirmed by colony PCR, qRT-PCR and whole genome sequencing. RNA-seq reads of WT and Δ*hfq* were aligned to the *Xff* Tem1 reference genome (GCF_000007245.1) and visualized using CLC Main Workbench 20.0.4 (https://digitalinsights.qiagen.com/).

Nutrient downshift assay

For sudden nutrient downshift assays, pre-cultured *Xff* cultures were split in half, pelleted at 4'000 x *g* for 15 min at RT and resuspended in either PD2 or 3G10-R media[82]. Depending on the assay, cultures were incubated for 4 h, 24 h or 4 days at 28 °C and 140 rpm. Then, cells were pelleted at 4'000 x *g* for 15 min and flash frozen in liquid nitrogen and stored at -80 °C

414 until further use. Supernatants were filtered through 0.22 µm filters (Millipore, SEGTPT0045)
415 and kept at 4 °C until further use.
416

417 ***Biofilm and planktonic growth measurements***

418 Biofilm formation of *Xff* was quantified using crystal violet assays as described before[83]. In
419 brief, 200 µL bacterial cultures were grown in 96-well plates at 28° C and 140 rpm. After 4 h,
420 8 h, 24 h and 96 h the supernatant was transferred to a new plate and planktonic growth was
421 quantified by OD_{600}. To measure biofilm growth, the plate was washed twice with 200 µL 1x
422 PBS and stained with 200 µL 0.1% (w/v) crystal violet (Merck V5265) for 20 min. Then, the
423 crystal violet solution was removed, and the wells were washed twice with 1x PBS. The bound
424 dye was recovered with 33% acetic acid (w/v), and the absorbance was measured at 570 nm.
425 A total of three biological replicates per strain were measured with twelve technical replicates
426 each.
427

428 ***EPS staining***

429 EPS were quantified using a phenol-sulfuric acid assay[15]. In brief, *Xff* cultures were grown in
430 25 mL PD2 until they reached $OD_{600} > 0.2$, then they were pelleted at 7'000 rpm for 20 min at
431 4 °C 10 mL of supernatant was mixed with 30 mL cold 96% ethanol and incubated for 30 min
432 at -80 °C, then centrifuged at 7'000 rpm for 20 min at 4 °C. Pellets were washed twice with 10
433 mL cold 70% ethanol and pellets were disrupted by adding 10 mL of water and glass beads,
434 followed by incubation for 1 h at 250 rpm. Then, 100 µL from each sample was collected and
435 mixed with 100 µL 5% phenol and 500 µL concentrated sulfuric acid and put on ice for a few
436 minutes to cool down. Absorbance was measured at 488 nm and EPS concentrations were
437 calculated based on a standard curve of known concentrations of glucose. A total of three
438 biological replicates per strain were measured with six technical replicates each.
439

440 ***Aggregation assay***

441 Cell aggregation of each strain was quantified based on[15]. Briefly, *Xff* cultures were grown in
442 25 mL PD2 to reach $OD_{600} > 0.2$. Then cultures were left standing for 20 min for settling of the
443 cell aggregates. 1 mL supernatant from the top of culture was taken and its absorbance was
444 measured at 540 nm (OD_s). Then the whole culture was vortexed thoroughly, 1 mL of culture
445 was taken and dispersed with tissue homogenizer for 1 min, and the turbidity was measured at

540 nm (OD_t). The percentage of cell aggregation was calculated by [(OD_t-OD_s)/OD_t] x100. A total of three biological replicate per strain was measured, with eight technical replicates each.

Motility assay

Motility was assessed based on the protocol from[84] with slight modifications. *Xff* strains grown on PD3 plates were collected and resuspended in 1xPBS, and OD_{600} was adjusted to 0.5. Six droplets of 10 µL for each strain were dropped on PD3 with 1% agar supplemented with a final concentration of 1 mM $CaCl_2$ to promote motility. After 3 days of incubation at 28 °C, the fringe morphology of the colonies was imaged using THUNDER Imager (Leica, Germany) with a HC PL Fluotar L 40×/0.60 dry objective and images were analysed using Fiji/ImageJ[85]. A total of three biological replicates per strain were measured with five technical replicates each.

Cell viability assay

The cell viability assay was performed based on[86] using a GFP-tagged version of *Xff* Tem1. In brief, *Xff* cultures were stained with 20 µM Propidium iodide (PI, SigmaAldrich, #81845) for 5 min and samples were imaged using THUNDER Imager (Leica, Germany) with a HC PL Fluotar L 40×/0.60 dry objective. The samples were excited at 510 nm, and the emission was detected at 535 nm (GFP) or 590 nm (PI). As a positive control, bacteria were killed by boiling at 98 °C for 5 min prior to staining and imaging.

EV isolation and nanoparticle tracking analysis

Xff-EV isolation and enzyme treatments was performed as described previously[28]. In brief, 200 mL cultures were centrifuged at 4’000 x *g* for 15 min and supernatants were filtered through 0.22 µm filters (Milipore, SEGTPT0045). Filtered supernatants were centrifuged at 38’000 x *g* for 1 h to remove cellular debris, then further centrifuged at 150’000 x *g* for 4 h and pellets were purified using qEV2 iZON size exclusion chromatography (SEC)-columns (iZon qEV2 columns, 70 nm series, IC2-70, France). *Xf*-EV containing fractions were split into two and kept untreated or treated with 100 µg Proteinase K (ProtK, 800U, NEB, P81075) for 30 min at 37 °C and reaction was stopped by addition of 6.6 µL of 100 mM PMSF and incubation at room temperature for 5 min. Then, fractions were concentrated using Amicon centrifugal columns 30 kDa (Milipore, UFC9030). For hypotonic treatments, concentrated EVs were

resuspended in hypotonic buffer (2 mM Tris-HCl, 1 mM MgCl2, 1 mM KCl)[87] and incubated over-night at 4 °C.

Vesiculation assays and NTA measurements

Particle numbers in filtered supernatants (4'000 x *g*, 15 min, then 0.22 µm filters Millipore, SEGTPT0045) after nutrient downshift were measured using nanopore tracking analyser (Zeta View, Particle Metrix, Germany). Supernatants were diluted to a concentration which resulted in approx. 200-300 particles per window; vesicle size and charge (Zeta Potential, ζ) were determined with three measurements per samples for at least three biological replicates per condition.

Transmission electron microscopy and immunogold labelling

For transmission electron microscopy (TEM), bacterial cells were negatively stained with 1% uranyl acetate. Microscopy was carried out at 200 kV using a JEOL F200 (JEOL, Japan), equipped with a 20 mega pixel CMOS camera. For immune-negative staining untreated SEC-purified *Xff*-EVs, Proteinase K-treated or hypotonic treated *Xff*-EVs were incubated with the primary antibody (Goat polyclonal antibody to HFQ, antibodies.com A121619) and visualized using secondary antibody (donkey anti-goat, coupled to 10 nm colloidal gold, dilution: 1:20) as previously reported[88]. In brief, 15 µL EV fractions were applied to mesh nickel grids and incubated with primary antibody for 30 min and secondary antibody for 30 min, negatively stained with 1% uranyl acetate for 2 minutes, and air dried. The immuno-negative stained samples were investigated using a Zeiss EM912 (Zeiss, Oberkochen, Germany) at 80 kV acceleration voltage. Images were acquired using a 2k × 2k slow-speed CCD camera (TRS Tröndle Restlichverstärker-Systeme, Moorenweis, Germany).

RNA isolation and RNA sequencing

Total RNA was isolated from pellets using Trizol and RNA was purified using RNA Clean & Concentrator Kit with DNase treatment (ZymoResearch, R1013) following standard manufacturer's guidelines (for total RNA) or sRNA purification protocols (for sRNA). RNA integrity and size was checked using a Bioanalyzer (Agilent). Ribosomal RNA (rRNA) depletion, library preparation and sequencing was performed by Novogene (Munich, Germany) using Illumina NovaSeq X Plus Series with 150-nt read length in paired-read mode. For total

RNA-seq of *Xff* Tem1 WT and Δ*hfq* 4 replicates per condition (genotype, media) were sequenced with 10M reads per sample and for sRNA-seq of *Xff* Tem1 WT RNA two replicates per media condition were sequenced with 16M reads per sample. For sRNA-seq, rRNA depletion was skipped, and libraries were prepared without fragmentation.

Transcriptomic analysis

The data was pre-processed, mapped, and counted with Curare v.0.6.0[89]. This workflow used Trim Galore v.0.6.10 (https://www.bioinformatics.babraham.ac. uk/projects/trim_galore/) for quality control and adapter trimming with default settings. Mapping was performed with Bowtie 2 v.2.5.2 in "--very-sensitive" mode[90]. Mapping results in SAM format were converted with SAMtools v.1.18[91]. Using featureCounts[92], reads per transcript were counted. Differential expression analysis was carried out using DESeq2[93]. Regularized log-transformed (rlog) expression values obtained from DESeq2 were used to compute gene-wise Z-scores, representing relative expression levels across samples. Gene Ontology (GO) term enrichment analysis was conducted using the enricher()-function from the clusterProfiler package[94].

sRNA annotation

The workflow for sRNA annotation can be found in Supplemental Figure S6. In short, reads were processed and mapped using Curare v.0.6.0[89]. sRNA annotation with APERO[64] was performed on mapped reads of each media condition separately and for shared sRNAs among conditions on merged reads using SAMtools v.1.18[91]. For this, in a first step, candidates were filtered using wmax = 10, min_dist = 10, enrichment = 0.1, min_read_number = 0 (first module), readthrough_proportion = 0.01 (second module). In a second step, candidates were further filtered for size < 251; frequency > 99 and only intergenic and/or antisense sRNAs were kept. sRNAs of class "multiple" were discarded if they had one "CDS-spanning" annotation and otherwise were classified as "antisense" or "intergenic" accordingly. To determine overlapping sRNAs between media conditions, sRNAs were considered the same, if encoded on the same strand and overlapping possible start positions with same length. All shared sRNAs with > 5 reads in each media condition were analysed using featureCounts and DESeq2 to compare counts between media conditions.

Target prediction and sRNA folding

To predict targets of sRNAs, IntaRNA 2.0[65,95] was run with optimized parameters for genome-wide sRNA target prediction ("IntaRNAsTar"), with enriched or unique sRNAs to each media condition. To predict interactions of sRNAs with untranslated regions (UTRs), an annotation file which contains intergenic regions was generated by retrieving all sequences located in-between annotated coding sequences of the Reference genome of *Xff* Tem1 GCF_000007245.1[51]. Predicted interactions were manually checked for overlap with differentially expressed genes from transcriptomics. Secondary structures of sRNAs were obtained with Copra-Tool (http://rna.informatik.uni-freiburg.de; version 5.0.10)[96].

A. thaliana *infections with* Xff

14-day-old *A. thaliana* Colombia-0 seedlings grown on sterile 1/2-Murashige and Skoog media plates with 1% Agar were infected with *Xff* inoculum (1x PBS; OD_{600} 0.3) or mock infected (1xPBS). For infection, 5 µL inoculum was applied onto the end of the hypocotyl and seedlings were pierced 5-6 times with 27G needles. Whole seedlings were harvested three days after infection and tissue was flash-frozen and stored at -80 °C until further usage. For tissue-specific colonization assays, infected petioles ("local") were removed from the rest of the seedling and harvested separately.

DNA extraction and qPCRs on infected plant material

DNA of flash-frozen plant material was extracted using CTAB procedure[97]. Relative bacterial amounts were quantified from 10 ng DNA by qPCR with SYBR Green (ThermoFisher Scientific, A25742), according to the manufacturer's instructions (95 °C 3 min, 95 °C 20 s, 60 °C 30 s, 72 °C 40 s, 40 cycles, melting curve analysis) using *CDKA* and *Xf16S* primers[98].

***Tobacco infections with* Xff**

Nicotiana tabacum 'Petite Havana SR1' were grown under controlled conditions with 11 h light periods (100 µmol/s/m^2) at 22 °C during the day, and 18 °C during the night. Infections were performed as described previously[68,99]. Briefly, 5-week-old tobacco plants were infected with either *Xff* WT, Δ*hfq* (1x PBS, OD_{600} 0.5) or mock (1x PBS) inoculum at day 1, day 3, day 8 and day 10. For infections, 20 µL inoculum was injected near the base of the leaf axil using a 1 mL syringe with 27G needles into four leaves per plant. To increase symptom development, tobacco plants were only mildly watered, and symptoms were observed in 7 weeks post

infection for local symptoms at infected leaves and 8 weeks at systemic leaves. In total, four tobacco plants per treatment were infected and the infection was repeated once.

Statistical analysis

All downstream analysis were performed using R version 2025.09.2+418.

Acknowledgements

We like to thank members of the Robatzek laboratory for fruitful discussions in particular Eliana Mor for careful reading of the manuscript and valuable feedback. We acknowledge Patrick Blumenkamp, Liza Rouyer, Jin Yan Khoo, Santiago Priego-Cubero and Niklas Schandry for bioinformatics support. Funding for computational infrastructure was provided by TRR356 (DFG: 491090170) project I01 and HPC computing was performed on the BioHPC hosted at Leibniz Rechenzentrum Munich funded by the German Research Foundation (grant INST 86/2050-1 FUGG).

We further acknowledge the financial support from the Deutsche Forschungsgemeinschaft provided to S.R. (Heisenberg funding RO 3550/17-1 and RO 3550/18-1) and to A.R. and E.O. (RU5116 “exRNA” RO 3550/16-1 and RO 3550/16-2). Research in the S.R. lab is further supported by the European Research Council (ERC Adv Grant 884235 “MultiX”).

Disclosure of interest

The authors report no conflict of interest.

References

1. Rapicavoli J, Ingel B, Blanco-Ulate B, Cantu D, Roper C. Xylella fastidiosa: an examination of a re-emerging plant pathogen. *Molecular Plant Pathology*. 2018;19(4):786-800. doi:10.1111/mpp.12585

2. Sicard A, Zeilinger AR, Vanhove M, et al. Xylella fastidiosa: Insights into an Emerging Plant Pathogen. *Annual Review of Phytopathology*. 2018;56(Volume 56, 2018):181-202. doi:10.1146/annurev-phyto-080417-045849

3. Landa BB, Saponari M, Feitosa-Junior OR, et al. Xylella fastidiosa’s relationships: the bacterium, the host plants, and the plant microbiome. *New Phytologist*. 2022;234(5):1598-1605. doi:10.1111/nph.18089

4. Hopkins DL. Xylella Fastidiosa: Xylem-Limited Bacterial Pathogen of Plants. *Annual Review of Phytopathology*. 1989;27(Volume 27, 1989):271-290. doi:10.1146/annurev.py.27.090189.001415

5. Castro C, DiSalvo B, Roper MC. Xylella fastidiosa: A reemerging plant pathogen that threatens crops globally. *PLOS Pathogens*. 2021;17(9):e1009813. doi:10.1371/journal.ppat.1009813

6. Backus EA, Laudier D. Functional anatomy of the sharpshooter precibarial valve supports its role in probing behaviors that control inoculation of Xylella fastidiosa. *Sci Rep*. 2025;15(1):34078. doi:10.1038/s41598-025-14208-4

7. De La Fuente L, Merfa MV, Cobine PA, Coleman JJ. Pathogen Adaptation to the Xylem Environment. *Annu Rev Phytopathol*. 2022;60(1):163-186. doi:10.1146/annurev-phyto-021021-041716

8. Cruz LF, Cobine PA, De La Fuente L. Calcium Increases Xylella fastidiosa Surface Attachment, Biofilm Formation, and Twitching Motility. *Appl Environ Microbiol*. 2012;78(5):1321-1331. doi:10.1128/AEM.06501-11

9. Cruz LF, Parker JK, Cobine PA, De La Fuente L. Calcium-Enhanced Twitching Motility in Xylella fastidiosa Is Linked to a Single PilY1 Homolog. *Appl Environ Microbiol*. 2014;80(23):7176-7185. doi:10.1128/AEM.02153-14

10. Parker JK, Chen H, McCarty SE, Liu LY, De La Fuente L. Calcium transcriptionally regulates the biofilm machinery of Xylella fastidiosa to promote continued biofilm development in batch cultures. *Env Micro*. 2016;18(5):1620-1634. doi:10.1111/1462-2920.13242

11. Chen H, De La Fuente L. Calcium transcriptionally regulates movement, recombination and other functions of Xylella fastidiosa under constant flow inside microfluidic chambers. *Microbial Biotechnology*. 2020;13(2):548-561. doi:10.1111/1751-7915.13512

12. Killiny N, Almeida RPP. Xylella fastidiosa Afimbrial Adhesins Mediate Cell Transmission to Plants by Leafhopper Vectors. *Applied and Environmental Microbiology*. 2009;75(2):521-528. doi:10.1128/AEM.01921-08

13. De La Fuente L, Burr TJ, Hoch HC. Autoaggregation of Xylella fastidiosa Cells Is Influenced by Type I and Type IV Pili. *Applied and Environmental Microbiology*. 2008;74(17):5579-5582. doi:10.1128/AEM.00995-08

14. Killiny N, Martinez RH, Dumenyo CK, Cooksey DA, Almeida RPP. The Exopolysaccharide of Xylella fastidiosa Is Essential for Biofilm Formation, Plant Virulence, and Vector Transmission. *MPMI*. 2013;26(9):1044-1053. doi:10.1094/MPMI-09-12-0211-R

15. Castro C, Ndukwe I, Heiss C, et al. Xylella fastidiosa modulates exopolysaccharide polymer length and the dynamics of biofilm development with a β-1,4-endoglucanase. *mBio*. 2023;14(5):e01395-23. doi:10.1128/mbio.01395-23

16. Beaulieu ED, Ionescu M, Chatterjee S, Yokota K, Trauner D, Lindow S. Characterization of a Diffusible Signaling Factor from Xylella fastidiosa. *mBio*. 2013;4(1):10.1128/mbio.00539-12. doi:10.1128/mbio.00539-12

17. He YW, Deng Y, Miao Y, et al. DSF-family quorum sensing signal-mediated intraspecies, interspecies, and inter-kingdom communication. *Trends in Microbiology*. 2023;31(1):36-50. doi:10.1016/j.tim.2022.07.006

18. Dow M. Diversification of the Function of Cell-to-Cell Signaling in Regulation of Virulence Within Plant Pathogenic Xanthomonads. *Science Sig*. 2008;1(21):pe23-pe23. doi:10.1126/stke.121pe23

19. Pierce BK, Kirkpatrick BC. The PhoP/Q two-component regulatory system is essential for Xylella fastidiosa survival in Vitis vinifera grapevines. *Physiological and Molecular Plant Pathology*. 2015;89:55-61. doi:10.1016/j.pmpp.2014.12.003

20. Chatterjee S, Killiny N, Almeida RPP, Lindow SE. Role of Cyclic di-GMP in Xylella fastidiosa Biofilm Formation, Plant Virulence, and Insect Transmission. *MPMI*. 2010;23(10):1356-1363. doi:10.1094/MPMI-03-10-0057

21. de Souza AA, Ionescu M, Baccari C, da Silva AM, Lindow SE. Phenotype Overlap in Xylella fastidiosa Is Controlled by the Cyclic Di-GMP Phosphodiesterase Eal in Response to Antibiotic Exposure and Diffusible Signal Factor-Mediated Cell-Cell Signaling. *Appl Environ Microbiol*. 2013;79(11):3444-3454. doi:10.1128/AEM.03834-12

22. Newman KL, Almeida RPP, Purcell AH, Lindow SE. Cell-cell signaling controls Xylella fastidiosa interactions with both insects and plants. *PNAS*. 2004;101(6):1737-1742. doi:10.1073/pnas.0308399100

23. Chatterjee S, Wistrom C, Lindow SE. A cell–cell signaling sensor is required for virulence and insect transmission of Xylella fastidiosa. *PNAS*. 2008;105(7):2670-2675. doi:10.1073/pnas.0712236105

24. Walker NC. *Investigating Physiological Host Resistance Mechanisms to* Xylella Fastidiosa *Diseases Using XCT Imaging and Mathematical Modelling*. phd. University of Southampton; 2024. Accessed October 27, 2025. https://eprints.soton.ac.uk/490748/

25. Gouran H, Gillespie H, Nascimento R, et al. The Secreted Protease PrtA Controls Cell Growth, Biofilm Formation and Pathogenicity in Xylella fastidiosa. *Sci Rep*. 2016;6(1):31098. doi:10.1038/srep31098

26. Burbank LP, Stenger DC. The DinJ/RelE Toxin-Antitoxin System Suppresses Bacterial Proliferation and Virulence of Xylella fastidiosa in Grapevine. *Phytopathology®*. 2017;107(4):388-394. doi:10.1094/PHYTO-10-16-0374-R

27. Ionescu M, Zaini PA, Baccari C, Tran S, Da Silva AM, Lindow SE. Xylella fastidiosa outer membrane vesicles modulate plant colonization by blocking attachment to surfaces. *Proc Natl Acad Sci USA*. 2014;111(37). doi:10.1073/pnas.1414944111

28. Ruf A, Blumenkamp P, Ludwig C, et al. Extracellular Vesicles From Xylella fastidiosa Carry sRNAs and Genomic Islands, Suggesting Roles in Recipient Cells. *JEV*. 2025;14(6):e70102. doi:10.1002/jev2.70102

685 29. Nascimento R, Gouran H, Chakraborty S, et al. The Type II Secreted Lipase/Esterase LesA
686 is a Key Virulence Factor Required for Xylella fastidiosa Pathogenesis in Grapevines. *Sci*
687 *Rep*. 2016;6(1):18598. doi:10.1038/srep18598

688 30. Roper MC, Greve LC, Warren JG, Labavitch JM, Kirkpatrick BC. Xylella fastidios
689 Requires Polygalacturonase for Colonization and Pathogenicity in Vitis vinifera
690 Grapevines. *MPMI*. 2007;20(4):411-419. doi:10.1094/MPMI-20-4-0411

691 31. Pérez-Donoso AG, Sun Q, Roper MC, Greve LC, Kirkpatrick B, Labavitch JM. Cell Wall-
692 Degrading Enzymes Enlarge the Pore Size of Intervessel Pit Membranes in Healthy and
693 Xylella fastidiosa-Infected Grapevines. *Plant Physiology*. 2010;152(3):1748-1759.
694 doi:10.1104/pp.109.148791

695 32. Ingel B, Jeske DR, Sun Q, Grosskopf J, Roper MC. Xylella fastidiosa Endoglucanases
696 Mediate the Rate of Pierce's Disease Development in Vitis vinifera in a Cultivar-Dependent
697 Manner. *MPMI*. 2019;32(10):1402-1414. doi:10.1094/MPMI-04-19-0096-R

698 33. Ingel B, Castro C, Burbank L, et al. Xylella fastidiosa Requires the Type II Secretion
699 System for Pathogenicity and Survival in Grapevine. *MPMI*. 2023;36(10):636-646.
700 doi:10.1094/MPMI-03-23-0027-R

701 34. Matsumoto A, Young GM, Igo MM. Chromosome-Based Genetic Complementation
702 System for Xylella fastidiosa. *Applied and Environmental Microbiology*. 2009;75(6):1679-
703 1687. doi:10.1128/AEM.00024-09

704 35. Wang P, Lee Y, Igo MM, Roper MC. Tolerance to oxidative stress is required for maximal
705 xylem colonization by the xylem-limited bacterial phytopathogen, Xylella fastidiosa.
706 *Molecular Plant Pathology*. 2017;18(7):990-1000. doi:10.1111/mpp.12456

707 36. Toledo MAS, Schneider DR, Azzoni AR, et al. Characterization of an oxidative stress
708 response regulator, homologous to *Escherichia coli* OxyR, from the phytopathogen *Xylella*
709 *fastidiosa*. *Protein Expression and Purification*. 2011;75(2):204-210.
710 doi:10.1016/j.pep.2010.10.004

711 37. Barbosa RL, Benedetti CE. BigR, a Transcriptional Repressor from Plant-Associated
712 Bacteria, Regulates an Operon Implicated in Biofilm Growth. *J Bacteriol*.
713 2007;189(17):6185-6194. doi:10.1128/jb.00331-07

714 38. Guimarães BG, Barbosa RL, Soprano AS, et al. Plant Pathogenic Bacteria Utilize Biofilm
715 Growth-associated Repressor (BigR), a Novel Winged-helix Redox Switch, to Control
716 Hydrogen Sulfide Detoxification under Hypoxia *. *Journal of Biological Chemistry*.
717 2011;286(29):26148-26157. doi:10.1074/jbc.M111.234039

718 39. de Lira NPV, Pauletti BA, Marques AC, et al. BigR is a sulfide sensor that regulates a sulfur
719 transferase/dioxygenase required for aerobic respiration of plant bacteria under sulfide
720 stress. *Sci Rep*. 2018;8(1):3508. doi:10.1038/s41598-018-21974-x

721 40. Santiago-Frangos A, Woodson SA. Hfq chaperone brings speed dating to bacterial sRNA.
722 *WIREs RNA*. 2018;9(4):e1475. doi:10.1002/wrna.1475

723 41. Updegrove TB, Zhang A, Storz G. Hfq: the flexible RNA matchmaker. *Curr Opin*
724 *Microbiol*. 2016;30:133-138. doi:10.1016/j.mib.2016.02.003

42. Vogel J, Luisi BF. Hfq and its constellation of RNA. *Nat Rev Microbiol*. 2011;9(8):578-589. doi:10.1038/nrmicro2615

43. Peng J, Schachterle JK, Sundin GW. Orchestration of virulence factor expression and modulation of biofilm dispersal in Erwinia amylovora through activation of the Hfq-dependent small RNA RprA. *Molecular Plant Pathology*. 2021;22(2):255-270. doi:10.1111/mpp.13024

44. Chao Y, Vogel J. The role of Hfq in bacterial pathogens. *Current Opinion in Microbiology*. 2010;13(1):24-33. doi:10.1016/j.mib.2010.01.001

45. Wilms I, Möller P, Stock AM, Gurski R, Lai EM, Narberhaus F. Hfq Influences Multiple Transport Systems and Virulence in the Plant Pathogen Agrobacterium tumefaciens. *Journal of Bacteriology*. 2012;194(19):5209-5217. doi:10.1128/jb.00510-12

46. Zeng Q, Sundin GW. Genome-wide identification of Hfq-regulated small RNAs in the fire blight pathogen Erwinia amylovora discovered small RNAs with virulence regulatory function. *BMC Genomics*. 2014;15(1):414. doi:10.1186/1471-2164-15-414

47. Zeng Q, McNally RR, Sundin GW. Global Small RNA Chaperone Hfq and Regulatory Small RNAs Are Important Virulence Regulators in Erwinia amylovora. *J Bacteriol*. 2013;195(8):1706-1717. doi:10.1128/jb.02056-12

48. Mitre LK, Teixeira-Silva NS, Rybak K, et al. The Arabidopsis immune receptor EFR increases resistance to the bacterial pathogens Xanthomonas and Xylella in transgenic sweet orange. *Plant Biotechnol J*. 2021;19(7):1294-1296. doi:10.1111/pbi.13629

49. Francis M, Civerolo EL, Bruening G. Improved Bioassay of *Xylella fastidiosa* Using *Nicotiana tabacum* Cultivar SR1. *Plant Disease*. 2008;92(1):14-20. doi:10.1094/PDIS-92-1-0014

50. Ciraulo MB, Santos DS, Rodrigues AC de FO, et al. Transcriptome Analysis of the Phytobacterium Xylella fastidiosa Growing under Xylem-Based Chemical Conditions. *BioMed Research International*. 2010;2010(1):781365. doi:10.1155/2010/781365

51. Ruf, Robatzek. Genome Annotation Xff Temecula1 (NCBI accession GCF_000007245.1) with Bakta. Published online May 27, 2025. doi:10.5281/zenodo.13970768

52. Merfa MV, Zhu X, Shantharaj D, et al. Complete functional analysis of type IV pilus components of a reemergent plant pathogen reveals neofunctionalization of paralog genes. *PLoS Pathog*. 2023;19(2):e1011154. doi:10.1371/journal.ppat.1011154

53. Udekwu KI, Darfeuille F, Vogel J, Reimegård J, Holmqvist E, Wagner EGH. Hfq-dependent regulation of OmpA synthesis is mediated by an antisense RNA. *Genes Dev*. 2005;19(19):2355-2366. doi:10.1101/gad.354405

54. Wei C, Ding T, Chang C, Yu C, Li X, Liu Q. Global Regulator PhoP is Necessary for Motility, Biofilm Formation, Exoenzyme Production, and Virulence of Xanthomonas citri Subsp. citri on Citrus Plants. *Genes*. 2019;10(5):340. doi:10.3390/genes10050340

762 55. Pierce BK, Kirkpatrick BC. The PhoP/Q two-component regulatory system is essential for
763 *Xylella fastidiosa* survival in *Vitis vinifera* grapevines. *Physiological and Molecular Plant*
764 *Pathology*. 2015;89:55-61. doi:10.1016/j.pmpp.2014.12.003

765 56. Xu Z, Wu G, Wang B, Zhao Y, Liu F. TrpR-Like Protein PXO_00831, Regulated by the
766 Sigma Factor RpoD, Is Involved in Motility, Oxidative Stress Tolerance, and Virulence in
767 Xanthomonas oryzae pv. oryzae. *Phytopathology®*. 2023;113(2):170-182.
768 doi:10.1094/PHYTO-05-22-0165-R

769 57. Li S. Post-Transcriptional Regulation Mechanisms of sRNA rnTrpL in S. meliloti and E.
770 coli. Published online 2020. Accessed October 28, 2025. http://nbn-
771 resolving.de/urn:nbn:de:hebis:26-opus-155786

772 58. Evguenieva-Hackenberg E. Riboregulation in bacteria: From general principles to novel
773 mechanisms of the trp attenuator and its sRNA and peptide products. *WIREs RNA*.
774 2022;13(3):e1696. doi:10.1002/wrna.1696

775 59. London LY, Aubee JI, Nurse J, Thompson KM. Post-Transcriptional Regulation of RseA
776 by Small RNAs RyhB and FnrS in Escherichia coli. *Front Mol Biosci*. 2021;8.
777 doi:10.3389/fmolb.2021.668613

778 60. Shi XY, Dumenyo CK, Hernandez-Martinez R, Azad H, Cooksey DA. Characterization of
779 Regulatory Pathways in Xylella fastidiosa: Genes and Phenotypes Controlled by algU.
780 *Applied and Environmental Microbiology*. 2007;73(21):6748-6756.
781 doi:10.1128/AEM.01232-07

782 61. Dressaire C, Moreira RN, Barahona S, Alves de Matos AP, Arraiano CM. BolA Is a
783 Transcriptional Switch That Turns Off Motility and Turns On Biofilm Development. *mBio*.
784 2015;6(1):10.1128/mbio.02352-14. doi:10.1128/mbio.02352-14

785 62. Taguchi F, Inoue Y, Suzuki T, et al. Characterization of quorum sensing-controlled
786 transcriptional regulator MarR and Rieske (2Fe–2S) cluster-containing protein (Orf5),
787 which are involved in resistance to environmental stresses in Pseudomonas syringae pv.
788 tabaci 6605. *Molecular Plant Pathology*. 2015;16(4):376-387. doi:10.1111/mpp.12187

789 63. Ionescu M, Baccari C, Da Silva AM, Garcia A, Yokota K, Lindow SE. Diffusible Signal
790 Factor (DSF) Synthase RpfF of Xylella fastidiosa Is a Multifunction Protein Also Required
791 for Response to DSF. *J Bacteriol*. 2013;195(23):5273-5284. doi:10.1128/jb.00713-13

792 64. Leonard S, Meyer S, Lacour S, Nasser W, Hommais F, Reverchon S. APERO: a genome-
793 wide approach for identifying bacterial small RNAs from RNA-Seq data. *Nucleic Acids*
794 *Res*. 2019;47(15):e88-e88. doi:10.1093/nar/gkz485

795 65. Mann M, Wright PR, Backofen R. IntaRNA 2.0: enhanced and customizable prediction of
796 RNA–RNA interactions. *Nucleic Acids Res*. 2017;45(Web Server issue):W435-W439.
797 doi:10.1093/nar/gkx279

798 66. Feitosa-Junior OR, Stefanello E, Zaini PA, et al. Proteomic and Metabolomic Analyses of
799 Xylella fastidiosa OMV-Enriched Fractions Reveal Association with Virulence Factors and
800 Signaling Molecules of the DSF Family. *Phytopathology®*. 2019;109(8):1344-1353.
801 doi:10.1094/PHYTO-03-19-0083-R

67. Rogers EE. Evaluation of Arabidopsis thaliana as a Model Host for Xylella fastidiosa. *MPMI*. 2012;25(6):747-754. doi:10.1094/MPMI-11-10-0270

68. Francis M, Civerolo EL, Bruening G. Improved Bioassay of Xylella fastidiosa Using Nicotiana tabacum Cultivar SR1. *Plant Disease*. 2008;92(1):14-20. doi:10.1094/PDIS-92-1-0014

69. Schachterle JK, Zeng Q, Sundin GW. Three Hfq-dependent small RNAs regulate flagellar motility in the fire blight pathogen Erwinia amylovora. *Molecular Microbiology*. 2019;111(6):1476-1492. doi:10.1111/mmi.14232

70. Leonard S, Villard C, Nasser W, Reverchon S, Hommais F. RNA Chaperones Hfq and ProQ Play a Key Role in the Virulence of the Plant Pathogenic Bacterium Dickeya dadantii. *Front Microbiol*. 2021;12. doi:10.3389/fmicb.2021.687484

71. Shi Z, Wang Q, Wang S, Wang C, Zhang LH, Liang Z. Hfq Is a Critical Modulator of Pathogenicity of Dickeya oryzae in Rice Seeds and Potato Tubers. *Microorganisms*. 2022;10(5):1031. doi:10.3390/microorganisms10051031

72. Harfouche L, Haichar F el Z, Achouak W. Small regulatory RNAs and the fine-tuning of plant–bacteria interactions. *New Phytologist*. 2015;206(1):98-106. doi:10.1111/nph.13195

73. Gottesman S, Storz G. Bacterial Small RNA Regulators: Versatile Roles and Rapidly Evolving Variations. *Cold Spring Harb Perspect Biol*. 2011;3(12):a003798. doi:10.1101/cshperspect.a003798

74. Nitzan M, Rehani R, Margalit H. Integration of Bacterial Small RNAs in Regulatory Networks. *Annu Rev Biophys*. 2017;46(Volume 46, 2017):131-148. doi:10.1146/annurev-biophys-070816-034058

75. Huber M, Fröhlich KS, Radmer J, Papenfort K. Switching fatty acid metabolism by an RNA-controlled feed forward loop. *PNAS*. 2020;117(14):8044-8054. doi:10.1073/pnas.1920753117

76. Yu MSC, Chiang DM, Reithmair M, et al. The proteome of bacterial membrane vesicles in Escherichia coli—a time course comparison study in two different media. *Front Microbiol*. 2024;15. doi:10.3389/fmicb.2024.1361270

77. Malabirade A, Morgado-Brajones J, Trépout S, et al. Membrane association of the bacterial riboregulator Hfq and functional perspectives. *Sci Rep*. 2017;7(1):10724. doi:10.1038/s41598-017-11157-5

78. Turbant F, Waeytens J, Campidelli C, et al. Unraveling Membrane Perturbations Caused by the Bacterial Riboregulator Hfq. *Int J Mol Sci*. 2022;23(15):8739. doi:10.3390/ijms23158739

79. Mashburn-Warren L, Howe J, Garidel P, et al. Interaction of quorum signals with outer membrane lipids: insights into prokaryotic membrane vesicle formation. *Mol Microbiol*. 2008;69(2):491-502. doi:10.1111/j.1365-2958.2008.06302.x

80. Davis MJ. Isolation Media for the Pierce's Disease Bacterium. *Phytopathology*. 1980;70(5):425. doi:10.1094/Phyto-70-425

841 81. Kandel PP, Chen H, De La Fuente L. A Short Protocol for Gene Knockout and
842 Complementation in Xylella fastidiosa Shows that One of the Type IV Pilin Paralogs
843 (PD1926) Is Needed for Twitching while Another (PD1924) Affects Pilus Number and
844 Location. *Applied and Environmental Microbiology*. 2018;84(18):e01167-18.
845 doi:10.1128/AEM.01167-18

846 82. Leite B, Andersen PC, Ishida ML. Colony aggregation and biofilm formation in xylem
847 chemistry-based media for Xylella fastidiosa. *FEMS Microbiology Letters*.
848 2004;230(2):283-290. doi:10.1016/S0378-1097(03)00917-0

849 83. Reisner A, Krogfelt KA, Klein BM, Zechner EL, Molin S. In Vitro Biofilm Formation of
850 Commensal and Pathogenic Escherichia coli Strains: Impact of Environmental and Genetic
851 Factors. *Journal of Bacteriology*. 2006;188(10):3572-3581. doi:10.1128/jb.188.10.3572-
852 3581.2006

853 84. D'Attoma G, Morelli M, De La Fuente L, et al. Phenotypic Characterization and
854 Transformation Attempts Reveal Peculiar Traits of Xylella fastidiosa Subspecies pauca
855 Strain De Donno. *Microorganisms*. 2020;8(11):1832.
856 doi:10.3390/microorganisms8111832

857 85. Schindelin J, Arganda-Carreras I, Frise E, et al. Fiji: an open-source platform for
858 biological-image analysis. *Nat Methods*. 2012;9(7):676-682. doi:10.1038/nmeth.2019

859 86. Liang J, Klingl A, Lin YY, Boul E, Thomas-Oates J, Marín M. A subcompatible rhizobium
860 strain reveals infection duality in Lotus. *J Exp Bot*. 2019;70(6):1903-1913.
861 doi:10.1093/jxb/erz057

862 87. Cheng G, Li W, Ha L, et al. Self-Assembly of Extracellular Vesicle-like Metal–Organic
863 Framework Nanoparticles for Protection and Intracellular Delivery of Biofunctional
864 Proteins. *J Am Chem Soc*. 2018;140(23):7282-7291. doi:10.1021/jacs.8b03584

865 88. Janda M, Rybak K, Krassini L, et al. Biophysical and proteomic analyses of Pseudomonas
866 syringae pv. tomato DC3000 extracellular vesicles suggest adaptive functions during plant
867 infection. *mBio*. 2023;14(4):e03589-22. doi:10.1128/mbio.03589-22

868 89. Blumenkamp P, Pfister M, Diedrich S, Brinkrolf K, Jaenicke S, Goesmann A. Curare and
869 GenExVis: a versatile toolkit for analyzing and visualizing RNA-Seq data. *BMC*
870 *Bioinformatics*. 2024;25(1):138. doi:10.1186/s12859-024-05761-2

871 90. Langmead B, Salzberg SL. Fast gapped-read alignment with Bowtie 2. *Nat Methods*.
872 2012;9(4):357-359. doi:10.1038/nmeth.1923

873 91. Li H, Handsaker B, Wysoker A, et al. The Sequence Alignment/Map format and SAMtools.
874 *Bioinformatics*. 2009;25(16):2078-2079. doi:10.1093/bioinformatics/btp352

875 92. Liao Y, Smyth GK, Shi W. featureCounts: an efficient general purpose program for
876 assigning sequence reads to genomic features. *Bioinformatics*. 2014;30(7):923-930.
877 doi:10.1093/bioinformatics/btt656

878 93. Love MI, Huber W, Anders S. Moderated estimation of fold change and dispersion for
879 RNA-seq data with DESeq2. *Genome Biology*. 2014;15(12):550. doi:10.1186/s13059-014-
880 0550-8

881 94. Yu G, Wang LG, Han Y, He QY. clusterProfiler: an R package for comparing biological
882 themes among gene clusters. *OMICS*. 2012;16(5):284-287. doi:10.1089/omi.2011.0118

883 95. Busch A, Richter AS, Backofen R. IntaRNA: efficient prediction of bacterial sRNA targets
884 incorporating target site accessibility and seed regions. *Bioinformatics*. 2008;24(24):2849-
885 2856. doi:10.1093/bioinformatics/btn544

886 96. Raden M, Ali SM, Alkhnbashi OS, et al. Freiburg RNA tools: a central online resource for
887 RNA-focused research and teaching. *Nucleic Acids Research*. 2018;46(W1):W25-W29.
888 doi:10.1093/nar/gky329

889 97. Bemm F, Becker D, Larisch C, et al. Venus flytrap carnivorous lifestyle builds on herbivore
890 defense strategies. *Genome Res*. 2016;26(6):812-825. doi:10.1101/gr.202200.115

891 98. Ruf A, Thieron H, Nasfi S, et al. Broad-scale phenotyping in Arabidopsis reveals varied
892 involvement of RNA interference across diverse plant-microbe interactions. *Plant Direct*.
893 2024;8(11):e70017. doi:10.1002/pld3.70017

894 99. Fuente LDL, Parker JK, Oliver JE, et al. The Bacterial Pathogen Xylella fastidiosa Affects
895 the Leaf Ionome of Plant Hosts during Infection. *PLOS ONE*. 2013;8(5):e62945.
896 doi:10.1371/journal.pone.0062945

897

898 **Figure legends**

899 **Figure 1: Genetic disruption of *Hfq* (Δ*hfq*) locks *Xff* Tem1 cells in biofilm state and**
900 **reduces twitching motility**. **a), b)** In-vitro growth of *Xff* Tem1 WT (a) and Δ*hfq* (b) in PD2
901 medium in flasks after 7 days. **c)** Planktonic growth (OD_{600}), **d)** biofilm formation (assessed
902 by crystal violet staining), and **e)** ratio of growth states after 4 days of growth in PD2 comparing
903 WT and Δ*hfq*. **f**) EPS levels assessed by phenol-sulfuric acid assay, **g**) percentage of aggregated
904 cells in WT and Δ*hfq*. **h**), **i**) motility of WT and Δ*hfq* cells assessed by measuring fringe width
905 of colonies grown for 4 days on 1% Agar-PD3 plates supplemented with 1 mM $CaCl_2$, scale
906 bar indicates 0.5 mm. Each assay was repeated independently at least three times, with each
907 experiment comprising a minimum of five technical replicates. Data points from independent
908 experiments are indicated by different symbols. Statistical significance was assessed using
909 Student's *t*-test and significance levels are indicated by asterisks with p-values < 0.05 (*), <
910 0.01 (**), < 0.001 (***), < 0.0001 (****). **i**, **j**) Representative transmission electron
911 microscopy (TEM) micrographs of WT (i) and Δ*hfq* cells (j) sampled from planktonic growth
912 in PD2 media or biofilm cells attached to the flasks. Scale bars indicate 500 nm.
913
914 **Figure 2: Transcriptomic response to nutrient downshift is reduced in *Xff* Tem1 *Δhfq***
915 **compared to WT. a)** PCA plot of variance-stabilized RNA-seq data with respectively four
916 replicates of *Xff* Tem1 WT and Δ*hfq* in PD2 and 3G10-R medium. Samples cluster by genotype
917 along PC1 and by media along PC2. **b), c)** Bar plots of differentially expressed genes (DEGs)
918 in response to sudden nutrient downshift in WT and Δ*hfq* (b) and between genotypes in both
919 media (c). **d), e)** Volcano plots of DEGs in WT (d) and Δ*hfq* (e) in response to nutrient
920 downshift. **c)** Volcano plot of DEGs between WT and Δ*hfq* in PD2 medium (f) and 3G10-R
921 medium (g). Genes of the category "transcriptional regulators" are highlighted in green, and
922 genes mediating twitching motility are highlighted in blue. Genes were considered differently
923 expressed between conditions when fold change >/< 1.5 and Benjamini-Hochberg corrected
924 (BH-corrected) p-value < 0.05.
925
926 **Figure 3: Retraction pilus genes are not responsive to nutrient downshift in *Xff* Tem1**
927 **Δ*hfq*. a), b)** Fold change of expression of retraction ATPases *pilT* (PD_1147) and *pilU*
928 (PD_1148) and regulatory pilus gene c-di-GMP receptor *pilZ* (PD_1497) in response to
929 nutrient downshift in WT and Δ*hfq* (a) and when comparing WT and Δ*hfq* in PD2 and 3G10-
930 R (b). **c)** Fold change of expression of fimbrial, afimbrial and Type IV-pili genes comparing

WT and Δ*hfq* in PD2 and 3G10-R. Genes with a fold change >/<1.5 and Benjamini-Hochberg corrected p-value < 0.05 are indicated with asterisk (*). **d)** Enriched GO-terms of category "Molecular Functions" of differentially expressed genes in response to nutrient downshift in WT but not in Δ*hfq*.

Figure 4: Transcriptional response to nutrient downshift of regulatory pathways is Hfq-dependent. Heatmap of z-score–normalized gene expression across *Xff* Tem1 WT and Δ*hfq* in response to the sudden nutrient downshift of 4 replicates in each condition. Genes are clustered together by functions with **a)** transcriptional regulators**, b)** chemotaxis/quorum sensing signalling pathways and **c)** described virulence factors. High z-scores (orange) indicate higher expression relative to the gene's mean, and low z-scores (grey) indicate lower expression. *OmpA* serves as positive control for Hfq-dependency.

Figure 5: Identified small RNAs (sRNAs) and their targets in rich and xylem-mimicking growth conditions in *Xff* Tem1 WT. Sequencing of size-selected transcripts (< 200 nucleotides) of *Xff* Tem1 WT and consequent annotation with the APERO-pipeline identifies sRNA candidates which are unique to rich (PD2), or xylem-mimicking (3G10-R) conditions or shared across both media represented as Venn diagram **(a)**. Volcano plot of differential expression analysis of shared sRNAs in response to nutrient down shift with sRNAs considered differently expressed when fold change >/<1.5 and BH corrected p-value < 0.05 between the two medium conditions **(b)**. **c-h)** Examples for IntaRNA-predicted target interactions between identified sRNAs with untranslated regions (UTRs) of *Xff* Tem1 and secondary structures of sRNAs folded with RNAfold. Interaction sites of sRNAs with UTRs are indicated by orange circles. c) *cis* antisense interaction of *XF25802* and 5'-UTR of the *rpfG-rpfC o*peron, partially covering ribosomal binding site (RBS), d) secondary structure of *XF25802*. Interactions in *trans* between *XF37402* (e, f) and 5'-UTR of the *blh-bigR* operon and *XF65031* (g, h) and 5'-UTR of the *trpR* open reading frame.

Figure 6: Hfq affects *Xff* Tem1 vesiculation and is present at the corona of EVs. a) EV concentration 4 h after nutrient downshift was assessed via nanoparticle-tracking analysis (NTA) of culture supernatant of *Xff* Tem1 WT and Δ*hfq* with at least three biological replicates per condition and similar results were obtained for 2 independent experiments. Statistical differences were calculated with Student's *t*-test, significance levels are indicated by asterisks with p-values < 0.01 (**) or 'ns' for 'not-significant' when p-value > 0.05. **b)** Representative

transmission electron microscopy (TEM) images of immunogold stained *Xff*-EVs using anti-Hfq antibodies (black arrows), showing presence of Hfq in the vicinity of *Xff* Tem1-EV membranes (white arrows). Proteinase K (ProtK)-treated EVs show lower immunogold signals at EVs, while several signals were observed at membranes from burst EVs in hypotonic buffer. Two representative images are shown for each condition. Scale bars indicate 100 nm.

Figure 7: Genetic disruption of *Hfq* reduces *Xff* Tem1's ability to systemically infect host plants. a) Bacterial load in Arabidopsis seedlings infected with *Xff* Tem1 WT or Δ*hfq* in total tissue, normalized to infection levels in WT. **b)** Systemic infection with *Xff* Tem1 WT or Δ*hfq* in Arabidopsis at distal tissue (seedling without infected petiole) normalized to infection site (petiole). Bacterial load was assessed by quantitative (qPCR) with *Xff*-specific primers and normalized to plant material. **c), d)** Symptom development after infection of *Nicotiana tabacum* cv. SR1 with *Xff* Tem1 WT or Δ*hfq* in locally infected leaves (c, grey arrows in d) and at systemic, younger leaves (d, white arrows). Leaf scorching, seen as browning, indicates disease symptoms, whereas leaf bleaching arises from growth stress and occurs in both WT and Δ*hfq*-infected plants.

Figure 8: Working model integrating Hfq and sRNAs into regulatory networks governing transition between planktonic and biofilm growth in *Xff* Tem1. a) In the xylem, *Xff* Tem1 forms biofilms which requires the coordinated expression of fimbrial (*fim*), afimbrial (*afim*,) and pilus (*pil*) genes. Environmental signals in the xylem and the QS-system mediate the shift of *Xff* Tem1 to a planktonic growth state. Some cells egress from the biofilm and crawl against the xylem sap along the xylem vessels by twitching motility. For this, genes of attachment and aggregation are being downregulated while motility genes, in particular genes of the Type IV-pilus mediating the twitching motility, such as ATPases *pilT* and *pilU*, are upregulated. This ultimately enables *Xff* Tem1 to systemically spread throughout the plant. Hfq and sRNAs are integrated into transcriptional networks mediated by transcription factors such as *bigR, phoP*, and *trpR*, to mediate the transcriptional adjustment required to switch between biofilm and planktonic growth. The regulatory role of Hfq and sRNAs in this transition might further be enabled to a colony-wide level through their spread via EVs. **b)** In the absence of Hfq (Δ*hfq*), this sRNA-based transcriptional adjustment is hindered, locking *Xff* Tem1 cells in aggregated, biofilm-growth state, hindering the bacterium's systemic infection in the plant.

Supplemental Figure S1: Genetic disruption of *Hfq*. a) Scheme of the *Hfq*-containing operon in *Xff* Tem1 and the genetic disruption by homologous recombination introducing a kanamycin resistance cassette (KanR). **b)** Colony-PCRs conforming insertion of KanR into Hfq locus. **c)** Expression level of *hfq* assessed via qRT-PCR of *hfq* in Δ*hfq* mutants compared to WT cells. **d)** Read coverage of RNA sequences in *Xff* WT and Δ*hfq* mutants at the insertion site (arrow), including operon downstream of insertion site.

Supplemental Figure S2: Sudden nutrient downshift induces biofilm formation followed by transition to planktonic growth. **a)** Scheme of nutrient downshift in WT and Δ*hfq*. **b)** *Xff* Tem1 WT planktonic growth (OD_{600}), **c)** biofilm formation (crystal violet assay) and **d)** ratio of growth states over time following nutrient downshift. Experiments were repeated at least three times with similar results.

Supplemental Figure S3: Sudden nutrient downshift has no major effect on cell viability. a, b) Cell viability assay of *Xff* Tem1-GFP cells 4 h and 4 days after nutrient downshift in PD2 (a) and 3G10-R (b), showing GFP fluorescence of *Xff* Tem1-GFP (green channel), propidium iodide (PI) fluorescence (red channel) and phase contrast of bacterial cells (grey channel). Boiled cells are used as positive control. The scale bar indicates 20 µm.

Supplemental Figure S4: a) Expression of accessory pilus genes, fimbrial and afimbrial genes in response to nutrient downshift. Gene expression is shown as z-score over all conditions for 4 replicates per genotype and media condition. **b, c) Complete list of enriched GO-terms of DEGs** in response to nutrient downshift in WT (b) and in Δ*hfq* (c).

Supplemental Figure S5: a) Expression of biosynthetic genes responsive to sudden nutrient downshift. To compare genotypes and media conditions, gene expression is shown as z-score over all conditions for 4 replicates per condition. **b, c) Expression of transcriptional regulators in response to nutrient downshift which show differential expression in Δ*hfq* compared to WT.** Gene expression is shown as fold change comparing media conditions (b) and genotypes (c) and genes with a fold change >/<1.5 and p-value < 0.05 are indicated by asterisks (*).

Supplemental Figure S6: sRNA-seq workflow (a) and sRNA annotation using APERO (b, c, d). b) sRNA-classes according to their localization as classified by APERO-tool with

primary RNAs in 250 nt upstream of CDS in sense (P) and antisense (DIV), intergenic orphan RNA (O), overlapping start/stop codon respectively in sense (5U/3U) and antisense (5A/3A), and antisense (Ai) and sense (I) RNA overlapping CDS. sRNAs with multiple classes (*) were classified according to Material & Methods Section "sRNA analysis". **c, d, e)** number of identified sRNAs for each class in PD2 (c), in 3G10-R (d), and when sequencing reads of PD2 and 3G10-R were used together for annotation (e).

Supplemental Figure S7: Boxplot of fold change (log2) of genes in *bigR*, *rpfG/C* and *trpR* operon in response to the nutrient downshift in WT and Δ*hfq*. Each data point corresponds to the expression level of an individual gene in the operon.

Supplemental Figure S8: Symptom scoring of infected tobacco. a) Tobacco leaves 7 weeks after infection with *Xff* Tem1-WT ('WT'), *Xff* Tem1-Δ*hfq* ('Δ*hfq*') or PBS ('mock') and **b)** whole plants 8 weeks after mock infection.

1046

Figure 1

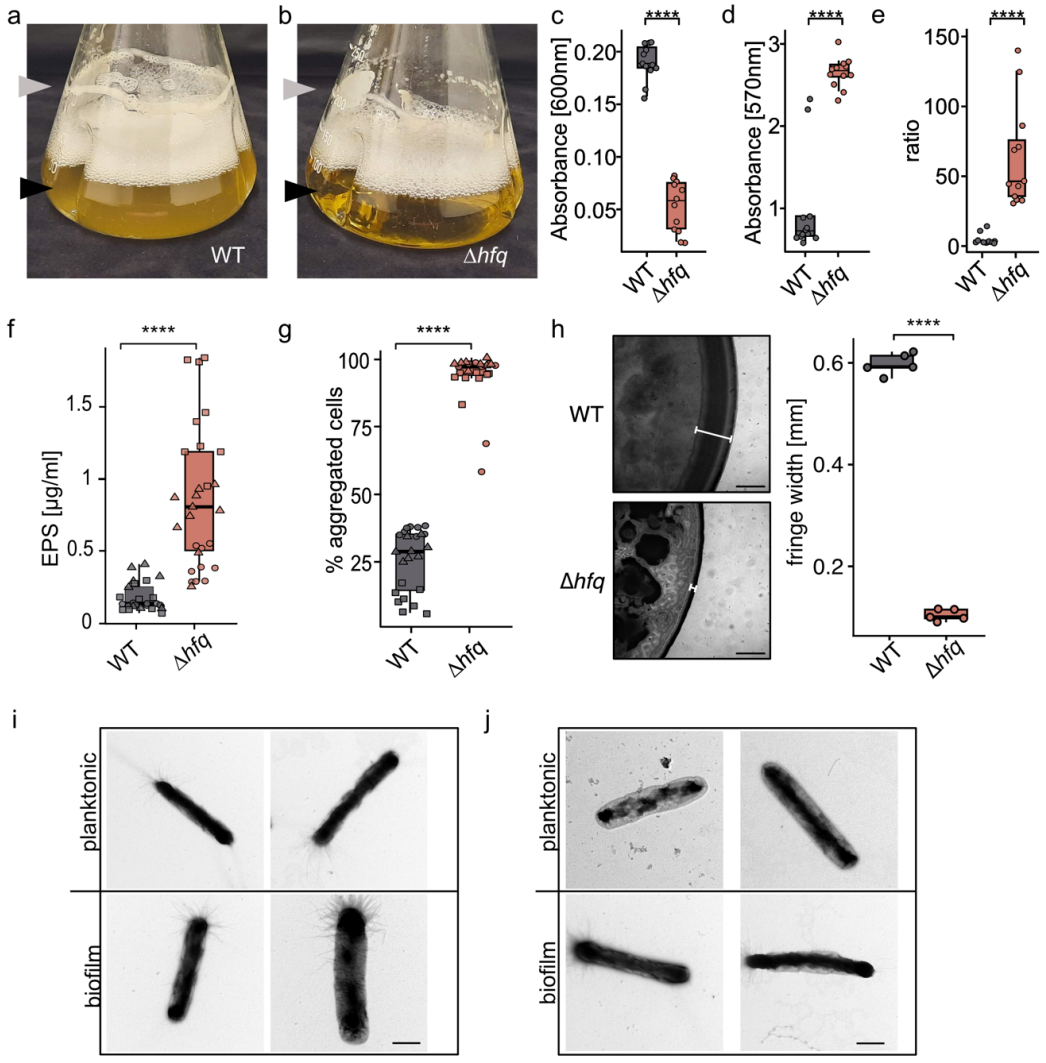

1047

Figure 2

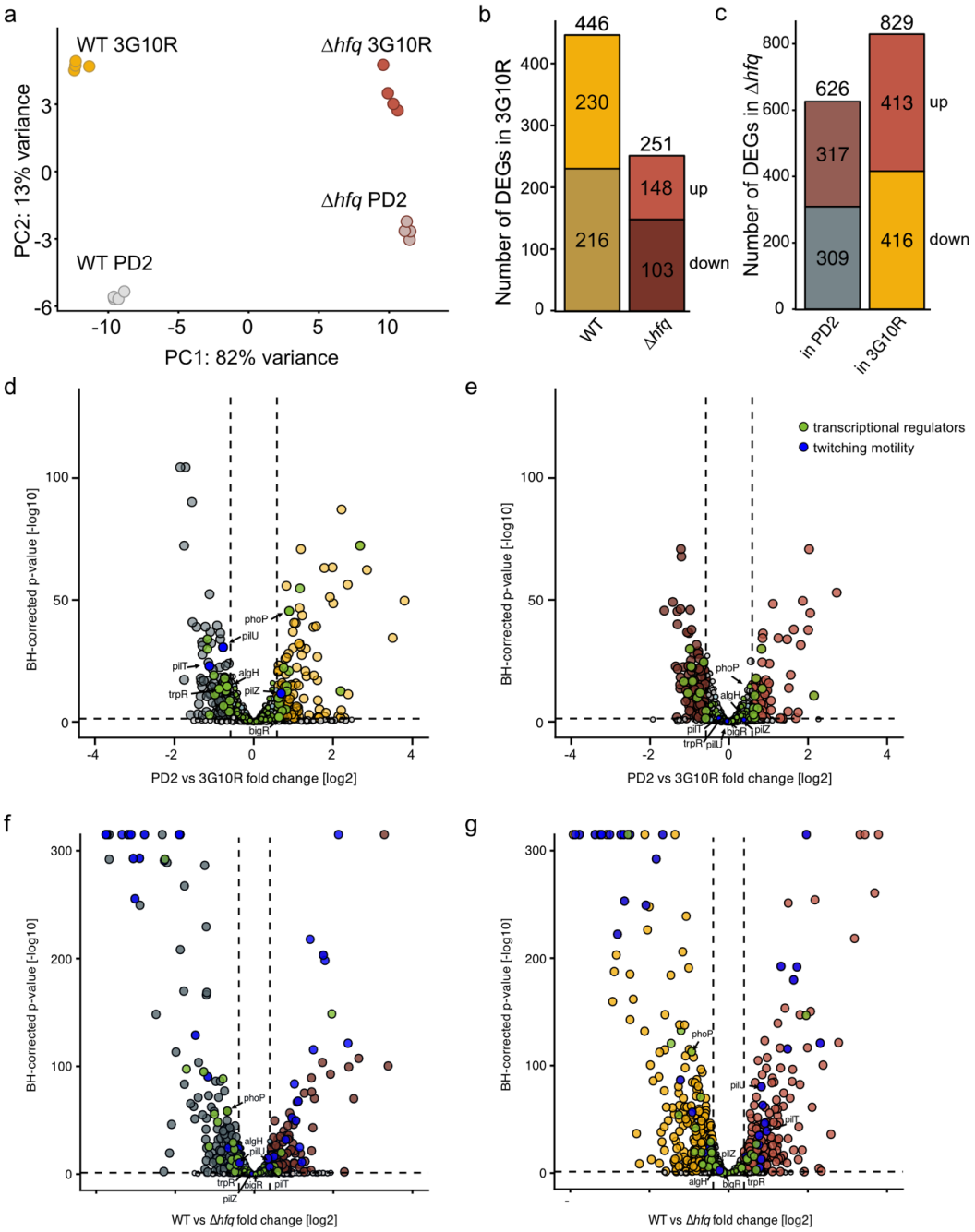

1048

Figure 3

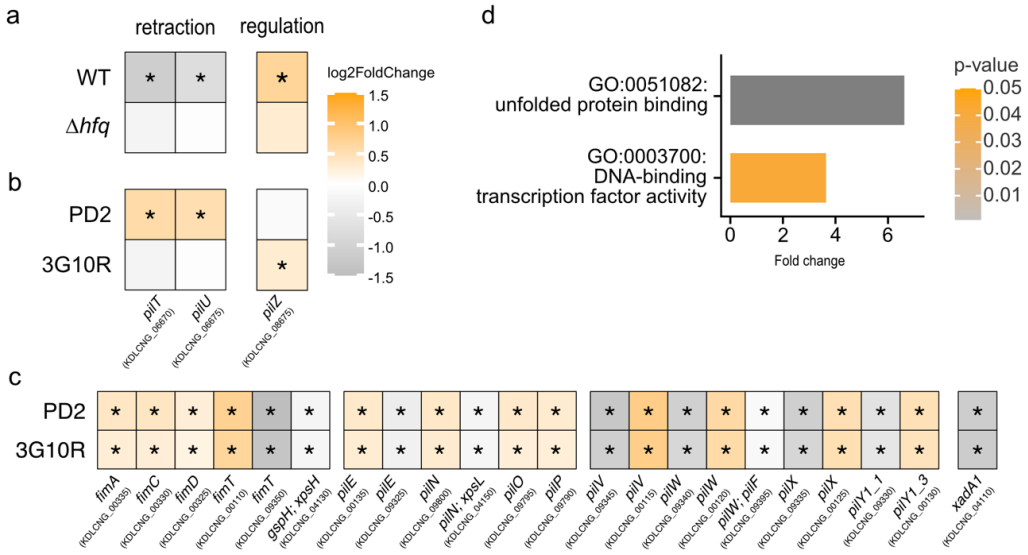

1049

Figure 4

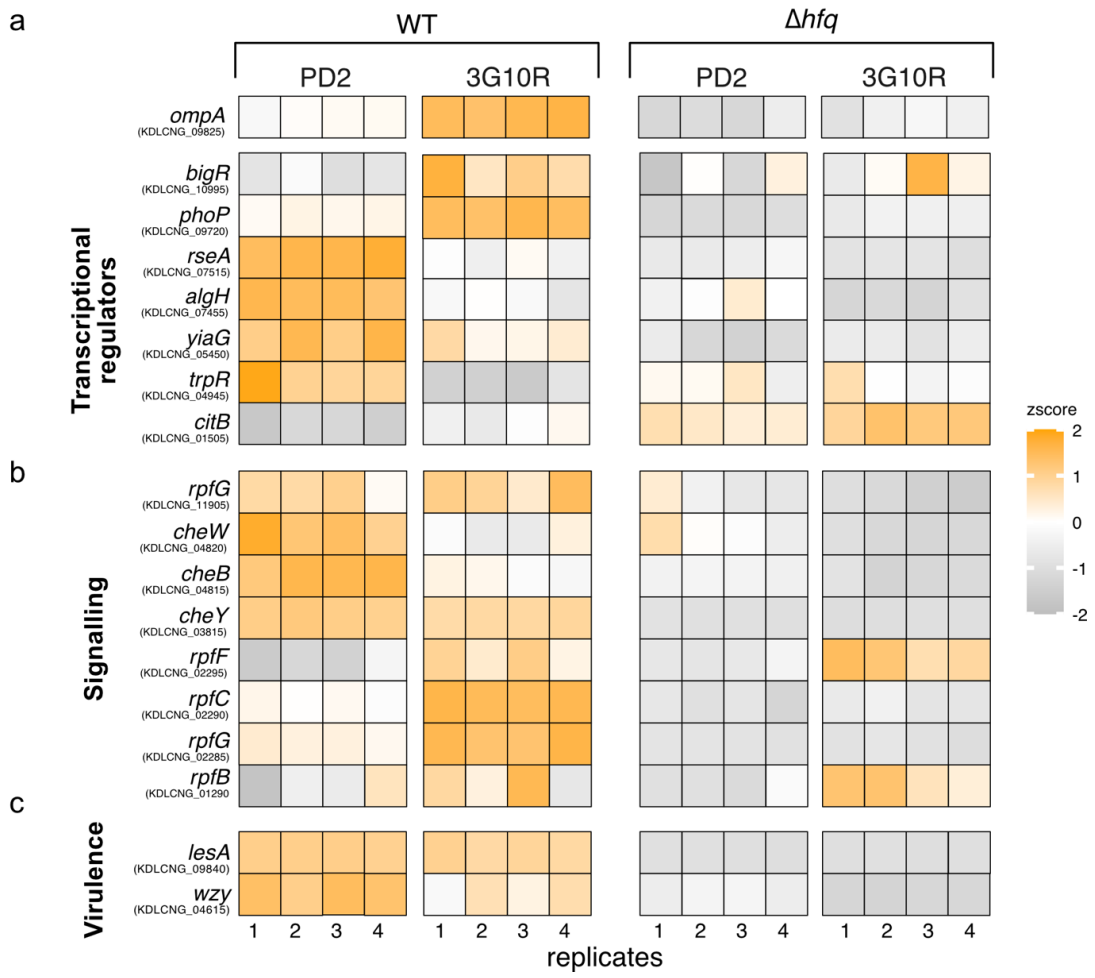

1050

Figure 5

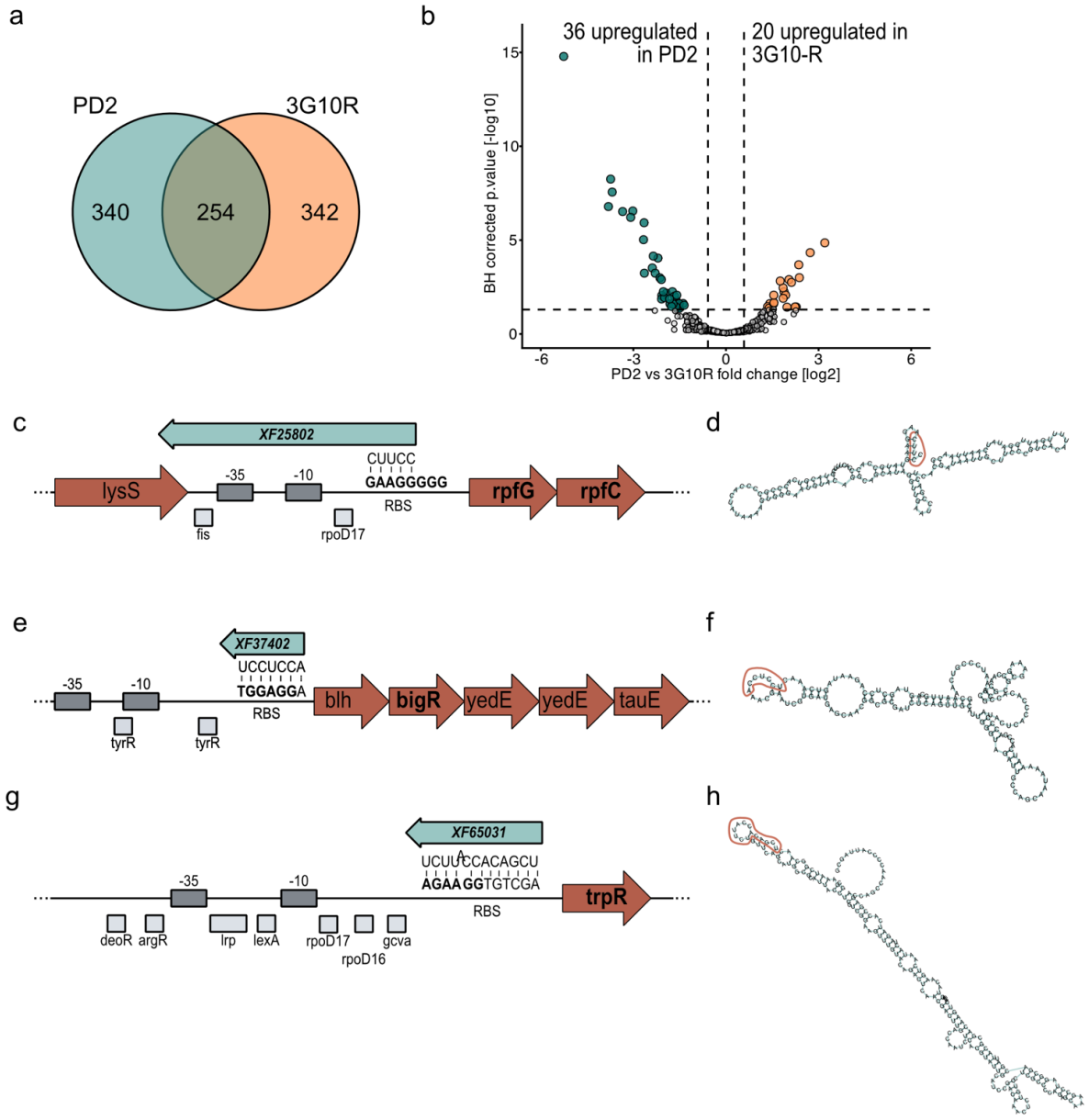

1051

Figure 6

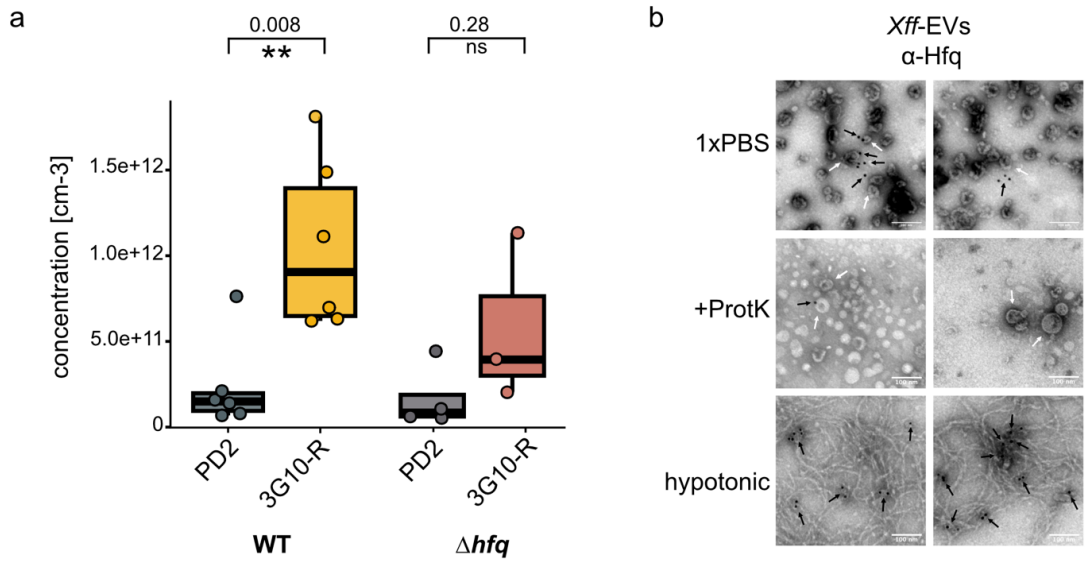

1052

Figure 7

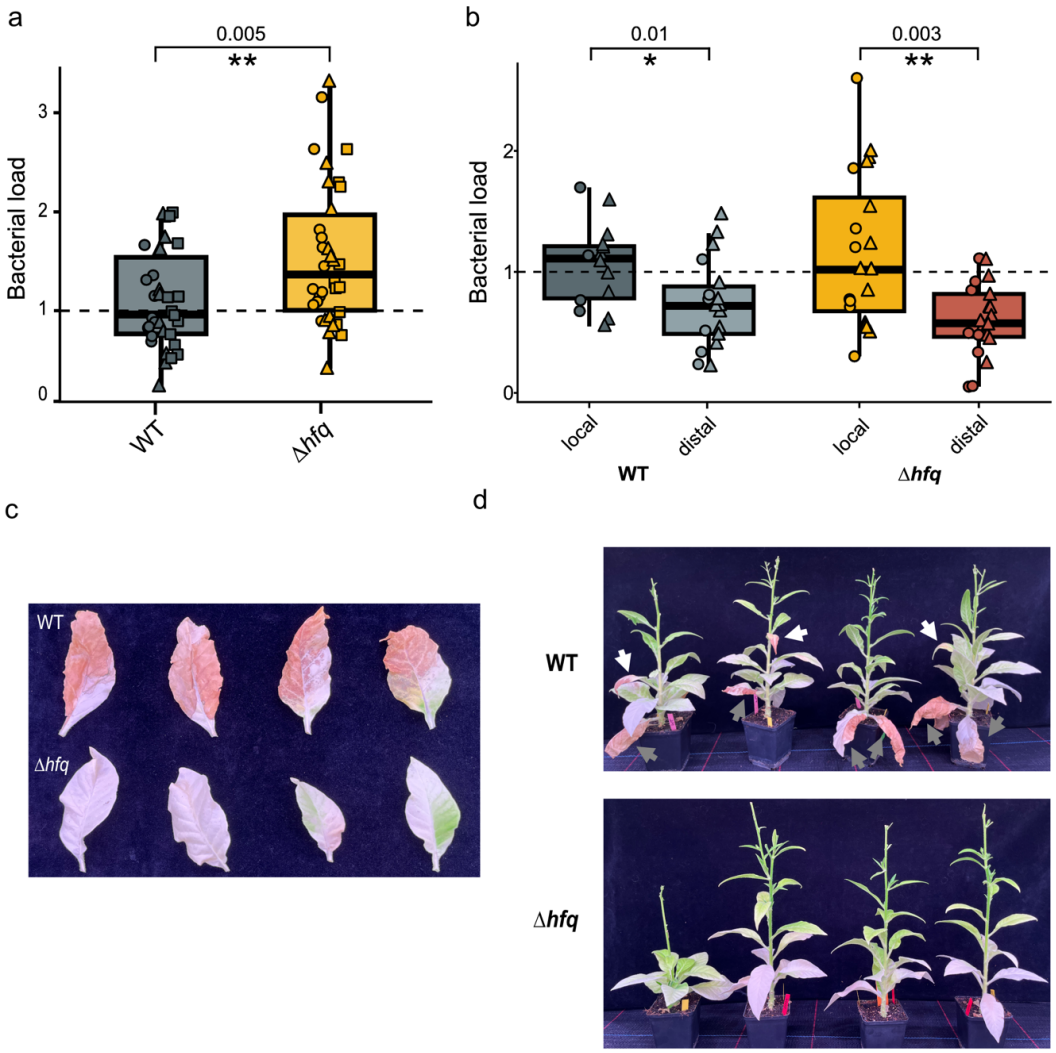

1053

Figure 8

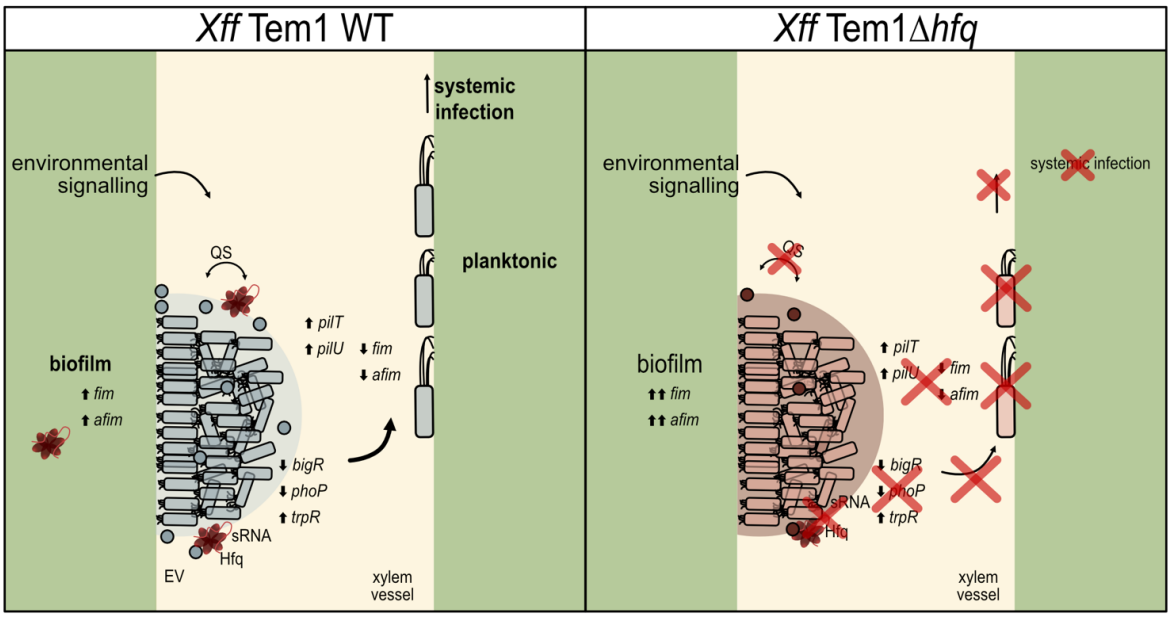

1054

Supplemental Figure S1

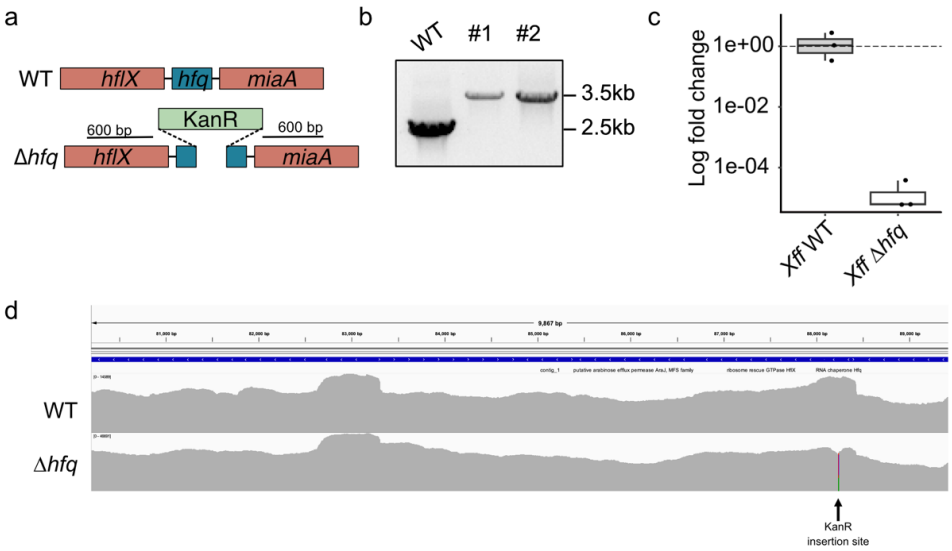

1055

Supplemental Figure S2

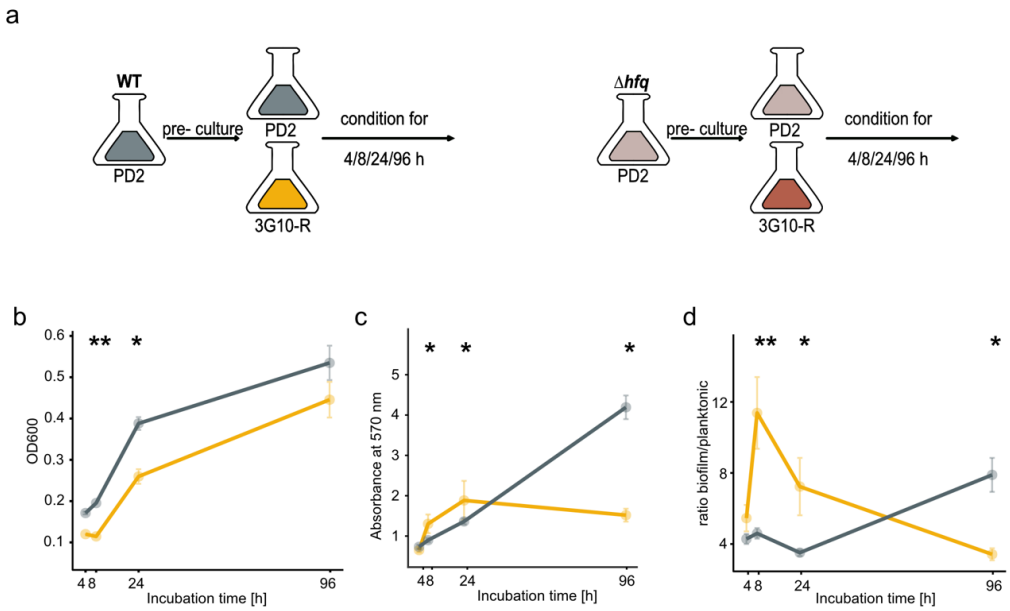

1056

Supplemental Figure S3

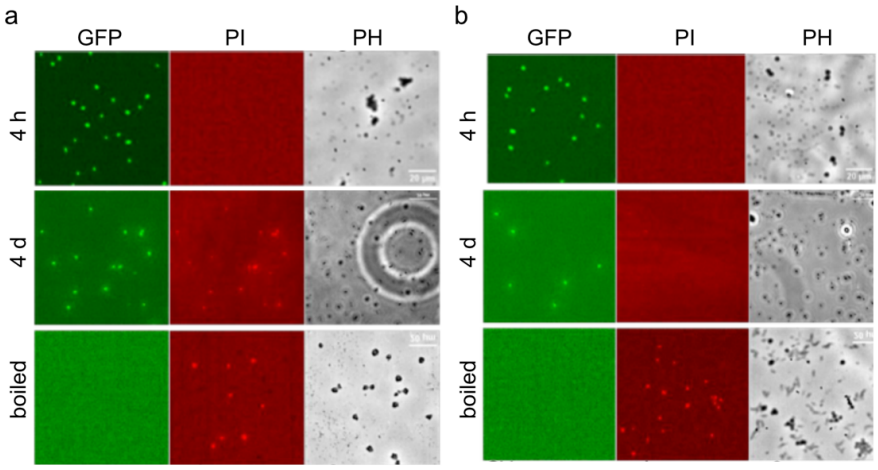

1057

Supplemental Figure S4

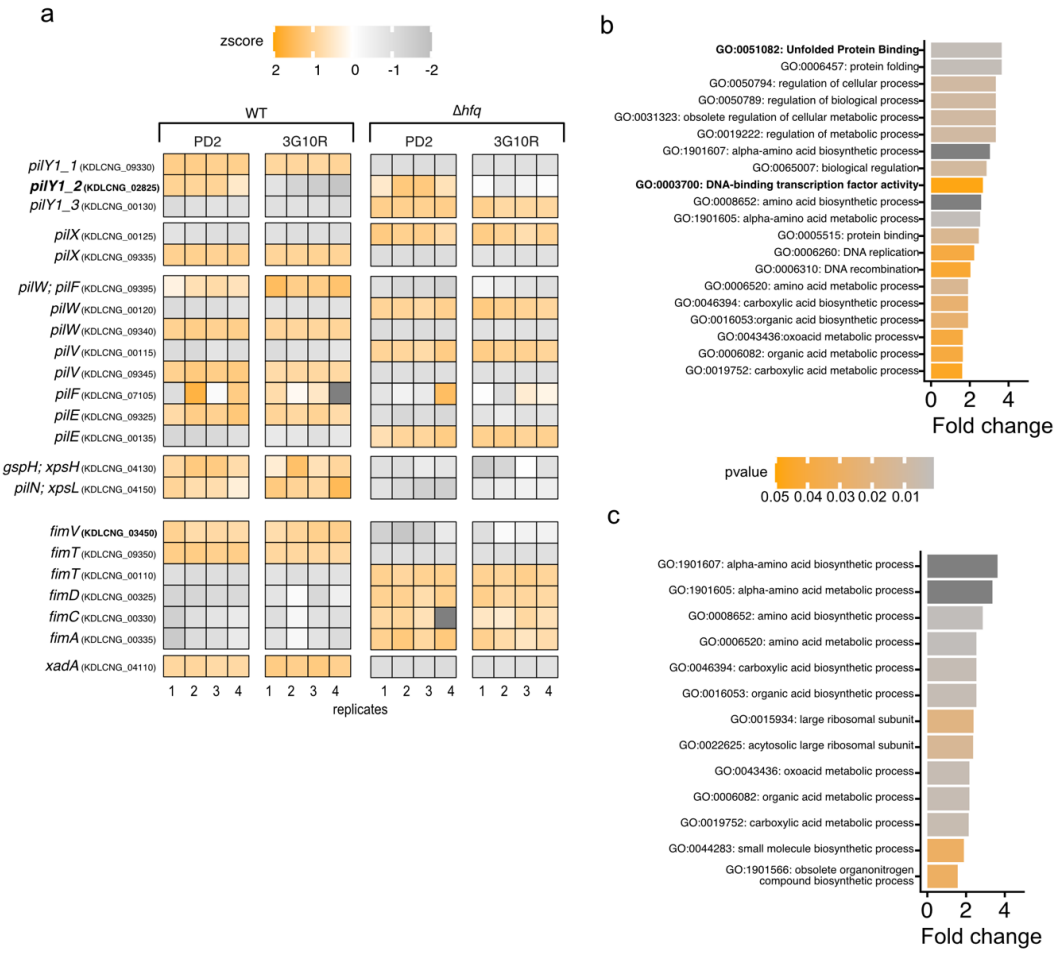

1058

Supplemental Figure S5

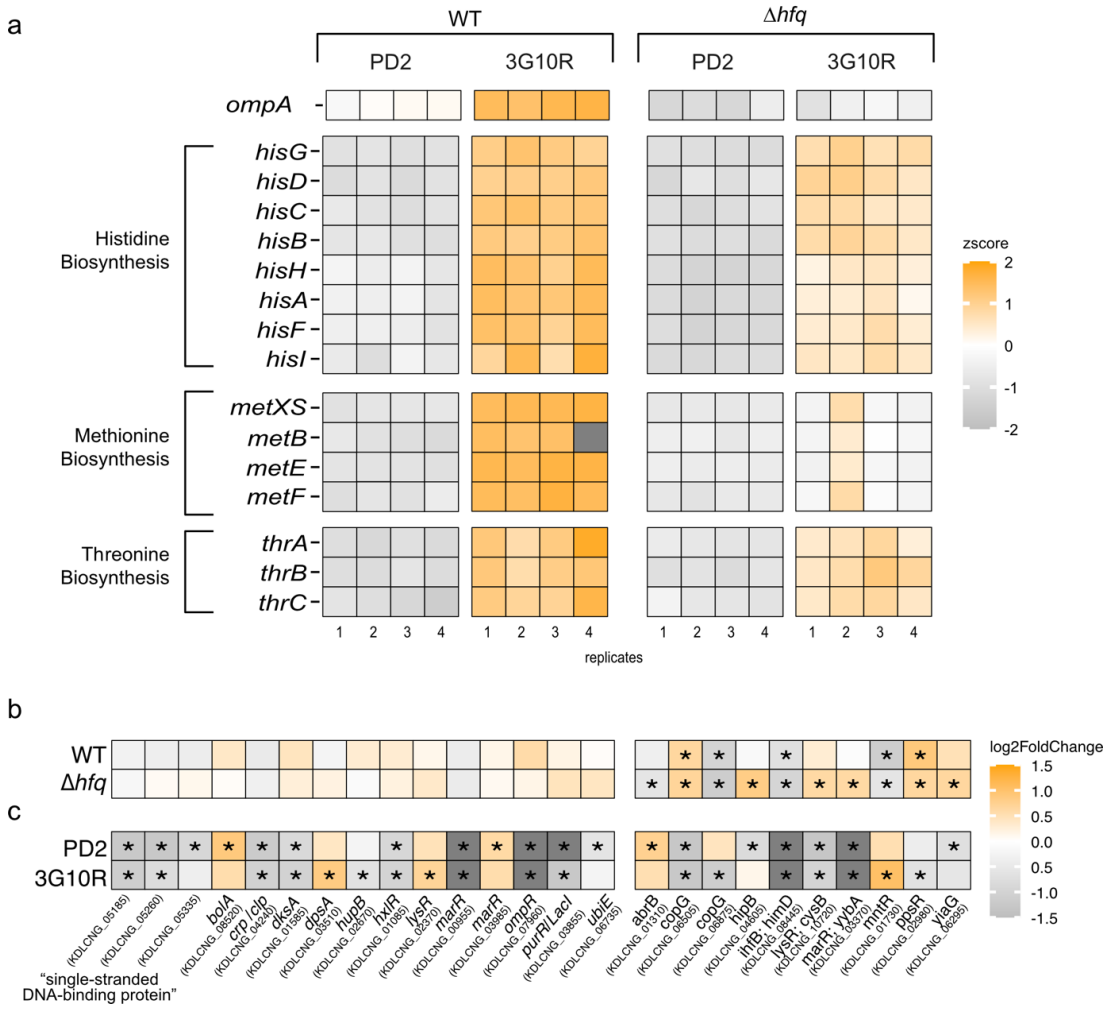

1059

Supplemental Figure S6

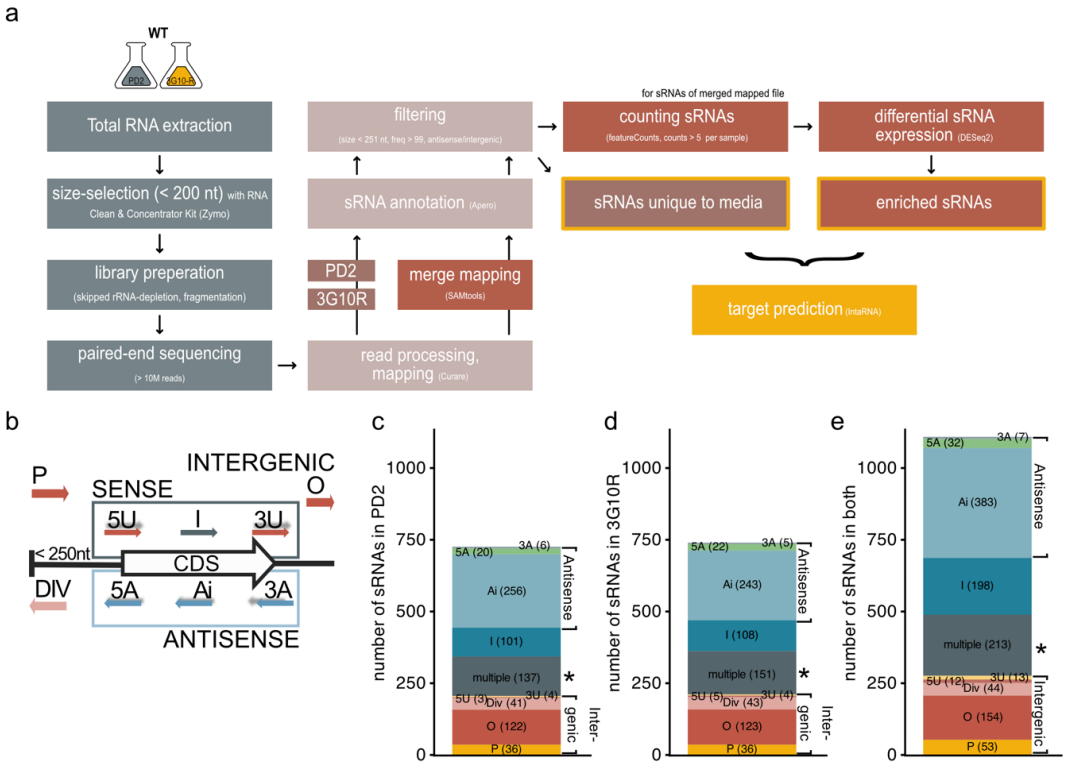

1060

Supplemental Figure S7

a

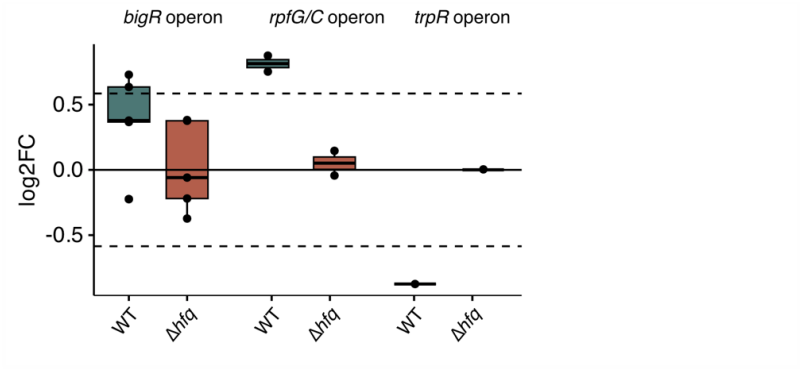

1061

Supplemental Figure S8

a

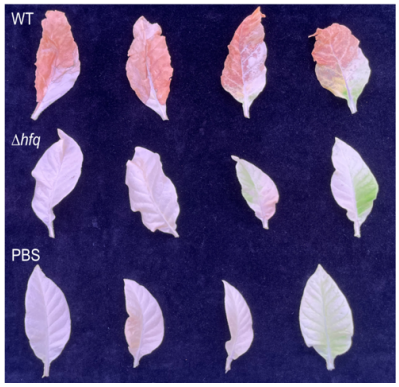

b

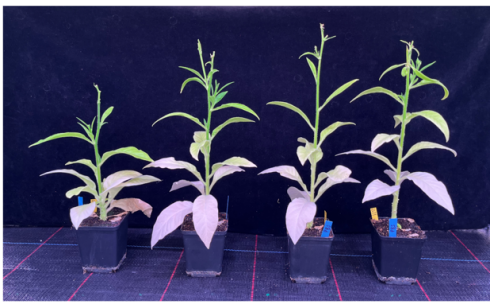

Discussion

Xf-EVs as delivery vehicles for Hfq, sXFs, toxins and GIs

The findings presented here give insights into the cargo of *Xylella fastidiosa*'s (*Xf*) extracellular vesicles (EVs) and the role they play in the communication with surrounding cells. The protein and nucleic acid cargo of *Xf*-EVs identified in Ruf et al., 2025 *JEV* [6] proposes EVs as shuttle agents for mechanisms involved in (1) cross-kingdom RNA interference (ckRNAi), (2) bacterial transcriptional regulation and (3) intraspecies competition and horizontal gene transfer (**Figure 4**).

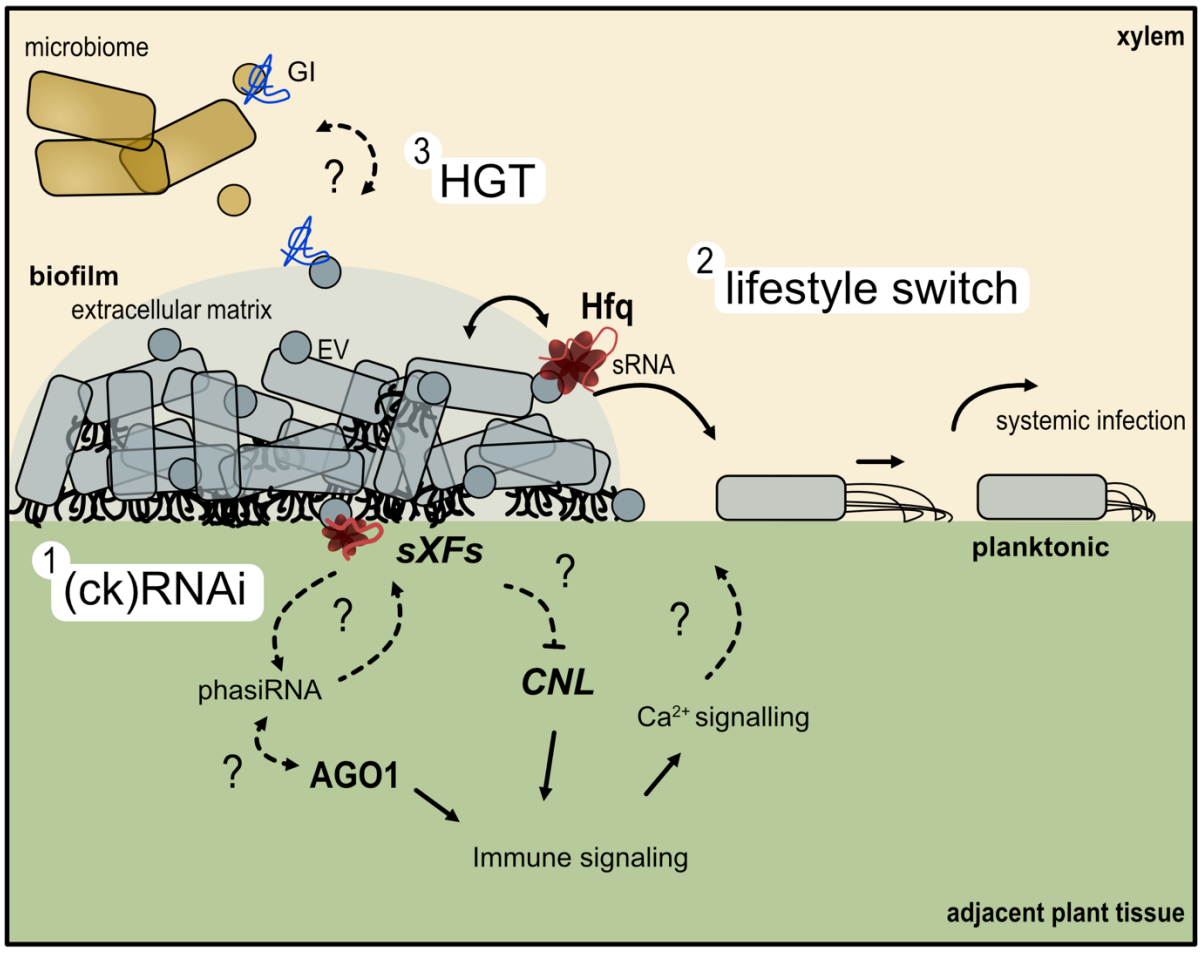

Figure 4: Proposed functions of *Xf*-EVs and sRNAs in cell-to-cell communication.
Xf resides in the xylem of host plants where delivery of sRNAs of class *sXFs* via EVs into adjacent plant tissue might silence immune receptors of class *CNL*. This could dampen early plant immune responses, a process negatively regulated by AGO1 in Arabidopsis (**1**). The dual targeting of *CNLs* by bacterial sRNAs and endogenous sRNAs could trigger amplification of the signal by phasiRNA production. The release of Ca^{2+} and other immune responses are potentially sensed by *Xf* cells and shape their growth. Hfq and sRNAs facilitate the lifestyle switch of *Xf* between biofilm and planktonic growth in response to environmental signals, which mediates *Xf*'s systemic infection (**2**). Genomic islands (GI) associated with EVs might facilitate horizontal gene transfer (HGT) among *Xf* cells and microbiome communities (**3**).

RNA-based communication across cellular borders

RNA-seq analysis of *Xf*-EVs revealed the presence of different classes of RNA, including small (s)RNAs in EVs of *Xf* subspecies *fastidiosa* strain Temecula1 (*Xff*). In addition to very conserved and well-studied bacterial non-coding (nc)RNAs, homologues of *Xanthomonas* sRNA-*Xcc1* are found at *Xff*-EVs, designated *sXF*s. In *Xanthomonas campestris* pv. *campestris* (*Xcc*), their expression is under the control of virulence regulon Hypersensitive Response and pathogenicity proteins G/X (HrpG/HrpX) but lack functional evidence[303]. We performed structural and functional predictions of *sXF*s by determining their fold, possible interactions with RNA-binding proteins (RBPs) and target prediction of bacterial and plant messenger (m)RNA.

The folding of *sXF*s revealed a three-loop structure and predicted *Xff*-mRNA targets of *sXF*s were categorized into two interactions. Category 1 *sXF*-mRNA interactions involve two loops of the *sXF* structure, while category 2 interactions only involve one loop. The third loop might engage in an interaction with the RNA chaperone Hfq. We propose that the interaction of *sXF*s with Hfq is based on their folding and the presence of several Hfq-binding motifs in one loop of *sXF*s. The association of Hfq with EVs was first identified via proteomics[6] and could be confirmed by visualizing their association employing immunogold staining methods[7].

Hfq associates with membranes as shown for interactions with *E.coli* [276,285,286]. The membrane interaction occurs between Hfq's amyloid-forming C-terminal region and negatively charged membrane lipids, while the N-terminal region of the protein binds sRNAs[277,285]. This interaction results in transient pore-formation in the inner membrane, followed by delivery of Hfq and sRNA into the periplasm, which might facilitate two crucial functions of Hfq; (i) Hfq-amyloids can shape the curvature of the outer membrane[276], possibly facilitating the formation of EVs and (ii) loading and protecting sRNAs in EVs[286]. Indeed, we found reduced amount of EVs in the knockout mutant of *hfq* (*Xff*Δ*hfq*) compared to *Xff* WT, which indicates a role of Hfq in formation of EVs in *Xff* [7].

In *E.coli*, Hfq retains its sRNA-binding function when interacting with membranes[277,285] and its loading to EVs is highly dynamic[283] which might allow loading and delivery of sRNAs to EVs, similar to the role of RBPs in eukaryotes[244,249,252].

Hfq is a matchmaker, bringing together sRNAs and their mRNA targets in bacteria[268]. We determined the overlap of identified mRNAs at EVs and *sXF*-mRNA targets, speculating that they might be bound by the EV-associated form of Hfq. Among the identified transcripts, we

found mRNAs coding for DNA transport Competence protein ComE which regulates DNA uptake and horizontal gene transfer (HGT) in Gram-negative bacteria, a process coordinated by Quorum Sensing (QS) in many bacteria[304]. For example, in the human bacterial pathogen *Vibrio cholera,* the induction of *ComE* expression by QS-signals is mediated by sRNAs, which facilitate the DNA uptake across neighbouring cells[305]. In *V. cholera*, the EV-associated protein Outer membrane-associated Biofilm Facilitating protein A (ObfA) modulates the expression of such regulatory sRNA and with that facilitates intra-species communication[306]. Another human bacterial pathogen, *Pseudomonas aeruginosa* (*Pa*), packages Hfq and sRNAs directly into EVs which modulate the expression of QS-regulatory genes[307]. This enables coordinated gene expression and communication across bacterial cells, mediated by Hfq and bound RNAs. EV-association of Hfq and RNAs predicted to regulate HGT proposes similar mechanisms in *Xff*.

Incorporation of bacterial sRNAs into eukaryotic pathways

Bacterial sRNAs associated with EVs could either regulate bacterial gene expression or be delivered to host plants. Several examples show that prokaryotic sRNAs can modify host target responses[133,256,257]. In particular, the highly conserved transfer RNAs (tRNAs) and their derivatives, tRNA fragments (tRFs), have been proposed to be shuttled between eukaryotic and prokaryotic cells. Bacterial RNAs can then be integrated into the eukaryotic host's RNA interference (RNAi) pathway to silence host genes. For example, the integration of rhizobial tRFs into the RNAi-pathway of soybeans depends on AGO1 and results in the downregulation of target genes[133], similar to eukaryotic cross-kingdom (ck)RNAi interactions[72,117,132]. Predicted plant mRNA targets of *sXF*s in model plant *Arabidopsis thaliana* (*At*) and *Xf* host plant *Vitis vinifera* (*Vv*) include several immunity genes, among which are four encoding *At* nucleotide-binding site (NBS) leucine-rich repeat (LRR) receptors (NLRs). The downregulation of a predicted target coiled coil domain-*NLR* (*CNL*) in response to infiltration with *Xf*-EVs in *At* indicates a ckRNAi-type mechanism for *Xf*-sRNAs delivered by EVs. However, for bacterial sRNAs to get integrated into the eukaryotic RNAi machinery to interfere with immune gene expression, several hurdles need to be overcome.

Firstly, secreted bacterial sRNAs need to be delivered into the host cells across the plant cell wall. For other systems, the delivery of EVs and their cargo depends on cell wall degrading enzymes (CWDEs)[1,219,222]. *Xf* encodes several CWDEs, one of which is a homologue of Xanthomonas LipA, also found in EVs, which might facilitate the delivery across the plant cell

wall[6,158,217]. Additionally, the most abundant ncRNAs found in *Xf*-EVs are protected from enzyme-treatments even in the presence of detergent, indicating a very stable protection of ncRNAs by EVs, which might further facilitate their delivery through the xylem. This protection could be based on an incorporation of ncRNAs into the EV membrane, potentially mediated by membrane-bound Hfq[286]. RNA modifications could also result in their strong protection. For example, in human cells, the glycosylation of sRNAs leads to the "presentation" of sRNAs on the cell surface[308]. Association of glycosylated RNAs with membranes and their biosynthesis via the canonical endosomal pathway[308] proposes an association of glycosylated sRNAs with EVs but awaits validation. In bacteria, glycosylation is a common post-translational modification of proteins, for example facilitating attachments to the host[309]. However, whether (s)RNAs are also being glycosylated in bacteria, and whether they associate with EVs, is currently not known.

Once arrived at a plasma membrane, the intracellular delivery of bacterial EVs with human and plant host cells can occur via membrane fusion and is mediated by nanodomains[232,310,311]. Insights into the composition of *Xf*-EV membranes, such as their lipopolysaccharides (LPS) and lipid composition, might shed light on how EV cargo, such as sRNAs, interact with EV-membranes and how EVs and their cargo interact with plant membranes.

Secondly, to enable the regulation of target genes in the host, bacterial sRNAs need to be adjusted to the eukaryotic RNAi machinery. Most bacterial sRNAs are around 50-500 nucleotides (nt) in length[262], but smaller populations of mostly transfer RNA (tRNA)-fragments (tRFs;15-49 nt) are reported[312]. With this, most bacterial sRNAs are longer than canonical eukaryotic sRNAs (20-24 nt). Eukaryotic unprocessed, precursor double-stranded (ds)RNA and primary(pri)-micro (mi) RNAs are diverse in length[313] but rely on secondary hairpin structures to be further processed by DCL endonucleases[314–317] before binding to AGOs. Bacterial sRNAs often form stable secondary structures, influenced by binding to RNA chaperones such as Hfq[268]. Hairpins might facilitate the processing of bacterial RNAs by eukaryotic DCLs and RNAses, adjusting them for AGO-binding. Other candidates which could facilitate incorporation of bacterial RNAs into eukaryotic pathways are fragments of very conserved RNA-building blocks such as tRNAs and ribosomal (r)RNAs. In particular, tRFs can be bound by AGO1 and mediate transcriptional changes in hosts, as shown for rhizobial tRFs facilitating nodulation in their host plant[133]. RNA-seq analysis of *Xf*-EV cargo revealed that almost 50% of all EV-associated transcripts encode tRNAs and sRNAs, indicating plenty of candidates for such interactions but require further validation.

Lastly, to achieve lasting post-transcriptional regulation based on bacterial sRNAs throughout the plant, the sRNA-signal requires amplification. The amplification of ckRNAi-signals is also important in eukaryote-eukaryote systems and relies on RNA-dependent RNA polymerases (RDRs)[289,318]. In Arabidopsis, RDR6, together with members of the DCL family, generates secondary siRNAs, including the production of phased siRNA (phasiRNAs) from miRNAs which amplifies their signal[319]. Two mechanisms have been proposed: in the "one-hit" model, a single miRNA-mediated cleavage initiates phasiRNA production downstream of the target site, whereas the "two-hit" model involves two miRNA target sites on the same transcript, resulting in processing upstream of the 3′ site[103,105]. One of the best studied miRNA superfamilies, *miR482/2118* and their secondary-derived phasiRNAs, targets many *NLR*s via the sequence of the very conserved ATP-binding site, the P-loop[98,106,320,321]. This process can keep *NLR* expression in-check in absence of immune triggers to avoid autoimmunity[102,319]. Intriguingly, the *sXF*-target site of the downregulated *CNL* is approximately 150 nt upstream of the endogenous P-loop target site of *miR482/2118*[6]. Whether a combined "two-hit"-targeting by bacterial sRNAs and endogenous miRNAs results in the production of phasiRNAs remains to be seen (**Figure 5**).

PhasiRNAs can either amplify the silencing of the primary target, target additional RNAs or extend their function cell non-autonomously[93,102,319]. Given the mobile nature of phasiRNAs and immune regulatory functions, it is not surprising that phasiRNAs are also important players in interactions with microbes[66,131]. For example, secondary siRNAs of Arabidopsis contribute to the defence against *Phytophthora*, which releases effectors to supress their biogenesis[66]. Endogenous phloem-traveling phasiRNAs are also required to achieve systemic resistance throughout the plant[111]. The lively traffic of phasiRNAs across cellular borders might represent a prominent entry point for bacterial sRNAs. By integrating sRNAs into endogenous phasiRNA-based silencing loops of *NLR*s, bacteria could keep *NLR* expression at bay to achieve successful infection. Membrane-association of RNA-induced silencing complexes (RISC) in plants[295], resulting in miRNA-based translation inhibition at the Endoplasmic Reticulum (ER)[322] and the production of phasiRNAs at membrane-bound polysomes[297], might

facilitate the exchange of RNAs from bacterial EVs to the eukaryotic machinery directly at the membrane.

RNA transport throughout plants occurs largely in the phloem[323,324]. Exchange between phloem and xylem stream[325–327] could explain how *Xf* sRNAs are being integrated into the endogenous sRNA-stream in the phloem. Immune responses to xylem-colonizing pathogens like *Xf* are speculated to be mediated by neighbouring tissue, as the xylem consists mostly of dead cells [139,147]. By integrating immunomodulatory sRNAs into the phloem stream, *Xf* might gain access to living tissue to interfere with immunity responses. Parenchyma cells, the sole living component of the xylem, are speculated to be implicated in the detection of xylem-colonizing microbes. Intriguingly, the xylem-colonizing rice pathogen *Xanthomonas oryzae* pv. *oryzae* delivers effectors directly into parenchyma cells via the T3SS to increase nutrient flux in the xylem[328]. Similarly, it is conceivable that the delivery of sRNAs via *Xf*-EVs into parenchyma cells also facilitates the growth of *Xf* in the xylem by reducing the expression of immunity receptors.

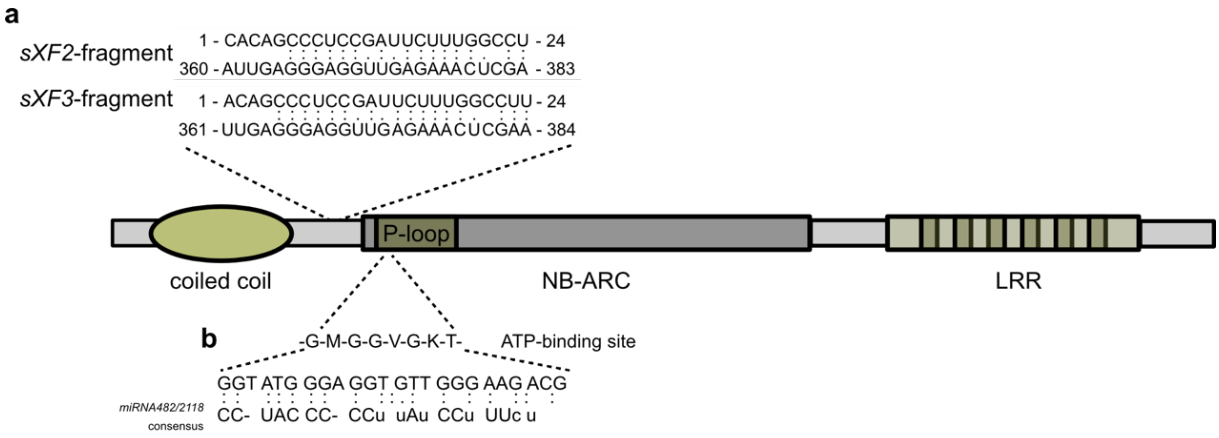

Figure 5: sRNA-target sites on *CNL*.

Target sites on *CNL* AT1G63350 of bacterial *sXF*s upstream of P-loop (**a**) and of endogenous *miRNA482/2118* at ATP-binding site P-loop (**b**).

Hfq regulates lifestyle switch in Xf

Despite its massive genome reduction, *Xf* did not lose Hfq, as shown for other bacteria[278], indicating important functions of Hfq and its associated sRNAs in *Xf*. Unlike protein-based regulations which allow more quantitative adjustments of gene expression levels, sRNA-based regulation allows a rapid switch between distinct states[299]. For example, many

bacterial pathogens rely on Hfq and sRNA-based regulation to coordinate lifestyle switches between planktonic and biofilm growth[329,330]. In Δ*hfq*, *Xff* cells are locked in aggregated, non-motile states resulting in biofilm growth and only local infection, indicating a similar role for Hfq and bound sRNAs in regulating lifestyle switches in *Xff* [7].

Transcriptomic analysis showed a reduced response of *Xff*Δ*hfq* to a sudden nutrient downshift, which triggers lifestyle changes in WT, and integrates the regulatory function of Hfq into transcription factor (TF) networks and signalling systems in *Xff*. Identified players include *e.g.* response regulator of the phosphate regulon PhoP[331,332], Biofilm growth-associated repressor (BigR)[333–335] and signalling components of the Diffusible Signal Factor (DSF)-mediated QS-system of *Xf,* which have reported roles in biofilm formation in *Xf* [5,336–339].
Hfq achieves functional specificity through bound sRNAs, the expression of which is highly dynamic and responsive to external stimuli and controlled by transcriptional regulators that sense environmental conditions[262,267,340,341].
The sRNA-seq after the nutrient-downshift in *Xff* proposes a similar quick adjustment of sRNA expression in *Xff. De novo* annotation of sRNAs and prediction of their mRNA targets, binding to coding and Untranslated Regions (UTR), resulted in a candidate list of genes encoding TFs and components of signalling systems which might get regulated by Hfq and bound sRNAs. This positions Hfq and sRNAs as central regulators of mechanisms that sense environmental signals and transduce them into transcriptional responses.

For example, while the expression of genes involved in DSF synthesis (*Regulator of Pathogenicity Factor F* (*rpfF*), *rpfB*) respond to changing conditions independent of Hfq, the transcriptional response of the two-component system of perception (*rpfC*) and signalling transduction (*rpfG*) of DSF-signals, are Hfq-dependent. Interestingly, both *rpfC* and *rpfG* are encoded in one operon, with an anti-sense sRNA targeting the operon's UTR. DSF signalling is conserved in many Xanthomonads, however in *Xf* several parts of the mechanisms, including the downstream signalling cascades, are not fully elucidated[337,342]. RpfG has a cyclic di-guanylate monophosphate (c-di-GMP) phosphodiesterase activity. This results in intracellular signalling which regulates gene expression mediated by c-di-GMP, a global bacterial second messenger[343,344]. Synergistic roles of c-di-GMP signalling, QS and Hfq in the regulation of biofilm formation and virulence have been reported for other bacteria[345,346]. For example, in plant pathogenic bacteria *Dickeya dadantii*, Hfq-bound sRNAs regulate the expression of a LysR-type transcriptional regulator and c-di-GMP diguanylate cyclases, creating a feed-

forward signalling circuit regulating the bacterium's virulence[347]. In the human bacterial pathogen *Pa*, the synergistic regulation of biofilm and virulence by QS and Hfq also extended to extracellular functions mediated by EVs. Besides directly disseminating QS-signals via EVs[348], *Pa* also packages Hfq and specific sRNAs into EVs, which modulate the transcription of QS-regulatory genes[307]. The previously described loading of DSFs into *Xf*-EVs[5,157], together with the here identified EV-associated form of Hfq and their sRNAs, proposes a similar dual function of *Xf*-EVs, but requires further validation.

The transcriptional responsiveness of the genes encoding the two-component system PhoP/PhoQ to the nutrient-downshift is also Hfq-dependent, another example how Hfq and bound sRNAs are involved in the regulation of transducing environmental signals. The receptor kinase PhoQ senses antimicrobial peptides and extracellular ion concentrations, such as Mg^{2+} and Ca^{2+}, resulting in the phosphorylation of transcriptional regulator PhoP[349,350]. This mechanism is essential to *Xf*'s virulence in grapevine[332]. Ca^{2+} also functions as a signalling molecule in plants, mediating immunity responses[351]. Ca^{2+} concentrations in leaves change in response to infection with *Xff* [60,61]. Could these plant signals also inform *Xf*'s lifestyle switch? For example, in phytopathogenic bacteria *Erwinia carotovora*, expression of virulence genes is modulated by total plant Ca^{2+} levels[352]. *In vitro*, Ca^{2+} influences *Xf*'s overall transcriptome, including the expression of attachment and motility genes as well as transcriptional regulators[54,63,64]. This, in turn, might influence the expression of regulatory sRNAs. Hence, the integration of sRNA-based regulatory functions into transcriptional networks of two-component systems and TFs most likely represents a mixed regulatory circuit, consisting of TFs and regulatory RNAs[353]. The regulatory feed-forward loop can amplify signals enabling the rapid adjustment of broad transcriptional programs required for the drastic lifestyle changes in response to changing environmental conditions. A well-characterized example of such a sRNA-integrated feed-forward loop consisting of the TF FadR and Fatty Acids regulated sRNA (FarS) in *V. cholerae*, where TF and sRNA-mediated regulation are coupled to coordinate the bacterium's fatty acid metabolism[354].

Taken together, sRNAs and Hfq play an important role in the regulation of lifestyle changes in *Xf*, an important virulence trait of the bacterium. Rather than directly regulating the expression of *e.g.* motility mediating genes, Hfq and bound sRNAs are being integrated into signal-response systems, such as QS- and environmental-sensing systems. This potentially amplifies the signalling of the regulatory networks and consequently facilitates the lifestyle switch.

Future work should reveal how expression of sRNAs is regulated in *Xf* and to what extend plant signals are influencing these regulatory circuits.
Overall, the sRNAs identified here, including conserved *sXF*s, point to cellular, extracellular, and cross-kingdom roles of *Xf*-sRNAs, revealing a regulatory layer of virulence in *Xf* that had not been explored before. Especially the reduced virulence observed in infection with *Xff*Δ*hfq*, highlights the importance of sRNA-based regulation and lays the foundation to study their function in regulating *Xf*'s virulence and life cycle.

However, target prediction and functional validation of bacterial sRNAs remains complicated[355]. Their homogeneity in length and secondary structure, coupled with small seed regions (< 10 nt), make it difficult to reliably predict interactions with targets. Our sRNA-annotation and target prediction pipeline consists of the tools APERO[356] and IntaRNA[357,358]. It starts from sequencing data of size-selected transcript leading to the identification of i) novel, unstructured bacterial sRNA candidates and ii) their mRNA target candidates. For example, the expression of the transcriptional regulator *bigR* which mediates biofilm formation, attachment and aggregation, and the QS-response regulator *rpfG*, are both Hfq-dependent and have sRNAs predicted to target the UTRs of their mRNAs. However, whether their expression is indeed mediated by interactions of Hfq-bound sRNAs with their Ribosome Binding Sites (RBS) requires further validation. This validation could be achieved by making use of translational GFP-fusion reporters which allow the study of the influence of bacterial sRNAs on targets[359,360]. Further, cross-referencing differentially expressed sRNAs and mRNAs in response to the sudden nutrient downshift with RNA interaction by ligation and sequencing (RIL-seq) data[361], should identify relevant sRNA-mRNA pairs associated with Hfq in both media conditions. Similar experiments in *Agrobacterium tumefaciens* identified 1697 mRNAs and 209 sRNAs associated with Hfq, resulting in the identification of over 50 previously unknown sRNAs[362].

Association of sRNAs and Hfq with *Xf*-EVs confirms their secretion from the cells. Applying WT EVs onto *Xff*Δ*hfq* cells could reveal if Hfq/sRNA-pairs delivered via EVs can modulate gene expression across cellular borders and help shape colony-wide transcriptional responses. By mutating only the C-ter of Hfq, the interaction face of Hfq with membranes[277,285], one might further be able to distinguish between cell autonomous and secreted functions of Hfq.

Target predictions of bacterial sRNAs with plant mRNAs included targets encoding immunity receptors. One of these immunity receptors, a *CNL*, showed differential expression following infection with *Xff* and *Xff*-EV-infiltration assays, representing an interesting candidate for a possible EV-mediated ckRNAi-interaction between *Xf* and its host plants. Established *in planta* "switch-on" reporters which are designed to visualize ckRNAi-interactions based on a relief of suppression of a fluorescent reporter in the presence of sRNA-mRNA interaction[117,289], could facilitate further validation. If the silencing of targets of *Xf* sRNAs can be validated *in planta*, the association of bacterial RNAs with host AGOs could further be investigated using AGO-immune purification followed by sequencing[363]. It would further be interesting to see if host targets are really being degraded by a "double-hit" of endogenous miRNA and *sXF*s, making use of degradome sequencing[364]. At this point, a combined mechanism of bacterial sRNAs getting integrated into endogenous host RNAi machinery and amplification remains still very speculative but would represent an intriguing novel way how bacterial sRNAs can act as effectors in plant infections.

For *Xf*, this would also represent the first report of an active suppression of immunity responses by interfering with the expression of an immune receptor. Because *Xf* lacks a T3SS and canonical effectors, research on its interactions with plants has primarily focused on PTI-typical immune responses[149,150] with two reports also showing HR-responses, a possible indication for ETI[161,162]. Contact-independent delivery via EVs could, on one hand, provide xylem-restricted *Xf* means to interfere with plant immune responses. On the other hand, if EVs and their cargo are transported beyond the xylem or interact with parenchyma cells in the xylem, they may also serve as key recognition cues for the plant immune system, triggering defences that limit *Xf* colonisation. The presence of MAMPs, such as EF-Tu, in *Xf*-EVs is speculated to trigger immune responses and restrict *Xf* infection success[149]. Additionally, the modification of the host membranes after fusion with bacterial EVs is proposed to result in intracellular host signalling[365]. However, whether nucleic acid cargo of EVs also trigger immune response is not known. Similarities between nucleic acid containing EVs and virus particles in size and cargo[366] and overlapping entry paths[227] begs the question whether plants respond similarly to bacterial (EV-) RNAs as to viruses.

Plant RNAi contributes to control of Xf *infections*

In eukaryotes, RNAi evolved as a "conserved immune mechanism to defend against invasive nucleic acids"[367]. Small interfering (si)RNAs, derived from viral or endogenous precursor dsRNA, regulate immune gene expression and degrade foreign RNA, protecting plants against pathogen attacks. Additionally, the non-cell autonomous functions of sRNAs help to coordinate immune responses across the whole plant[368–370]. Pathogens have evolved to interfere with this layer of immunity by secreting effectors targeting RNAi components[66,371]. This also includes the delivery of sRNAs which hijack the RNAi machinery to silence plant immunity genes[72]. By testing the interaction of several microbes with *At*, we observed different roles of plant RNAi components, namely AGOs and DCLs, for their interaction with the respective microbe[8]. For *Xff*, we revealed AGO1 as a negative regulator of *Xff* colonization in Arabidopsis, indicating an involvement of RNAi in the response to *Xf*. A potential integration of bacterial sRNAs into plant pathways to interfere with immune responses, begs the question if plants can detect and respond to such "foreign" RNA, other than viral RNA. Could proposed *sXF*-mediated ckRNAi engage RNAi components like AGO1 to sense bacterial RNA and initiate immune responses?

Detection of foreign sRNAs in plants

In humans, foreign sRNAs are Toll/Interleukin-1-like Receptor (TIR) ligands triggering immune responses[372,373]. The secondary structures marking of sRNAs marks them as foreign[374]. A plant homologue for such a perception is not known. While bacterial RNA can activate innate immunity responses in plants, underlying molecular mechanisms are not understood[375].
Most research on perception of foreign RNAs in plants has focused on viral infections, of which the presence of dsRNA is a hallmark[367]. Perception of (viral) dsRNA is proposed to be mediated by the PRR Somatic Embryogenesis Receptor-like Kinase 1 (SERK1), resulting in prototypical PAMP responses in Arabidopsis[376]. The EV-mediated delivery of bacterial sRNAs, potentially resulting in the association with plant membranes, might represent a critical detection point for the plant. Intracellular perception of (viral) RNA is mediated by RNAi components, in particular DCLs which can process dsRNA[367]. Recent discoveries propose a mechanism by which intracellular level of dsRNA and produced siRNAs are monitored by DCL4 and DLC2, with the saturation of DCL4 leading to the activation of DCL2, resulting in the activation of RNAi-independent immunity mediated by NLRs[377,378]. If bacterial sRNA-signals are indeed further amplified via phasiRNAs-pathways, elevated production of siRNAs might be

recognized by the same pathway. Which response NLRs are being triggered by DCL-dependant detection is still largely unknown[377]. TIR-only proteins have been proposed[76] with TIR domains of TNLs and TIR-only proteins exhibiting two distinct enzymatic activities: (i) nucleic acid hydrolase activity, cleaving dsRNA and DNA to produce 2′,3′-cAMP/cGMP, which promotes cell death[379], and (ii) NADase/ATPase activity, hydrolysing NAD^+ and ATP to generate signalling molecules that activate downstream immune pathways and cell death[82,83]. Intriguingly, the enzymatic activity of TIR-domains resulting in the production of signal molecules is a very conserved function in immunity throughout all domains of life[380–382]. Since DCL-dependent immunity activation depends on the production of siRNAs rather than consequent siRNA-based silencing[377,378], could it be a metabolic signal that activates NLRs rather than direct interaction of DCLs with NLRs?

The formation of biomolecular condensates has emerged as important player in the coordinating of stress responses and plant immune response[383,384]. Given the ability of TIR-domain proteins to undergo substrate-induced condensation[385] and DCLs to function within RNA-processing condensates[386], it is conceivable that the generation of subcellular reaction hubs with specific micro-environments leads to the interplay between DCLs and NLRs resulting in immune activation.

ckRNAi interactions or sRNA detection – a question of timing?

Overall, RNAi-mediated signals contribute to the regulation and activation of the plant immune system. Pathogens interfere with this layer of immunity to support their own growth. In the interaction of *Xff* and Arabidopsis, AGO1 negatively regulates *Xf* growth. If AGO1 is used to incorporate *sXF*s, as shown for rhizobial *tRF*s and the soybean homologue of Arabidopsis AGO1[133], AGO1 would represent a susceptibility factor to infection with *Xf*, its absence therefore reducing *Xf* colonization. However, AGO1 might also be involved in the detection of bacterial sRNAs. As ckRNAi is proposed to be relevant at early infection timepoints[289], detection of sRNAs by RNAi could be more relevant for the overall infection outcome. This might be the reason why EVs can supress *NLR* expression four hours after infiltration, but *ago1* mutants show increased bacterial load five days after infection. As a result, plant responses to infections with *Xff*Δ*hfq* compared to infections with *Xff* WT may provide a useful model for investigating sRNA-based responses, as Δ*hfq* knockout mutants show reduced levels of sRNAs[387,388]. Additionally, ongoing single-nuclei sequencing experiments will give insights

into tissue-specific responses of plants to infection with WT and *Xff*Δ*hfq* and could get scanned for potential interactors with bacterial RNAs or other EV cargo.

Vesiduction - EVs as mediators for HGT

In addition to RNA molecules, the DNA of three genomic islands was found associated with *Xff*-EVs[6]. Key components of the large protein complex of the T4-pilus, which mediates DNA uptake and natural competence in *Xf*, where also detected in *Xff*-EVs[36]. The OM-associated secretin PilQ is a porin responsible for the transport of DNA across the OM[36,389]. Two homologues of tip adhesin PilY and mayor pilin PilA stretch across the OM and might facilitate the capture of DNA from the extracellular space and retraction ATPases PilU/PilT might pull the DNA into the EV-lumen[390,391]. The periplasmic DNA-binding competence protein ComE is found in the lumen of *Xff*-EV, and facilitates DNA uptake and protection of DNA[304,392].

Hence, DNA of genomic islands found in *Xff*-EVs could either be the result of active release of genomic islands via EVs or the uptake of environmental DNA by EVs from dead *Xf* cells in the monoculture. DNA-seq of EVs from co-cultured *Xf* with other *Xf* strains, other bacteria or under natural conditions, could give insight on whether genomic islands are actively released via EVs or specifically taken up by EVs from the environment.

Association of genomic islands with EVs shows a clear specificity for some DNA fragments. A simple loading of enriched genomic DNA fragments is unlikely, since DNA of genomic islands is not found enriched in cellular DNA of *Xff* [6]. Whether association of genomic island with EVs is based on DNA modifications or requires additional co-factors remains to be studied. One interesting factor could be the DNA methylation patterns of genomic islands. Generally, the methylation of DNA marks DNA fragments as “own” and prevents degradation by restriction endonucleases, a system which protects bacterial cells against foreign DNA[393]. Unlike eukaryotes, methylation in prokaryotes is not actively remodelled but only removed passively during DNA replication[393]. Maybe counterintuitively, genomic exchange between bacteria is higher in species with more abundant Restriction-Modification Systems (RMS)[394]. Rather than blocking all genomic exchange, RMS and their specific methylation patterns facilitate genomic exchange between species with similar RMS, creating “highways” of genomic exchange[394]. RMS are prevalent in *Xylella* and vary across different lineages, resulting in a multitude of genomic DNA methylation patterns[395]. Methylation patterns of genomic islands associated with EVs might therefore provide a strain-specificity of DNA intergration.

Epigenetic profiling of EV-DNA using PacBio- or Nanopore-sequencing could shed light on such modifications[396]. These sequencing techniques would further also reveal the true length of DNA fragments associated with EVs. Previous DNA-seq was performed with Illumina sequencing, which includes fragmentation of DNA before sequencing. In *E.coli*, vesiduction efficiency showed no increased uptake times for fragments up to 15 kb, indicating that large DNA fragments can be transferred via EVs[397].

In *Pa*, efficiency of vesiduction is influenced by growth states of EV-releasing cells, with higher transformation efficiency of biofilm-derived EVs[210]. EV-association of membrane-binding compounds, including antimicrobial peptides in sublethal concentrations, can influence the exchange of EVs across bacterial cells[214]. Whether there is a specific uptake of EVs by, for example, "vesiduction-ready" cells, similar to receptor-mediated uptake of bacteriophages[398] or EV-uptake by eukaryotic cells[229], is currently not understood. This process might further be influenced by sRNAs contained in *Xff*-EVs which are predicted to target *e.g. ComE*[6]. A similar sRNA-based mechanism is *e.g.* observed for the extrachromosomal DNA transfer in *Salmonella enterica*[399].

Previous experiments in *Xf* showed high recombination rates across *Xf* cells when co-cultured with another *Xf* strain and under natural flow condition[32,34]. The authors also noted increasing levels of extracellular (ex)DNA during growth, without assessing what sequences the exDNA contained[34]. Biofilm matrixes consist of exDNA and could also be a source of DNA for capture by EVs. Release of exDNA is mediated via QS[400], and so is the release of EVs in *Xf* [5] and its natural competence[34]. To what extent measured exDNA is associated with EVs and how this influences HGT remains to be assessed.

Natural competence rates vary in different strains of *Xf*, with lower rates in *Xfp* strain 'DeDonno' compared to *Xff* strain 'Temecula1'[35]. Under the same growth conditions, we showed reduced production of EVs and lack of T4-pilus components at *Xf*-EVs of subsp. *pauca* strain 'DeDonno'[6], which might additionally influence competence in subspecies *pauca*.

Compared to other bacterial pathogens with broad host ranges, *Xf* has unusually high recombination rates[34,401] and HGT is believed to facilitate adjustment to novel hosts and environments[25–31], highlighting the importance of HGT for *Xf*. Genomic islands associated with *Xf*-EVs encode proteins important for their own mobility (Helicases, DNA polymerase, Recombinase, Integrase) but also contain genes encoding for toxins, sRNAs and many proteins with unknown functions. The vesiduction-mediated dissemination of the sRNA-island

harbouring five copies of *sXF*s implies that *sXF*s can be horizontally transferred. This is akin to many other virulence-associated sRNAs in bacteria[402] and has been proposed for the *Xanthomonadacea* sRNA-*Xcc1*, the homologues of *sXFs*[303]. Initial evidence suggests that *sXF*s target plant *NLR*s, functioning as virulence factors in *Xff,* but require further validation. Studying the conservation of *sXF*s and their targets across different *Xf* lineages and hosts could give insight into what role they play in the virulence and host specificity of *Xf.*

Antibacterial toxins to establish niche dominance and enlarge available gene pool

In addition to sRNAs and genomic islands, we identified several antimicrobial toxins as cargo of *Xf*-EVs. The growth of *Xylella* is restricted to two distinct environments: the xylem of its host plants and the foregut of insect vectors. Both environments are colonized by microbiomes, including bacterial, fungal and viral populations[403–406]. In the xylem, nutrients for microbial growth are limited, making it a very competitive environment[407]. Bacteriocin, one of the most enriched proteins in *Xf*-EVs of both *Xf* subspecies, has anti-microbial properties[408]. Delivering hydrophobic antimicrobial proteins and toxins in the aqueous xylem environment via EVs might help *Xf* to establish its niche dominance by indirect intraspecies competition[403,409–413]. The death of competing microorganisms in the xylem further releases DNA, which enlarges the available gene pool for HGT[414].

Across microbial communities in the ocean, EVs facilitate "marine HGT"[415] and our data suggests that EVs might play similar roles for xylem communities. This highlights vesiduction as a general mechanism to support HGT in aqueous environments. In summary, EV-mediated transfer of DNA, sRNAs, and toxins likely promotes HGT in the xylem, potentially enhancing *Xf*'s adaptability to new hosts.

Are Xf-*EVs facilitating the delivery of molecules in the aqueous xylem environment?*

Xylella's genome is very small and has lost all secretion systems which could directly deliver molecules either into the host or inject into competitive bacterial strains (T3SS; T6SS)[416]. Bacterial social behaviour requires communication among neighbouring cells, allowing coordination of cooperative strategies within the same species[417]. *Xf*, like many other bacteria, coordinates its social behaviour through the secretion of QS-factors[337,339]. In its

biological niche, the xylem, *Xf* might be required to indirectly deliver molecules over longer paths to reach cooperating *Xf* cells, competitive microbial strains and host cells. EVs represent prime candidates for such a delivery.

Xf-EVs not only mediate the spread of QS-molecules[157] but are themselves regulated by the QS-system, which coordinates lifestyle changes[5]. We could extend this knowledge, proposing EVs as important players in HGT, another form of bacterial social behaviour. *Xf*-EVs carry (i) Genomic islands, (ii) proteins facilitating DNA uptake, (iii) bacteriocin which might enlarge the available gene pool and (iv) sRNAs which are predicted to regulate HGT.

The dependency on Hfq and sRNAs, both present as cargos of *Xff*-EVs, for a coordinated lifestyle switch in response to changing environmental conditions, broadens our understanding of how *Xf* regulates this process. The reduced virulence of the *Xff*Δ*hfq* mutant further underscores the importance of this regulatory mechanism for *Xf*'s pathogenicity.

In addition to their roles in bacterial communication, *Xf*-EVs may also serve as vehicles for delivering molecules into plant tissues. We could confirm the association of known virulence factors with *Xf*-EVs and propose sRNAs of class *sXF*s as new virulence factors associated with EVs. They potentially mediate the expression of *NLR*s through a ckRNAi-type interaction. The negative regulatory function of AGO1 in infection with *Xf* in *At*, opens new avenues in understanding the underlying mechanisms on how plants can sense the presence of xylem-inhabiting microbes and their RNAs.

Open questions

i) Can we distinguish between different subpopulation of EVs, *e.g.* by making use of single-EV sequencing[418]? Do these subpopulations carry different cargo, fulfilling different roles? How do growth conditions and plant signals influence *Xf*-EV-cargo?

ii) How is cargo sorted and loaded into EVs? Can modification of EV components and cargo (lipids, proteins, DNA, RNA) explain loading specificity and their very strong protection in *Xf*-EVs? Do such modifications also play a role in the uptake of EVs by certain cellular subpopulations (*e.g.* competent cells) or tissues (role of receptors)?

iii) Can we confirm the regulation of gene expression by EV-delivered RNA molecules across cellular borders?

iv) Do *Xf*-EVs enter plant target cells or merge with the plasma membrane to deliver their cargo? Do CWDEs, similarly as suggested in fungal pathogens, play a role in their delivery?

v) Can bacterial sRNAs be integrated into the RNAi-pathway or do they function with other components? What plant proteins (DCL?) incorporate them? Can we find secondary, phased RNAs produced in response to treatment with bacterial sRNAs?

vi) Do bacterial RNAs elicit plant immune responses? Are they similar to viral defence responses?

vii) How does *Xf*'s restriction to the xylem influence the detection of the bacteria by the plant and what role do EVs play in triggering immune responses?

viii) Is association of DNA with *Xf*-EVs the result of uptake of environmental DNA by EVs or the result of active release of the genomic islands from the EV-producing cell? To what degree do EVs influence HGT in *Xf*?

Save the olive trees – an outlook for RNA-based methods to fight Xf

Given the rise of RNA-based plant protection tools against eukaryotic pathogens[419], and the recent development of antibacterial gene silencing strategies[260], our findings on the importance of RNA-mediated signalling for *Xf* virulence indicate that comparable approaches could be explored for controlling *Xf*. For example, it could be interesting to moonlight specific RNA classes or generate RNAs which stay bound to Hfq and hence block its activity. Genomic interruption of Hfq locks *Xf* in biofilm growth and interferes with QS-signalling and sensing of environmental signals. This also leads to reduced systemic infection, making Hfq a promising target to control infection with *Xf*. In eukaryotes, the identification of interaction partners of AGO proteins has led to the development of peptides which can bind and block AGO functions[420]. Since the protein-interactome of Hfq is relatively well-studied[421] and its crystal-structure, including RNA binding sites, is resolved[269,422,423], a similar peptide might be developed to block Hfq function. If expressed in the plant or delivered extracellularly, both peptide or RNAs would need to be delivered to the xylem. Antimicrobial peptides infiltrated in tobacco leaves showed promising protective results against *Xf* infection[424,425]. Additionally, sprayed dsRNA can colocalize with xylem structures, which might facilitate targeting of *Xf* with RNA[426,427]. A biological control of adhesion and retention of *Xf* in the insect vectors could also reduce the spread of *Xf* [40]. RNAi-based techniques have been successfully tested against

other insect-borne diseases[428–430] but would require better understanding of molecular components regulating *Xf* transmission by insects[431].

References

1. Ruf, A., Oberkofler, L., Robatzek, S. & Weiberg, A. Spotlight on plant RNA-containing extracellular vesicles. *Current Opinion in Plant Biology* **69**, 102272 (2022).
2. Ruf, A. & Robatzek, S. “Messenger RNA just entered the chat”: The next layer of cross-kingdom RNA transfer. *Cell Host & Microbe* **32**, 7–8 (2024).
3. Thieron, H. *et al.* Practical advice for extracellular vesicle isolation in plant–microbe interactions: Concerns, considerations, and conclusions. *J Extracell Vesicles* **13**, e70022 (2024).
4. Landa, B. B. *et al.* Xylella fastidiosa’s relationships: the bacterium, the host plants, and the plant microbiome. *New Phytologist* **234**, 1598–1605 (2022).
5. Ionescu, M. *et al.* Xylella fastidiosa outer membrane vesicles modulate plant colonization by blocking attachment to surfaces. *Proc. Natl. Acad. Sci. U.S.A.* **111**, (2014).
6. Ruf, A. *et al.* Extracellular Vesicles From Xylella fastidiosa Carry sRNAs and Genomic Islands, Suggesting Roles in Recipient Cells. *JEV* **14**, e70102 (2025).
7. Ruf, A. *et al.* Hfq is integrated into transcriptional networks in Xylella fastidiosa supporting lifestyle transitions and systemic infection in plants. *unpublished* (unpublished).
8. Ruf, A. *et al.* Broad-scale phenotyping in Arabidopsis reveals varied involvement of RNA interference across diverse plant-microbe interactions. *Plant Direct* **8**, e70017 (2024).
9. FAO. *Gross Domestic Product and Agriculture Value Added 2014–2023*. https://openknowledge.fao.org/handle/20.500.14283/cd5490en (2025) doi:10.4060/cd5490en.
10. FAO. *FAO’s Plant Production and Protection Division*. (FAO, 2022). doi:10.4060/cc2447en.
11. Miller, S. A., Testen, A. L., Jacobs, J. M. & Ivey, M. L. L. Mitigating Emerging and Reemerging Diseases of Fruit and Vegetable Crops in a Changing Climate. *Phytopathology* **114**, 917–929 (2024).
12. Subbarao, K. V., Sundin, G. W. & Klosterman, S. J. Focus Issue Articles on Emerging and Re-Emerging Plant Diseases. *Phytopathology*® **105**, 852–854 (2015).
13. Saponari, M., Giampetruzzi, A., Loconsole, G., Boscia, D. & Saldarelli, P. Xylella fastidiosa in Olive in Apulia: Where We Stand. *APS* **109**, 175–186 (2019).
14. EPPO, S. A. Xylella fastidiosa in the EPPO region. *Short notes Xylella* https://www.eppo.int/ACTIVITIES/plant_quarantine/shortnotes_qps/shortnotes_xylella.
15. De La Fuente, L., Navas-Cortés, J. A. & Landa, B. B. Ten Challenges to Understanding and Managing the Insect-Transmitted, Xylem-Limited Bacterial Pathogen Xylella fastidiosa. *Phytopathology* **114**, 869–884 (2024).
16. Pfitzer, R. *et al.* Effects of succession crops and soil tillage on suppressing the syndrome ‘basses richesses’ vector Pentastiridius leporinus in sugar beet. *Pest ManagmSci* **80**, 3379–3388 (2024).
17. Mahillon, M. *et al.* From insect endosymbiont to phloem colonizer: comparative genomics unveils the lifestyle transition of phytopathogenic Arsenophonus strains. *mSystems* **10**, e01496-24 (2025).
18. Malinowski, R., Singh, D., Kasprzewska, A., Blicharz, S. & Basińska-Barczak, A. Vascular tissue – boon or bane? How pathogens usurp long-distance transport in plants and the defence mechanisms deployed to counteract them. *New Phytologist* **243**, 2075–2092 (2024).

19. Mansfield, J. *et al.* Top 10 plant pathogenic bacteria in molecular plant pathology. *Molecular Plant Pathology* **13**, 614–629 (2012).
20. Yaschenko, A. E., Alonso, J. M. & Stepanova, A. N. Arabidopsis as a model for translational research. *Plant Cell* **37**, koae065 (2025).
21. Kirzinger, M. W. B., Nadarasah, G. & Stavrinides, J. Insights into Cross-Kingdom Plant Pathogenic Bacteria. *Genes* **2**, 980–997 (2011).
22. Authority (EFSA), E. F. S. *et al.* Update of the Xylella spp. host plant database – Systematic literature search up to 30 June 2024. *EFSA J* **23**, e9241 (2025).
23. Roper, C., Castro, C. & Ingel, B. *Xylella fastidiosa*: bacterial parasitism with hallmarks of commensalism. *Current Opinion in Plant Biology* **50**, 140–147 (2019).
24. Nunney, L., Azad, H. & Stouthamer, R. An Experimental Test of the Host-Plant Range of Nonrecombinant Strains of North American Xylella fastidiosa subsp. multiplex. *Phytopathology* **109**, 294–300 (2019).
25. Potnis, N. *et al.* Patterns of inter- and intrasubspecific homologous recombination inform eco-evolutionary dynamics of Xylella fastidiosa. *The ISME Journal* **13**, 2319–2333 (2019).
26. Nunney, L., Schuenzel, E. L., Scally, M., Bromley, R. E. & Stouthamer, R. Large-Scale Intersubspecific Recombination in the Plant-Pathogenic Bacterium Xylella fastidiosa Is Associated with the Host Shift to Mulberry. *Appl Environ Microbiol* **80**, 3025–3033 (2014).
27. Nunney, L., Hopkins, D. L., Morano, L. D., Russell, S. E. & Stouthamer, R. Intersubspecific Recombination in Xylella fastidiosa Strains Native to the United States: Infection of Novel Hosts Associated with an Unsuccessful Invasion. *Appl Environ Microbiol* **80**, 1159–1169 (2014).
28. Nunney, L. *et al.* Population Genomic Analysis of a Bacterial Plant Pathogen: Novel Insight into the Origin of Pierce's Disease of Grapevine in the U.S. *PLOS ONE* **5**, e15488 (2010).
29. Nunney, L., Yuan, X., Bromley, R. E. & Stouthamer, R. Detecting Genetic Introgression: High Levels of Intersubspecific Recombination Found in Xylella fastidiosa in Brazil. *Appl Environ Microbiol* **78**, 4702–4714 (2012).
30. Almeida, R. P. P. *et al.* Genetic Structure and Biology of Xylella fastidiosa Strains Causing Disease in Citrus and Coffee in Brazil. *Appl Environ Microbiol* **74**, 3690–3701 (2008).
31. Coletta-Filho, H. D., Francisco, C. S., Lopes, J. R. S., Muller, C. & Almeida, R. P. P. Homologous Recombination and Xylella fastidiosa Host–Pathogen Associations in South America. *Phytopathology* **107**, 305–312 (2017).
32. Kandel, P. P., Lopez, S. M., Almeida, R. P. P. & De La Fuente, L. Natural Competence of Xylella fastidiosa Occurs at a High Frequency Inside Microfluidic Chambers Mimicking the Bacterium's Natural Habitats. *Appl Environ Microbiol* **82**, 5269–5277 (2016).
33. Kandel, P. P., Almeida, R. P. P., Cobine, P. A. & De La Fuente, L. Natural Competence Rates Are Variable Among Xylella fastidiosa Strains and Homologous Recombination Occurs In Vitro Between Subspecies fastidiosa and multiplex. *MPMI* **30**, 589–600 (2017).
34. Kung, S. H. & Almeida, R. P. P. Natural Competence and Recombination in the Plant Pathogen Xylella fastidiosa. *Appl Environ Microbiol* **77**, 5278–5284 (2011).

35. D'Attoma, G. *et al.* Phenotypic Characterization and Transformation Attempts Reveal Peculiar Traits of Xylella fastidiosa Subspecies pauca Strain De Donno. *Microorganisms* **8**, 1832 (2020).
36. Merfa, M. V. *et al.* Complete functional analysis of type IV pilus components of a reemergent plant pathogen reveals neofunctionalization of paralog genes. *PLoS Pathog* **19**, e1011154 (2023).
37. Firrao, G., Scortichini, M. & Pagliari, L. Orthology-Based Estimate of the Contribution of Horizontal Gene Transfer from Distantly Related Bacteria to the Intraspecific Diversity and Differentiation of Xylella fastidiosa. *Pathogens* **10**, 46 (2021).
38. Beaber, J. W., Hochhut, B. & Waldor, M. K. SOS response promotes horizontal dissemination of antibiotic resistance genes. *Nature* **427**, 72–74 (2004).
39. Shvetsov, A. V. *et al.* Structure of RecX protein complex with the presynaptic RecA filament: Molecular dynamics simulations and small angle neutron scattering. *FEBS Letters* **588**, 948–955 (2014).
40. Krugner, R., Sisterson, M. S., Backus, E. A., Burbank, L. P. & Redak, R. A. Sharpshooters: a review of what moves Xylella fastidiosa. *Austral Entom* **58**, 248–267 (2019).
41. Castro, C., DiSalvo, B. & Roper, M. C. Xylella fastidiosa: A reemerging plant pathogen that threatens crops globally. *PLOS Pathogens* **17**, e1009813 (2021).
42. Lucas, W. J. *et al.* The Plant Vascular System: Evolution, Development and Functions. *J Int Plant Bio* **55**, 294–388 (2013).
43. Pickard, W. F. The ascent of sap in plants. *Progress in Biophysics and Molecular Biology* **37**, 181–229 (1981).
44. Cosgrove, D. J. Structure and growth of plant cell walls. *Nat Rev Mol Cell Biol* **25**, 340–358 (2024).
45. Zhong, R., Cui, D. & Ye, Z.-H. Secondary cell wall biosynthesis. *New Phytologist* **221**, 1703–1723 (2019).
46. Oda, Y. & Fukuda, H. Initiation of Cell Wall Pattern by a Rho- and Microtubule-Driven Symmetry Breaking. *Science* **337**, 1333–1336 (2012).
47. Sugiyama, Y. *et al.* A Rho-actin signaling pathway shapes cell wall boundaries in Arabidopsis xylem vessels. *Nat Commun* **10**, 468 (2019).
48. Carluccio, G. *et al.* Xylem Embolism and Pathogens: Can the Vessel Anatomy of Woody Plants Contribute to X. fastidiosa Resistance? *Pathogens* **12**, 825 (2023).
49. Scholander, P. F., Bradstreet, E. D., Hemmingsen, E. A. & Hammel, H. T. Sap Pressure in Vascular Plants. *Science* **148**, 339–346 (1965).
50. Chu, L. T. *et al.* Development of a tomato xylem-mimicking microfluidic system to study Ralstonia pseudosolanacearum biofilm formation. *Front. Bioeng. Biotechnol.* **12**, (2024).
51. Munzert, K. S. & Engelsdorf, T. Plant cell wall structure and dynamics in plant–pathogen interactions and pathogen defence. *J Exp Bot* **76**, 228–242 (2025).
52. De La Fuente, L., Burr, T. J. & Hoch, H. C. Autoaggregation of Xylella fastidiosa Cells Is Influenced by Type I and Type IV Pili. *Applied and Environmental Microbiology* **74**, 5579–5582 (2008).
53. Guilhabert, M. R. & Kirkpatrick, B. C. Identification of Xylella fastidiosa Antivirulence Genes: Hemagglutinin Adhesins Contribute to X. fastidiosa Biofilm Maturation and Colonization and Attenuate Virulence. *MPMI* **18**, 856–868 (2005).

54. Cruz, L. F., Cobine, P. A. & De La Fuente, L. Calcium Increases Xylella fastidiosa Surface Attachment, Biofilm Formation, and Twitching Motility. *Appl Environ Microbiol* **78**, 1321–1331 (2012).
55. De La Fuente, L. *et al.* Assessing Adhesion Forces of Type I and Type IV Pili of Xylella fastidiosa Bacteria by Use of a Microfluidic Flow Chamber. *Appl Environ Microbiol* **73**, 2690–2696 (2007).
56. Feitosa-Junior, O. R. *et al.* The XadA Trimeric Autotransporter Adhesins in Xylella fastidiosa Differentially Contribute to Cell Aggregation, Biofilm Formation, Insect Transmission and Virulence to Plants. *MPMI* **35**, 857–866 (2022).
57. Killiny, N., Martinez, R. H., Dumenyo, C. K., Cooksey, D. A. & Almeida, R. P. P. The Exopolysaccharide of Xylella fastidiosa Is Essential for Biofilm Formation, Plant Virulence, and Vector Transmission. *MPMI* **26**, 1044–1053 (2013).
58. Anbumani, S. *et al.* Controlled spatial organization of bacterial growth reveals key role of cell filamentation preceding Xylella fastidiosa biofilm formation. *npj Biofilms Microbiomes* **7**, 86 (2021).
59. Meng, Y. *et al.* Upstream Migration of Xylella fastidiosa via Pilus-Driven Twitching Motility. *J Bacteriol* **187**, 5560–5567 (2005).
60. Oliver, J. E. *et al.* Ionome Changes in Xylella fastidiosa–Infected Nicotiana tabacum Correlate With Virulence and Discriminate Between Subspecies of Bacterial Isolates. *MPMI* **27**, 1048–1058 (2014).
61. Fuente, L. D. L. *et al.* The Bacterial Pathogen Xylella fastidiosa Affects the Leaf Ionome of Plant Hosts during Infection. *PLOS ONE* **8**, e62945 (2013).
62. Rapicavoli, J., Ingel, B., Blanco-Ulate, B., Cantu, D. & Roper, C. Xylella fastidiosa: an examination of a re-emerging plant pathogen. *Molecular Plant Pathology* **19**, 786–800 (2018).
63. Cruz, L. F., Parker, J. K., Cobine, P. A. & De La Fuente, L. Calcium-Enhanced Twitching Motility in Xylella fastidiosa Is Linked to a Single PilY1 Homolog. *Appl Environ Microbiol* **80**, 7176–7185 (2014).
64. Parker, J. K., Chen, H., McCarty, S. E., Liu, L. Y. & De La Fuente, L. Calcium transcriptionally regulates the biofilm machinery of Xylella fastidiosa to promote continued biofilm development in batch cultures. *Env Micro* **18**, 1620–1634 (2016).
65. Newman, M.-A., Sundelin, T., Nielsen, J. T. & Erbs, G. MAMP (microbe-associated molecular pattern) triggered immunity in plants. *Front. Plant Sci.* **4**, (2013).
66. Hou, Y. *et al.* A Phytophthora Effector Suppresses Trans-Kingdom RNAi to Promote Disease Susceptibility. *Cell Host & Microbe* **25**, 153-165.e5 (2019).
67. Tang, D., Wang, G. & Zhou, J.-M. Receptor Kinases in Plant-Pathogen Interactions: More Than Pattern Recognition. *Plant Cell* **29**, 618–637 (2017).
68. Dodds, P. N. & Rathjen, J. P. Plant immunity: towards an integrated view of plant–pathogen interactions. *Nat Rev Genet* **11**, 539–548 (2010).
69. Zhou, J.-M. & Zhang, Y. Plant Immunity: Danger Perception and Signaling. *Cell* **181**, 978–989 (2020).
70. Toruño, T. Y., Stergiopoulos, I. & Coaker, G. Plant-Pathogen Effectors: Cellular Probes Interfering with Plant Defenses in Spatial and Temporal Manners. *Annu. Rev. Phytopathol.* **54**, 419–441 (2016).

71. Chanclud, E. & Morel, J.-B. Plant hormones: a fungal point of view. *Mol Plant Pathol* **17**, 1289–1297 (2016).
72. Weiberg, A. *et al.* Fungal small RNAs suppress plant immunity by hijacking host RNA interference pathways. *Science* **342**, 118–123 (2013).
73. Collemare, J., O'Connell, R. & Lebrun, M.-H. Nonproteinaceous effectors: the terra incognita of plant–fungal interactions. *New Phytologist* **223**, 590–596 (2019).
74. Cui, H., Tsuda, K. & Parker, J. E. Effector-Triggered Immunity: From Pathogen Perception to Robust Defense. *Annual Review of Plant Biology* **66**, 487–511 (2015).
75. Takken, F. L., Albrecht, M. & Tameling, W. I. Resistance proteins: molecular switches of plant defence. *Current Opinion in Plant Biology* **9**, 383–390 (2006).
76. Huang, S. *et al.* NLR signaling in plants: from resistosomes to second messengers. *Trends in Biochemical Sciences* **48**, 776–787 (2023).
77. Wang, J. *et al.* Reconstitution and structure of a plant NLR resistosome conferring immunity. *Science* **364**, eaav5870 (2019).
78. Bi, G. *et al.* The ZAR1 resistosome is a calcium-permeable channel triggering plant immune signaling. *Cell* **184**, 3528-3541.e12 (2021).
79. Adachi, H. *et al.* An N-terminal motif in NLR immune receptors is functionally conserved across distantly related plant species. *eLife* **8**, e49956 (2019).
80. Ibrahim, T. *et al.* A helper NLR targets organellar membranes to trigger immunity. 2024.09.19.613839 Preprint at https://doi.org/10.1101/2024.09.19.613839 (2024).
81. Huang, S., Li, E., Jia, F., Han, Z. & Chai, J. Assembly and functional mechanisms of plant NLR resistosomes. *Current Opinion in Structural Biology* **90**, 102977 (2025).
82. Wan, L. *et al.* TIR domains of plant immune receptors are NAD+-cleaving enzymes that promote cell death. *Science* **365**, 799–803 (2019).
83. Horsefield, S. *et al.* NAD+ cleavage activity by animal and plant TIR domains in cell death pathways. *Science* **365**, 793–799 (2019).
84. Yu, X. *et al.* PTI-ETI synergistic signal mechanisms in plant immunity. *Plant Biotechnol J* **22**, 2113–2128 (2024).
85. Jones, J. D. G., Staskawicz, B. J. & Dangl, J. L. The plant immune system: From discovery to deployment. *Cell* **187**, 2095–2116 (2024).
86. Tsuda, K. & Somssich, I. E. Transcriptional networks in plant immunity. *New Phytologist* **206**, 932–947 (2015).
87. Javed, T. & Gao, S.-J. WRKY transcription factors in plant defense. *Trends in Genetics* **39**, 787–801 (2023).
88. Muhammad, T., Zhang, F., Zhang, Y. & Liang, Y. RNA Interference: A Natural Immune System of Plants to Counteract Biotic Stressors. *Cells* **8**, 38 (2019).
89. Wang, J., Mei, J. & Ren, G. Plant microRNAs: Biogenesis, Homeostasis, and Degradation. *Front. Plant Sci.* **10**, (2019).
90. Martín-Merchán, A., Moro, B., Bouet, A. & Bologna, N. G. Domain organization, expression, subcellular localization, and biological roles of ARGONAUTE proteins in Arabidopsis. *J Exp Bot* **74**, 2374–2388 (2023).
91. Iwakawa, H. & Tomari, Y. Life of RISC: Formation, action, and degradation of RNA-induced silencing complex. *Molecular Cell* **82**, 30–43 (2022).

92. Curaba, J. & Chen, X. Biochemical Activities of *Arabidopsis* RNA-dependent RNA Polymerase 6*. *Journal of Biological Chemistry* **283**, 3059–3066 (2008).
93. Felippes, F. F. de, Ott, F. & Weigel, D. Comparative analysis of non-autonomous effects of tasiRNAs and miRNAs in Arabidopsis thaliana. *Nucleic Acids Res* **39**, 2880–2889 (2011).
94. Zou, Y. *et al.* Transcriptional Regulation of the Immune Receptor FLS2 Controls the Ontogeny of Plant Innate Immunity. *Plant Cell* **30**, 2779–2794 (2018).
95. Tian, D., Traw, M. B., Chen, J. Q., Kreitman, M. & Bergelson, J. Fitness costs of R-gene-mediated resistance in Arabidopsis thaliana. *Nature* **423**, 74–77 (2003).
96. Li, S.-X., Liu, Y., Zhang, Y.-M., Chen, J.-Q. & Shao, Z.-Q. Convergent reduction of immune receptor repertoires during plant adaptation to diverse special lifestyles and habitats. *Nat. Plants* **11**, 248–262 (2025).
97. Deng, Y. *et al.* A role for small RNA in regulating innate immunity during plant growth. *PLOS Pathogens* **14**, e1006756 (2018).
98. Zhai, J. *et al.* MicroRNAs as master regulators of the plant NB-LRR defense gene family via the production of phased, trans-acting siRNAs. *Genes Dev.* **25**, 2540–2553 (2011).
99. Li, F. *et al.* MicroRNA regulation of plant innate immune receptors. *PNAS* **109**, 1790–1795 (2012).
100. Shivaprasad, P. V. *et al.* A MicroRNA Superfamily Regulates Nucleotide Binding Site–Leucine-Rich Repeats and Other mRNAs. *Plant Cell* **24**, 859–874 (2012).
101. Zhang, Y., Xia, R., Kuang, H. & Meyers, B. C. The Diversification of Plant NBS-LRR Defense Genes Directs the Evolution of MicroRNAs That Target Them. *Mol Biol Evol* **33**, 2692–2705 (2016).
102. López-Márquez, D. *et al.* Regulation of plant immunity via small RNA-mediated control of NLR expression. *J Exp Bot* **74**, 6052–6068 (2023).
103. Fei, Q., Xia, R. & Meyers, B. C. Phased, Secondary, Small Interfering RNAs in Posttranscriptional Regulatory Networks. *Plant Cell* **25**, 2400–2415 (2013).
104. de Vries, S., de Vries, J. & Rose, L. E. The Elaboration of miRNA Regulation and Gene Regulatory Networks in Plant–Microbe Interactions. *Genes (Basel)* **10**, 310 (2019).
105. Liao, L., Xie, B., Guan, P., Jiang, N. & Cui, J. New insight into the molecular mechanism of miR482/2118 during plant resistance to pathogens. *Front Plant Sci* **13**, 1026762 (2022).
106. Canto-Pastor, A. *et al.* Enhanced resistance to bacterial and oomycete pathogens by short tandem target mimic RNAs in tomato. *PNAS* **116**, 2755–2760 (2019).
107. Boccara, M. *et al.* The Arabidopsis miR472-RDR6 Silencing Pathway Modulates PAMP- and Effector-Triggered Immunity through the Post-transcriptional Control of Disease Resistance Genes. *PLOS Pathogens* **10**, e1003883 (2014).
108. Niu, D. *et al.* Bacillus cereus AR156 primes induced systemic resistance by suppressing miR825/825* and activating defense-related genes in Arabidopsis. *J Int Plant Bio* **58**, 426–439 (2016).
109. Nie, P. *et al.* Function of miR825 and miR825* as Negative Regulators in Bacillus cereus AR156-elicited Systemic Resistance to Botrytis cinerea in Arabidopsis thaliana. *International Journal of Molecular Sciences* **20**, 5032 (2019).

110. Jiang, C. *et al.* Bacillus cereus AR156 triggers induced systemic resistance against Pseudomonas syringae pv. tomato DC3000 by suppressing miR472 and activating CNLs-mediated basal immunity in Arabidopsis. *Molecular Plant Pathology* **21**, 854–870 (2020).
111. Shine, M. B. *et al.* Phased small RNA–mediated systemic signaling in plants. *Sci Adv* **8**, eabm8791 (2022).
112. Vaucheret, H. Plant ARGONAUTES. *Trends in Plant Science* **13**, 350–358 (2008).
113. Navarro, L. *et al.* A Plant miRNA Contributes to Antibacterial Resistance by Repressing Auxin Signaling. *Science* **312**, 436–439 (2006).
114. Ellendorff, U., Fradin, E. F., de Jonge, R. & Thomma, B. P. H. J. RNA silencing is required for Arabidopsis defence against Verticillium wilt disease. *J Exp Bot* **60**, 591–602 (2009).
115. Li, Y. *et al.* Identification of MicroRNAs Involved in Pathogen-Associated Molecular Pattern-Triggered Plant Innate Immunity. *Plant Physiology* **152**, 2222–2231 (2010).
116. Cao, J.-Y., Xu, Y.-P., Zhao, L., Li, S.-S. & Cai, X.-Z. Tight regulation of the interaction between Brassica napus and Sclerotinia sclerotiorum at the microRNA level. *Plant Mol Biol* **92**, 39–55 (2016).
117. Dunker, F. *et al.* Oomycete small RNAs bind to the plant RNA-induced silencing complex for virulence. *eLife* **9**, e56096 (2020).
118. Shen, D. *et al.* Identification and characterization of microRNAs in oilseed rape (Brassica napus) responsive to infection with the pathogenic fungus Verticillium longisporum using Brassica AA (Brassica rapa) and CC (Brassica oleracea) as reference genomes. *New Phytologist* **204**, 577–594 (2014).
119. Yu, X. *et al.* Malus hupehensis miR168 Targets to ARGONAUTE1 and Contributes to the Resistance against Botryosphaeria dothidea Infection by Altering Defense Responses. *Plant Cell Physiol* **58**, 1541–1557 (2017).
120. Bjornson, M., Pimprikar, P., Nürnberger, T. & Zipfel, C. The transcriptional landscape of Arabidopsis thaliana pattern-triggered immunity. *Nat. Plants* **7**, 579–586 (2021).
121. Maier, B. A. *et al.* A general non-self response as part of plant immunity. *Nat. Plants* **7**, 696–705 (2021).
122. Kong, X., Yang, M., Le, B. H., He, W. & Hou, Y. The master role of siRNAs in plant immunity. *Mol Plant Pathol* **23**, 1565–1574 (2022).
123. Song, L., Fang, Y., Chen, L., Wang, J. & Chen, X. Role of non-coding RNAs in plant immunity. *Plant Comm* **2**, (2021).
124. Zhang, S., Li, C., Si, J., Han, Z. & Chen, D. Action Mechanisms of Effectors in Plant-Pathogen Interaction. *International Journal of Molecular Sciences* **23**, 6758 (2022).
125. Boch, J. & Bonas, U. Xanthomonas AvrBs3 Family-Type III Effectors: Discovery and Function. *Annu. Rev. Phytopathol.* **48**, 419–436 (2010).
126. Navarro, L., Jay, F., Nomura, K., He, S. Y. & Voinnet, O. Suppression of the MicroRNA Pathway by Bacterial Effector Proteins. *Science* **321**, 964–967 (2008).
127. Mosher, R. A. & Baulcombe, D. C. Bacterial pathogens encode suppressors of RNA-mediated silencing. *Genome Biol* **9**, 237 (2008).
128. Thiébeauld, O. *et al.* A bacterial effector directly targets Arabidopsis Argonaute 1 to suppress Pattern-triggered immunity and cause disease. 215590 Preprint at https://doi.org/10.1101/215590 (2023).

129. Wang, M. *et al.* Bidirectional cross-kingdom RNAi and fungal uptake of external RNAs confer plant protection. *Nat Plants* **2**, 16151 (2016).
130. Zhang, T. *et al.* Cotton plants export microRNAs to inhibit virulence gene expression in a fungal pathogen. *Nat Plants* **2**, 1–6 (2016).
131. Cai, Q. *et al.* Plants send small RNAs in extracellular vesicles to fungal pathogen to silence virulence genes. *Science* https://doi.org/10.1126/science.aar4142 (2018) doi:10.1126/science.aar4142.
132. Silvestri, A. *et al.* A fungal sRNA silences a host plant transcription factor to promote arbuscular mycorrhizal symbiosis. *New Phytologist* **246**, 924–935 (2025).
133. Ren, B., Wang, X., Duan, J. & Ma, J. Rhizobial tRNA-derived small RNAs are signal molecules regulating plant nodulation. *Science* **365**, (2019).
134. Wong-Bajracharya, J. *et al.* The ectomycorrhizal fungus Pisolithus microcarpus encodes a microRNA involved in cross-kingdom gene silencing during symbiosis. *PNAS* **119**, e2103527119 (2022).
135. Lipka, V. & Panstruga, R. Dynamic cellular responses in plant–microbe interactions. *Current Opinion in Plant Biology* **8**, 625–631 (2005).
136. Ryder, L. S. *et al.* The appressorium at a glance. *J Cell Sci* **135**, jcs259857 (2022).
137. Pel, M. J. C. & Pieterse, C. M. J. Microbial recognition and evasion of host immunity. *J Exp Bot* **64**, 1237–1248 (2013).
138. Venturas, M. D., Sperry, J. S. & Hacke, U. G. Plant xylem hydraulics: What we understand, current research, and future challenges. *J Int Plant Bio* **59**, 356–389 (2017).
139. Yadeta, K. & Thomma, B. The xylem as battleground for plant hosts and vascular wilt pathogens. *Front. Plant Sci.* **4**, (2013).
140. Wang, R., Li, J. & Liang, Y. Role of ROS signaling in the plant defense against vascular pathogens. *Current Opinion in Plant Biology* **81**, 102617 (2024).
141. Kim, J.-Y. *et al.* Distinct identities of leaf phloem cells revealed by single cell transcriptomics. *Plant Cell* **33**, 511–530 (2021).
142. Furch, A. C. U. *et al.* Transformation of flg22 perception into electrical signals decoded in vasculature leads to sieve tube blockage and pathogen resistance. *Science Advances* **11**, eads6417 (2025).
143. Cao, Y. *et al.* The Expression Pattern of a Rice Disease Resistance Gene Xa3/Xa26 Is Differentially Regulated by the Genetic Backgrounds and Developmental Stages That Influence Its Function. *Genetics* **177**, 523–533 (2007).
144. Cao, J. *et al.* Autophagy-Like Cell Death Regulates Hydrogen Peroxide and Calcium Ion Distribution in Xa3/Xa26-Mediated Resistance to Xanthomonas oryzae pv. oryzae. *International Journal of Molecular Sciences* **21**, 194 (2020).
145. De Lorenzo, G., Ferrari, S., Cervone, F. & Okun, E. Extracellular DAMPs in Plants and Mammals: Immunity, Tissue Damage and Repair. *Trends Immunol* **39**, 937–950 (2018).
146. Wang, W. *et al.* Plant extracellular vesicles contribute to the amplification of immune signals during systemic acquired resistance. *Plant Cell Rep* **44**, 16 (2024).
147. De La Fuente, L., Merfa, M. V., Cobine, P. A. & Coleman, J. J. Pathogen Adaptation to the Xylem Environment. *Annu. Rev. Phytopathol.* **60**, 163–186 (2022).
148. Dow, J. M. & Daniels, M. J. Xylella genomics and bacterial pathogenicity to plants. *Yeast* **17**, 263–271 (2000).

149. Mitre, L. K. *et al.* The Arabidopsis immune receptor EFR increases resistance to the bacterial pathogens Xanthomonas and Xylella in transgenic sweet orange. *Plant Biotechnol J* **19**, 1294–1296 (2021).
150. Rapicavoli, J. N. *et al.* Lipopolysaccharide O-antigen delays plant innate immune recognition of Xylella fastidiosa. *Nat Commun* **9**, 390 (2018).
151. Burbank, L. P. & Ochoa, J. Evidence for Elicitation of an Oxidative Burst in Vitis vinifera by Xylella fastidiosa Cold Shock Protein Peptide csp20. *PhytoFront* **2**, 339–341 (2022).
152. Fritschi, F. B., Lin, H. & Walker, M. A. Scanning Electron Microscopy Reveals Different Response Pattern of Four Vitis Genotypes to Xylella fastidiosa Infection. *Plant Disease* **92**, 276–286 (2008).
153. Ingel, B. *et al.* Xylella fastidiosa causes transcriptional shifts that precede tylose formation and starch depletion in xylem. *Mol Plant Pathol* **22**, 175–188 (2021).
154. Wallis, C. M. & Chen, J. Grapevine Phenolic Compounds in Xylem Sap and Tissues Are Significantly Altered During Infection by Xylella fastidiosa. *Phytopathology* **102**, 816–826 (2012).
155. Wallis, C. M. *et al.* Impact of phenolic compounds on progression of Xylella fastidiosa infections in susceptible and PdR1-locus containing resistant grapevines. *PLOS ONE* **15**, e0237545 (2020).
156. Lee, S. A., Wallis, C. M., Rogers, E. E. & Burbank, L. P. Grapevine phenolic compounds influence cell surface adhesion of Xylella fastidiosa and bind to lipopolysaccharide. *PLOS ONE* **15**, e0240101 (2020).
157. Feitosa-Junior, O. R. *et al.* Proteomic and Metabolomic Analyses of Xylella fastidiosa OMV-Enriched Fractions Reveal Association with Virulence Factors and Signaling Molecules of the DSF Family. *Phytopathology*® **109**, 1344–1353 (2019).
158. Roper, M. C., Greve, L. C., Warren, J. G., Labavitch, J. M. & Kirkpatrick, B. C. Xylella fastidios Requires Polygalacturonase for Colonization and Pathogenicity in Vitis vinifera Grapevines. *MPMI* **20**, 411–419 (2007).
159. Pérez-Donoso, A. G. *et al.* Cell Wall-Degrading Enzymes Enlarge the Pore Size of Intervessel Pit Membranes in Healthy and Xylella fastidiosa-Infected Grapevines. *Plant Physiology* **152**, 1748–1759 (2010).
160. Ingel, B., Jeske, D. R., Sun, Q., Grosskopf, J. & Roper, M. C. Xylella fastidiosa Endoglucanases Mediate the Rate of Pierce's Disease Development in Vitis vinifera in a Cultivar-Dependent Manner. *MPMI* **32**, 1402–1414 (2019).
161. Sertedakis, M. *et al.* Expression of putative effectors of different Xylella fastidiosa strains triggers cell death-like responses in various Nicotiana model plants. *Mol Plant Pathol* **23**, 148–156 (2022).
162. Abou Kubaa, R., Giampetruzzi, A., Altamura, G., Saponari, M. & Saldarelli, P. Infections of the Xylella fastidiosa subsp. pauca Strain "De Donno" in Alfalfa (Medicago sativa) Elicits an Overactive Immune Response. *Plants* **8**, 335 (2019).
163. Zaini, P. A. *et al.* Molecular Profiling of Pierce's Disease Outlines the Response Circuitry of Vitis vinifera to Xylella fastidiosa Infection. *Front. Plant Sci.* **9**, (2018).
164. Rodrigues, C. M., de Souza, A. A., Takita, M. A., Kishi, L. T. & Machado, M. A. RNA-Seq analysis of Citrus reticulata in the early stages of Xylella fastidiosa infection reveals auxin-related genes as a defense response. *BMC Genomics* **14**, 1–13 (2013).

165. Hückelhoven, R. Transport and secretion in plant–microbe interactions. *Current Opinion in Plant Biology* **10**, 573–579 (2007).
166. Jian, Y. *et al.* How plants manage pathogen infection. *EMBO Rep* **25**, 31–44 (2024).
167. Costa, T. R. D. *et al.* Secretion systems in Gram-negative bacteria: structural and mechanistic insights. *Nat Rev Microbiol* **13**, 343–359 (2015).
168. Simpson, A. J. G. *et al.* The genome sequence of the plant pathogen Xylella fastidiosa. *Nature* **406**, 151–157 (2000).
169. Ingel, B. *et al.* Xylella fastidiosa Requires the Type II Secretion System for Pathogenicity and Survival in Grapevine. *MPMI* **36**, 636–646 (2023).
170. Jha, G., Rajeshwari, R. & Sonti, R. V. Bacterial Type Two Secretion System Secreted Proteins: Double-Edged Swords for Plant Pathogens. *MPMI* **18**, 891–898 (2005).
171. Johnson, T. L. *et al.* The Type II Secretion System Delivers Matrix Proteins for Biofilm Formation by Vibrio cholerae. *J Bacteriol* **196**, 4245–4252 (2014).
172. Naskar, S., Hohl, M., Tassinari, M. & Low, H. H. The structure and mechanism of the bacterial type II secretion system. *Mol Microbiol* **115**, 412–424 (2021).
173. Denise, R., Abby, S. S. & Rocha, E. P. C. Diversification of the type IV filament superfamily into machines for adhesion, protein secretion, DNA uptake, and motility. *PLOS Biology* **17**, e3000390 (2019).
174. Burdman, S., Bahar, O., Parker, J. K. & De La Fuente, L. Involvement of Type IV Pili in Pathogenicity of Plant Pathogenic Bacteria. *Genes* **2**, 706–735 (2011).
175. Piepenbrink, K. H. DNA Uptake by Type IV Filaments. *Front. Mol. Biosci.* **6**, (2019).
176. Dörr, J., Hurek, T. & Reinhold-Hurek, B. Type IV pili are involved in plant–microbe and fungus–microbe interactions. *Mol Microbiol* **30**, 7–17 (1998).
177. Mattick, J. S. Type IV Pili and Twitching Motility. *Annu Rev Microbiol* **56**, 289–314 (2002).
178. Wadhwa, N. & Berg, H. C. Bacterial motility: machinery and mechanisms. *Nat Rev Microbiol* **20**, 161–173 (2022).
179. U. Stotz, H., Brotherton, D. & Inal, J. Communication is key: extracellular vesicles as mediators of infection and defence during host–microbe interactions in animals and plants. *FEMS Microbiology Reviews* **46**, fuab044 (2022).
180. van Niel, G. *et al.* Challenges and directions in studying cell–cell communication by extracellular vesicles. *Nat Rev Mol Cell Biol* **23**, 369–382 (2022).
181. Woith, E., Fuhrmann, G. & Melzig, M. F. Extracellular Vesicles—Connecting Kingdoms. *International Journal of Molecular Sciences* **20**, 5695 (2019).
182. Girbardt, M. Über die Substruktur von Polystictus versicolor L. *Archiv. Mikrobiol.* **28**, 255–269 (1957).
183. Couch, Y. *et al.* A brief history of nearly EV-erything – The rise and rise of extracellular vesicles. *JEV* **10**, e12144 (2021).
184. Pan, B.-T. & Johnstone, R. M. Fate of the transferrin receptor during maturation of sheep reticulocytes in vitro: Selective externalization of the receptor. *Cell* **33**, 967–978 (1983).
185. Cocucci, E., Racchetti, G. & Meldolesi, J. Shedding microvesicles: artefacts no more. *Trends in Cell Biology* **19**, 43–51 (2009).

186. Rai, A., Claridge, B., Lozano, J. & Greening, D. W. The Discovery of Extracellular Vesicles and Their Emergence as a Next-Generation Therapy. *Circulation R* **135**, 198–221 (2024).
187. Toyofuku, M., Nomura, N. & Eberl, L. Types and origins of bacterial membrane vesicles. *Nat Rev Microbiol* **17**, 13–24 (2019).
188. Guerrero-Mandujano, A., Hernández-Cortez, C., Ibarra, J. A. & Castro-Escarpulli, G. The outer membrane vesicles: Secretion system type zero. *Traffic* **18**, 425–432 (2017).
189. Schwechheimer, C. & Kuehn, M. J. Outer-membrane vesicles from Gram-negative bacteria: biogenesis and functions. *Nat Rev Microbiol* **13**, 605–619 (2015).
190. Nagakubo, T., Nomura, N. & Toyofuku, M. Cracking Open Bacterial Membrane Vesicles. *Front. Microbiol.* **10**, (2020).
191. Pérez-Cruz, C., Delgado, L., López-Iglesias, C. & Mercade, E. Outer-Inner Membrane Vesicles Naturally Secreted by Gram-Negative Pathogenic Bacteria. *PLOS ONE* **10**, e0116896 (2015).
192. Pérez-Cruz, C. *et al.* New Type of Outer Membrane Vesicle Produced by the Gram-Negative Bacterium Shewanella vesiculosa M7T: Implications for DNA Content. *Appl Environ Microbiol* **79**, 1874–1881 (2013).
193. Kadurugamuwa, J. L. & Beveridge, T. J. Virulence factors are released from Pseudomonas aeruginosa in association with membrane vesicles during normal growth and exposure to gentamicin: a novel mechanism of enzyme secretion. *J Bacteriol* **177**, 3998–4008 (1995).
194. McBroom, A. J. & Kuehn, M. J. Release of outer membrane vesicles by Gram-negative bacteria is a novel envelope stress response. *Mol Micro* **63**, 545–558 (2007).
195. Schwechheimer, C. & Kuehn, M. J. Synthetic Effect between Envelope Stress and Lack of Outer Membrane Vesicle Production in Escherichia coli. *J Bacteriol* **195**, 4161–4173 (2013).
196. McMillan, H. M. & Kuehn, M. J. The extracellular vesicle generation paradox: a bacterial point of view. *EMBO J* **40**, e108174 (2021).
197. Deng, J., Li, W., Wang, Z., Zeng, J. & Cai, Q. KatB, a bacterial extracellular vesicles (EVs)-secreted catalase, detoxifies reactive oxygen species (ROS) and promotes pathogen proliferation in plants. *J Int Plant Bio* **n/a**, (2025).
198. Lin, J. *et al.* A Pseudomonas T6SS effector recruits PQS-containing outer membrane vesicles for iron acquisition. *Nat Commun* **8**, 14888 (2017).
199. Janda, M. *et al.* Biophysical and proteomic analyses of Pseudomonas syringae pv. tomato DC3000 extracellular vesicles suggest adaptive functions during plant infection. *mBio* **14**, e03589-22 (2023).
200. McMillan, H. M. & Kuehn, M. J. Proteomic Profiling Reveals Distinct Bacterial Extracellular Vesicle Subpopulations with Possibly Unique Functionality. *Appl Environ Microbiol* **89**, e0168622 (2023).
201. Mashburn, L. M. & Whiteley, M. Membrane vesicles traffic signals and facilitate group activities in a prokaryote. *Nature* **437**, 422–425 (2005).
202. Fan, M. *et al.* The Legionella autoinducer LAI-1 is delivered by outer membrane vesicles to promote interbacterial and interkingdom signaling. *Journal of Biological Chemistry* **299**, (2023).

203. Bala, A., Kumar, L., Chhibber, S. & Harjai, K. Augmentation of virulence related traits of pqs mutants by Pseudomonas quinolone signal through membrane vesicles. *J Basic Micro* **55**, 566–578 (2015).
204. Toyofuku, M. *et al.* Membrane vesicle-mediated bacterial communication. *The ISME Journal* **11**, 1504–1509 (2017).
205. Winans, S. C. Bacterial speech bubbles. *Nature* **437**, 330–330 (2005).
206. Arnold, B. J., Huang, I.-T. & Hanage, W. P. Horizontal gene transfer and adaptive evolution in bacteria. *Nat Rev Microbiol* **20**, 206–218 (2022).
207. Zhu, L.-T. *et al.* Diverse functional genes harboured in extracellular vesicles from environmental and human microbiota. *JEV* **11**, 12292 (2022).
208. Marinacci, B., Krzyżek, P., Pellegrini, B., Turacchio, G. & Grande, R. Latest Update on Outer Membrane Vesicles and Their Role in Horizontal Gene Transfer: A Mini-Review. *Membranes* **13**, 860 (2023).
209. Dell'Annunziata, F. *et al.* Gene Transfer Potential of Outer Membrane Vesicles of Gram-Negative Bacteria. *Int J Mol Sci* **22**, 5985 (2021).
210. Johnston, E. L. *et al.* Planktonic and Biofilm-Derived Pseudomonas aeruginosa Outer Membrane Vesicles Facilitate Horizontal Gene Transfer of Plasmid DNA. *Microb Spectrum* **11**, e05179-22 (2023).
211. Li, P. *et al.* Horizontal gene transfer via OMVs co-carrying virulence and antimicrobial-resistant genes is a novel way for the dissemination of carbapenem-resistant hypervirulent Klebsiella pneumoniae. *Front. Microbiol.* **13**, (2022).
212. Wang, Z. *et al.* Dissemination of virulence and resistance genes among Klebsiella pneumoniae via outer membrane vesicle: An important plasmid transfer mechanism to promote the emergence of carbapenem-resistant hypervirulent Klebsiella pneumoniae. *Transboundary and Emerging Diseases* **69**, e2661–e2676 (2022).
213. Soler, N. & Forterre, P. Vesiduction: the fourth way of HGT. *Environmental Microbiology* **22**, 2457–2460 (2020).
214. Tran, F., Gangan, M. S., Weaver, B. P. & Boedicker, J. Q. Membrane-Binding Biomolecules Influence the Rate of Vesicle Exchange between Bacteria. *Appl Environ Microbiol* **88**, e01346-22 (2022).
215. Tashiro, Y. *et al.* Interaction of Bacterial Membrane Vesicles with Specific Species and Their Potential for Delivery to Target Cells. *Front. Microbiol.* **8**, (2017).
216. Li, C. *et al.* T6SS secretes an LPS-binding effector to recruit OMVs for exploitative competition and horizontal gene transfer. *ISME J* **16**, 500–510 (2022).
217. Nascimento, R. *et al.* The Type II Secreted Lipase/Esterase LesA is a Key Virulence Factor Required for Xylella fastidiosa Pathogenesis in Grapevines. *Sci Rep* **6**, 18598 (2016).
218. Santiago, A. D. S. *et al.* The Antitoxin Protein of a Toxin-Antitoxin System from Xylella fastidiosa Is Secreted via Outer Membrane Vesicles. *Front. Microbiol.* **7**, (2016).
219. Rutter, B. D. & Innes, R. W. Extracellular Vesicles Isolated from the Leaf Apoplast Carry Stress-Response Proteins. *Plant Physiol* **173**, 728–741 (2017).
220. Regente, M. *et al.* Plant extracellular vesicles are incorporated by a fungal pathogen and inhibit its growth. *Journal of Experimental Botany* **68**, 5485–5495 (2017).
221. Janda, M. & Robatzek, S. Extracellular vesicles from phytobacteria: Properties, functions and uses. *Biotechnology Advances* **58**, 107934 (2022).

222. de la Canal, L. & Pinedo, M. Extracellular vesicles: a missing component in plant cell wall remodeling. *Journal of Experimental Botany* **69**, 4655–4658 (2018).
223. Salvachúa, D. *et al.* Outer membrane vesicles catabolize lignin-derived aromatic compounds in Pseudomonas putida KT2440. *PNAS* **117**, 9302–9310 (2020).
224. Dora, S., Terrett, O. M. & Sánchez-Rodríguez, C. Plant–microbe interactions in the apoplast: Communication at the plant cell wall. *Plant Cell* **34**, 1532–1550 (2022).
225. Zhang, B., Gao, Y., Zhang, L. & Zhou, Y. The plant cell wall: Biosynthesis, construction, and functions. *J Int Plant Bio* **63**, 251–272 (2021).
226. O'Donoghue, E. J. & Krachler, A. M. Mechanisms of outer membrane vesicle entry into host cells. *Cell Microb* **18**, 1508–1517 (2016).
227. van Dongen, H. M., Masoumi, N., Witwer, K. W. & Pegtel, D. M. Extracellular Vesicles Exploit Viral Entry Routes for Cargo Delivery. *Microb MolBio* **80**, 369–386 (2016).
228. French, K. C., Antonyak, M. A. & Cerione, R. A. Extracellular vesicle docking at the cellular port: Extracellular vesicle binding and uptake. *Seminars in Cell & Developmental Biology* **67**, 48–55 (2017).
229. Mulcahy, L. A., Pink ,Ryan Charles & and Carter, D. R. F. Routes and mechanisms of extracellular vesicle uptake. *JEV* **3**, 24641 (2014).
230. Morris, K. V. & Witwer, K. W. The evolving paradigm of extracellular vesicles in intercellular signaling and delivery of therapeutic RNAs. *Molecular Therapy* **30**, 2393–2394 (2022).
231. Wang, W. *et al.* Plant extracellular vesicles contribute to the amplification of immune signals during systemic acquired resistance. *Plant Cell Rep* **44**, 16 (2024).
232. Tran, T. M. *et al.* Potentiation of plant defense by bacterial outer membrane vesicles is mediated by membrane nanodomains. *The Plant Cell* **34**, 395–417 (2022).
233. Jarsch, I. K. & Ott, T. Perspectives on Remorin Proteins, Membrane Rafts, and Their Role During Plant–Microbe Interactions. *MPMI* **24**, 7–12 (2011).
234. Li, R. *et al.* A Membrane Microdomain-Associated Protein, Arabidopsis Flot1, Is Involved in a Clathrin-Independent Endocytic Pathway and Is Required for Seedling Development. *Plant Cell* **24**, 2105–2122 (2012).
235. Rutter, B. D. & Innes, R. W. Growing pains: addressing the pitfalls of plant extracellular vesicle research. *New Phytol* **228**, 1505–1510 (2020).
236. Lécrivain, A.-L. & Beckmann, B. M. Bacterial RNA in extracellular vesicles: A new regulator of host-pathogen interactions? *Biochimica et Biophysica Acta (BBA) - Gene Regulatory Mechanisms* **1863**, 194519 (2020).
237. Zhou, Q. *et al.* Extracellular vesicles: Their functions in plant–pathogen interactions. *Mol Plant Pathol* **23**, 760–771 (2022).
238. Rybak, K. & Robatzek, S. Functions of Extracellular Vesicles in Immunity and Virulence. *Plant Physiol.* **179**, 1236–1247 (2019).
239. Solé, M. *et al.* Xanthomonas campestris pv. vesicatoria Secretes Proteases and Xylanases via the Xps Type II Secretion System and Outer Membrane Vesicles. *J Bacteriol* **197**, 2879–2893 (2015).
240. Chowdhury, C. & Jagannadham, M. V. Virulence factors are released in association with outer membrane vesicles of *Pseudomonas syringae* pv. tomato T1 during normal growth. *Biochimica et Biophysica Acta (BBA) - Proteins and Proteomics* **1834**, 231–239 (2013).

241. Kaparakis-Liaskos, M. & Ferrero, R. L. Immune modulation by bacterial outer membrane vesicles. *Nat Rev Immunol* **15**, 375–387 (2015).
242. Bielaszewska, M. *et al.* Host cell interactions of outer membrane vesicle-associated virulence factors of enterohemorrhagic Escherichia coli O157: Intracellular delivery, trafficking and mechanisms of cell injury. *PLOS Pathogens* **13**, e1006159 (2017).
243. Rompikuntal, P. K. *et al.* Perinuclear Localization of Internalized Outer Membrane Vesicles Carrying Active Cytolethal Distending Toxin from Aggregatibacter actinomycetemcomitans. *Infect Immun* **80**, 31–42 (2012).
244. He, B. *et al.* RNA-binding proteins contribute to small RNA loading in plant extracellular vesicles. *Nat. Plants* **7**, 342–352 (2021).
245. He, B., Hamby, R. & Jin, H. Plant extracellular vesicles: Trojan horses of cross-kingdom warfare. *FASEB BioAdvances* **3**, 657–664 (2021).
246. Kwon, S. *et al.* mRNA Inventory of Extracellular Vesicles from Ustilago maydis. *J Fungi (Basel)* **7**, 562 (2021).
247. Kusch, S., Singh, M., Thieron, H., Spanu, P. D. & Panstruga, R. Site-specific analysis reveals candidate cross-kingdom small RNAs, tRNA and rRNA fragments, and signs of fungal RNA phasing in the barley–powdery mildew interaction. *Mol Plant Pathol* **24**, 570–587 (2023).
248. Wang, S. *et al.* Plant mRNAs move into a fungal pathogen via extracellular vesicles to reduce infection. *Cell Host & Microbe* **32**, 93-105.e6 (2024).
249. Karimi, H. Z. *et al.* Arabidopsis apoplastic fluid contains sRNA- and circular RNA-protein complexes that are located outside extracellular vesicles. *The Plant Cell* koac043 (2022) doi:10.1093/plcell/koac043.
250. Wang, Y., Wang, Y. & Wang, Y. Apoplastic Proteases: Powerful Weapons against Pathogen Infection in Plants. *Plant Comm* **1**, (2020).
251. Tsatsaronis, J. A., Franch-Arroyo, S., Resch, U. & Charpentier, E. Extracellular Vesicle RNA: A Universal Mediator of Microbial Communication? *Trends in Microbiology* **26**, 401–410 (2018).
252. Villarroya-Beltri, C. *et al.* Sumoylated hnRNPA2B1 controls the sorting of miRNAs into exosomes through binding to specific motifs. *Nat Commun* **4**, 2980 (2013).
253. Garcia-Martin, R. *et al.* MicroRNA sequence codes for small extracellular vesicle release and cellular retention. *Nature* 1–6 (2021) doi:10.1038/s41586-021-04234-3.
254. Koppers-Lalic, D. *et al.* Nontemplated Nucleotide Additions Distinguish the Small RNA Composition in Cells from Exosomes. *Cell Reports* **8**, 1649–1658 (2014).
255. Choi, J.-W., Kim, S.-C., Hong, S.-H. & Lee, H.-J. Secretable Small RNAs via Outer Membrane Vesicles in Periodontal Pathogens. *J Dent Res* **96**, 458–466 (2017).
256. Koeppen, K. *et al.* A Novel Mechanism of Host-Pathogen Interaction through sRNA in Bacterial Outer Membrane Vesicles. *PLoS Pathog* **12**, e1005672 (2016).
257. Wu, Y. *et al.* Suppression of host plant defense by bacterial small RNAs packaged in outer membrane vesicles. *Plant Communications* 100817 (2024) doi:10.1016/j.xplc.2024.100817.
258. Lambertz, U. *et al.* Small RNAs derived from tRNAs and rRNAs are highly enriched in exosomes from both old and new world Leishmania providing evidence for conserved exosomal RNA Packaging. *BMC Genomics* **16**, 1–26 (2015).

259. Tosar, J. P. & Cayota, A. Extracellular tRNAs and tRNA-derived fragments. *RNA Biol* **17**, 1149–1167 (2020).
260. Ravet, A. *et al.* Vesicular and non-vesicular extracellular small RNAs direct gene silencing in a plant-interacting bacterium. *Nat Commun* **16**, 3533 (2025).
261. Diallo, I. & Provost, P. RNA-Sequencing Analyses of Small Bacterial RNAs and their Emergence as Virulence Factors in Host-Pathogen Interactions. *Int J Mol Sci* **21**, 1627 (2020).
262. Carrier, M.-C., Lalaouna, D. & Massé, E. Broadening the Definition of Bacterial Small RNAs: Characteristics and Mechanisms of Action. *Annu Rev Microbiol* **72**, 141–161 (2018).
263. Kawamoto, H., Koide, Y., Morita, T. & Aiba, H. Base-pairing requirement for RNA silencing by a bacterial small RNA and acceleration of duplex formation by Hfq. *Mol Micro* **61**, 1013–1022 (2006).
264. Papenfort, K., Bouvier, M., Mika, F., Sharma, C. M. & Vogel, J. Evidence for an autonomous 5′ target recognition domain in an Hfq-associated small RNA. *PNAS* **107**, 20435–20440 (2010).
265. Fröhlich, K. S. & Vogel, J. Activation of gene expression by small RNA. *Current Opinion in Microbiology* **12**, 674–682 (2009).
266. Storz, G., Opdyke, J. A. & Zhang, A. Controlling mRNA stability and translation with small, noncoding RNAs. *Current Opinion in Microbiology* **7**, 140–144 (2004).
267. Santiago-Frangos, A. & Woodson, S. A. Hfq chaperone brings speed dating to bacterial sRNA. *WIREs RNA* **9**, e1475 (2018).
268. Holmqvist, E. & Vogel, J. RNA-binding proteins in bacteria. *Nat Rev Microbiol* **16**, 601–615 (2018).
269. Updegrove, T. B., Zhang, A. & Storz, G. Hfq: the flexible RNA matchmaker. *Curr Opin Microbiol* **30**, 133–138 (2016).
270. Gorski, S. A., Vogel, J. & Doudna, J. A. RNA-based recognition and targeting: sowing the seeds of specificity. *Nat Rev Mol Cell Biol* **18**, 215–228 (2017).
271. Link, T. M., Valentin-Hansen, P. & Brennan, R. G. Structure of Escherichia coli Hfq bound to polyriboadenylate RNA. *PNAS* **106**, 19292–19297 (2009).
272. Someya, T. *et al.* Crystal structure of Hfq from Bacillus subtilis in complex with SELEX-derived RNA aptamer: insight into RNA-binding properties of bacterial Hfq. *Nucleic Acids Res* **40**, 1856–1867 (2012).
273. Robinson, K. E., Orans, J., Kovach, A. R., Link, T. M. & Brennan, R. G. Mapping Hfq-RNA interaction surfaces using tryptophan fluorescence quenching. *Nucleic Acids Res* **42**, 2736–2749 (2014).
274. Wang, L. *et al.* Structural insights into the recognition of the internal A-rich linker from OxyS sRNA by Escherichia coli Hfq. *Nucleic Acids Res* **43**, 2400–2411 (2015).
275. Horstmann, N., Orans, J., Valentin-Hansen, P., Shelburne, S. A., III & Brennan, R. G. Structural mechanism of Staphylococcus aureus Hfq binding to an RNA A-tract. *Nucleic Acids Res* **40**, 11023–11035 (2012).
276. Turbant, F. *et al.* Unraveling Membrane Perturbations Caused by the Bacterial Riboregulator Hfq. *Int J Mol Sci* **23**, 8739 (2022).

277. Berbon, M. *et al.* Hfq C-terminal region forms a β-rich amyloid-like motif without perturbing the N-terminal Sm-like structure. *Commun Biol* **6**, 1075 (2023).
278. Sobrero, P. & Valverde, C. The bacterial protein Hfq: much more than a mere RNA-binding factor. *Critical Reviews in Microbiology* **38**, 276–299 (2012).
279. Harfouche, L., Haichar, F. el Z. & Achouak, W. Small regulatory RNAs and the fine-tuning of plant–bacteria interactions. *New Phytologist* **206**, 98–106 (2015).
280. Gottesman, S. & Storz, G. Bacterial Small RNA Regulators: Versatile Roles and Rapidly Evolving Variations. *Cold Spring Harb Perspect Biol* **3**, a003798 (2011).
281. Beisel, C. L. & Storz, G. Base pairing small RNAs and their roles in global regulatory networks. *FEMS Microbiology Reviews* **34**, 866–882 (2010).
282. Wu, Y. *et al.* A key antisense sRNA modulates the oxidative stress response and virulence in Xanthomonas oryzae pv. oryzicola. *PLOS Pathogens* **17**, e1009762 (2021).
283. Yu, M. S. C. *et al.* The proteome of bacterial membrane vesicles in Escherichia coli—a time course comparison study in two different media. *Front. Microbiol.* **15**, (2024).
284. Eddy, J. L., Gielda, L. M., Caulfield, A. J., Rangel, S. M. & Lathem, W. W. Production of Outer Membrane Vesicles by the Plague Pathogen Yersinia pestis. *PLOS ONE* **9**, e107002 (2014).
285. Malabirade, A. *et al.* Membrane association of the bacterial riboregulator Hfq and functional perspectives. *Sci Rep* **7**, 10724 (2017).
286. Turbant, F. *et al.* Interactions and Insertion of Escherichia coli Hfq into Outer Membrane Vesicles as Revealed by Infrared and Orientated Circular Dichroism Spectroscopies. *Int J Mol Sci* **24**, 11424 (2023).
287. Olsen, A. S., Møller-Jensen, J., Brennan, R. G. & Valentin-Hansen, P. C-Terminally Truncated Derivatives of *Escherichia coli* Hfq Are Proficient in Riboregulation. *Journal of Molecular Biology* **404**, 173–182 (2010).
288. Velez, M. & Arluison, V. Does the Hfq Protein Contribute to RNA Cargo Translocation into Bacterial Outer Membrane Vesicles? *Pathogens* **14**, 399 (2025).
289. Cheng, A.-P. *et al.* A fungal RNA-dependent RNA polymerase is a novel player in plant infection and cross-kingdom RNA interference. *PLOS Pathogens* **19**, e1011885 (2023).
290. Diallo, I. *et al.* A tRNA-derived fragment present in E. coli OMVs regulates host cell gene expression and proliferation. *PLOS Pathogens* **18**, e1010827 (2022).
291. Garcia-Silva, M. R. *et al.* Gene Expression Changes Induced by Trypanosoma cruzi Shed Microvesicles in Mammalian Host Cells: Relevance of tRNA-Derived Halves. *Biomed Res I* **2014**, 305239 (2014).
292. Lalaouna, D. *et al.* A 3′ External Transcribed Spacer in a tRNA Transcript Acts as a Sponge for Small RNAs to Prevent Transcriptional Noise. *Molecular Cell* **58**, 393–405 (2015).
293. Kumar, P., Anaya, J., Mudunuri, S. B. & Dutta, A. Meta-analysis of tRNA derived RNA fragments reveals that they are evolutionarily conserved and associate with AGO proteins to recognize specific RNA targets. *BMC Biol* **12**, 78 (2014).
294. Li, Z. & Stanton, B. A. Transfer RNA-Derived Fragments, the Underappreciated Regulatory Small RNAs in Microbial Pathogenesis. *Front. Microbiol.* **12**, (2021).
295. Brodersen, P. *et al.* Isoprenoid biosynthesis is required for miRNA function and affects membrane association of ARGONAUTE 1 in Arabidopsis. *PNAS* **109**, 1778–1783 (2012).

296. Jouannet, V. *et al.* Cytoplasmic Arabidopsis AGO7 accumulates in membrane-associated siRNA bodies and is required for ta-siRNA biogenesis | The EMBO Journal. https://www.embopress.org/doi/full/10.1038/emboj.2012.20 (2012).
297. Li, S. *et al.* Biogenesis of phased siRNAs on membrane-bound polysomes in Arabidopsis. *eLife* **5**, e22750 (2016).
298. Pieretti, I. *et al.* The complete genome sequence of Xanthomonas albilineans provides new insights into the reductive genome evolution of the xylem-limited Xanthomonadaceae. *BMC Genomics* **10**, 616 (2009).
299. Mehta, P., Goyal, S. & Wingreen, N. S. A quantitative comparison of sRNA-based and protein-based gene regulation. *Mol Systems Bio* **4**, 221 (2008).
300. Storz, G., Vogel, J. & Wassarman, K. M. Regulation by Small RNAs in Bacteria: Expanding Frontiers. *Molecular Cell* **43**, 880–891 (2011).
301. Jørgensen, M. G., Pettersen, J. S. & Kallipolitis, B. H. sRNA-mediated control in bacteria: An increasing diversity of regulatory mechanisms. *Biochimica et Biophysica Acta (BBA) - Gene Regulatory Mechanisms* **1863**, 194504 (2020).
302. Papenfort, K. & Melamed, S. Small RNAs, Large Networks: Posttranscriptional Regulons in Gram-Negative Bacteria. *Annu Rev Microbiol* **77**, 23–43 (2023).
303. Chen, X.-L. *et al.* sRNA-Xcc1, an integron-encoded transposon- and plasmid-transferred trans-acting sRNA, is under the positive control of the key virulence regulators HrpG and HrpX of Xanthomonas campestris pathovar campestris. *RNA Biol* **8**, 947–953 (2011).
304. Johnston, C., Martin, B., Fichant, G., Polard, P. & Claverys, J.-P. Bacterial transformation: distribution, shared mechanisms and divergent control. *Nat Rev Microbiol* **12**, 181–196 (2014).
305. Antonova, E. S. & Hammer, B. K. Quorum-sensing autoinducer molecules produced by members of a multispecies biofilm promote horizontal gene transfer to Vibrio cholerae. *FEMS Microbiol Lett* **322**, 68–76 (2011).
306. Ebenberger, S. P. *et al.* The activity of the quorum sensing regulator HapR is modulated by the bacterial extracellular vesicle (BEV)-associated protein ObfA of Vibrio cholerae. *JEV* **13**, e12507 (2024).
307. Jia, T. *et al.* Hfq-binding small RNA PqsS regulates Pseudomonas aeruginosa pqs quorum sensing system and virulence. *npj Biofilms Microbiomes* **10**, 82 (2024).
308. Flynn, R. A. *et al.* Small RNAs are modified with N-glycans and displayed on the surface of living cells. *Cell* **184**, 3109-3124.e22 (2021).
309. Lu, Q., Li, S. & Shao, F. Sweet Talk: Protein Glycosylation in Bacterial Interaction With the Host. *Trends in Microbiology* **23**, 630–641 (2015).
310. Bomberger, J. M. *et al.* Long-Distance Delivery of Bacterial Virulence Factors by Pseudomonas aeruginosa Outer Membrane Vesicles. *PLOS Pathogens* **5**, e1000382 (2009).
311. Jäger, J., Keese, S., Roessle, M., Steinert, M. & Schromm, A. B. Fusion of Legionella pneumophila outer membrane vesicles with eukaryotic membrane systems is a mechanism to deliver pathogen factors to host cell membranes. *Cell Microb* **17**, 607–620 (2015).
312. Ghosal, A. *et al.* The extracellular RNA complement of Escherichia coli. *Microb Open* **4**, 252–266 (2015).

313. Jodder, J. Regulation of pri-MIRNA processing: mechanistic insights into the miRNA homeostasis in plant. *Plant Cell Rep* **40**, 783–798 (2021).
314. Manavella, P. A., Koenig, D. & Weigel, D. Plant secondary siRNA production determined by microRNA-duplex structure. *PNAS* **109**, 2461–2466 (2012).
315. Nguyen, T. D., Trinh, T. A., Bao, S. & Nguyen, T. A. Secondary structure RNA elements control the cleavage activity of DICER. *Nat Commun* **13**, 2138 (2022).
316. Wei, X. *et al.* Structural basis of microRNA processing by Dicer-like 1. *Nat. Plants* **7**, 1389–1396 (2021).
317. Fukudome, A. & Fukuhara, T. Plant dicer-like proteins: double-stranded RNA-cleaving enzymes for small RNA biogenesis. *J Plant Res* **130**, 33–44 (2017).
318. Kellari, L. M. *et al.* Cross-kingdom RNAi induced by a beneficial endophytic fungus to its host requires transitivity and amplification of silencing signals. *Plant Biol* **27**, 504–514 (2025).
319. Liu, Y., Teng, C., Xia, R. & Meyers, B. C. PhasiRNAs in Plants: Their Biogenesis, Genic Sources, and Roles in Stress Responses, Development, and Reproduction. *The Plant Cell* **32**, 3059–3080 (2020).
320. Arikit, S. *et al.* An Atlas of Soybean Small RNAs Identifies Phased siRNAs from Hundreds of Coding Genes. *Plant Cell* **26**, 4584–4601 (2014).
321. Xia, R., Xu, J., Arikit, S. & Meyers, B. C. Extensive Families of miRNAs and PHAS Loci in Norway Spruce Demonstrate the Origins of Complex phasiRNA Networks in Seed Plants. *Mol Biol Evol* **32**, 2905–2918 (2015).
322. Li, S. *et al.* MicroRNAs Inhibit the Translation of Target mRNAs on the Endoplasmic Reticulum in Arabidopsis. *Cell* **153**, 562–574 (2013).
323. Ryabov, E. V., van Wezel, R., Walsh, J. & Hong, Y. Cell-to-Cell, but Not Long-Distance, Spread of RNA Silencing That Is Induced in Individual Epidermal Cells. *J Virol* **78**, 3149–3154 (2004).
324. Voinnet, O. Three decades of mobile RNA silencing within plants: what have we learnt? *J Exp Bot* eraf312 (2025) doi:10.1093/jxb/eraf312.
325. van Bel, A. J. E. Xylem-Phloem Exchange Via the Rays: The Undervalued Route of Transport. *J Exp Bot* **41**, 631–644 (1990).
326. Geßler, A., Weber, P., Schneider, S. & Rennenberg, H. Bidirectional exchange of amino compounds between phloem and xylem during long-distance transport in Norway spruce trees (Picea abies [L.] Karst). *J Exp Bot* **54**, 1389–1397 (2003).
327. Zhang, L. *et al.* Altered Xylem-Phloem Transfer of Amino Acids Affects Metabolism and Leads to Increased Seed Yield and Oil Content in Arabidopsis. *Plant Cell* **22**, 3603–3620 (2010).
328. Redzich, L. *et al.* Differentiation of Xanthomonas oryzae pv. oryzae in vitro and during rice leaf infection. 2025.10.12.680524 Preprint at https://doi.org/10.1101/2025.10.12.680524 (2025).
329. Chambers, J. R. & Sauer, K. Small RNAs and their role in biofilm formation. *Trends in Microbiology* **21**, 39–49 (2013).
330. Mitra, A. & Mukhopadhyay, S. Regulation of biofilm formation by non-coding RNA in prokaryotes. *Current Research in Pharmacology and Drug Discovery* **4**, 100151 (2023).

331. Wei, C. *et al.* Global Regulator PhoP is Necessary for Motility, Biofilm Formation, Exoenzyme Production, and Virulence of Xanthomonas citri Subsp. citri on Citrus Plants. *Genes* **10**, 340 (2019).
332. Pierce, B. K. & Kirkpatrick, B. C. The PhoP/Q two-component regulatory system is essential for Xylella fastidiosa survival in Vitis vinifera grapevines. *Physiological and Molecular Plant Pathology* **89**, 55–61 (2015).
333. Barbosa, R. L. & Benedetti, C. E. BigR, a Transcriptional Repressor from Plant-Associated Bacteria, Regulates an Operon Implicated in Biofilm Growth. *J Bacteriol* **189**, 6185–6194 (2007).
334. Guimarães, B. G. *et al.* Plant Pathogenic Bacteria Utilize Biofilm Growth-associated Repressor (BigR), a Novel Winged-helix Redox Switch, to Control Hydrogen Sulfide Detoxification under Hypoxia *. *Journal of Biological Chemistry* **286**, 26148–26157 (2011).
335. de Lira, N. P. V. *et al.* BigR is a sulfide sensor that regulates a sulfur transferase/dioxygenase required for aerobic respiration of plant bacteria under sulfide stress. *Sci Rep* **8**, 3508 (2018).
336. Newman, K. L., Almeida, R. P. P., Purcell, A. H. & Lindow, S. E. Cell-cell signaling controls Xylella fastidiosa interactions with both insects and plants. *PNAS* **101**, 1737–1742 (2004).
337. Chatterjee, S., Wistrom, C. & Lindow, S. E. A cell–cell signaling sensor is required for virulence and insect transmission of Xylella fastidiosa. *PNAS* **105**, 2670–2675 (2008).
338. Wang, N., Li, J.-L. & Lindow, S. E. RpfF-Dependent Regulon of Xylella fastidiosa. *Phytopathology* **102**, 1045–1053 (2012).
339. Ionescu, M. *et al.* Diffusible Signal Factor (DSF) Synthase RpfF of Xylella fastidiosa Is a Multifunction Protein Also Required for Response to DSF. *J Bacteriol* **195**, 5273–5284 (2013).
340. Vogel, J. *et al.* RNomics in Escherichia coli detects new sRNA species and indicates parallel transcriptional output in bacteria. *Nucleic Acids Res* **31**, 6435–6443 (2003).
341. Beisel, C. L., Updegrove, T. B., Janson, B. J. & Storz, G. Multiple factors dictate target selection by Hfq-binding small RNAs. *EMBO J* **31**, 1961–1974 (2012).
342. Dow, M. Diversification of the Function of Cell-to-Cell Signaling in Regulation of Virulence Within Plant Pathogenic Xanthomonads. *Science Sig* **1**, pe23–pe23 (2008).
343. Valentini, M. & Filloux, A. Biofilms and Cyclic di-GMP (c-di-GMP) Signaling: Lessons from Pseudomonas aeruginosa and Other Bacteria. *J Biol Chem* **291**, 12547–12555 (2016).
344. de Souza, A. A., Ionescu, M., Baccari, C., da Silva, A. M. & Lindow, S. E. Phenotype Overlap in Xylella fastidiosa Is Controlled by the Cyclic Di-GMP Phosphodiesterase Eal in Response to Antibiotic Exposure and Diffusible Signal Factor-Mediated Cell-Cell Signaling. *Appl Environ Microbiol* **79**, 3444–3454 (2013).
345. Condinho, M. *et al.* The role of RNA regulators, quorum sensing and c-di-GMP in bacterial biofilm formation. *FEBS Open Bio* **13**, 975–991 (2023).
346. Fu, Y. *et al.* The Multiple Regulatory Relationship Between RNA-Chaperone Hfq and the Second Messenger c-di-GMP. *Front. Microbiol.* **12**, (2021).

347. Yuan, X. *et al.* A feed-forward signalling circuit controls bacterial virulence through linking cyclic di-GMP and two mechanistically distinct sRNAs, ArcZ and RsmB. *Env Micro* **21**, 2755–2771 (2019).
348. Mashburn-Warren, L. *et al.* Interaction of quorum signals with outer membrane lipids: insights into prokaryotic membrane vesicle formation. *Mol Microbiol* **69**, 491–502 (2008).
349. Groisman, E. A. The Pleiotropic Two-Component Regulatory System PhoP-PhoQ. *J Bacteriol* **183**, 1835–1842 (2001).
350. Mao, M., He, L. & Yan, Q. An updated overview on the bacterial PhoP/PhoQ two-component signal transduction system. *Front. Cell. Infect. Microbiol.* **15**, (2025).
351. Köster, P., DeFalco, T. A. & Zipfel, C. Ca2+ signals in plant immunity. *The EMBO Journal* **41**, e110741 (2022).
352. Flego, D., Pirhonen, M., Saarilahti, H., Palva, T. K. & Palva, E. T. Control of virulence gene expression by plant calcium in the phytopathogen Erwinia carotovora. *Mol Micro* **25**, 831–838 (1997).
353. Nitzan, M., Rehani, R. & Margalit, H. Integration of Bacterial Small RNAs in Regulatory Networks. *Annu Rev Biophys* **46**, 131–148 (2017).
354. Huber, M., Fröhlich, K. S., Radmer, J. & Papenfort, K. Switching fatty acid metabolism by an RNA-controlled feed forward loop. *PNAS* **117**, 8044–8054 (2020).
355. Li, W., Ying, X., Lu, Q. & Chen, L. Predicting sRNAs and Their Targets in Bacteria. *genom. proteom. bioinform.* **10**, 276–284 (2012).
356. Leonard, S. *et al.* APERO: a genome-wide approach for identifying bacterial small RNAs from RNA-Seq data. *Nucleic Acids Res* **47**, e88–e88 (2019).
357. Mann, M., Wright, P. R. & Backofen, R. IntaRNA 2.0: enhanced and customizable prediction of RNA–RNA interactions. *Nucleic Acids Res* **45**, W435–W439 (2017).
358. Raden, M. *et al.* Freiburg RNA tools: a central online resource for RNA-focused research and teaching. *Nucleic Acids Research* **46**, W25–W29 (2018).
359. Urban, J. H. & Vogel, J. A Green Fluorescent Protein (GFP)-Based Plasmid System to Study Post-Transcriptional Control of Gene Expression In Vivo. in *Riboswitches: Methods and Protocols* (ed. Serganov, A.) 301–319 (Humana Press, Totowa, NJ, 2009). doi:10.1007/978-1-59745-558-9_22.
360. Gao, X., Liu, Z. & Han, Y. Target Validation of sRNA with a GFP Reporter Gene Fusion System. in *Yersinia Pestis Protocols* (ed. Yang, R.) 115–120 (Springer, Singapore, 2018). doi:10.1007/978-981-10-7947-4_12.
361. Melamed, S. *et al.* Mapping the small RNA interactome in bacteria using RIL-seq. *Nat Protoc* **13**, 1–33 (2018).
362. Möller, P. *et al.* Profound Impact of Hfq on Nutrient Acquisition, Metabolism and Motility in the Plant Pathogen Agrobacterium tumefaciens. *PLOS ONE* **9**, e110427 (2014).
363. Dunker, F., Lederer, B. & Weiberg, A. Plant ARGONAUTE Protein Immunopurification for Pathogen Cross Kingdom Small RNA Analysis. *Bio Protoc* **11**, e3911 (2021).
364. Lin, S.-S., Chen, Y. & Lu, M.-Y. J. Degradome Sequencing in Plants. in *Plant MicroRNAs: Methods and Protocols* (ed. de Folter, S.) 197–213 (Springer, New York, NY, 2019). doi:10.1007/978-1-4939-9042-9_15.

365. Prince, A. *et al.* Lipid Specificity of the Fusion of Bacterial Extracellular Vesicles with the Host Membrane. *J. Phys. Chem. B* **128**, 8116–8130 (2024).
366. Nolte-'t Hoen, E., Cremer, T., Gallo, R. C. & Margolis, L. B. Extracellular vesicles and viruses: Are they close relatives? *PNAS* **113**, 9155–9161 (2016).
367. Lozano-Durán, R. Viral Recognition and Evasion in Plants. *Annu. Rev. Plant Biol.* **75**, 655–677 (2024).
368. Yan, Y. Insights into Mobile Small-RNAs Mediated Signaling in Plants. *Plants* **11**, 3155 (2022).
369. Yan, Y. & Ham, B.-K. The Mobile Small RNAs: Important Messengers for Long-Distance Communication in Plants. *Front. Plant Sci.* **13**, (2022).
370. Chen, W. *et al.* A Genetic Network for Systemic RNA Silencing in Plants. *Plant Physiol* **176**, 2700–2719 (2018).
371. Ye, W. & Ma, W. Filamentous pathogen effectors interfering with small RNA silencing in plant hosts. *Current Opinion in Microbiology* **32**, 1–6 (2016).
372. Nemeth, K., Bayraktar, R., Ferracin, M. & Calin, G. A. Non-coding RNAs in disease: from mechanisms to therapeutics. *Nat Rev Genet* **25**, 211–232 (2024).
373. Chen, X., Liang, H., Zhang, J., Zen, K. & Zhang, C.-Y. microRNAs are ligands of Toll-like receptors. *RNA* **19**, 737–739 (2013).
374. Koski, G. K. *et al.* Cutting Edge: Innate Immune System Discriminates between RNA Containing Bacterial versus Eukaryotic Structural Features That Prime for High-Level IL-12 Secretion by Dendritic Cells1. *J Immunol* **172**, 3989–3993 (2004).
375. Lee, B., Park, Y.-S., Lee, S., Song, G. C. & Ryu, C.-M. Bacterial RNAs activate innate immunity in Arabidopsis. *New Phytologist* **209**, 785–797 (2016).
376. Niehl, A., Wyrsch, I., Boller, T. & Heinlein, M. Double-stranded RNAs induce a pattern-triggered immune signaling pathway in plants. *New Phytologist* **211**, 1008–1019 (2016).
377. Nielsen, C. P. S. *et al.* Sensing of viral RNA in plants via a DICER-LIKE Ribonuclease. 2023.01.10.523395 Preprint at https://doi.org/10.1101/2023.01.10.523395 (2023).
378. Nielsen, C. P. S. *et al.* Evidence for an RNAi-independent role of Arabidopsis DICER-LIKE2 in growth inhibition and basal antiviral resistance. *Plant Cell* **36**, 2289–2309 (2024).
379. Yu, D. *et al.* TIR domains of plant immune receptors are 2′,3′-cAMP/cGMP synthetases mediating cell death. *Cell* **185**, 2370-2386.e18 (2022).
380. Essuman, K., Milbrandt, J., Dangl, J. L. & Nishimura, M. T. Shared TIR enzymatic functions regulate cell death and immunity across the tree of life. *Science* **377**, eabo0001 (2022).
381. Jia, A. *et al.* TIR-catalyzed ADP-ribosylation reactions produce signaling molecules for plant immunity. *Science* **377**, eabq8180 (2022).
382. Huang, S. *et al.* Identification and receptor mechanism of TIR-catalyzed small molecules in plant immunity. *Science* **377**, eabq3297 (2022).
383. Peng, J., Yu, Y. & Fang, X. Stress sensing and response through biomolecular condensates in plants. *Plant Communications* **6**, 101225 (2025).
384. Wang, W. & Gu, Y. The emerging role of biomolecular condensates in plant immunity. *Plant Cell* **34**, 1568–1572 (2022).

385. Song, W. *et al.* Substrate-induced condensation activates plant TIR domain proteins. *Nature* **627**, 847–853 (2024).
386. Li, Q., Liu, Y. & Zhang, X. Biomolecular condensates in plant RNA silencing: insights into formation, function, and stress responses. *Plant Cell* **36**, 227–245 (2024).
387. Moon, K. & Gottesman, S. Competition among Hfq-binding small RNAs in Escherichia coli. *Mol Micro* **82**, 1545–1562 (2011).
388. Zeng, Q. & Sundin, G. W. Genome-wide identification of Hfq-regulated small RNAs in the fire blight pathogen Erwinia amylovora discovered small RNAs with virulence regulatory function. *BMC Genomics* **15**, 414 (2014).
389. Palchevskiy, V. & Finkel, S. E. Escherichia coli Competence Gene Homologs Are Essential for Competitive Fitness and the Use of DNA as a Nutrient. *J Bacteriol* **188**, 3902–3910 (2006).
390. Laurenceau, R. *et al.* A Type IV Pilus Mediates DNA Binding during Natural Transformation in Streptococcus pneumoniae. *PLOS Pathogens* **9**, e1003473 (2013).
391. Craig, L., Pique, M. E. & Tainer, J. A. Type IV pilus structure and bacterial pathogenicity. *Nat Rev Microbiol* **2**, 363–378 (2004).
392. Seitz, P. & Blokesch, M. Cues and regulatory pathways involved in natural competence and transformation in pathogenic and environmental Gram-negative bacteria. *FEMS Microbiology Reviews* **37**, 336–363 (2013).
393. Anton, B. P. & Roberts, R. J. Beyond Restriction Modification: Epigenomic Roles of DNA Methylation in Prokaryotes. *Annu Rev Microbiol* **75**, 129–149 (2021).
394. Oliveira, P. H., Touchon, M. & Rocha, E. P. C. Regulation of genetic flux between bacteria by restriction–modification systems. *PNAS* **113**, 5658–5663 (2016).
395. O'Leary, M. L. & Burbank, L. P. Natural Recombination among Type I Restriction-Modification Systems Creates Diverse Genomic Methylation Patterns among Xylella fastidiosa Strains. *Appl Environ Microbiol* **89**, e01873-22 (2023).
396. Liu, L. *et al.* Recent Advances in the Genomic Profiling of Bacterial Epigenetic Modifications. *Biotech J* **14**, 1800001 (2019).
397. Tran, F. & Boedicker, J. Q. Plasmid Characteristics Modulate the Propensity of Gene Exchange in Bacterial Vesicles. *J Bacteriol* **201**, 10.1128/jb.00430-18 (2019).
398. Bertozzi Silva, J., Storms, Z. & Sauvageau, D. Host receptors for bacteriophage adsorption. *FEMS Microbiol Lett* **363**, fnw002 (2016).
399. Papenfort, K., Espinosa, E., Casadesús, J. & Vogel, J. Small RNA-based feedforward loop with AND-gate logic regulates extrachromosomal DNA transfer in Salmonella. *PNAS* **112**, E4772–E4781 (2015).
400. Ibáñez de Aldecoa, A. L., Zafra, O. & González-Pastor, J. E. Mechanisms and Regulation of Extracellular DNA Release and Its Biological Roles in Microbial Communities. *Front. Microbiol.* **8**, (2017).
401. Didelot, X. & Maiden, M. C. J. Impact of recombination on bacterial evolution. *Trends in Microbiology* **18**, 315–322 (2010).
402. Dutcher, H. A. & Raghavan, R. Origin, Evolution, and Loss of Bacterial Small RNAs. *Micro Spectrum* **6**, 10.1128/microbiolspec.rwr-0004–2017 (2018).
403. Anguita-Maeso, M. *et al.* Xylella fastidiosa Infection Reshapes Microbial Composition and Network Associations in the Xylem of Almond Trees. *Front. Microbiol.* **13**, (2022).

404. Anguita-Maeso, M. *et al.* Metabolomic, Ionomic and Microbial Characterization of Olive Xylem Sap Reveals Differences According to Plant Age and Genotype. *Agronomy* **11**, 1179 (2021).
405. Sun, Y.-D., Spellman-Kruse, A. & Folimonova, S. Y. Blaze a New Trail: Plant Virus Xylem Exploitation. *Int J Mol Sci* **23**, 8375 (2022).
406. Marques, M. *et al.* Rhizosphere-xylem sap connections in the olive tree microbiome: implications for biostimulation approaches. *J. Appl. Microbiol.* **135**, lxae152 (2024).
407. Fatima, U. & Senthil-Kumar, M. Plant and pathogen nutrient acquisition strategies. *Front. Plant Sci.* **6**, (2015).
408. Sugrue, I., Ross, R. P. & Hill, C. Bacteriocin diversity, function, discovery and application as antimicrobials. *Nat Rev Microbiol* **22**, 556–571 (2024).
409. Lacava, P. T., Araújo, W. L., Marcon, J., Maccheroni, W., Jr & Azevedo, J. L. Interaction between endophytic bacteria from citrus plants and the phytopathogenic bacteria Xylella fastidiosa, causal agent of citrus-variegated chlorosis. *Letters in Applied Microbiology* **39**, 55–59 (2004).
410. Deyett, E. *et al.* Microbial Landscape of the Grapevine Endosphere in the Context of Pierce's Disease. *Phytobiomes Journal* **1**, 138–149 (2017).
411. Giampetruzzi, A. *et al.* Differences in the Endophytic Microbiome of Olive Cultivars Infected by Xylella fastidiosa across Seasons. *Pathogens* **9**, 723 (2020).
412. Vergine, M. *et al.* The Xylella fastidiosa-Resistant Olive Cultivar "Leccino" Has Stable Endophytic Microbiota during the Olive Quick Decline Syndrome (OQDS). *Pathogens* **9**, 35 (2020).
413. Zicca, S. *et al.* Antagonistic activity of olive endophytic bacteria and of *Bacillus* spp. strains against *Xylella fastidiosa*. *Microbiological Research* **236**, 126467 (2020).
414. Wholey, W.-Y., Kochan, T. J., Storck, D. N. & Dawid, S. Coordinated Bacteriocin Expression and Competence in Streptococcus pneumoniae Contributes to Genetic Adaptation through Neighbor Predation. *PLOS Pathogens* **12**, e1005413 (2016).
415. Lücking, D., Mercier, C., Alarcón-Schumacher, T. & Erdmann, S. Extracellular vesicles are the main contributor to the non-viral protected extracellular sequence space. *ISME Commun* **3**, 112 (2023).
416. Moreira, L. M., De Souza, R. F., Digiampietri, L. A., Da Silva, A. C. R. & Setubal, J. C. Comparative analyses of Xanthomonas and Xylella complete genomes. *OMICS* **9**, 43–76 (2005).
417. Asfahl, K. L. & Schuster, M. Social interactions in bacterial cell–cell signaling. *FEMS Microbiol Rev* **41**, 92–107 (2017).
418. Luo, T. *et al.* Transcriptomic Features in a Single Extracellular Vesicle via Single-Cell RNA Sequencing. *Small Methods* **6**, e2200881 (2022).
419. Zhao, J.-H., Liu, Q.-Y., Xie, Z.-M. & Guo, H.-S. Exploring the challenges of RNAi-based strategies for crop protection. *Adv. Biotechnol.* **2**, 23 (2024).
420. Danner, J., Pai, B., Wankerl, L. & Meister, G. Peptide-Based Inhibition of miRNA-Guided Gene Silencing. in *Drug Target miRNA: Methods and Protocols* (ed. Schmidt, M. F.) 199–210 (Springer, New York, NY, 2017). doi:10.1007/978-1-4939-6563-2_14.

421. Caillet, J., Baron, B., Boni, I. V., Caillet-Saguy, C. & Hajnsdorf, E. Identification of protein-protein and ribonucleoprotein complexes containing Hfq. *Sci Rep* **9**, 14054 (2019).
422. Sauter, C., Basquin, J. & Suck, D. Sm-like proteins in Eubacteria: the crystal structure of the Hfq protein from Escherichia coli. *Nucleic Acids Res* **31**, 4091–4098 (2003).
423. Schulz, E. C. *et al.* Intermolecular base stacking mediates RNA-RNA interaction in a crystal structure of the RNA chaperone Hfq. *Sci Rep* **7**, 9903 (2017).
424. Moll, L. *et al.* Antimicrobial Peptides With Antibiofilm Activity Against Xylella fastidiosa. *Front. Microbiol.* **12**, (2021).
425. El Handi, K. *et al.* Exploring Active Peptides with Antimicrobial Activity In Planta against Xylella fastidiosa. *Biology* **11**, 1685 (2022).
426. Koch, A. *et al.* An RNAi-Based Control of Fusarium graminearum Infections Through Spraying of Long dsRNAs Involves a Plant Passage and Is Controlled by the Fungal Silencing Machinery. *PLOS Pathogens* **12**, e1005901 (2016).
427. Liu, S. *et al.* Evaluation of dsRNA delivery methods for targeting macrophage migration inhibitory factor MIF in RNAi-based aphid control. *J Plant Dis Prot* **128**, 1201–1212 (2021).
428. Airs, P. M. & Bartholomay, L. C. RNA Interference for Mosquito and Mosquito-Borne Disease Control. *Insects* **8**, 4 (2017).
429. Singh, A. D., Wong, S., Ryan, C. P. & Whyard, S. Oral delivery of double-stranded RNA in larvae of the yellow fever mosquito, Aedes aegypti: Implications for pest mosquito control. *J Insect Sci* **13**, 69 (2013).
430. Yadav, M., Dahiya, N. & Sehrawat, N. Mosquito gene targeted RNAi studies for vector control. *Funct Integr Genomics* **23**, 180 (2023).
431. Backus, E. A. & Shugart, H. J. The vector regulation hypothesis: dynamic competition between pathogen and vector behaviors constrains Xylella fastidiosa biofilm development in sharpshooter foreguts. *Appl Environ Microbiol* **90**, e01102-24 (2024).

Appendices

List of Appendices

Appendix 1: Ruf, Alessa*, Lorenz Oberkofler*, Silke Robatzek, and Arne Weiberg. 'Spotlight on Plant RNA-Containing Extracellular Vesicles'. *Current Opinion in Plant Biology* 69 (1 October **2022**): 102272. https://doi.org/10.1016/j.pbi.2022.102272.

Appendix 2: Ruf, Alessa, and Silke Robatzek. '"Messenger RNA Just Entered the Chat": The next Layer of Cross-Kingdom RNA Transfer'. *Cell Host & Microbe* 32, no. 1 (10 January **2024**): 7–8. https://doi.org/10.1016/j.chom.2023.12.002.

Appendix 3: Thieron, Hannah*, Laura Krassini*, Seomun Kwon*, Sebastian Fricke, Sabrine Nasfi, Lorenz Oberkofler, Alessa **Ruf**, Julia Kehr, Karl-Heinz Kogel, Arne Weiberg, Michael Feldrbügge, Silke Robatzek, Ralph Panstruga. 'Practical Advice for Extracellular Vesicle Isolation in Plant–Microbe Interactions: Concerns, Considerations, and Conclusions'. *Journal of Extracellular Vesicles* 13, no. 12 (December **2024**): e70022. https://doi.org/10.1002/jev2.70022.

Appendix 1

Available online at www.sciencedirect.com

ScienceDirect

Current Opinion in Plant Biology

Spotlight on plant RNA-containing extracellular vesicles

Alessa Ruf[a], Lorenz Oberkofler[a], Silke Robatzek and Arne Weiberg

Abstract

Extracellular vesicles (EVs) carrying RNA have attracted growing attention in plant cell biology. For a long time, EV release or uptake through the rigid plant cell wall was considered to be impossible and RNA outside cells to be unstable. Identified EV biomarkers have brought new insights into functional roles of EVs to transport their RNA cargo for systemic spread in plants and into plant-invading pathogens. RNA-binding proteins supposedly take over key functions in EV-mediated RNA secretion and transport, but the mechanisms of RNA sorting and EV translocation through the plant cell wall and plasma membrane are not understood. Characterizing the molecular players and the cellular mechanisms of plant RNA-containing EVs will create new knowledge in cell-to-cell and inter-organismal communication.

Addresses

LMU Munich Biocenter, Großhaderner Straße 4, 82152 Planegg-Martinsried, DE, Germany

Corresponding author: Weiberg, Arne (a.weiberg@lmu.de)

[a] Co-first authors.

Current Opinion in Plant Biology 2022, **69**:102272

This review comes from a themed issue on **Cell biology and cell signalling (2022)**

Edited by **Dr. Stefanie Sprunck**, **Dr. Claus Schwechheimer** and **Dr. Miyo Morita**

For complete overview of the section, please refer the article collection - Cell biology and cell signalling (2022)

Available online 11 August 2022

https://doi.org/10.1016/j.pbi.2022.102272

Keywords

Extracellular vesicle, Extracellular RNA, RNA communication, Plant defense, Cell-wall remodeling, MVB, Biomarker, Tetraspanin, Syntaxin, Papillary matrix, EXPO, ckRNAi, Post-transcriptional modification, RNA sorting, RNA loading, RNA secretion, Polysome, RNA-Binding protein, Apoplast wash fluid.

Abbreviations

Extracellular vesicle, (EV); extracellular RNA, (exRNA); cross-kingdom RNA interference, (ckRNAi); RNA-binding protein, (RBP); multivesicular body, (MVB); exocyst-positive organelle, (EXPO); tetraspanin, (TET); PEN1, (PENETRATION1); tiny RNA, (tyRNA); small RNA, (sRNA); small interfering RNA, (siRNA); microRNA, (miRNA); long noncoding RNA, (lncRNA); circular RNA, (circRNA); trans-Golgi network, (TGN); cell wall degrading enzyme, (CWDE); remorin, (Rem); spray-induce gene silencing, (SIGS); apoplast wash fluid, (AWF).

Introduction

In plants, cell non-autonomous RNAs pass from cell-to-cell and travel over long distances between plant organs via the phloem vascular system. These mobile RNAs function as morphogens or gene regulatory molecules, which modulate diverse biological processes such as plant development, nutrient allocation, stress responses, antiviral defense, and root nodule symbiosis [1,2].

In recent years, RNA has been acknowledged to act as mediator in plants to communicate with other organisms in their environment, opening an exciting new chapter of inter-species and cross-kingdom RNA communication. Important key questions regarding RNA transport remain open: i) how are RNAs secreted from a donor cell, ii) how are RNAs selected for secretion, iii) how are RNAs stabilized outside the cell, iv) how are RNAs taken up by a recipient cell, and v) how can RNAs pass through the cell walls of plants and plant-interacting organisms? New results place plant extracellular vesicles (EV) into the center of cell-to-cell and inter-organismal RNA communication providing the function of potential RNA delivery chassis. In this short review, we discuss recent findings addressing RNA-containing EVs in plants.

EVs in plants

EVs are membrane-surrounded nanoparticles of 10−1000 nm in size that are found in all kingdoms of life [3−5]. Plant EVs were first described in carrot cell cultures in the 1960s [6]. Since plant cells are enveloped by a complex cell wall, the cellular release of particles as large as EVs was inconceivable. Additional hints for the existence of plant EVs came from transmission electron microscopic images of barley cells infected with the powdery mildew fungus *Blumeria graminis* [7] and *Arabidopsis thaliana* infected with *Golovinomyces orontii* [8], indicating EV-like structures in the papillary matrix beneath the pathogen infection sites and in encasements of haustoria, respectively. Imaging of the

periarbuscular space during plant-microbe symbiosis further revealed EVs associated with membrane tubules [9,10]. A new wave of plant EV studies using *A. thaliana* apoplast wash fluids (AWF) has been seen in recent years, with multiple advanced EV isolation methods were developed over the last few years that increased the quality of purified EVs [11–13]. These recent advances and technology developments make it now possible to analyse the proteins and RNA molecules present at EVs.

Biogenesis of plant EVs

Currently, two biogenesis routes of plant EVs are proposed: i) EVs derived from multivesicular body (MVB) endosomes, resembling the biogenesis pathway of exosomes as known in mammalian systems [14], and ii) EVs derived from the exocyst-positive organelle (EXPO) [15] (Figure 1a).

A role of MVBs in the biogenesis of plant EVs has been proposed since their co-occurrence was observed in microscopic images [6–8], but a mechanistic link between MVBs and EVs was missing. With the advent of the first plant EV biomarkers, tetraspanins (TET) and the syntaxin PENETRATION1 (PEN1), this link could be drawn. TETs are prominent biomarkers of mammalian exosomes [16]. Apart from roles in exosome biogenesis, selection of cargo, and exosome uptake, TETs have various functions in cell adhesion, motility, membrane fusion, signaling and protein trafficking [17]. The partial co-localization of the *A. thaliana* TET8 with the known MVB marker Rab5-like GTPase, ARA6 [18], suggests that TET8 positive EVs in plants are exosome-like and MVB-derived [19] and that other EVs, which are not labeled with TET8, might also be secreted from MVBs.

The plasma membrane-localized PEN1 has also been established as a plant EV biomarker [20]. Syntaxins are membrane-integrated proteins of the SNARE family mediating membrane fusion and are involved in vesicle-mediated transport within cells [21]. PEN1 has been

Figure 1

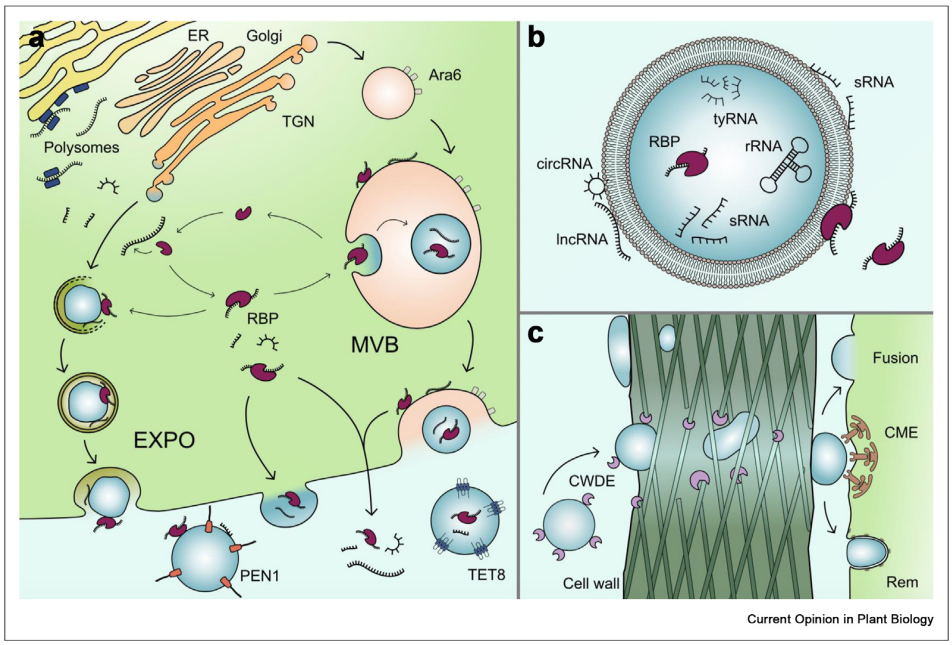

Plant RNA-containing EVs—biogenesis, types of RNA cargo, and plant cellular uptake. (**a**): Possible EV biogenesis routes, loading of RNAs, and cellular EV release in plants. Plant EVs might derive either from the endocytic pathway including the *trans*-Golgi network (TGN) and multivesicular body (MVB) endosomes or from the exocyst-positive organelles (EXPO), or by shedding from the plasma membrane, a process known in animals and bacteria but not yet reported in plants. So far, the identification of two EV biomarkers, TET8 and PEN1, allows the differentiation between two types of plant EVs. RNA-binding proteins (RBP) seem to play important roles in RNA loading into EV precursors and for exRNA stability. A site of RNA loading into vesicles could be membrane-bound polysomes. RBPs and exRNAs could also be secreted into the apoplast independent of membrane vesicles. (**b**): Different types of RNAs are identified to associate with plant EVs. RNAs and RBPs can be located inside the EV or attached to the EV outer surface. (**c**): Passage of EVs through the plant cell wall might involve active cell wall remodeling through EV-associated cell wall-degrading enzymes (CWDE). Cell wall as well as EV plasticity could further facilitate their cell wall passage. Intracellular delivery of EV cargo might occur via clathrin-mediated endocytosis (CME), clathrin-independent EV fusion with the plasma membrane, or might involve interaction with remorins (Rem)-rich nanodomains.

first established as a biomarker for the papillary matrix, which forms beneath attempted penetration sites in non-host response to powdery mildew fungi [22]. The presence of PEN1−positive EVs in the papillary matrix suggested the secretion in the form of intraluminal vesicles from MVBs, which is consistent with ARA6-labeled organelles accumulating near the fungal attack site [23]. The proteome of PEN1-positive EVs shares high similarity with endomembrane proteomes [19] and the partial co-localization of ARA6 with TET8 [19,24] would argue that other EVs could be derived from MVBs and they could include PEN1 vesicles, too.

However, PEN1- and TET8-positive EVs do not co-localize [24], thus they are considered as two distinct classes of plant EVs. An alternative route of EV biogenesis could be via EXPO, a spherical, double-membrane compartment, which is thought to form in an autophagosome-like manner and represent an unconventional secretion pathway unique in plants [15]. The EXPO marker Exo70E2 does not co-localize with MVBs and the endocytic pathway in *A. thaliana*. EXPO internal vesicles could fuse with the plasma membrane and thereby release plant EVs (Figure 1a). Given the heterogeneity expected in plant EV population, it is likely that the EXPO and other secretory pathways might contribute to EV biogenesis. This is supported by findings that EXO70B2 co-localizes with the exocyst core subunit SEC6 and PEN1 in the membrane domain of papillae, and interaction between EXO70B2 and PEN1 [25]. However, the assembly of the secretory VAMP721/722-PEN1-SNAP33 SNARE ternary complex, which is mediated by the small GTPase RABA2a occurs independent of exocyst function [26]. This suggests that RABA2a-SNARE- and exocyst-mediated secretion are largely separate pathways, but this remains to be shown under pathogen infection. Being at the plasma membrane, PEN1-positive EVs could also emerge by shedding from the plasma membrane and thus, representing yet another biogenesis route. While this has been found for mammalian cells [27] and bacteria [28], no evidence of plasma membrane budding exists in plants at the moment.

How do plant EVs traverse the cell wall?

Physically, the size of an EV particle is too big to fit through the dense cell wall network of lignin, pectin, and (hemi-)cellulose fibrils. However, a passive diffusion might occur due to the dynamics of the cell wall, which could be at sites of plant infection or cell wall genesis [29,30]. Since cell wall-degrading enzymes are found at plant EVs [20,31,32], the vesicles could perturb the cell wall, turning EV cell wall transmission into an active process (Figure 1c). Plant EVs typically occur as a spherical structure when isolated, but tubular shapes could be conceivable and have been observed in bacteria [33,34], which could promote cell wall passage [35] (Figure 1).

Plant EVs might fuse to the plasma membrane of target cells to release their content intracellularly. EV fusion might occur via clathrin-mediated endocytosis (CME) or independent of CME. Moreover, protein microdomains of the plasma membrane, such as remorins, might facilitate EV fusion and cargo release as shown for the interaction between bacterial vesicles and the plant plasma membrane [36] (Figure 1c).

Plant EVs contain RNAs

Regulatory small RNAs mediate inter-species communication, with EVs being a prime suspect for RNA transport. EVs isolated from the AWF of *A. thaliana* leaves infected with the fungal pathogen *Botrytis cinerea* contained diverse plant small-interfering RNAs (siRNAs) and microRNAs (miRNAs), some of them translocating into the infecting pathogen [19]. The EVs carrying antifungal RNAs are TET8 positive. RNA content of EVs found in mammals are rather diverse, spanning from miRNAs, siRNAs, small nuclear/nucleolar RNAs, Y-RNAs, ribosomal RNAs, transfer RNAs, other types of non-coding RNAs to messenger RNAs, fragmented and in full length [37,38]. It is very likely that plant EVs comprise such diverse RNA spectra, too. Indeed, tiny RNAs (tyRNAs) of 10−17 nucleotides in length, long noncoding RNAs (lncRNAs), circular RNAs (circRNAs), and small RNAs (sRNAs) are present at Arabidopsis EVs [39,40]. Interestingly, several types of RNAs co-purifying in EV samples are protected against MNase treatment alone [19], while others are degraded by Trypsin and RNAse A co-treatment [40]. Hence, identified EV-RNAs might be encapsulated inside EVs, but might also being located outside of EVs where they might be protected by RNA-binding proteins against enzymatic degradation (Figure 1b).

Small RNAs found in plant EVs do not reflect the profile of cellular RNAs suggesting selective loading. For instance, tyRNAs in *A. thaliana* were enriched in EVs compared to cellular RNAs [39], and only some siRNAs of the same RNA precursor can be detected in EVs. Similarly, miRNA166, but not miR822 was detected in EVs, although both miRNAs are abundant in plant cell extracts [19]. This observation raises the question of how small RNAs are sorted for EV secretion.

First insights into RNA sorting and loading were given by studying the plant EV proteome, in particular RNA-binding proteins (RBPs). TET8 positive EVs contain the RBPs ARGONAUTE1 (AGO1), two annexins (ANNs), ANN1 and ANN2, and two DEAD-box RNA helicases (RHs), RH11 and RH37 [24]. Co-IP

experiments suggest that AGO1, RH11, and RH37 specifically interact with EV-enriched small RNAs. *A. thaliana ago1-27*, *rh11rh37*, and *ann1ann2* mutants revealed reduction but not completely abolished signal from EV-enriched siRNA and miRNA. Thus, other RBPs and mechanisms are likely involved in the loading process. The RBP Glycine-rich protein (GRP)7 was found in *A. thaliana* AWF [20], and exRNAs revealed an enriched level of N6-methyladenine (m^6A) modification [40]. A mammalian homolog of GRP7 is HNRNPA2B1 that interacts with m^6A-RNAs [41], thus GRP7 might specifically bind to m^6A-RNAs for secretion. Moreover, HNRNPA2B1 is also involved in miRNA sorting into exosomes [42], but a link of GRP7 to plant EVs is not evident. Another possibility could be RNA sequence motifs, which would be recognized by sorting RBPs. Such RNA sorting sequences (EXOmotif) and non-template additions of 3' end uridylation have been described in mammalian exosome miRNAs [43,44] and are postulated as functional RNA secretion signals. Loading specificity of RNAs into EVs could also be determined by RNA subcellular localization. For instance, RNAs found in membrane-bound polysomes [45–47] could be at side of EV loading. Despite all these hints, to date a mechanistic understanding of RNA loading into EVs remains incomplete, both in plants and animals.

Functions of EV-associated RNAs

Diversity of EVs and associated RNAs points toward a broad range of biological functions, from removal of cellular nonsense RNAs to cell-to-cell, intra-organismal, and inter-species/cross-kingdom RNA communication. Several findings highlight a role of plant EVs in defense response against infecting pathogens. For instance, EV-like structures accumulated around hyphal infection sites of fungi [8,48,49] and EV quantities isolated from the *A. thaliana* AWF increased during pathogen infection [8,19,50,51]. Moreover, EVs contain several proteins and RNAs known or being predicted to have antimicrobial activities [19,20].

Cross-kingdom RNAi (ckRNAi) in plant–microbial interaction is well characterized in the pathosystem *A. thaliana*/*B. cinerea*. The fungal pathogen *B. cinerea* secretes siRNAs during infection that enter the plant cells and hijack the plant's own AGO1/RNA-induced silencing complex to suppress important plant immunity-related genes [52]. Of note, ckRNAi is bidirectional [53], and *A. thaliana* natural miRNAs and siRNAs suppress *B. cinerea* genes relevant for infection [19]. These antifungal RNAs are secreted in TET8-positive EVs, and fungal mycelium treated with *A. thaliana* EVs induced gene silencing *in vitro*. Furthermore, antifungal activity of sunflower EVs were found [32], but a role exRNAs or ckRNAi is not clear in this case. Also, ckRNAi has been demonstrated in plant–oomycete interaction [54] and in symbiotic interactions of root nodule forming Rhizobia and of an ectomycorrhiza fungus [55,56]. RNA exchange has been reported between plants of the same species [57], as well as in parasitic plants of the genus *Cuscuta* [58,59]. We speculate that plant EVs are involved in these inter-organismal and inter-kingdom interactions, too.

Conclusions

How is exRNA secreted and transported in plants? EV-mediated exRNA transport for intercellular communication is widely accepted in mammals [60], and is now suggested in plants. However, our mechanistic understanding of plant EV biogenesis, their cellular release and uptake, and their biological functions remain obscure. RNAs seem to be selected for secretion in EVs, but how RNA sorting is regulated and where RNAs are loaded into vesicles is not known. RBPs are postulated to mediate these RNA processes. This raises the questions: how is EV production, EV-RNA loading, and EV release regulated in plants, and is EV secretion under the control of plant immune signaling pathway(s)? In this complicated situation, the identification of the two plant EV biomarkers, TET8 and PEN1, has been a milestone in plant EV research. We expect that more biomarkers representing plant EVs originated from unconventional secretion pathways will be obtained in the future. These biomarkers not only link EVs to the MVB secretion pathway and to plasma membrane interaction, but also allow EV quantification, purification, and *in situ* localization. This is a promising starting point to dissect their molecular cargo, which in turn will reveal information on the biogenesis pathway(s) and their biological functions. Standardized protocols and guidelines provided by the International Society of Extracellular Vesicles (ISEV) consortium and shared databases led to an increase of understanding biogenesis and role of EVs in animals. In our opinion, standardization in plant EV research is key to progress in a similar speed as in the mammalian field [61,62].

ExRNA communication between plants and associated (micro)-organisms is bidirectional, which allows for pathogens and parasites to manipulate host plants through exRNAs for infection. This raises the question: How do plants respond to microbe-derived EVs, which can contain RNAs [63]?. For example, bacterial outer membrane vesicles integrate into the plant plasma membrane [36], likely releasing their content into plant cells. Moreover, bacterial EVs might have immunogenic or immune-suppressive effects on host plants [64]. A next milestone will be to find out how plants recognize and respond to microbial EVs, which will uncover new functions in microbial virulence and plant immunity.

Understanding the mechanistic basis of how exRNAs are secreted and taken up by plants and their interacting microbes bears great potential for innovative RNAi-based crop protection strategies [65,66]. Spray-induced gene

silencing (SIGS) is based on antimicrobial RNAs that are topically applied onto plant surfaces to suppress the infecting pathogen [53,67,68]. Translating gained knowledge on EV-mediated RNA delivery could help to improve SIGS, making agricultural production systems more sustainable and eco-friendlier in the future.

Declaration of competing interest

The authors declare that they have no known competing financial interests or personal relationships that could have appeared to influence the work reported in this article.

Acknowledgments

We would like to thank Vera Göhre for proofreading and editorial suggestions and Federico Bergonzini for his advice in drawing the figure. This work was supported by the German Research Foundation (DFG) through the Collaborative Research Center SFB924 and the DFG Research Unit RU5116 "exRNA".

References

Papers of particular interest, published within the period of review, have been highlighted as:

* of special interest
** of outstanding interest

1. Liu L, Chen X: **Intercellular and systemic trafficking of RNAs in plants**. *Nat Plants* 2018, **4**:869–878.

2. Maizel A, Markmann K, Timmermans M, Wachter A: **To move or not to move: roles and specificity of plant RNA mobility**. *Curr Opin Plant Biol* 2020, **57**:52–60.

3. Stotz HU, Brotherton D, Inal J: **Communication is key: extracellular vesicles as mediators of infection and defence during host-microbe interactions in animals and plants**. *FEMS Microbiol Rev* 2022, **46**.

4. van Niel G, D'Angelo G, Raposo G: **Shedding light on the cell biology of extracellular vesicles**. *Nat Rev Mol Cell Biol* 2018, **19**:213–228.

5. Woith E, Fuhrmann G, Melzig MF: **Extracellular vesicles-connecting kingdoms**. *Int J Mol Sci* 2019, **20**.

6. Halperin W, Jensen WA: **Ultrastructural changes during growth and embryogenesis in carrot cell cultures**. *J Ultrastruct Res* 1967, **18**:428–443.

7. An Q, van Bel AJ, Huckelhoven R: **Do plant cells secrete exosomes derived from multivesicular bodies?** *Plant Signal Behav* 2007, **2**:4–7.

8. Micali CO, Neumann U, Grunewald D, Panstruga R, O'Connell R: **Biogenesis of a specialized plant-fungal interface during host cell internalization of *Golovinomyces orontii* haustoria**. *Cell Microbiol* 2011, **13**:210–226.

9. Ivanov S, Austin 2nd J, Berg RH, Harrison MJ: **Extensive membrane systems at the host-arbuscular mycorrhizal fungus interface**. *Nat Plants* 2019, **5**:194–203.

10. Roth R, Hillmer S, Funaya C, Chiapello M, Schumacher K, Lo Presti L, Kahmann R, Paszkowski U: **Arbuscular cell invasion coincides with extracellular vesicles and membrane tubules**. *Nat Plants* 2019, **5**:204–211.

11. * Chen A, He B, Jin H: **Isolation of extracellular vesicles from Arabidopsis**. *Curr Protoc* 2022, **2**:e352.
Describes detailed protocols for the isolation of plant EVs from apoplastic wash fluids of *Arabidopsis thaliana*, discussing areas of troubleshooting and improvements.

12. Huang Y, Wang S, Cai Q, Jin H: **Effective methods for isolation and purification of extracellular vesicles from plants**. *J Integr Plant Biol* 2021, **63**:2020–2030.

13. * Rutter BD, Rutter KL, Innes RW: **Isolation and quantification of plant extracellular vesicles**. *Bio Protoc* 2017, **7**:e2533.
Highlights potential challenges in studying plant EVs, and lessons learnt from EV research in mammalian systems. Addresses experimental approaches regarding isolation of vesicles with a special focus on RNA isolation from plant EVs.

14. Hessvik NP, Llorente A: **Current knowledge on exosome biogenesis and release**. *Cell Mol Life Sci* 2018, **75**:193–208.

15. Wang J, Ding Y, Wang J, Hillmer S, Miao Y, Lo SW, Wang X, Robinson DG, Jiang L: **EXPO, an exocyst-positive organelle distinct from multivesicular endosomes and autophagosomes, mediates cytosol to cell wall exocytosis in Arabidopsis and tobacco cells**. *Plant Cell* 2010, **22**:4009–4030.

16. Colombo M, Raposo G, Thery C: **Biogenesis, secretion, and intercellular interactions of exosomes and other extracellular vesicles**. *Annu Rev Cell Dev Biol* 2014, **30**:255–289.

17. Andreu Z, Yanez-Mo M: **Tetraspanins in extracellular vesicle formation and function**. *Front Immunol* 2014, **5**:442.

18. Ebine K, Fujimoto M, Okatani Y, Nishiyama T, Goh T, Ito E, Dainobu T, Nishitani A, Uemura T, Sato MH, *et al.*: **A membrane trafficking pathway regulated by the plant-specific RAB GTPase ARA6**. *Nat Cell Biol* 2011, **13**:853–859.

19. ** Cai Q, Qiao L, Wang M, He B, Lin FM, Palmquist J, Huang SD, Jin H: **Plants send small RNAs in extracellular vesicles to fungal pathogen to silence virulence genes**. *Science* 2018, **360**:1126–1129.
Proof-of-principle study of EV-based cross-kingdom RNAi in a fungal–plant interaction. Identification of TET8 as a plant EV biomarker.

20. ** Rutter BD, Innes RW: **Extracellular vesicles isolated from the leaf apoplast carry stress-response proteins**. *Plant Physiol* 2017, **173**:728–741.
First study on plant EV proteome and comparative analysis of EV-proteins under bacterial infection. Identification of PEN1 as a plant EV biomarker.

21. More K, Klinger CM, Barlow LD, Dacks JB: **Evolution and natural history of membrane trafficking in eukaryotes**. *Curr Biol* 2020, **30**:R553–R564.

22. Meyer D, Pajonk S, Micali C, O'Connell R, Schulze-Lefert P: **Extracellular transport and integration of plant secretory proteins into pathogen-induced cell wall compartments**. *Plant J* 2009, **57**:986–999.

23. Nielsen ME, Feechan A, Bohlenius H, Ueda T, Thordal-Christensen H: **Arabidopsis ARF-GTP exchange factor, GNOM, mediates transport required for innate immunity and focal accumulation of syntaxin PEN1**. *Proc Natl Acad Sci U S A* 2012, **109**:11443–11448.

24. ** He B, Cai Q, Qiao L, Huang CY, Wang S, Miao W, Ha T, Wang Y, Jin H: **RNA-binding proteins contribute to small RNA loading in plant extracellular vesicles**. *Nat Plants* 2021, **7**:342–352.
Suggests a role for RBPs in the selective loading of sRNAs in TET8-positive EVs. Identified RBPs include AGO1, DEAD-box RNA helicases 11 and 37 as well as annexins. Immunity against *B. cinerea* was decreased in respective RBP mutant lines and transcripts of fungal target genes of plant EV-sRNAs were no longer repressed. These results demonstrate for the first time how RNAs are selectively loaded into plant EVs.

25. Ortmannova J, Sekeres J, Kulich I, Santrucek J, Dobrev P, Zarsky V, Pecenkova T: **Arabidopsis EXO70B2 exocyst subunit contributes to papillae and encasement formation in antifungal defence**. *J Exp Bot* 2022, **73**:742–755.

26. Pang L, Ma Z, Zhang X, Huang Y, Li R, Miao Y, Li R: **The small GTPase RABA2a recruits SNARE proteins to regulate the secretory pathway in parallel with the exocyst complex in Arabidopsis**. *Mol Plant* 2022, **15**:398–418.

27. Rilla K: **Diverse plasma membrane protrusions act as platforms for extracellular vesicle shedding**. *J Extracell Vesicles* 2021, **10**, e12148.

28. Sartorio MG, Pardue EJ, Feldman MF, Haurat MF: **Bacterial outer membrane vesicles: from discovery to applications**. *Annu Rev Microbiol* 2021, **75**:609–630.

Appendix 1

29. Dora S, Terrett OM, Sanchez-Rodriguez C: **Plant-microbe interactions in the apoplast: communication at the plant cell wall**. *Plant Cell* 2022, **34**:1532–1550.

30. Zhang B, Gao Y, Zhang L, Zhou Y: **The plant cell wall: biosynthesis, construction, and functions**. *J Integr Plant Biol* 2021, **63**:251–272.

31. de la Canal L, Pinedo M: **Extracellular vesicles: a missing component in plant cell wall remodeling**. *J Exp Bot* 2018, **69**: 4655–4658.

32. Regente M, Pinedo M, San Clemente H, Balliau T, Jamet E, de la Canal L: **Plant extracellular vesicles are incorporated by a fungal pathogen and inhibit its growth**. *J Exp Bot* 2017, **68**: 5485–5495.

33. McCaig WD, Koller A, Thanassi DG: **Production of outer membrane vesicles and outer membrane tubes by *Francisella novicida***. *J Bacteriol* 2013, **195**:1120–1132.

34. Santos S, Arauz LJ, Baruque-Ramos J, Lebrun I, Carneiro SM, Barreto SA, Schenkman RP: **Outer membrane vesicles (OMV) production of *Neisseria meningitidis* serogroup B in batch process**. *Vaccine* 2012, **30**:6064–6069.

35. Zhang H, Goh NS, Wang JW, Pinals RL, Gonzalez-Grandio E, Demirer GS, Butrus S, Fakra SC, Del Rio Flores A, Zhai R, *et al.*: **Nanoparticle cellular internalization is not required for RNA delivery to mature plant leaves**. *Nat Nanotechnol* 2022, **17**: 197–205.

36. * Tran TM, Chng CP, Pu X, Ma Z, Han X, Liu X, Yang L, Huang C, Miao Y: **Potentiation of plant defense by bacterial outer membrane vesicles is mediated by membrane nanodomains**. *Plant Cell* 2022, **34**:395–417.

Provides evidence for a direct interaction between the *Arabidopsis* plasma membrane and *Xanthomonas* OMVs, suggesting that bacterial vesicles can integrate and remain in the host plasma membrane. Highlights the role of remorin-rich nanodomains in the interaction between the plant plasma membrane and bacterial OMVs. Computational modeling suggests an increase in the plant plasma membrane lipid order upon interaction with bacterial OMVs, which may underline a potentiated immune response.

37. Gruner HN, McManus MT: **Examining the evidence for extracellular RNA function in mammals**. *Nat Rev Genet* 2021, **22**: 448–458.

38. Kim KM, Abdelmohsen K, Mustapic M, Kapogiannis D, Gorospe M: **RNA in extracellular vesicles**. *Wiley Interdiscip Rev RNA* 2017, **8**.

39. Baldrich P, Rutter BD, Karimi HZ, Podicheti R, Meyers BC, Innes RW: **Plant extracellular vesicles contain diverse small RNA species and are enriched in 10- to 17-nucleotide "tiny" RNAs**. *Plant Cell* 2019, **31**:315–324.

40. ** Karimi HZ, Baldrich P, Rutter BD, Borniego L, Zajt KK, Meyers BC, Innes RW: **Arabidopsis apoplastic fluid contains sRNA- and circular RNA-protein complexes that are located outside extracellular vesicles**. *Plant Cell* 2022, **34**:1863–1881.

Reports results that RNA species identified in the apoplast of *A. thaliana* include sRNAs and lncRNAs, which were detected externally and not inside of EVs, associating with EV membranes and RBPs. Many identified RNA molecules seem to be circRNAs. Two RBPs, *AGO2* and *GRP7* were identified to be involved in the secretion or stabilization of extracellular circRNAs. These results represent a big leap forward in understanding the diversity and localization of extracellular RNAs in plants.

41. Alarcon CR, Goodarzi H, Lee H, Liu X, Tavazoie S, Tavazoie SF: **HNRNPA2B1 is a mediator of m(6)A-dependent nuclear RNA processing events**. *Cell* 2015, **162**:1299–1308.

42. Villarroya-Beltri C, Gutierrez-Vazquez C, Sanchez-Cabo F, Perez-Hernandez D, Vazquez J, Martin-Cofreces N, Martinez-Herrera DJ, Pascual-Montano A, Mittelbrunn M, Sanchez-Madrid F: **Sumoylated hnRNPA2B1 controls the sorting of miRNAs into exosomes through binding to specific motifs**. *Nat Commun* 2013, **4**:2980.

43. Garcia-Martin R, Wang G, Brandao BB, Zanotto TM, Shah S, Kumar Patel S, Schilling B, Kahn CR: **MicroRNA sequence codes for small extracellular vesicle release and cellular retention**. *Nature* 2022, **601**:446–451.

44. Koppers-Lalic D, Hackenberg M, Bijnsdorp IV, van Eijndhoven MAJ, Sadek P, Sie D, Zini N, Middeldorp JM, Ylstra B, de Menezes RX, *et al.*: **Nontemplated nucleotide additions distinguish the small RNA composition in cells from exosomes**. *Cell Rep* 2014, **8**:1649–1658.

45. Jouannet V, Moreno AB, Elmayan T, Vaucheret H, Crespi MD, Maizel A: **Cytoplasmic Arabidopsis AGO7 accumulates in membrane-associated siRNA bodies and is required for ta-siRNA biogenesis**. *EMBO J* 2012, **31**:1704–1713.

46. Li S, Le B, Ma X, Li S, You C, Yu Y, Zhang B, Liu L, Gao L, Shi T, *et al.*: **Biogenesis of phased siRNAs on membrane-bound polysomes in Arabidopsis**. *Elife* 2016, **5**.

47. Li S, Liu L, Zhuang X, Yu Y, Liu X, Cui X, Ji L, Pan Z, Cao X, Mo B, *et al.*: **MicroRNAs inhibit the translation of target mRNAs on the endoplasmic reticulum in Arabidopsis**. *Cell* 2013, **153**:562–574.

48. An Q, Ehlers K, Kogel KH, van Bel AJ, Huckelhoven R: **Multivesicular compartments proliferate in susceptible and resistant MLA12-barley leaves in response to infection by the biotrophic powdery mildew fungus**. *New Phytol* 2006, **172**: 563–576.

49. An Q, Huckelhoven R, Kogel KH, van Bel AJ: **Multivesicular bodies participate in a cell wall-associated defence response in barley leaves attacked by the pathogenic powdery mildew fungus**. *Cell Microbiol* 2006, **8**:1009–1019.

50. Movahed N, Cabanillas DG, Wan J, Vali H, Laliberte JF, Zheng H: **Turnip mosaic virus components are released into the extracellular space by vesicles in infected leaves**. *Plant Physiol* 2019, **180**:1375–1388.

51. Xin XF, Nomura K, Underwood W, He SY: **Induction and suppression of PEN3 focal accumulation during *Pseudomonas syringae pv. tomato* DC3000 infection of Arabidopsis**. *Mol Plant Microbe Interact* 2013, **26**:861–867.

52. Weiberg A, Wang M, Lin FM, Zhao H, Zhang Z, Kaloshian I, Huang HD, Jin H: **Fungal small RNAs suppress plant immunity by hijacking host RNA interference pathways**. *Science* 2013, **342**:118–123.

53. Wang M, Weiberg A, Lin FM, Thomma BP, Huang HD, Jin H: **Bidirectional cross-kingdom RNAi and fungal uptake of external RNAs confer plant protection**. *Nat Plants* 2016, **2**, 16151.

54. Dunker F, Trutzenberg A, Rothenpieler JS, Kuhn S, Prols R, Schreiber T, Tissier A, Kemen A, Kemen E, Huckelhoven R, *et al.*: **Oomycete small RNAs bind to the plant RNA-induced silencing complex for virulence**. *Elife* 2020, **9**, e56096.

55. Ren B, Wang X, Duan J, Ma J: **Rhizobial tRNA-derived small RNAs are signal molecules regulating plant nodulation**. *Science* 2019, **365**:919–922.

56. Wong-Bajracharya J, Singan VR, Monti R, Plett KL, Ng V, Grigoriev IV, Martin FM, Anderson IC, Plett JM: **The ectomycorrhizal fungus *Pisolithus microcarpus* encodes a microRNA involved in cross-kingdom gene silencing during symbiosis**. *Proc Natl Acad Sci U S A* 2022:119.

57. * Betti F, Ladera-Carmona MJ, Weits DA, Ferri G, Iacopino S, Novi G, Svezia B, Kunkowska AB, Santaniello A, Piaggesi A, *et al.*: **Exogenous miRNAs induce post-transcriptional gene silencing in plants**. *Nat Plants* 2021, **7**:1379–1388.

Shows that plant-produced miRNAs are signaling molecules, affecting gene expression in nearby plants. Target genes of exogenous miRNAs were found silenced in WT *A. thaliana* plants when co-cultured with plants overexpressing miRNAs. Silencing occurred in an AGO1 and RDR6-dependant manner, indicating the importance of secondary siRNA to induce PTGS via exogenous miRNAs in plants.

58. Kim G, LeBlanc ML, Wafula EK, dePamphilis CW, Westwood JH: **Plant science. Genomic-scale exchange of mRNA between a parasitic plant and its hosts**. *Science* 2014, **345**:808–811.

59. Shahid S, Kim G, Johnson NR, Wafula E, Wang F, Coruh C, Bernal-Galeano V, Phifer T, dePamphilis CW, Westwood JH, *et al.*: **MicroRNAs from the parasitic plant *Cuscuta campestris* target host messenger RNAs**. *Nature* 2018, **553**:82–85.

60. Maas SLN, Breakefield XO, Weaver AM: **Extracellular vesicles: unique intercellular delivery vehicles**. *Trends Cell Biol* 2017, **27**:172–188.

Appendix 1

61. * Pinedo M, de la Canal L, de Marcos Lousa C: **A call for rigor and standardization in plant extracellular vesicle research**. *J Extracell Vesicles* 2021, **10**, e12048.
Underlines the need for standardization in the research of plant EVs in order to progress in a similar way than the mammalian EV research. Focusses on the nomenclature and characterization of plant EVs.

62. Thery C, Witwer KW, Aikawa E, Alcaraz MJ, Anderson JD, Andriantsitohaina R, Antoniou A, Arab T, Archer F, Atkin-Smith GK, *et al.*: **Minimal information for studies of extracellular vesicles 2018 (MISEV2018): a position statement of the International Society for Extracellular Vesicles and update of the MISEV2014 guidelines**. *J Extracell Vesicles* 2018, **7**, 1535750.

63. Kwon S, Rupp O, Brachmann A, Blum CF, Kraege A, Goesmann A, Feldbrugge M: **mRNA inventory of extracellular vesicles from *ustilago maydis***. *J Fungi* 2021, **7**.

64. McMillan HM, Kuehn MJ: **The extracellular vesicle generation paradox: a bacterial point of view**. *EMBO J* 2021, **40**, e108174.

65. Kameli N, Dragojlovic-Kerkache A, Savelkoul P, Stassen FR: **Plant-derived extracellular vesicles: current findings, challenges, and future applications**. *Membranes* 2021:11.

66. Yang C, Zhang M, Merlin D: **Advances in plant-derived edible nanoparticle-based lipid nano-drug delivery systems as therapeutic nanomedicines**. *J Mater Chem B* 2018, **6**: 1312–1321.

67. Koch A, Biedenkopf D, Furch A, Weber L, Rossbach O, Abdellatef E, Linicus L, Johannsmeier J, Jelonek L, Goesmann A, *et al.*: **An RNAi-based control of *Fusarium graminearum* infections through spraying of long dsRNAs involves a plant passage and is controlled by the fungal silencing machinery**. *PLoS Pathog* 2016, **12**, e1005901.

68. Mitter N, Worrall EA, Robinson KE, Li P, Jain RG, Taochy C, Fletcher SJ, Carroll BJ, Lu GQ, Xu ZP: **Clay nanosheets for topical delivery of RNAi for sustained protection against plant viruses**. *Nat Plants* 2017, **3**, 16207.

Appendix 2

Cell Host & Microbe
Previews

CellPress

"Messenger RNA just entered the chat": The next layer of cross-kingdom RNA transfer

Alessa Ruf[1] and Silke Robatzek[1,*]
[1]LMU Munich Biocenter, Großhadener Strasse 4, 82152 Planegg, DE, Germany
*Correspondence: robatzek@bio.lmu.de
https://doi.org/10.1016/j.chom.2023.12.002

Infectious fungi send small RNAs into plant cells to enhance their virulence by silencing defense-related genes. In this issue of *Cell Host & Microbe*, Wang and colleagues show that full-length messenger RNA is transported in vesicles from plants to fungi, becoming translated by fungal ribosomes and reducing fungal pathogenicity.

Cross-kingdom RNA transfer exists between plant hosts and microbes to orchestrate the infection outcome. Ten years ago, these processes were discovered in the fungal pathogen *Botrytis cinerea*, which exports small RNAs (sRNAs) that exploit the plant RNA interference (RNAi) machinery to silence defense genes and promote disease.[1] Cross-kingdom RNAi has since been found relevant for other fungal pathogens and many different types of plant-microbe interactions, including pathogenic oomycetes, beneficial fungi, and rhizobacteria.[2–5] The transfer is bidirectional as sRNA is transported from the host to the microbes and aids the plant defense against pathogens.[6] Cross-kingdom transferred sRNAs include microRNAs (miRNAs) and dsRNA-derived small interfering RNAs (siRNAs) but also rRNA- and tRNA-derived fragments. Do plants and microbes transfer other RNA biotypes too? In this preview, we highlight the recent finding by Wang et al. that *Arabidopsis thaliana,* a cousin of mustard plants*,* transfers messenger RNA (mRNA) into *Botrytis cinerea*, where it is translated and the corresponding protein reducing pathogen virulence.[7]

RNA transfer between cells is mediated by extracellular vesicles (EVs), which are membrane-enclosed nanoscale particles released from cells of all organisms and carry a variety of RNA, DNA, protein, and lipid cargo. In *Arabidopsis thaliana*, distinct EV types have been described, of which EVs positive for tetraspanin 8 (TET8), a homologue of mammalian EV-enriched tetraspanins CD9, CD63, and CD81, likely resemble exosomes derived from multivesicular bodies. Focusing on TET8-positive EVs,[8] Wang et al. explored the mRNA contents of plant exosomes in response to *Botrytis cinerea* infection.

In agriculture, *Botrytis cinerea* causes gray mold, one of the most destructive plant diseases. It is ubiquitously present in the form of airborne spores and can infect over 200 crop species. Gray mold leads to soft rot of all aerial plant parts and is particularly important in post-harvest spoilage of fruits. It is a difficult disease to control and thus, knowledge is needed of how plants defend themselves against this fungus.

Using *Arabidopsis thaliana* as an experimental model, Wang et al. showed that EVs isolated from extracellular fluids of infected leaves contain sequence reads of numerous mRNAs and full-length transcripts of at least 15 mRNAs. It is critical to ensure that the vesicles were not debris from plant cells undergoing cell death, which is a disease symptom of infection with a necrotrophic fungus. To rule this out, the authors confirmed the quality of the extracellular fluids by (1) collecting the fluids at the early, biotrophic infection stage where no cell death occurs and (2) showing that the fluids did not contain chloroplast and mitochondrial proteins. The mRNA profiles of EVs were distinct from total mRNA profiles. The authors selected four infection-induced EV-mRNAs for further investigations. These RNAs were resistant to nuclease and proteinase treatments of EVs, hinting that they could be luminal EV cargoes. The authors found the corresponding full-length transcripts in TET8-positive EVs using immunocapture of the vesicles from infected leaves.

Next, the authors visualized selected mRNAs in plant EVs. They used an improved version of the Three-Way Junction-4 x Broccoli (3WJ-4xBro) RNA reporter system. Full-length *SAG21*, *APS1*, *PRXIIC*, and *HEL* transcripts tagged with fluorescent RNA aptamers expressed *in planta* were observed in TET8-positive EVs. This was not the case for *OEP6* transcripts, which is abundant in total mRNA but is not found in EVs. To show mRNA transfer into fungal cells, stable *Arabidopsis thaliana* lines expressing RNA aptamer-tagged *SAG21* and *APS1* transcripts were infected with *Botrytis cinerea*. Labeled transcripts could be detected in fungal protoplasts. Transfer of mRNA transcripts into fungal cells could also be shown after co-incubation of fungal cells with EVs isolated from the reporter lines. The authors observed no transfer of tagged *OEP6* transcripts into fungal cells. The transfer of tagged *SAG21* and *APS1* transcripts was significantly reduced in *tet8*/*tet9* mutant plants. Moreover, proteins potentially coding for fluorescence protein-tagged mRNAs expressed *in planta* were not found in TET8-positive EVs. This provides experimental evidence of mRNA transfer from plant to fungal cells via EVs.

To examine if plant mRNAs transferred to *Botrytis cinerea* are being translated, the authors performed immunocapture of fungal ribosomes (TRAP-seq) using a fungal strain expressing the ribosome protein large subunit 23 with a yellow fluorescence protein (YFP) tag (*Bc*RPL23-YFP). This strain showed no obvious phenotypic differences to wild type *Botrytis cinerea.* The authors identified over 300 actively translated plant mRNA molecules in the fungus, including *SAG21*, *APS1*, *PRXIIC*, and *HEL*. Their full-length transcripts were only detected in immunopurified *Bc*RPL23-YFP from infected leaves. This demonstrates that

CellPress

Cell Host & Microbe
Previews

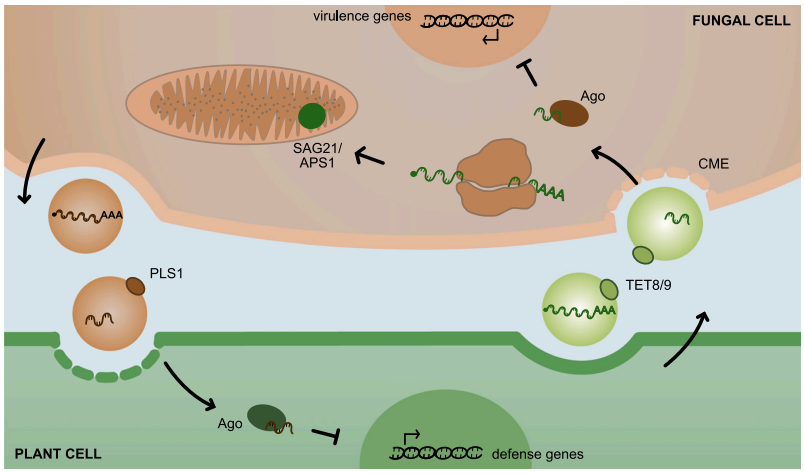

Figure 1. EV-mediated RNA transfer between plant and fungal cells

Plants secrete TET8/9-positive EVs, which contain sRNA and mRNA molecules. Clathrin-mediated endocytosis (CME) facilitates the uptake of sRNAs into fungal cells, to date reported for *Sclerotinia sclerotiorum*. Transferred plant sRNA molecules can be incorporated into the RNAi complex of fungi and lead to the silencing of virulence genes. Now Wang et al. show that plant mRNA molecules are transferred into cells of the fungus *Botrytis cinerea*. The transferred plant mRNAs are translated in the fungal cell. Many of these transcripts seem to have mitochondrial targets or localisation. Fungal EVs contain sRNA and mRNA molecules; punchless-1 (PLS1), fungal tetraspanin found at *B. cinerea* EVs.

transferred plant mRNAs are translated into proteins in the fungus.

Wang and co-workers noted many of the fungal translated plant mRNAs code for mitochondrial proteins. To test whether they influence the infection outcome, the authors analyzed the virulence of *Botrytis cinerea* ectopically expressing plant mRNA transcripts. Both *in vitro* growth and infection success in *Arabidopsis thaliana* were reduced in these strains. This indicates that expressed, exogenous plant transcripts can interfere with fungal life. Conversely, *Arabidopsis thaliana* mutants, in which the respective genes were deleted, were more susceptible to *Botrytis cinerea* infection.

Overall, Wang et al. have expanded our view on cross-kingdom RNA transfer (Figure 1): (1) Plants send mRNAs into fungal cells via EVs, (2) transferred plant mRNAs are then translated in the fungus, and (3) the translated proteins interfere with fungal growth. The authors not only identify a key mechanism in driving immunity but also characterize at least two mRNAs that comprise the infection success of *Botrytis cinerea*. A strength of this study is the combination of gene expression analysis, live-imaging techniques, the creation and use of genetically modified plant and fungal lines to understand RNA transfer at the plant-fungal interface.

This work now raises some intriguing questions: (1) Is cross-kingdom mRNA transfer bidirectional? There is evidence that fungal EVs contain intact, spliced, and poly(A)-tailed mRNAs.[9] (2) How are the transferred mRNAs selectively loaded into EVs? Loading of sRNA into TET8-positive EVs was shown to be partly dependent on EV-associated RNA-binding proteins (RBPs), including Argonaute 1, two annexins, and two RNA-helicases.[10] (3) Does cross-kingdom mRNA transfer also occur between plants and other microbes, including oomycetes and beneficial fungi? The discovery of cross-kingdom RNA transfer has led to the development of RNA-based crop protection strategies based on dsRNA-molecules.[6] Will we be able to trick pathogens into translating their own pesticide in the future by delivering it as an mRNA via nanoparticles?

DECLARATION OF INTERESTS

The authors declare no competing interests.

REFERENCES

1. Weiberg, A., Wang, M., Lin, F.M., Zhao, H., Zhang, Z., Kaloshian, I., Huang, H.D., and Jin, H. (2013). Fungal small RNAs suppress plant immunity by hijacking host RNA interference pathways. Science *342*, 118–123.

2. Kusch, S., Singh, M., Thieron, H., Spanu, P.D., and Panstruga, R. (2023). Site-specific analysis reveals candidate cross-kingdom small RNAs, tRNA and rRNA fragments, and signs of fungal RNA phasing in the barley-powdery mildew interaction. Mol. Plant Pathol. *24*, 570–587.

3. Wong-Bajracharya, J., Singan, V.R., Monti, R., Plett, K.L., Ng, V., Grigoriev, I.V., Martin, F.M., Anderson, I.C., and Plett, J.M. (2022). The ectomycorrhizal fungus *Pisolithus microcarpus* encodes a microRNA involved in cross-kingdom gene silencing during symbiosis. Proc. Natl. Acad. Sci. USA. *119*, e2103527119.

4. Dunker, F., Trutzenberg, A., Rothenpieler, J.S., Kuhn, S., Pröls, R., Schreiber, T., Tissier, A., Kemen, A., Kemen, E., Hückelhoven, R., and Weiberg, A. (2020). Oomycete small RNAs bind to the plant RNA-induced silencing complex for virulence. Elife *9*, e56096.

5. Ren, B., Wang, X., Duan, J., and Ma, J. (2019). Rhizobial tRNA-derived small RNAs are signal molecules regulating plant nodulation. Science (New York, N.Y.) *365*, 919–922.

6. Wang, M., Weiberg, A., Lin, F.M., Thomma, B.P.H.J., Huang, H.D., and Jin, H. (2016). Bidirectional cross-kingdom RNAi and fungal uptake of external RNAs confer plant protection. Nat. Plants *2*, 16151.

7. Wang, S., He, B., Wu, H., Cai, Q., Ramírez-Sánchez, O., Abreu-Goodger, C., Birch, P.R.J., and Jin, H. (2023). Plant mRNAs move into a fungal pathogen via extracellular vesicles to reduce infection. Cell Host Microbe *32*, 93–105.

8. Cai, Q., Halilovic, L., Shi, T., Chen, A., He, B., Wu, H., and Jin, H. (2023). Extracellular vesicles: cross-organismal RNA trafficking in plants, microbes, and mammalian cells. Extracell. Vesicles Circ. Nucl. Acids *4*, 262–282.

9. Kwon, S., Rupp, O., Brachmann, A., Blum, C.F., Kraege, A., Goesmann, A., and Feldbrügge, M. (2021). mRNA Inventory of Extracellular Vesicles from Ustilago maydis. J. Fungi *7*, 562.

10. He, B., Cai, Q., Qiao, L., Huang, C.Y., Wang, S., Miao, W., Ha, T., Wang, Y., and Jin, H. (2021). RNA-binding proteins contribute to small RNA loading in plant extracellular vesicles. Nat. Plants *7*, 342–352.

Appendix 3

Received: 12 June 2024 | Accepted: 24 November 2024

DOI: 10.1002/jev2.70022

PERSPECTIVE

Practical advice for extracellular vesicle isolation in plant–microbe interactions: Concerns, considerations, and conclusions

Hannah Thieron[1] | **Laura Krassini**[2] | **Seomun Kwon**[3] | **Sebastian Fricke**[4] | **Sabrine Nasfi**[5] | **Lorenz Oberkofler**[2] | **Alessa Ruf**[2] | **Julia Kehr**[4] | **Karl-Heinz Kogel**[5] | **Arne Weiberg**[2] | **Michael Feldbrügge**[3] | **Silke Robatzek**[2] | **Ralph Panstruga**[1]

[1]Unit for Plant Molecular Cell Biology, Institute for Biology I, RWTH Aachen University, Aachen, Germany

[2]LMU Munich Biocenter, Ludwig-Maximilian-University of Munich, Munich, Germany

[3]Institute for Microbiology, Cluster of Excellence on Plant Sciences, Heinrich-Heine University Düsseldorf, Düsseldorf, Germany

[4]Institute of Plant Science and Microbiology, Department of Biology, Universität Hamburg, Hamburg, Germany

[5]Institute of Phytopathology, Research Centre for BioSystems, Land Use and Nutrition, Justus-Liebig-University Giessen, Giessen, Germany

Correspondence
Ralph Panstruga, Unit for Plant Molecular Cell Biology, Institute for Biology I, RWTH Aachen University, Aachen, Germany.
Email: panstruga@bio1.rwth-aachen.de

Funding information
European Research Council, Grant/Award Number: 884235; Deutsche Forschungsgemeinschaft, Grant/Award Numbers: 433194101, SFB924/3TP15

Abstract

In recent years, extracellular vesicles (EVs) have emerged as novel key players in plant–microbe interactions. While it is immensely useful to draw on the established "minimal information for studies of extracellular vesicles" (MISEV) guidelines and precedents in mammalian systems, working with plants and their associated microbes poses specific challenges. To navigate researchers through these obstacles, we offer detailed step-by-step suggestions for those embarking on EV research in the context of plant–microbe interactions. The advice is based on recent publications and our collective experience from the diverse plant and microbe systems studied in a dedicated research consortium. We provide considerations for experimental design, optimization, quality control, and recommendations on how to increase yield, purity, and reproducibility of EV isolation. With this perspective article, we aim not only to assist researchers in our field but also to promote discussions on plant and microbe EVs in the broader EV community.

KEYWORDS

plant-microbe interactions, EV isolation, EV size profile, EV marker, EV quality control, biological fluid, axenic culture, apoplastic wash fluid

1 | BACKGROUND

Extracellular vesicles (EVs) are central mediators in inter-cellular and inter-organismal communication across diverse biological systems. These membranous structures can be generated and released via different cellular pathways and cell types to the extracellular space (Box 1; Colombo et al., 2014). In the interaction of plants with both pathogenic and beneficial microbes, EVs have garnered significant interest owing to their potential to modulate the relationship between both partners (Cai, Qiao, et al., 2018; Chalupowicz et al., 2023; Wang et al., 2016).

Hannah Thieron, Laura Krassini, and Seomun Kwon contributed equally to the study.

Particle types defined by the minimal information for studies of extracellular vesicles (MISEV) guideline and examples thereof from the field of plant–microbe interactions

Extracellular vesicles (EVs): "Particles that are released from cells, are delimited by a lipid bilayer, and cannot replicate on their own" (Welsh et al., 2024). Example: In samples derived from colonized plants, these can be of plant or microbe origin.
Non-vesicular extracellular particles (NVEPs): "Multimolecular assemblies that are released from cells and do not have a lipid bilayer (non-vesicular extracellular particle fraction" (Welsh et al., 2024). Example: If working with plant samples one might look out for RuBisCo complexes or lipoproteins. For samples originating from liquid cultures, particles from the medium might be contaminants.
Extracellular particles (EPs): "Umbrella term for all particles outside the cell, including EVs and NVEPs" (Welsh et al., 2024). Example: See above as for EVs and NVEPs.
EV mimetic: "EV-like particles that are produced through direct artificial manipulation" (Welsh et al., 2024). Example: Unintentionally generated vesicles derived from cell lysis, for example, by infiltration or centrifugation during apoplastic wash fluid (AWF) isolation.
Artificial cell-derived vesicles (ACDVs): "EV mimetics that are produced in the laboratory under conditions of induced cell disruption, such as extrusion" (Welsh et al., 2024). Example: In the plant field, vesicles sourced from juices or disrupted tissue have also been termed "plant-derived nanovesicles" (PDNVs; Pinedo et al., 2021).

Examples of known and suggested EV markers for plants and plant-colonizing microbes

Plants
- *Arabidopsis thaliana*: PENETRATION1 (PEN1) and PATELLIN1 (PATL1) (Rutter & Innes, 2017), TETRASPANIN8 (TET8) (Cai, Qiao, et al., 2018), EXOCYST COMPONENT OF 70 kDa PROTEIN E2 (EXO70E2) (Wang et al., 2010)
- *Sorghum bicolor*: *A. thaliana* PENETRATION (PEN1) orthologs (Chaya et al., 2024)

Phytopathogenic fungi
- *Botrytis cinerea*: PUNCHLESS1 (PLS1) (He et al., 2023)
- *Colletotrichum higginsianum*: Brain modulosignalin homolog1 (Bmh1) (Rutter et al., 2022)
- *Fusarium graminearum*: Suppressor of Rvs167 mutation (Sur7) (Garcia-Ceron et al., 2021)
- *Fusarium oxysporum* f.sp. *vasinfectum*: Heat shock protein of 70 kDa (Hsp70) (Bleackley et al., 2020)
- *Zymoseptoria tritici*: Suppressor of Rvs167 mutation (Sur7) (Hill & Solomon, 2020)

Phytopathogenic oomycetes
- *Phytophthora sojae*: TETRASPANIN1 (TET1), TETRASPANIN3 (TET3) (Zhu et al., 2023)

Phytopathogenic bacteria
- *Pseudomonas syringae* pv. *tomato* DC3000: Outer membrane protein F (OprF), Ampicillin C (AmpC) (Janda et al., 2023)
- *Xanthomonas oryzae*: ELONGATION FACTOR-Thermo unstable (EF-Tu) (Bahar et al., 2016)
- *Xylella fastidiosa*: Lipase/esterase A (LesA), Motility protein B (MopB) (Nascimento et al., 2016)

Research efforts discerning the composition of EV cargos of plants and associated microbes, at present, typically focus on proteins and various RNA classes, including small RNAs, messenger RNAs, long non-coding RNAs, circular RNAs, and fragments of transfer as well as ribosomal RNAs (Kusch et al., 2023; Kwon et al., 2021; Ruf et al., 2022; Wang et al., 2023). In particular, the bidirectional RNA exchange between plants and microbes has been suggested to tune the interaction in several systems (Cai, Qiao, et al., 2018; Cheng et al., 2023; Dunker et al., 2020; Wang et al., 2016; Weiberg et al., 2013; Wong-Bajracharya et al., 2022) and is serving as a blueprint for the development of novel types of pesticides (Cai, He, et al., 2018). Accordingly, there is an increasing interest in studying EVs and their cargos in the context of plant–microbe interactions, which necessitates suitable EV isolation protocols.

However, EV isolation procedures in plant, microbial, and mammalian systems vary due to differences in physiology (e.g., the presence/absence of a cell wall; Brown et al., 2015) and cultivation. The current lack of recommendations for experimental procedures and documentation standards regarding plant(-microbe) systems in the MISEV (minimal information for studies of extracellular vesicles) guideline hinders reproducibility and comparability across such studies (Welsh et al., 2024). Consequently,

the importance of well-documented and reproducible workflows cannot be overstated, serving as the foundation for robust scientific conclusions. Previous reviews have sought to address these issues for EV isolations from (healthy) plants (Pinedo et al., 2021; Rutter & Innes, 2020). Nonetheless, further refinements and tailored protocols specific to this field are urgently needed, especially for scientists studying plant–microbe interactions.

In this perspective article, we attempt to provide comprehensive support for the establishment and optimization of EV isolation procedures in the context of plant–microbe interactions. Drawing upon recent advancements and novel insights from first-hand experience gained in the context of a dedicated research consortium (Research Unit FOR5116 "exRNA" funded by the Deutsche Forschungsgemeinschaft [DFG]; https://www.biologie.uni-hamburg.de/en/forschung/forschungsverbuende/dfg-ru5116.html), we wish to supply researchers new to this burgeoning field with practical advice to master the complexities of EV isolation. These include hints regarding the cultivation of organisms and the retrieval of biological fluids for EV isolation, the actual EV isolation procedure, and measures for EV quality control. By this, we aim to empower scientists to elucidate the nuanced mechanisms governing potential cross-kingdom plant–microbe communication mediated by EVs or to discover novel potential colonization strategies enabled by EVs.

2 | CULTIVATION AND RETRIEVAL OF BIOLOGICAL FLUIDS FOR EV ISOLATION

Living cells can release EVs into their environment. Depending on the cell type and organism of interest, this environment can be very diverse in the plant–microbe field. Appropriate cultivation of the source organisms significantly influences the experimental EV isolation success. Isolation of EVs typically requires some kind of biological fluid as starting material, which is ideally fully devoid of cells and cellular debris. The latter is usually achieved through filtration (0.22 or 0.45 µm pore size) and low-speed centrifugation of EV-containing samples (reviewed in Pinedo et al., 2021; Rutter & Innes, 2020). Plant samples are typically centrifuged at 10,000 × *g* (Cai, He, et al. 2018; Cai, Qiao, et al., 2018; Regente et al., 2009; Rutter & Innes, 2017), fungal samples between 4000 × *g* and 15,000 × *g* (in some instances by two consecutive cleaning steps; Bleackley et al., 2020; Hill & Solomon, 2020; Kwon et al., 2021; Rutter et al., 2022), and bacterial samples between 4500 × *g* and 10,000 × *g* (Bahar et al., 2016; Janda et al., 2023; McMillan & Kuehn, 2023; Nascimento et al., 2016). In cases involving microbial or liquid plant cultures (e.g., plant cell suspension cultures, plant tissue cultures, or hydroponic systems), EVs can be directly isolated from culture supernatants (De Palma et al., 2020; Janda et al., 2023; Kocholata et al., 2022; Kwon et al., 2021). For whole plants grown in soil or other solid substrates (e.g., mineral composites such as vermiculite or solid media for in vitro cultivation), growth conditions need to be optimized to isolate apoplastic wash fluid (AWF)—a frequently used source for EV isolation from plants approximating the full repertoire of naturally secreted EVs. AWF is a liquid commonly obtained by infiltrating buffer into the intercellular space (apoplast) and subsequent centrifugation of the infiltrated plant specimens to collect the buffer along with (nano-)particles and molecules present in the apoplast (O'Leary et al., 2014).

2.1 | Plants

For plants grown on solid substrates, AWF can be isolated from entire seedlings or adult plants, isolated leaves, and potentially roots, as accomplished in many different plant species (Chen et al., 2022; Kusch et al., 2023; Regente et al., 2017; Rutter & Innes, 2017). Preceding growth conditions notably affect buffer infiltration. For instance, high humidity supports infiltration efficiency, because stomata are wide open (Chincinska, 2021; Rumyantseva et al., 2023). We, therefore, recommend increasing the humidity at least several hours before buffer infiltration by covering plants with a lid. However, it is crucial to note that adjusting humidity levels may alter plant gene expression and hence affect the interaction with any microbes under study (Yao et al., 2023).

Apart from AWF, EVs have also been isolated from the liquid medium of plant cell or tissue cultures (Boccia et al., 2022; Kocholata et al., 2022). On the one hand, this approach reduces potential contaminations due to cell damage through infiltration-centrifugation steps during AWF isolation, and a direct comparison could be used to identify these in AWF samples. On the other hand, plant liquid culture experiments neglect the systemic context and are restricted to systems for which the microbe of study can be co-cultivated. Hydroponic plant systems also offer the possibility to retrieve EVs from the medium but are not necessarily suitable for all types of plant–microbe interactions (De Palma et al., 2020).

Disruptive methods such as tissue blending are unsuitable for EV isolation due to associated contamination from cellular debris. This can lead to the generation of artificial cell-derived vesicles, EV mimetics, which in the plant field, have been termed "plant-derived nanovesicles" (Box 1; Pinedo et al., 2021). In general, the generation of such plant-derived nanovesicles is undesirable in the context of EV isolation. However, comparing their characteristics with those of EVs can support the existence of unique EV profiles. Depending on the plant species, obtaining sufficient AWF volume for EV isolation can be challenging. To enhance AWF yield, we suggest employing young(er) plants with soft(er) tissue and optimising buffer infiltration with an efficient vacuum pump (employed vacuum typically between 25 and 45 kPa; Figueir et al., 2018; Regente et al., 2008). Vacuum infiltration is followed by a very low-speed centrifugation step. Applied centrifugation forces range between 400 and 900 × *g* depending on

the plant species (Cai, Qiao, et al., 2018; Regente et al., 2008; Rutter & Innes, 2017). We do not recommend exceeding 900 × *g* unless a higher force is necessary to obtain the fluid (Lohaus et al., 2001). Further, customized growth conditions are proposed to find the best balance between plant age and leaf size—larger and younger leaves will yield more AWF than smaller or older leaves (Chen et al., 2022). Significant scale-up may be necessary for sufficient AWF (and thus EV) yield, especially when microbial EVs should be co-enriched. In cases where infiltration is aggravated due to high lignin content or cuticular waxes, one might consider using low amounts of a non-ionic detergent (e.g., Tween 20) in the infiltration buffer to break surface tension (Nouchi et al., 2012). If the EVs are stable, this treatment is unlikely to affect their integrity and might aid their stability during storage (van de Wakker et al., 2022). However, attention should be paid when performing measurements of the zeta potential (an indicator of particle surface charge) as it might be altered (Midekessa et al., 2020).

We further advise assessing cell viability of infiltrated plant tissue post-AWF isolation, for example, using trypan blue staining to visualize potential damage (e.g., dead cells; Mulaosmanovic et al., 2020) and/or inspect the retrieved AWF by microscopy for organelle debris potentially released because of cell injury during its isolation. At the molecular level, immunoblotting of AWF samples with antibodies targeting abundant intracellular proteins (e.g., of endomembrane or cytoplasmic origin, e.g., chloroplast components) should complement these efforts to validate proper AWF isolation. In principle, such cellular content could also result from organelle secretion, which has been described recently for animal cells (Suh & Lee, 2024). However, although we cannot exclude the possibility that certain plant species or cell types may secrete organelles, this has not been reported to the best of our knowledge. Hence, we consider any organelle debris detected in AWF samples rather a putative byproduct of the unavoidably harsh conditions of the isolation process. Recurring cytoplasmic contamination is often indicated by green (chlorophyll-based) coloration in the case of leaf-derived AWF. In such instances, we recommend streamlining the AWF isolation to minimize the damage to the plant material. This may include selecting an infiltration buffer that does not compromise cell integrity, as do high detergent or non-isotonic salt concentrations; opting for the lowest effective infiltration time; centrifuging as slowly and shortly as possible; and handling the plant samples with great care (avoid agitation and tissue damage). Special attention is warranted when working with plants infected by necrotrophic or hemibiotrophic pathogens, which cause cell damage and tissue lesions during pathogenesis. In these instances, AWF should be preferably collected at the early infection stage before necrotic lesions occur. The above-outlined methods can be used to confirm that pathogen growth has not yet compromised plant cell integrity.

2.2 | Culturable microorganisms

Several plant-associated microbes can be cultivated in vitro. While EVs from microbial axenic cultures (i.e., cultures in the absence of the plant) are most likely not equivalent to those produced during interaction with their plant hosts, the relative ease of handling and scalability are advantageous for an initial survey of EV characteristics and EV-associated molecules.

As outlined above for plants, the first step is choosing appropriate growth conditions since these can impact EV production and EV cargo (Jonca et al., 2021; McMillan & Kuehn, 2023; Welsh et al., 2024). It is further important to consider the microbial growth or developmental stage at the time point of EV isolation and any potential factor that may impinge on the physiology and cellular activities. EV biogenesis and the permeability of cellular barriers, such as the microbial cell wall, can vary greatly depending on the cellular morphology influenced by the growth conditions. Furthermore, the biological functions of EVs can differ depending on the microbial growth stage (Saad et al., 2024) and lifestyle (Johnston et al., 2023). The latter can be influenced by growing the microbes in liquid media or on agar plates for biofilm formation, and EVs can be isolated from both conditions (Janda et al., 2023). Multicellular growth forms such as bacterial biofilms or mycelia of fungi and oomycetes may increase the heterogeneity of EVs. For mycelia, EV diffusion into the medium can be hindered, for example, by the cell wall (Rutter et al., 2022). Because of the aforementioned variability, experimental details such as nutrient composition and pH of the culture medium, aeration/rotation, cultivation time, growth phase, and temperature should be well documented and reported to increase reproducibility (Welsh et al., 2024).

Opting for liquid culture over colonized plant materials is usually a compromise between relevance to the biological question and EV yield. In some systems, culture conditions can be adjusted to allow the microbial cells to simulate developmentally and transcriptionally certain stages of plant colonization, for example, by the addition of plant extracts or dedicated salts (Kwon et al., 2021; Li et al., 2022). Moreover, there are media known that resemble specific plant locations, such as the apoplast (Rico & Preston, 2008) or xylem (Hiery et al., 2013; Neumann & Dobinson, 2003), or that trigger virulence in phytobacteria (Wengelnik et al., 1996) or mimic symbiotic conditions (Li et al., 2022). It is helpful to understand, for example, based on existing transcriptomics or proteomics data, to what extent a given culture condition simulates the situation *in planta*. If -omics resources are limited for testing different conditions, one could use expression levels of hallmark genes for colonization that are specifically upregulated during certain infection stages as an indicator of whether the growth conditions mimic the *in planta* situation. We propose using defined media composition for microbial cultures instead of complex media with ill-defined components of natural origin, such as yeast extract, which may contain EV-like nanoparticles. Contamination from such components can be reduced by filtration or ultracentrifugation, similar to how blood sera are particle-depleted before their addition to mammalian cell cultures (Lehrich et al., 2021). The potential effect of this procedure on the growth of the microorganisms should be, however, assessed carefully.

If unavoidable, the unconditioned complex medium should be included in all experiments as an important negative control for comparison (Welsh et al., 2024).

Any optimization to increase the viability and the intactness of the EV-secreting microbes during culture and harvesting of conditioned media would reduce the contamination by EV mimetics (Box 1). In general, high cell viability (commonly ≥95%, certified by vital staining) at the time point of EV isolation is advised (Shekari et al., 2023). However, a compromise may be necessary to increase the EV yield. For example, starvation (Debbi et al., 2022) or cell wall stress (Olicón-Hernández et al., 2015) may increase the release of EV-like particles (Box 1). In some fungi, such as *Colletotrichum higginsianum*, it may be necessary to use cell wall-degrading enzymes to break apart the mycelium partially and to release EVs from the paramural space (Rutter et al., 2022). We recommend taking such steps with caution, because several studies have demonstrated that the vesicle cargo of some bacterial and fungal species is influenced by nutrient availability (Bahar et al., 2016; Dauros Hill & Solomon, 2020; Hong et al., 2019; McMillan & Kuehn, 2023; Singorenko et al., 2017). It must also be noted that many commercially available protoplasting enzyme preparations tend to be crude mixtures with additional proteinase and RNase activities and are often derived from fungi, which may confound any -omics analyses of fungal EVs. While such organism-specific treatments may be necessary to yield sufficient EV quantities, it is important to address the potential consequences on the cellular status, the occurrence of putative contaminants, and the biological relevance of the EVs obtained.

Prior to EV isolation, microbial cells must be removed from the culture medium. This can be achieved by centrifugation and/or filtration. Centrifugation time and force, as well as filtration pressure, should be reduced as much as possible to prevent cell lysis and minimize changes in cell physiology. At this point, defined aliquots of the cells should be snap-frozen for later comparison with the isolated EVs. This can be done by an immunoblot or gene expression analysis via quantitative reverse transcriptase-polymerase chain reaction (qRT-PCR), for example. To address any putative contamination of the EV preparations with living cells, it is suggested to introduce streak controls of the samples on a solid medium. These should take place instantly after the removal of microbial cells from the liquid culture and after obtaining the crude EV suspension. A quick quality control via microscopy and, optionally, organelle staining, would be beneficial to address contamination from dead or lysed cells before proceeding with EV isolation. It should be noted, though, that certain organisms may secrete organelles, similar to various animal cell types that recently have been reported to secrete mitochondria (Suh & Lee, 2024), which would render such organelles unsuitable as markers for cell lysis. If cellular, non-EV marker proteins are already known, an aliquot from each step in preparing the biological fluid and EV isolation can be tested for cellular contamination by immunoblotting.

3 | EV ISOLATION

Once the biological source fluid (e.g., AWF or culture medium) has been obtained and cleared of cellular material, EV isolation can proceed. The methods published for the isolation of EVs from plants, plant-colonizing microbes, and colonized plants include a combination of differential ultracentrifugation, ultrafiltration, size exclusion chromatography, and density gradient centrifugation (Bleackley et al., 2020; Cai, Qiao, et al., 2018; Janda et al., 2023; Kwon et al., 2021; Regente et al., 2017; Rutter & Innes, 2017). We encourage researchers to explore diverse methods used in the plant–microbe field, especially if generating sufficient quantities of biological source fluid is critical (Rutter et al., 2022). In these instances, scientists might consider a low specificity/high recovery approach such as a precipitation (polymer)-based method to obtain more EVs in the crude pellet (Welsh et al., 2024). For detailed considerations on designing a suitable differential ultracentrifugation protocol, we refer to the review by Rutter & Innes (2020). It should be noted that the appropriate procedure depends on the size and density of EVs of the targeted organism(s), which may differ between biological fluids obtained from uncolonized and colonized plants. Thus, centrifugation force and rotors should be selected with great care as this might influence the accumulation of different EV subclasses or even contaminants (Box 1), making it necessary to establish the ideal rotor type for the given system. Fixed angle rotors have a higher pelleting efficiency (lower k-factor) compared to swing-out rotors that hold equivalent sample tube volumes and, therefore, may be more suitable for obtaining the crude EV pellets from a larger volume of starting biological fluid, while swing-out rotors are essential for density gradients. For a detailed overview of the effect of rotor types on EV isolation, we refer the readers to a previous study (Cvjetkovic et al., 2014). Common centrifugation forces are between 40,000 and 100,000 × *g* in the case of plants and fungi (Bleackley et al., 2020; Cai, Qiao, et al., 2018; Hill & Solomon, 2020; Kwon et al., 2021; Regente et al., 2009; Rutter & Innes, 2017; Rutter et al., 2022), and between 31,000 and 150,000 × *g* in case of bacteria (Bahar et al., 2016; Janda et al., 2023; McMillan & Kuehn, 2023; Nascimento et al., 2016). In general, centrifugation time should be minimized as prolonged centrifugation time can lead to the accumulation of impurities (Box 1), cause artifacts, and might affect EV integrity (Cvjetkovic et al., 2014). Typical centrifugation times for an EV pelleting step (in some instances several runs are performed) are usually 60 min for plant AWF (Cai, Qiao, et al., 2018; Regente et al., 2009; Rutter & Innes, 2017), between 60 and 90 min for fungal cultures (Bleackley et al., 2020; Hill & Solomon, 2020; Kwon et al., 2021; Rutter et al., 2022), and between 90 and 180 min for bacterial cultures (Bahar et al., 2016; Janda et al., 2023; McMillan & Kuehn, 2023; Nascimento et al., 2016). Purification of crude EV pellets obtained by any of the abovementioned methods is recommended, particularly for explorative downstream analyses such as any -omics approaches and should exploit different physical and biochemical properties than the initial EV isolation procedure (Welsh et al., 2024).

A specific challenge when isolating EVs in the context of plant–microbe interactions is distinguishing between the EVs originating from the different organisms or even separating them physically. In the case of bacterial OMVs, researchers might benefit from recent advancements. For example, a fluorescent probe sensitive to outer membrane vesicles (OMVs) with aggregation-induced emission (AIE) characteristics that could aid in distinguishing between plant and bacterial EVs has been reported lately (Wang et al., 2023). Alternatively, the separation of OMVs from plant EVs in a mixture could, at some point, be facilitated by targeting bacterial lipopolysaccharides exploiting a secreted effector protein of the bacterial species *Cupriavidus necator* (Hofer, 2021). If technically possible, the separate characterization of plant- and microbe-derived EVs enables the assessment of changes that occur during plant colonization. This can be, for example, achieved by measuring the zeta potential, which in addition to EV size, can reveal differences in EV surface charge (see below; Janda et al., 2023). It is important to note that isolating EVs from the natural interaction site rather than from (co-)cultivated plants and microbes may allow for conclusions with higher biological relevance. Allocation of EV-associated molecules is possible if reference datasets are available for each organism, even when no specific EV markers (see below) have been identified yet. If desired, plant- and microbe-derived EVs may be separated by immunoaffinity capture or fluorescence-activated cell sorting (He et al., 2021; Kondratov et al., 2020). However, for these procedures, reliable EV biomarkers and suitable antibodies are required, which remain an exception for many species (as discussed below). Particularly for obligate biotrophic microbes, which cannot be cultivated without their host plant, the establishment of EV biomarkers would be highly desired to capture microbe-derived EVs from the colonized plant tissue.

4 | EV QUALITY CONTROL PARAMETERS

To characterize isolated particles and to verify if these are genuine EVs (see Box 1 for alternative particle categories), we recommend three types of analysis: (1) an estimation of EV particle size and concentration measurements, (2) visual inspection by electron microscopy, and (3) molecular analysis for the presence of EV biomarker proteins. In agreement with the MISEV guideline, we advise to use at least two of these independent yet complementing methods (Théry et al., 2018; Welsh et al., 2024).

4.1 | EV size profiles and concentration

Common single particle-based methods to analyse the size and concentration of nanoparticles in plant EV samples are nanoparticle tracking analysis (NTA) and dynamic light scattering (Welsh et al., 2024). To measure the sample concentration, NTA is a popular method since besides the concentration, it determines the size profile and, depending on the manufacturer, the zeta potential, which represents the overall electric charge of the EV's surface (Varga et al., 2020; Welsh et al., 2024). Both, changes in the zeta potential and the size profile in EV samples derived from infected plants as compared to uncolonized plants and microbial EVs can be a hint for the co-presence of plant and microbial EVs (Janda et al., 2023). Nonetheless, NTA does not distinguish between EVs and other spherical particles (Box 1) such as bigger protein complexes. Further, the concentration of smaller particles such as EVs in polydisperse samples might be underrepresented due to the intense light scattering of larger particles, preventing smaller particles from being tracked (Filipe et al., 2010). Newer NTA generations include lasers to detect EV particles via a fluorescence light detector. If available, measuring EVs with fluorescently labelled biomarkers (see below) or staining of EVs with lipophilic dyes or probes prior to the measurement can enable a more precise estimation of the EV size profile and concentration, as fewer non-EV or non-lipid contaminants, respectively, will be measured. However, it is crucial to include appropriate controls, such as buffer only, to demonstrate that unbound dye has been removed from the sample. Of note, the binding of antibodies or the intercalation of membrane dyes could lead to a distortion of the actual particle size (Varga et al., 2020). One also has to consider that NTA and dynamic light scattering measure, in fact, the hydrodynamic diameter and provide an overestimation of the actual EV diameter, which has to be taken into account when comparing it with size estimates from electron micrographs (Varga et al., 2020). We, therefore, encourage researchers to explore also advanced single-particle analysers (e.g. nanoflow cytometry or microfluidic resistive pulse sensing) that at present are not commonly used in the field.

The EV quantity can also be derived based on the total lipid, protein, or nucleic acid content (Bahar et al., 2016; McMillan & Kuehn, 2023; McMillan et al., 2021). For protein concentration measurements, commonly used methods are the Bradford assay or staining with bicinchoninic acid (BCA). However, the respective substances also react with reducing sugars and phospholipids and do not discriminate contaminants from EVs (Théry et al., 2018). The total lipid content is typically quantified by staining EVs with lipid dyes such as FM4-64, DiOC6, and DiR, followed by fluorescence intensity measurements (Rutter & Innes, 2017). Some dyes stain nucleic acids, such as RiboGreen, or the RNA dye SYTOTM RNASelectTM (Fortunato et al., 2021). While the single-particle-based techniques can give further information on different EV (sub-)populations by measuring size, such differences cannot be revealed by quantifying total lipid, nucleic acid, or protein concentrations (Welsh et al., 2024).

4.2 | Morphology

Electron microscopic techniques are the method of choice to characterize the morphological features of EVs. In addition, electron microscopy can provide information about the purity of EV samples and the potential occurrence of different EV (sub-)populations (Bahar et al., 2016; Janda et al., 2023; McMillan et al., 2021; Rutter & Innes, 2017). Currently, the most precise albeit tedious approach is cryo-electron microscopy (Chernyshev et al., 2015; Skliar et al., 2018). Other frequently used electron microscopic techniques like transmission or scanning electron microscopy will underestimate the diameter of EVs as these will desiccate in the process of sample preparation (Bachurski et al., 2019; Chuo et al., 2018). In transmission electron micrographs, EVs typically appear as cup-shaped structures (Panagopoulou et al., 2020; Rutter et al., 2020), whereas in scanning electron micrographs, EVs are usually spherical blebs (Chernyshev et al., 2015; Janda et al., 2023). Attention should be given when the electron micrographs reveal impurities such as flagellar structures when working with bacterial EVs (Janda et al., 2023) or organellar structures when working with plant or fungal samples as they are indicators of impurities. These contaminants can have severe effects on any downstream experiments and it might be necessary to optimize the purification process before proceeding with further analyses.

4.3 | EV biomarkers and molecular cargo

There are ongoing efforts to establish suitable EV markers in the plant(-microbe) field. EV biomarkers are molecules (in particular proteins) that are characteristic of EVs or EV sub-types of a given organism (Welsh et al., 2024). They can significantly improve the EV quality and quantity assessment, might allow for EV purification via immunoaffinity capture, and increase the portfolio for experimental downstream analyses (He et al., 2021). We encourage following the MISEV guidelines regarding the recommendation to establish at least two different positive EV biomarkers. Ideally, one of these should be an integral membrane or glycosylphosphatidylinositol (GPI)-anchored protein (or outer membrane for Gram-negative bacteria) and the other a cytosolic (or periplasmic for Gram-negative bacteria) protein with lipid- or membrane protein-binding ability. It is advised to establish additionally one negative marker, which could be a common co-isolated contaminant, for example, a constituent of non-vesicular extracellular particles (Théry et al., 2018; Box 1). Moreover, a proper EV biomarker should be abundant in the EV fractions for easy and reliable detection.

For finding organism-specific EV markers, there is a benefit in using organisms that can be grown in liquid culture, as EVs are obtained from a single species and it is easier to avoid contaminations from lysed cells due to handling. For obligate parasites or symbionts, the mixture of EVs obtained and the potential homology of proteins and nucleic acids in mixed samples may complicate the analyses. A first step to establish a new EV biomarker might be a proteomic survey, which can provide a list of candidate proteins. Such data can be used to select candidates that show potential relevance for plant–microbe interactions (e.g., association of a protein with a nucleic acid of interest; Cai, Qiao, et al., 2018), or that have homology to established marker proteins in other biological systems. Currently, there are only a handful of commonly tested EV markers in the field, including a homolog of human tetraspanin CD63 in the dicotyledonous reference plant *Arabidopsis thaliana* (TET8; Cai, He, et al., 2018; Cai, Qiao, et al., 2018; Box 2). Orthologs of well-established mammalian EV markers such as tetraspanins are absent in certain fungi and bacteria, but other biomarker proteins have been suggested for these organisms (Box 2). Larger collections of EV proteomics data such as Vesiclepedia or EVpedia (Chitti et al., 2024; Kim et al., 2015), which also include established EV biomarkers, can help deciding which candidate protein(s) to select.

If specific antibodies are available or epitope-tagged protein variants can be expressed, the candidate list can be further narrowed down based on protease protection or immunoaffinity capture assays to gain information on which proteins are rather inside the EV lumen than only loosely associated with the EV surface (forming the so-called EV corona; Heidarzadeh et al., 2023). Particularly useful would be an EV-associated integral membrane protein with both an "extracellular" and "cytosolic" terminus. These termini could be labelled by genetic engineering with a reporter tag on the luminal side (e.g., for EV quantification) and with an epitope tag on the extra-vesicular side (e.g. for immunoaffinity capture). However, such an approach requires the genetic manipulation of the organism(s) of interest to express labelled EV markers, which is not always possible.

Protease protection assays are commonly used to determine the localization of EV-associated proteins. They are based on the proteolytic digestion of EV-associated proteins in the presence or the absence of an EV-disrupting detergent (Cvjetkovic et al., 2016). A typical protease protection assay would include EVs treated with buffer-only, protease-only, detergent-only, and protease with detergent. Harsh protease treatments may compromise the integrity of EVs and could lead to false results where even intraluminal proteins are degraded (Foers et al., 2018). Therefore, we highly recommend including the detergent-only control. If, for example, luminescence originating from EVs with luciferase-tagged intraluminal proteins increases with the detergent-only control but disappears upon protease treatment, the protease concentration should be reduced (Bonsergent et al., 2021). If there is already evidence suggesting that the protein of interest is a cargo, a less invasive alternative to determine the localization might

be immunoaffinity capture or immunogold labelling. However, EVs will only be able to bind to the solid phase or be markable if the epitope for the antibody is present on the outside of the EV.

A similar approach could be used for EV-associated nucleic acids (nuclease protection assay). Many EV-associated nucleic acids are protected by proteins (He et al., 2021). Hence, addition of a protease might be necessary in addition to the nuclease to access the nucleic acid for digestion (Zand Karimi et al., 2022). This setup increases the complexity of required controls further. Protease and nuclease treatments should be carried out on fresh EVs and may require a washing step to remove the respective hydrolytic enzyme sufficiently. Therefore, these would be performed immediately after obtaining a crude EV preparation, before further purification. As some proteins can be associated with the EV corona but still be relevant for the plant–microbe interaction, it may be important to optimize protease treatment to suit the biological question at hand. If it is not possible to generate transgenic organisms that express tagged EV markers, surface labelling with membrane-impermeant biotinylation reagents may help distinguishing internal and external cargo (Cvjetkovic et al., 2016).

4.4 | Controls

Stepwise quality checks are necessary during optimization and troubleshooting of an EV isolation protocol. The effect of altering each step in the protocol should be assessed by the above-mentioned approaches. While this may be a tedious process, it is necessary for maximising the EV yield (as opposed to other EV-like particles, Box 1), assessing suitable storage conditions, or decreasing intracellular and other contaminants. During initial method establishment and troubleshooting for sources of contamination, it is useful to include the liquid medium (if any), buffers, or even filtered distilled water as negative controls to determine the extent of nanoparticle contamination derived from the materials, equipment, and handling. It is further important to assess for contaminants following the removal of cells from the medium or AWF, and also after subsequent centrifugation or filtration steps. If ultracentrifugation is used to pellet EVs, then it may be informative to examine the supernatant for EVs, especially if the EV pellet is loose or difficult to see. It is not uncommon to deal with EV pellets that are not visible to the naked eye. If ultrafiltration is used to concentrate the samples, it is worth testing for EVs bound to the membrane or eluting with the filtrate. The same ideas apply to immunoaffinity capture, where one would compare the input crude EVs, the supernatant after each wash step, the eluate, and the beads after elution.

In the mammalian field, EVs are typically stored for longer periods at −80°C; however, preserving EV integrity during storage remains a matter of debate (Görgens et al., 2022). Similarly, experience within the Research Unit FOR5116 has revealed that the suitability for EV storage greatly depends on the source organism and is generally improved when so-called low-bind tubes are used (Evtushenko et al., 2020). We recommend initially comparing stored EVs that have undergone freeze-thawing and fresh EVs for their intactness (e.g., by transmission electron microscopy or NTA), content (e.g., by Bioanalyzer-based nucleic acid profiling), and biological activity (e.g., by enzymatic or other functional assays). EV storage conditions are dependent on the purpose and the biological question at hand. Generally, measurements of morphology, biophysical size and concentration, for example, by NTA or electron microscopy, should be performed with fresh EVs, which we propose to store short-term (e.g., overnight) at 4°C with gentle rotation, if necessary. However, it may be possible to snap-freeze freshly prepared EV samples for subsequent protein and nucleic acid analyses, for example, in case it is challenging to extract EV content on the same day that the EVs are obtained. Ideally, freshly prepared EVs are directly used for protein or nucleic acid extraction up to a point where the samples are safe for storage.

5 | CONCLUDING REMARKS

Here we present a practical proposal for establishing EV work in the field of plant–microbe interactions (see Figure 1 for a proposed workflow and Table 1 for a synopsis of questions and recommendations). While the existing MISEV guidelines and resources from the mammalian field are highly informative, the diversity and complexity of our systems, comprising two interacting organisms, present specific challenges. There are no one-size-fits-all solutions for striking a balance between sufficient EV yield and purity and identifying specific molecular markers. We encourage scientists to be creative to bypass these obstacles. At the same time, adapting protocols to the EV research in the context of plant–microbe interactions, the thorough use of controls, and precise documentation are essential for creating new field-specific standards. An open exchange of challenges and solutions can help the plant–microbe EV field to grow in the future.

AUTHOR CONTRIBUTIONS

Hannah Thieron: Conceptualization (equal); visualization (lead); writing—original draft (equal); writing—review and editing (equal). **Laura Krassini**: Conceptualization (equal); writing—original draft (equal); writing—review and editing (equal). **Seomun Kwon**: Conceptualization (equal); writing—original draft (equal); writing—review and editing (equal). **Sebastian Fricke**: Conceptualization (supporting); writing—review and editing (supporting). **Sabrine Nasfi**: Conceptualization (supporting);

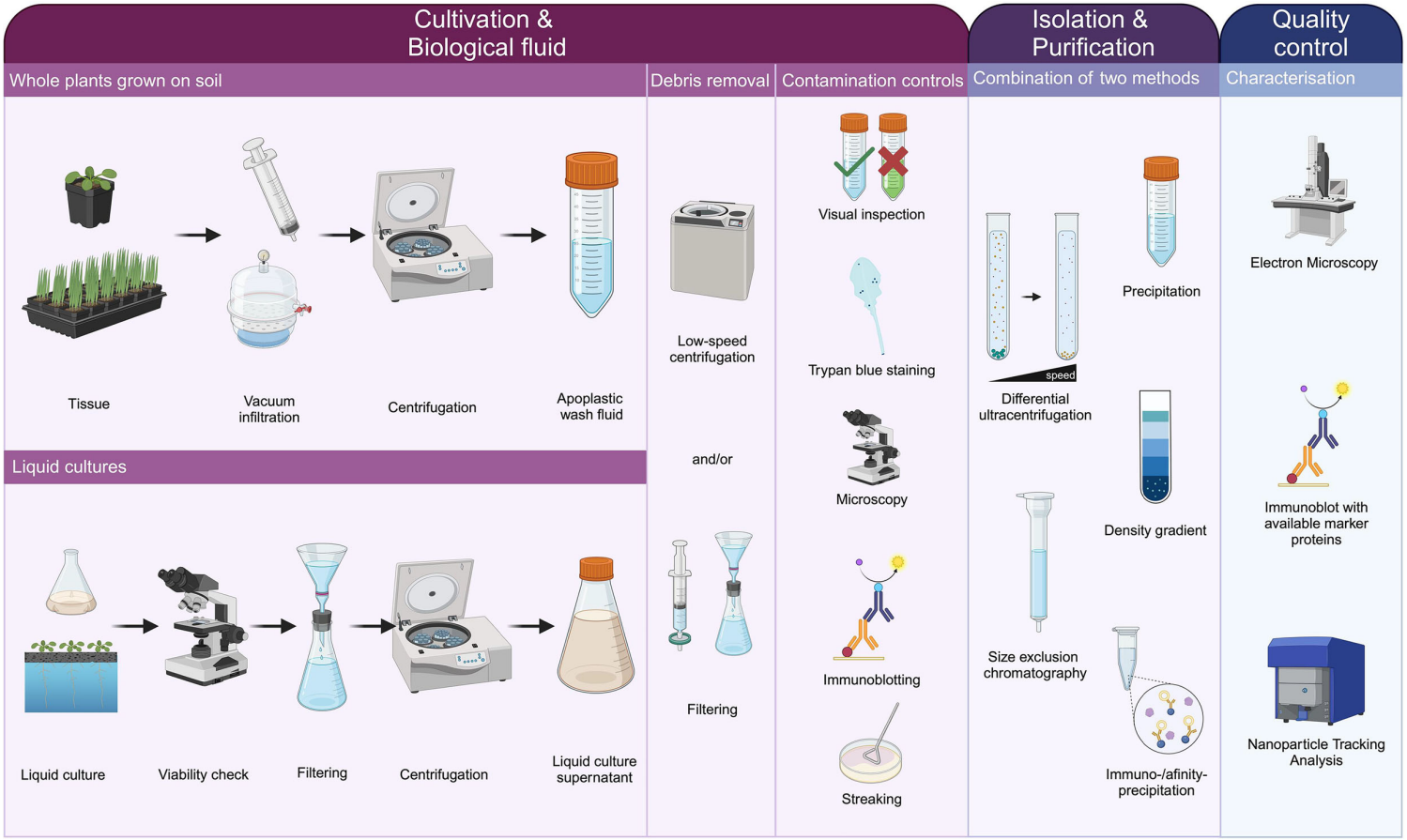

FIGURE 1 A workflow for designing EV isolation procedures from different sources in plant–microbe systems. The growth conditions of the source organism and the research question determine the downstream workflow for EV isolation. Cultivation and biological fluid: For plants grown on soil, the biological fluid, AWF, is commonly obtained by vacuum infiltration followed by very low-speed centrifugation. Removal of cellular debris involves low-speed centrifugation and filtering. Contamination controls for the tissue include visual inspection of the AWF colour (if applicable), viability stains (e.g., trypan blue), microscopy for organelle debris, and immunoblotting targeting intracellular proteins. When organisms are grown in liquid culture (e.g., microbes, plant cell cultures, hydroponic systems), the culture supernatant or medium serves as the biological fluid. For cell cultures, viability checks of source cells before harvesting the supernatant are advised. Removal of intact cells and larger debris involves filtering and centrifugation, followed by another step of low-speed centrifugation and/or filtering for cell debris. Controls for contamination with live cells or cell debris are microscopy, immunoblotting with known non-EV markers, and streaking of the cell-free culture supernatant, where applicable. Isolation and purification of EVs can be achieved by precipitation via polymers, differential ultracentrifugation, density gradient centrifugation, size exclusion chromatography, or immuno-/affinity-purification. Details may vary based on research questions and the manageability of obtaining biological fluid. We refer to the MISEV 2023 guidelines for a detailed register of pros and cons for the different approaches (Welsh et al., 2024). Working with crude EV samples is acceptable for pilot studies, but purification with a second method exploiting different physical and biological properties should be performed for thorough examination. Quality control and initial characterization of isolated (and purified) EVs largely overlap. Two independent methods are recommended for EV characterization, with regular quality control suggested. Electron microscopy confirms the presence of typical structures, and nanoparticle tracking validates consistent particle size isolation, both independent of knowledge about biomarkers. If available, EVs can be tested for the presence of suitable marker proteins by immunoblotting. When EVs are isolated from unicellular organisms, streaking of the EV pellet aids in corroborating that no replicating entities are present. Created with BioRender.com. AWF, apoplastic wash fluid; EV, extracellular vesicles; MISEV, minimal information for studies of extracellular vesicles.

Appendix 3

TABLE 1 Synopsis of questions and recommendations for EV isolation in plant–microbe interactions.

Question	Recommendation	Sample type	Reference
1) Cultivation			
a) How to obtain microbial EVs from axenic cultures that are biologically relevant for plant–microbe interactions?	- Try different media mimicking *in planta* conditions. *e.g., apoplast or xylem* - Compare the transcriptome and proteome of cultured cells to those from colonised plant material to determine how representative the cultures are. *e.g., are the so-called "plant-specific" genes, or those important for plant colonization up-regulated? Are the developmental stage, morphology, and physiology of the cultured cells matching the colonization stage of interest?*	Liquid culture	(Hiery et al., 2013; Jonca et al., 2021; Kwon et al., 2021; Li et al., 2022; McMillan & Kuehn, 2023; Rico & Preston, 2008; Wengelnik et al., 1996)
b) How to cultivate my organism for good EV yield?	- Scale up *It may be too laborious to harvest the biological fluid, isolate the EVs, and perform quality controls and extractions on the same day. To determine a stopping point, test for stability of the biological material from suitable steps in the procedure, when stored*, e.g., *biological fluid, EV pellet, or suspension*	All	–
	- Adjust conditions to open stomata to improve infiltration *e.g., humidity or light conditions* - Use younger plants	Plants grown on soil	(Chincinska, 2021; Nouchi et al., 2012; Rumyantseva et al., 2023)
	- Optimise conditions for cultivation *e.g., rich vs. minimal medium, pH etc.* - Increase surface area exposed to medium e.g., smaller mycelial clumps for fungi - Degrade the cell wall to release paramural vesicles *Stress conditions may increase vesiculation but can compromise the biological relevance of the EV cargos*	Liquid culture	(McMillan & Kuehn, 2023; Rutter et al., 2022)
c) How to choose the right cultivation time?	- Perform vesicle isolation in a time series to check for EV yield and relevant EV cargos if known - Check for cell viability by staining (ideally ≥95%; see below)	Liquid culture	(Janda et al., 2023; Shekari et al., 2023)
2) Obtaining biological fluid and EV isolation			
a) How to increase apoplastic fluid yield?	- Optimise vacuum pressure for infiltration - Optimise centrifugation time and force *The goal is to find a balance between infiltration/extraction efficiency and cell integrity (see 2b)* - Use surfactants to decrease the leaf hydrophobicity *Should only be considered in extreme cases when no AWF can be obtained otherwise* - Use more plants	Plants grown on soil	RU5116 (own experience) (Nouchi et al., 2012)
b) How and when to check for contamination with cells/cell debris?	- Immunoblotting with antibodies directed against endomembrane/cytoplasmic contaminants - Perform (light) microscopy (check for organelle contamination) *Consider the possibility of bona fide secretion of organelles, especially for organisms other than plants*	All	(Delaunois et al., 2013)
	After infiltration/centrifugation: - Green AWF and pellets indicate cell lysis - Trypan blue staining	Plants grown on soil	(Mulaosmanovic et al., 2020) RU5116 (own experience)
	- Viability staining (e.g., propidium iodide) staining of cultures just prior to EV isolation (ideally ≥95% viable) - Check via microscopy: - Cell morphology and signs of lysis before and after removing them from culture supernatant - Cell-free culture supernatant for carried over cells and debris - Streak cell-free culture supernatant and EV suspension on agar plate to check for contamination with living cells *It is possible to work as sterile as possible under the clean bench, with sterile filtered solutions and sterilised ultracentrifuge tubes*	Liquid culture	RU5116 (own experience) (Janda et al., 2023; Shekari et al., 2023)

(Continues)

Appendix 3

TABLE 1 (Continued)

2) Obtaining biological fluid and EV isolation			
c) How to reduce contamination from cell lysis?	- Settle with the lowest possible time for infiltration; find a balance between yield and purity (see above) - Handle the leaves with great care when blotting dry and otherwise - Choose infiltration buffer that does not compromise cell integrity	Plants grown on soil	(O'Leary et al., 2014)
	- Minimise centrifugation force and time - Apply gentle vacuum when filtering	All	RU5116 (own experience)
d) How to determine which EV subpopulations are relevant for my biological question?	- Further purify and fractionate crude EV preparation according to their biophysical properties or known markers, e.g., size exclusion chromatography, density gradients, immunoaffinity capture, fluorescence-activated cell sorting, or advanced single-particle analysers - Check resulting fractions for molecules of interest	All	(Bleackley et al., 2020; Cai, Qiao, et al., 2018; Garcia-Ceron et al., 2021; Rutter & Innes, 2017)
e) What is the best ultracentrifugation force/duration for isolating my vesicles?	- Dependent on the size and density of the EVs, of the organism(s), and of the density of the used media/buffer - Different pellets have to be compared if not much is known about the organism - Centrifuge as short as possible	All	(Rutter & Innes, 2020)
f) How to distinguish between plant vesicles and microbe vesicles?	- Take advantage of specific plant and microbial vesicle markers if available - Comparison of properties from EVs isolated from microbe, plant, and colonised plant	All	(Janda et al., 2023)
3) Quality check			
a) How to determine if a protein or nucleic acid of interest is EV cargo?	- Carry out immunoaffinity capture assay - Carry out nuclease or protease protection assays: - Check if luminal cargo is removed after treatment with detergent (Triton X-100 etc.) and hydrolytic enzyme (e.g., protease or nuclease) *One might check for sufficient EV disruption under the electron microscope*	All	(Bonsergent et al., 2021; Huang et al., 2021; Kwon et al., 2021; Zand Karimi et al., 2022)
b) How to identify the correct storage conditions?	- Check EVs in NTA/transmission electron microscopy for aggregate formation - Perform immunoblot analysis with antibodies directed against intraluminal cargo *Protein integrity is used as a proxy for EV integrity* - Perform immunoaffinity capture *Signal intensity in subsequent immunoblot analysis should decrease if EVs were disrupted and membrane fragments fused in random orientation* - Use low-bind tubes - Some EVs cannot be frozen *In some cases, freezing can have a negative effect on the properties of the EVs. In these cases, short-term storage of the EVs at 4°C with slight rotation can be considered.*	All	FOR5116 (own experience) (Evtushenko et al., 2020; Görgens et al., 2022)
c) How to differentiate EVs from other particles?	- Perform NTA (size profile and zeta potential) - Stain with a lipophilic dye (e.g., FM4-64, DiOC6, DiR) - Transmission electron microscopy (TEM) - Comparison of the results obtained using the above methods with literature - Use of advanced single-particle analysers such as nanoflow cytometry or microfluidic resistive pulse sensing *Try to compare recorded EV properties with the ones of closely related species or universal EV properties where applicable, e.g., NTA size profiles and zeta potentials or cup-shaped structures in TEM micrographs, respectively. Consider testing differing experimental conditions until the ideal cultivation/isolation procedure is found.*	All	(Welsh et al., 2024)

Abbreviation: EV, extracellular vesicles.

writing—review and editing (supporting). **Lorenz Oberkofler**: Conceptualization (supporting); writing—review and editing (supporting). **Alessa Ruf**: Conceptualization (supporting); writing—review and editing (supporting). **Julia Kehr**: Funding acquisition (equal); supervision (equal); writing—review and editing (supporting). **Karl-Heinz Kogel**: Funding acquisition (equal); supervision (equal); writing—review and editing (supporting). **Arne Weiberg**: Funding acquisition (equal); supervision (equal); writing—review and editing (equal). **Michael Feldbrügge**: Funding acquisition (equal); supervision (equal); writing—review and editing (supporting). **Silke Robatzek**: Funding acquisition (equal); supervision (equal); writing—review and editing (support-

ing). **Ralph Panstruga**: Conceptualization (supporting); funding acquisition (equal); project administration (lead); supervision (lead); writing—review and editing (lead).

ACKNOWLEDGEMENTS

We appreciate the usage of BioRender (https://www.biorender.com/) to create Figure 1. This work was enabled by grants within the research unit FOR5116 "exRNA" funded by the Deutsche Forschungsgemeinschaft (DFG; project number 433194101). Individual grants of this research unit comprise FE 448/15-1 to M.F., KE 856/8-1 to J.K., KO 1208/30-1 to K.-H.K., PA 861/22-1 to R.P., RO 3550/16-1 to S.R., and WE 5707/2-1 to A.W.). Work in the lab of S.R. in the context of this article was further funded by a project within the DFG-funded Collaborative Research Centre SFB924 "Yield" (SFB924/3TP15) and the Advanced Grant "MultiX" (grant number 884235) of the European Research Council (ERC). S.N. was supported by a Dr. Ernst-Leopold Klipstein Foundation scholarship.

Open access funding enabled and organized by Projekt DEAL.

CONFLICT OF INTEREST STATEMENT

The authors declare no conflicts of interests.

DATA AVAILABILITY STATEMENT

Data sharing not applicable to this article as no datasets were generated or analysed during the current study.

ORCID

Hannah Thieron https://orcid.org/0000-0002-0670-7328
Laura Krassini https://orcid.org/0009-0005-7613-910X
Seomun Kwon https://orcid.org/0000-0002-0514-1465
Sebastian Fricke https://orcid.org/0009-0004-0859-4437
Sabrine Nasfi https://orcid.org/0000-0001-5916-0824
Lorenz Oberkofler https://orcid.org/0000-0002-9506-2751
Alessa Ruf https://orcid.org/0000-0003-0919-9717
Julia Kehr https://orcid.org/0000-0003-3617-9981
Karl-Heinz Kogel https://orcid.org/0000-0003-1226-003X
Arne Weiberg https://orcid.org/0000-0003-4300-4864
Michael Feldbrügge https://orcid.org/0000-0003-0046-983X
Silke Robatzek https://orcid.org/0000-0002-9788-322X
Ralph Panstruga https://orcid.org/0000-0002-3756-8957

REFERENCES

Bachurski, D., Schuldner, M., Nguyen, P.-H., Malz, A., Reiners, K. S., Grenzi, P. C., Babatz, F., Schauss, A. C., Hansen, H. P., Hallek, M., & Pogge von Strandmann, E. (2019). Extracellular vesicle measurements with nanoparticle tracking analysis—An accuracy and repeatability comparison between NanoSight NS300 and ZetaView. *Journal of Extracellular Vesicles*, *8*, 1596016. https://doi.org/10.1080/20013078.2019.1596016

Bahar, O., Mordukhovich, G., Luu, D. D., Schwessinger, B., Daudi, A., Jehle, A. K., Felix, G., & Ronald, P. C. (2016). Bacterial outer membrane vesicles induce plant immune responses. *Molecular Plant-Microbe Interactions*, *29*(5), 374–384. https://doi.org/10.1094/MPMI-12-15-0270-R

Bitto, N. J., Petrovski, S., Hill, A. F., & Kaparakis-Liaskos, M. (2023). Planktonic and biofilm-derived *Pseudomonas aeruginosa* outer membrane vesicles facilitate horizontal gene transfer of plasmid DNA. *Microbiology Spectrum*, *11*, e05179–e05122. https://doi.org/10.1128/spectrum.05179-22

Bleackley, M. R., Samuel, M., Garcia-Ceron, D., McKenna, J. A., Lowe, R. G. T., Pathan, M., Zhao, K., Ang, C. S., Mathivanan, S., & Anderson, M. A. (2020). Extracellular vesicles from the cotton pathogen *Fusarium oxysporum* f. sp. *vasinfectum* induce a phytotoxic response in plants. *Frontiers in Plant Science*, *10*, 1610. https://doi.org/10.3389/fpls.2019.01610

Boccia, E., Alfieri, M., Belvedere, R., Santoro, V., Colella, M., Del Gaudio, P., Moros, M., Dal Piaz, F., Petrella, A., Leone, A., & Ambrosone, A. (2022). Plant hairy roots for the production of extracellular vesicles with antitumor bioactivity. *Communications Biology*, *5*(1), 848. https://doi.org/10.1038/s42003-022-03781-3

Bonsergent, E., Grisard, E., Buchrieser, J., Schwartz, O., Théry, C., & Lavieu, G. (2021). Quantitative characterization of extracellular vesicle uptake and content delivery within mammalian cells. *Nature Communications*, *12*, 1864. https://doi.org/10.1038/s41467-021-22126-y

Brown, L., Wolf, J. M., Prados-Rosales, R., & Casadevall, A. (2015). Through the wall: Extracellular vesicles in Gram-positive bacteria, mycobacteria and fungi. *Nature Reviews Microbiology*, *13*(10), 620–630. https://doi.org/10.1038/nrmicro3480

Cai, Q., He, B., Kogel, K. H., & Jin, H. (2018a). Cross-kingdom RNA trafficking and environmental RNAi — nature's blueprint for modern crop protection strategies. *Current Opinion in Microbiology*, *46*, 58–64. https://doi.org/10.1016/j.mib.2018.02.003

Cai, Q., Qiao, L., Wang, M., He, B., Lin, F., Palmquist, J., & Jin, H. (2018b). Plants send small RNAs in extracellular vesicles to fungal pathogen to silence virulence genes. *Science*, *360*(6393), 1126–1129. https://doi.org/10.1126/science.aar4142

Chalupowicz, L., Mordukhovich, G., Assoline, N., Katsir, L., Sela, N., & Bahar, O. (2023). Bacterial outer membrane vesicles induce a transcriptional shift in arabidopsis towards immune system activation leading to suppression of pathogen growth in planta. *Journal of Extracellular Vesicles*, *12*(1), 12285. https://doi.org/10.1002/jev2.12285

Chaya, T., Banerjee, A., Rutter, B. D., Adekanye, D., Ross, J., Hu, G., Innes, R. W., & Caplan, J. L. (2024). The extracellular vesicle proteomes of *Sorghum bicolor* and *Arabidopsis thaliana* are partially conserved. *Plant Physiology*, *194*(3), 1481–1497. https://doi.org/10.1093/plphys/kiad644

Chen, A., He, B., & Jin, H. (2022). Isolation of extracellular vesicles from arabidopsis. *Current Protocols*, *2*(1), e352. https://doi.org/10.1002/cpz1.352

Appendix 3

Cheng, A. P., Lederer, B., Oberkofler, L., Huang, L., Johnson, N. R., Platten, F., Dunker, F., Tisserant, C., & Weiberg, A. (2023). A fungal RNA-dependent RNA polymerase is a novel player in plant infection and cross-kingdom RNA interference. *PLoS Pathogens*, *19*(12), e1011885. https://doi.org/10.1371/journal.ppat.1011885

Chernyshev, V. S., Rachamadugu, R., Tseng, Y. H., Belnap, D. M., Jia, Y., Branch, K. J., Butterfield, A. E., Pease, L. F., Bernard, P. S., & Skliar, M. (2015). Size and shape characterization of hydrated and desiccated exosomes. *Analytical and Bioanalytical Chemistry*, *407*(12), 3285–3301. https://doi.org/10.1007/s00216-015-8535-3

Chincinska, I. A. (2021). Leaf infiltration in plant science: Old method, new possibilities. *Plant Methods*, *17*(1), 83. https://doi.org/10.1186/s13007-021-00782-x</./bib>

Chitti, S. V., Gummadi, S., Kang, T., Shahi, S., Marzan, A. L., Neveda, C., Sanwlani, R., Bramich, K., Stewart, S., Petrovska, M., Sen, B., Ozkan, A., Akinfenwa, M., Foneska, P., & Mathivanan, S. (2024). Vesiclepedia 2024: An extracellular vesicles and extracellular particles repository. *Nucleic Acids Research*, *52*(D1), D1694–1D698. https://doi.org/10.1093/nar/gkad1007

Chuo, S. T. Y., Chien, J. C. Y., & Lai, C. P. K. (2018). Imaging extracellular vesicles: Current and emerging methods. *Journal of Biomedical Science*, *25*, 91. https://doi.org/10.1186/s12929-018-0494-5

Colombo, M., Raposo, G., & Théry, C. (2014). Biogenesis, secretion, and intercellular interactions of exosomes and other extracellular vesicles. *Annual Review of Cell and Developmental Biology*, *30*, 255–289. https://doi.org/10.1146/annurev-cellbio-101512-122326

Cvjetkovic, A., Jang, S. C., Konečná, B., Höög, J. L., Sihlbom, C., Lässer, C., & Lötvall, J. (2016). Detailed analysis of protein topology of extracellular vesicles-evidence of unconventional membrane protein orientation. *Scientific Reports*, *6*, 36338. https://doi.org/10.1038/srep36338

Cvjetkovic, A., Lötvall, J., & Lässer, C. (2014). The influence of rotor type and centrifugation time on the yield and purity of extracellular vesicles. *Journal of Extracellular Vesicles*, *3*(1), 23111. https://doi.org/10.3402/jev.v3.23111

Dauros Singorenko, P., Chang, V., Whitcombe, A., Simonov, D., Hong, J., Phillips, A., Swift, S., & Blenkiron, C. (2017). Isolation of membrane vesicles from prokaryotes: A technical and biological comparison reveals heterogeneity. *Journal of Extracellular Vesicles*, *6*(1), 1324731. https://doi.org/10.1080/20013078.2017.1324731

Debbi, L., Guo, S., Safina, D., & Levenberg, S. (2022). Boosting extracellular vesicle secretion. *Biotechnology Advances 2*, *59*, 107983. https://doi.org/10.1016/j.biotechadv.2022.107983

Delaunois, B., Colby, T., Belloy, N., Conreux, A., Harzen, A., Baillieul, F., Clément, C., Schmidt, J., Jeandet, P., & Cordelier, S. (2013). Large-scale proteomic analysis of the grapevine leaf apoplastic fluid reveals mainly stress-related proteins and cell wall modifying enzymes. *BMC Plant Biology*, *13*, 24. https://doi.org/10.1186/1471-2229-13-24

De Palma, M., Ambrosone, A., Leone, A., Del Gaudio, P., Ruocco, M., Turi, L., Bokka, R., Fiume, I., Tucci, M., & Pocsfalvi, G. (2020). Plant roots release small extracellular vesicles with antifungal activity. *Plants*, *9*(12), 1777. https://doi.org/10.3390/plants9121777

Dunker, F., Trutzenberg, A., Rothenpieler, J. S., Kuhn, S., Pröls, R., Schreiber, T., Tissier, A., Kemen, A., Kemen, E., Hückelhoven, R., & Weiberg, A. (2020). Oomycete small RNAs bind to the plant RNA-induced silencing complex for virulence. *Elife*, *9*, e56096. https://doi.org/10.7554/eLife.56096

Evtushenko, E. G., Bagrov, D. V., Lazarev, V. N., Livshits, M. A., & Khomyakova, E. (2020). Adsorption of extracellular vesicles onto the tube walls during storage in solution. *PLoS ONE*, *15*(12), e0243738. https://doi.org/10.1371/journal.pone.0243738

Figueiredo, J., Sousa Silva, M., & Figueiredo, A. (2018). Subtilisin-like proteases in plant defence: The past, the present and beyond. *Molecular Plant Pathology*, *19*(4), 1017–1028. https://doi.org/10.1111/mpp.12567

Filipe, V., Hawe, A., & Jiskoot, W. (2010). Critical evaluation of nanoparticle tracking analysis (NTA) by NanoSight for the measurement of nanoparticles and protein aggregates. *Pharmaceutical Research*, *27*(5), 796–810. https://doi.org/10.1007/s11095-010-0073-2

Foers, A. D., Chatfield, S., Dagley, L. F., Scicluna, B. J., Webb, A. I., Cheng, L., Hill, A. F., Wicks, I. P., & Pang, K. C. (2018). Enrichment of extracellular vesicles from human synovial fluid using size exclusion chromatography. *Journal of Extracellular Vesicles*, *7*(1), 1490145. https://doi.org/10.1080/20013078.2018.1490145

Fortunato, D., Mladenović, D., Criscuoli, M., Loria, F., Veiman, K. L., Zocco, D., Koort, K., & Zarovni, N. (2021). Opportunities and pitfalls of fluorescent labeling methodologies for extracellular vesicle profiling on high-resolution single-particle platforms. *International Journal of Molecular Sciences*, *22*(19), 10510. https://doi.org/10.3390/ijms221910510

Garcia-Ceron, D., Lowe, R. G. T., McKenna, J. A., Brain, L. M., Dawson, C. S., Clark, B., Berkowitz, O., Faou, P., Whelan, J., Bleackley, M. R., & Anderson, M. A. (2021). Extracellular vesicles from *Fusarium graminearum* contain protein effectors expressed during infection of corn. *Journal of Fungi*, *7*(11), 977. https://doi.org/10.3390/jof7110977

Görgens, A., Corso, G., Hagey, D. W., Jawad Wiklander, R., Gustafsson, M. O., Felldin, U., Lee, Y., Bostancioglu, R. B., Sork, H., Liang, X., Zheng, W., Mohammad, D. K., van de Wakker, S. I., Vader, P., Zickler, A. M., Mamand, D. R., Ma, L., Holme, M. N., Stevens, M. M., … El Andaloussi, S. (2022). Identification of storage conditions stabilizing extracellular vesicles preparations. *Journal of Extracellular Vesicles*, *11*(6), 12238. https://doi.org/10.1002/jev2.12238

He, B., Cai, Q., Qiao, L., Huang, C. Y., Wang, S., Miao, W., Ha, T., Wang, Y., & Jin, H. (2021). RNA-binding proteins contribute to small RNA loading in plant extracellular vesicles. *Nature Plants*, *7*(3), 342–352. https://doi.org/10.1038/s41477-021-00863-8

He, B., Wang, H., Liu, G., Chen, A., Calvo, A., Cai, Q., & Jin, H. (2023). Fungal small RNAs ride in extracellular vesicles to enter plant cells through clathrin-mediated endocytosis. *Nature Communications*, *14*(1), 1–15. https://doi.org/10.1038/s41467-023-40093-4

Heidarzadeh, M., Zarebkohan, A., Rahbarghazi, R., & Sokullu, E. (2023). Protein corona and exosomes: New challenges and prospects. *Cell Communication and Signaling*, *21*, 64. https://doi.org/10.1186/s12964-023-01089-1

Hiery, E., Adam, S., Reid, S., Hofmann, J., Sonnewald, S., & Burkovski, A. (2013). Genome-wide transcriptome analysis of *Clavibacter michiganensis* subsp. *michiganensis* grown in xylem mimicking medium. *Journal of Biotechnology*, *168*(4), 348–354. https://doi.org/10.1016/j.jbiotec.2013.09.006

Hill, E. H., & Solomon, P. S. (2020). Extracellular vesicles from the apoplastic fungal wheat pathogen *Zymoseptoria tritici*. *Fungal Biology and Biotechnology*, *7*, 13. https://doi.org/10.1186/s40694-020-00103-2

Hofer, U. (2021). Lassoing OMVs with an LPS receptor. *Nature Reviews Microbiology*, *19*(11), 682. https://doi.org/10.1038/s41579-021-00633-5

Hong, J., Dauros-Singorenko, P., Whitcombe, A., Payne, L., Blenkiron, C., Phillips, A., & Swift, S. (2019). Analysis of the *Escherichia coli* extracellular vesicle proteome identifies markers of purity and culture conditions. *Journal of Extracellular Vesicles*, *8*(1), 1632099. https://doi.org/10.1080/20013078.2019.1632099

Huang, Y., Wang, S., Cai, Q., & Jin, H. (2021). Effective methods for isolation and purification of extracellular vesicles from plants. *Journal of Integrative Plant Biology*, *63*(12), 2020–2030. https://doi.org/10.1111/jipb.13181

Janda, M., Rybak, K., Krassini, L., Meng, C., Feitosa-junior, O., Stigliano, E., Szulc, B., Menke, F. L. H., Malone, J. G., Brachmann, A., Klingl, A., Ludwig, C., & Robatzek, S. (2023). Biophysical and proteomic analyses of *Pseudomonas syringae* pv. tomato DC3000 extracellular vesicles suggest adaptive functions during plant infection. *MBio*, *14*, e03589–e03522. https://doi.org/10.1128/mbio.03589-22

Jonca, J., Waleron, M., Czaplewska, P., Bogucka, A., Steć, A., Dziomba, S., Jasiecki, J., Rychłowski, M., & Waleron, K. (2021). Membrane vesicles of pectobacterium as an effective protein secretion system. *International Journal of Molecular Sciences*, *22*(22), 12574. https://doi.org/10.3390/ijms222212574

Kim, D. K., Lee, J., Kim, S. R., Choi, D. S., Yoon, Y. J., Kim, J. H., Go, G., Nhung, D., Hong, K., Jang, S. C., Kim, S. H., Park, K. S., Kim, O. Y., Park, H. T., Seo, J. H., Aikawa, E., Baj-Krzyworzeka, M., van Balkom, B. W., Belting, M., … Gho, Y. S. (2015). EVpedia: A community web portal for extracellular vesicles research. *Bioinformatics*, *31*(6), 933–939. https://doi.org/10.1093/bioinformatics/btu741

Kocholata, M., Prusova, M., Auer Malinska, H., Maly, J., & Janouskova, O. (2022). Comparison of two isolation methods of tobacco-derived extracellular vesicles, their characterization and uptake by plant and rat cells. *Scientific Reports*, *12*, 19896. https://doi.org/10.1038/s41598-022-23961-9

Kondratov, K., Nikitin, Y., Fedorov, A., Kostareva, A., Mikhailovskii, V., Isakov, D., Ivanov, A., & Golovkin, A. (2020). Heterogeneity of the nucleic acid repertoire of plasma extracellular vesicles demonstrated using high-sensitivity fluorescence-activated sorting. *Journal of Extracellular Vesicles*, *9*(1), 1743139. https://doi.org/10.1080/20013078.2020.1743139

Kusch, S., Singh, M., Thieron, H., Spanu, P. D., & Panstruga, R. (2023). Site-specific analysis reveals candidate cross-kingdom small RNAs, tRNA and rRNA fragments, and signs of fungal RNA 2 phasing in the barley-powdery mildew interaction. *Molecular Plant Pathology*, *24*(6), 570–587. https://doi.org/10.1111/mpp.13324

Kwon, S., Rupp, O., Brachmann, A., Blum, C. F., Kraege, A., Goesmann, A., & Feldbrügge, M. (2021). mRNA inventory of extracellular vesicles from *Ustilago maydis*. *Journal of Fungi*, *7*(7), 562. https://doi.org/10.3390/jof7070562

Lehrich, B. M., Liang, Y., & Fiandaca, M. S. (2021). Foetal bovine serum influence on in vitro extracellular vesicle analyses. *Journal of Extracellular Vesicles*, *10*(3), e12061. https://doi.org/10.1002/jev2.12061

Li, D., Li, Z., Wu, J., Tang, Z., Xie, F., Chen, D., Lin, H., & Li, Y. (2022). Analysis of outer membrane vesicles indicates that glycerophospholipid metabolism contributes to early symbiosis between *Sinorhizobium fredii* HH103 and soybean. *Molecular Plant-Microbe Interactions*, *35*(4), 311–322. https://doi.org/10.1094/MPMI-11-21-0288-R

Lohaus, G., Pennewiss, K., Sattelmacher, B., Hussmann, M., & Hermann Muehling, K. (2001). Is the infiltration-centrifugation technique appropriate for the isolation of apoplastic fluid? A critical evaluation with different plant species. *Physiologia Plantarum*, *111*(4), 457–465. https://doi.org/10.1034/j.1399-3054.2001.1110405.x

McMillan, H. M., & Kuehn, M. J. (2023). Proteomic profiling reveals distinct bacterial extracellular vesicle subpopulations with possibly unique functionality. *Applied and Environmental Microbiology*, *89*(1), e01686–e01622. https://doi.org/10.1128/aem.01686-22

McMillan, H. M., Rogers, N., Wadle, A., Hsu-Kim, H., Wiesner, M. R., Kuehn, M. J., & Hendren, C. O. (2021). Microbial vesicle-mediated communication: Convergence to understand interactions within and between domains of life. *Environmental Science: Processes and Impacts*, *23*(5), 664–677. https://doi.org/10.1039/d1em00022e

Midekessa, G., Godakumara, K., Ord, J., Viil, J., Lättekivi, F., Dissanayake, K., Kopanchuk, S., Rinken, A., Andronowska, A., Bhattacharjee, S., Rinken, T., & Fazeli, A. (2020). Zeta potential of extracellular vesicles: Toward understanding the attributes that determine colloidal stability. *ACS Omega*, *5*(27), 16701–16710. https://doi.org/10.1021/acsomega.0c01582

Mulaosmanovic, E., Lindblom, T. U. T., Bengtsson, M., Windstam, S. T., Mogren, L., Marttila, S., Stützel, H., & Alsanius, B. W. (2020). High-throughput method for detection and quantification of lesions on leaf scale based on trypan blue staining and digital image analysis. *Plant Methods*, *16*, 62. https://doi.org/10.1186/s13007-020-00605-5

Nascimento, R., Gouran, H., Chakraborty, S., Gillespie, H. W., Almeida-Souza, H. O., Tu, A., Rao, B. J., Feldstein, P. A., Bruening, G., Goulart, L. R., & Dandekar, A. M. (2016). The type II secreted lipase/esterase LesA is a key virulence factor required for *Xylella fastidiosa* pathogenesis in grapevines. *Scientific Reports*, *6*, 18598. https://doi.org/10.1038/srep18598

Neumann, M. J., & Dobinson, K. F. (2003). Sequence tag analysis of gene expression during pathogenic growth and microsclerotia development in the vascular wilt pathogen *Verticillium dahliae*. *Fungal Genetics and Biology*, *38*(1), 54–62. https://doi.org/10.1016/S1087-1845(02)00507-8

Nouchi, I., Hayashi, K., Hiradate, S., Ishikawa, S., Fukuoka, M., Chen, C. P., & Kobayashi, K. (2012). Overcoming the difficulties in collecting apoplastic fluid from rice leaves by the infiltration-centrifugation method. *Plant and Cell Physiology*, *53*(9), 1659–1668. https://doi.org/10.1093/pcp/pcs102

O'Leary, B. M., Rico, A., McCraw, S., Fones, H. N., & Preston, G. M. (2014). The infiltration-centrifugation technique for extraction of apoplastic fluid from plant leaves using *Phaseolus vulgaris* as an example. *Journal of Visualized Experiments: JoVE*, *19*(94), e52113. https://doi.org/10.3791/52113

Olicón-Hernández, D. R., Hernández-Lauzardo, A. N., Pardo, J. P., Peña, A., Velázquez-del Valle, M. G., & Guerra-Sánchez, G. (2015). Influence of chitosan and its derivatives on cell development and physiology of *Ustilago maydis*. *International Journal of Biological Macromolecules*, *79*, 654–660. https://doi.org/10.1016/j.ijbiomac.2015.05.057

Panagopoulou, M. S., Wark, A. W., Birch, D. J. S., & Gregory, C. D. (2020). Phenotypic analysis of extracellular vesicles: A review on the applications of fluorescence. *Journal of Extracellular Vesicles*, *9*(1), 1710020. https://doi.org/10.1080/20013078.2019.1710020

Pinedo, M., Canal, L., & Marcos Lousa, C. (2021). A call for Rigor and standardization in plant extracellular vesicle research. *Journal of Extracellular Vesicles*, *10*(6), e12048. https://doi.org/10.1002/jev2.12048

Regente, M., Corti Monzón, G., & De La Canal, L. (2008). Phospholipids are present in extracellular fluids of imbibing sunflower seeds and are modulated by hormonal treatments. *Journal of Experimental Botany*, *59*(3), 553–562. https://doi.org/10.1093/jxb/erm329

Regente, M., Corti-Monzón, G., Maldonado, A. M., Pinedo, M., Jorrín, J., & de la Canal, L. (2009). Vesicular fractions of sunflower apoplastic fluids are associated with potential exosome marker proteins. *FEBS Letters*, *583*(20), 3363–3366. https://doi.org/10.1016/j.febslet.2009.09.041

Regente, M., Pinedo, M., Clemente, H. S., Balliau, T., Jamet, E., & De La Canal, L. (2017). Plant extracellular vesicles are incorporated by a fungal pathogen and inhibit its growth. *Journal of Experimental Botany*, *68*(20), 5485–5495. https://doi.org/10.1093/jxb/erx355

Rico, A., & Preston, G. M. (2008). *Pseudomonas syringae* pv. tomato DC3000 uses constitutive and apoplast-induced nutrient assimilation pathways to catabolize nutrients that are abundant in the tomato apoplast. *Molecular Plant-Microbe Interactions*, *21*(2), 269–282. https://doi.org/10.1094/MPMI-21-2-0269

Ruf, A., Oberkofler, L., Robatzek, S., & Weiberg, A. (2022). Spotlight on plant RNA-containing extracellular vesicles. *Current Opinion in Plant Biology*, *69*, 102272. https://doi.org/10.1016/j.pbi.2022.102272

Rumyantseva, N. I., Valieva, A. I., Kostyukova, Y. A., & Ageeva, M. V. (2023). The effect of leaf plasticity on the isolation of apoplastic fluid from leaves of tartary buckwheat plants grown in vivo and in vitro. *Plants*, *12*(23), 4048. https://doi.org/10.3390/plants12234048

Rutter, B. D., Chu, T. T. H., Dallery, J. F., Zajt, K. K., O'Connell, R. J., & Innes, R. W. (2022). The development of extracellular vesicle markers for the fungal phytopathogen *Colletotrichum higginsianum*. *Journal of Extracellular Vesicles*, *11*(5), e12216. https://doi.org/10.1002/jev2.12216

Rutter, B. D., & Innes, R. W. (2017). Extracellular vesicles isolated from the leaf apoplast carry stress-response proteins. *Plant Physiology*, *173*(1), 728–741. https://doi.org/10.1104/pp.16.01253

Rutter, B. D., & Innes, R. W. (2020). Growing pains: Addressing the pitfalls of plant extracellular vesicle research. *New Phytologist*, *228*(5), 1505–1510. https://doi.org/10.1111/nph.16725

Saad, M. G., Beyenal, H., & Dong, W. J. (2024). Dual roles of the conditional extracellular vesicles derived from *Pseudomonas aeruginosa* biofilms: Promoting and inhibiting bacterial biofilm growth. *Biofilm*, *7*, 100183. https://doi.org/10.1016/j.bioflm.2024.100183

Appendix 3

Shekari, F., Alibhai, F. J., Baharvand, H., Börger, V., Bruno, S., Davies, O., Giebel, B., Gimona, M., Salekdeh, G. H., Martin-Jaular, L., Mathivanan, S., Nelissen, I., Nolte-'t Hoen, E., O'Driscoll, L., Perut, F., Pluchino, S., Pocsfalvi, G., Salomon, C., Soekmadji, C., … Nieuwland , R. (2023). Cell culture-derived extracellular vesicles: Considerations for reporting cell culturing parameters. *Journal of Extracellular Biology*, *2*(10), e115. https://doi.org/10.1002/jex2.115

Skliar, M., Chernyshev, V. S., Belnap, D. M., Sergey, G. V., Al-Hakami, S. M., Bernard, P. S., Stijleman, I. J., & Rachamadugu, R. (2018). Membrane proteins significantly restrict exosome mobility. *Biochemical and Biophysical Research Communications*, *501*(4), 1055–1059. https://doi.org/10.1016/j.bbrc.2018.05.107

Suh, J., & Lee, Y. S. (2024). Mitochondria as secretory organelles and therapeutic cargos. *Experimental and Molecular Medicine*, *56*, 66–85. https://doi.org/10.1038/s12276-023-01141-7

Théry, C., Witwer, K. W., Aikawa, E., Alcaraz, M. J., Anderson, J. D., Andriantsitohaina, R., Antoniou, A., Arab, T., Archer, F., Atkin-Smith, G. K., Ayre, D. C., Bach, J. M., Bachurski, D., Baharvand, H., Balaj, L., Baldacchino, S., Bauer, N. N., Baxter, A. A., Bebawy, M., … Zuba-Surma, E. K. (2018). Minimal information for studies of extracellular vesicles 2018 (MISEV2018): A position statement of the International Society for Extracellular Vesicles and update of the MISEV2014 guidelines. *Journal of Extracellular Vesicles*, *7*(1), 1535750. https://doi.org/10.1080/20013078.2018.1535750

van de Wakker, S. I., van Oudheusden, J., Mol, E. A., Roefs, M. T., Zheng, W., Görgens, A., El Andaloussi, S., Sluijter, J. P. G., & Vader, P. (2022). Influence of short term storage conditions, concentration methods and excipients on extracellular vesicle recovery and function. *European Journal of Pharmaceutics and Biopharmaceutics*, *170*, 59–69. https://doi.org/10.1016/j.ejpb.2021.11.012

Varga, Z., Fehér, B., Kitka, D., Wacha, A., Bóta, A., Berényi, S., Pipich, V., & Fraikin, J. L. (2020). Size measurement of extracellular vesicles and synthetic liposomes: The impact of the hydration shell and the protein corona. *Colloids and Surfaces B: Biointerfaces*, *192*, 111053. https://doi.org/10.1016/j.colsurfb.2020.111053

Wang, F., Ho, P. Y., Kam, C., Yang, Q., Liu, J., Wang, W., Zhao, E., & Chen, S. (2023). An AIE-active probe for efficient detection and high-throughput identification of outer membrane vesicles. *Aggregate*, *4*(4), e312. https://doi.org/10.1002/agt2.312

Wang, J., Ding, Y., Wang, J., Hillmer, S., Miao, Y., Lo, S. W., Wang, X., Robinson, D. G., & Jiang, L. (2010). EXPO, an exocyst-positive organelle distinct from multivesicular endosomes and autophagosomes, mediates cytosol to cell wall exocytosis in Arabidopsis and tobacco cells. *Plant Cell*, *22*(12), 4009–4030. https://doi.org/10.1105/tpc.110.080697

Wang, M., Weiberg, A., Lin, F.-M., Thomma, B. P. H. J., Huang, H.-D., & Jin, H. (2016). Bidirectional cross-kingdom RNAi and fungal uptake of external RNAs confer plant protection. *Nature Plants*, *2*, 16151. https://doi.org/10.1038/nplants.2016.151

Wang, S., He, B., Wu, H., Cai, Q., Ramírez-Sánchez, O., Abreu-Goodger, C., Birch, P. R. J., & Jin, H. (2023). Plant mRNAs move into a fungal pathogen via extracellular vesicles to reduce infection. *Cell Host & Microbe*, *32*(1), 93–105. https://doi.org/10.1016/j.chom.2023.11.020

Weiberg, A., Wang, M., Lin, F.-M., Zhao, H., Zhang, Z., Kaloshian, I., Huang, H.-D., & Jin, H. (2013). Fungal small RNAs suppress plant immunity by hijacking host RNA interference pathways. *Science*, *342*(6154), 118–123. https://doi.org/10.1126/science.1239705

Welsh, J. A., Goberdhan, D. C. I., O'Driscoll, L., Buzas, E. I., Blenkiron, C., Bussolati, B., Cai, H., Di Vizio, D., Driedonks, T. A. P., Erdbrügger, U., Falcon-Perez, J. M., Fu, Q. L., Hill, A. F., Lenassi, M., Lim, S. K., Mahoney, M. G., Mohanty, S., Möller, A., Nieuwland, R., … Witwer, K. W. (2024). Minimal information for studies of extracellular vesicles (MISEV2023): From basic to advanced approaches. *Journal of Extracellular Vesicles*, *13*(2), e12404. https://doi.org/10.1002/jev2.12404

Wengelnik, K., Marie, C., Russel, M., & Bonas, U. (1996). Expression and localization of HrpA1, a protein of *Xanthomonas campestris* pv. *vesicatoria* essential for pathogenicity and induction of the hypersensitive reaction. *Journal of Bacteriology*, *178*(4), 1061–1069. https://doi.org/10.1128/jb.178.4.1061-1069.1996

Wong-Bajracharya, J., Singan, V. R., Monti, R., Plett, K. L., Ng, V., Grigoriev, I. V., Martin, F. M., Anderson, I. C., & Plett, J. M. (2022). The ectomycorrhizal fungus *Pisolithus microcarpus* encodes a microRNA involved in cross-kingdom gene silencing during symbiosis. *Proceedings of the National Academy of Sciences of the United States of America*, *119*(3), e2103527119. https://doi.org/10.1073/pnas.2103527119

Yao, L., Jiang, Z., Wang, Y., Hu, Y., Hao, G., Zhong, W., Wan, S., & Xin, X. (2023). High air humidity dampens salicylic acid pathway and NPR1 function to promote plant disease. *EMBO Journal*, *42*(21), e113499. https://doi.org/10.15252/embj.2023113499

Zand Karimi, H., Baldrich, P., Rutter, B. D., Borniego, L., Zajt, K. K., Meyers, B. C., & Innes, R. W. (2022). Arabidopsis apoplastic fluid contains SRNA- and circular RNA-protein complexes that are located outside extracellular vesicles. *Plant Cell*, *34*(5), 1863–1881. https://doi.org/10.1093/plcell/koac043

Zhu, J., Qiao, Q., Sun, Y., Xu, Y., Shu, H., Zhang, Z., Liu, F., Wang, H., Ye, W., Dong, S., Wang, Y., Ma, Z., & Wang, Y. (2023). Divergent sequences of tetraspanins enable plants to specifically recognize microbe-derived extracellular vesicles. *Nature Communications*, *14*, 4877. https://doi.org/10.1038/s41467-023-40623-0

How to cite this article: Thieron, H., Krassini, L., Kwon, S., Fricke, S., Nasfi, S., Oberkofler, L., Ruf, A., Kehr, J., Kogel, K.-H., Weiberg, A., Feldbrügge, M., Robatzek, S., & Panstruga, R. (2024). Practical advice for extracellular vesicle isolation in plant–microbe interactions: Concerns, considerations, and conclusions. *Journal of Extracellular Vesicles*, *13*, e70022. https://doi.org/10.1002/jev2.70022

Acknowledgement

The unfolding climate crisis, raising fascism and increasing inequality make me very anxious and often not very optimistic about the future. Being able to perform research and working on a topic even, if it's as small as vesicles, often gave me a sense of purpose.

None of this would have been possible without the constant support of my supervisor and mentor Silke! When I started this project, you were recommended to me by someone who considers themselves "your number one fan". Now, I am happy to join this club - thank you for showing me how to be a better scientist, and that academia doesn't suck after all ;).

I would also like to express my gratitude to my TAC committee, Arne Weiberg and Wolfgang Enard for their guidance and advice on this project. The same is true for the help from many other experts and collaborators including Kai Papenfort, Christina Ludwig, Lionel Navarro, Andreas Brachmann and Andreas Klingl. Thank you all so much for your advice, I have learnt a lot from all of you.

Danke Mama & Papa, dass ihr mich überall besuchen kommt, mir immer zuhört und mich in allem unterstützt! Auch wenn die Sprachen und Länder alle paar Jahre wechseln, auf euch kann ich mir immer verlassen.

Das gleiche gilt für meine (mehr oder weniger) „daheim gebliebenen" Freunde: Alena, Carla, Jannik, Malte und Sophia. Für jedes Wochenende, dass ich mit euch verbringe, ohne auch nur eine Sekunde an Vesikel oder Xylella zu denken, bin ich euch unendlich dankbar. Ihr erinnert mich daran, dass der Rest der Welt auch dann noch existiert, wenn das letzte Experiment doch nicht geklappt hat. Wie cool ist es, dass ich euch überall mitbringen kann und ihr euch einfach mit den neuen Freunden mischt. Ihr seid die Beschden.

And then there is of course the new friends I made along the way, for whom I am also eternally grateful. Thank you, Jin, for making me a better, kinder person. Thank you, Lorenz for being my scientific sparring partner and such a good friend. Thank you, Eliana for being my fellow sufferer and the ultimate nomenclature guide. Thank you, Zane and Gabi, noble prize(s) incoming for you any day now and thank you Santi for always having an open ear. Thank you

for all the evenings at Frische Bier, at Sofa and on the Couch – I don’t know how I would have come out of this, without you.
It is a lot easier, coming to work when you are being welcomed into a lovely office every morning, thank you Constance, Marta and Xuanyu for all your girl power. The same is true for every lunch break with the people of the department, thank you for all the laughter, level 3 bioinformatics support (Niklas!), advise and coffees together. The same goes for all my colleagues of the research unit, in particular my co-authors Hannah, Sabrine and Patrick, what a joy it has been learning from you and working alongside you. A big part of this work would not have been possible without my super students, Tora, Vincent and Elif! Thank you for all your efforts, discussions and your patience while I tried to figure out how to be a supervisor myself. I would also like to thank all recent and former members of the AG Robatzek and Genetics, for all your support, help, advice and open ears along the way. In particular to Kasia and Eliana for proof-reading my thesis! I am also very grateful for the technical support from the ultimate power team of Chappy, Irma, Jessi, Marta and Ute! There are also lots of other people, I was fortunate enough to learn from along the way including former supervisors, study colleagues and friends: Thank you, merci, gracias, danke und 谢谢.

Un grand merci à la belle-famille bretonne, qui m’ont accueillie plusieurs fois chez eux pour le télétravail dans un tout nouveau bureau et avec tout service compris : verres de rouge à midi, pauses plouf le soir, et atelier pomme ou “lance patate” pour se changer les idées. Merci aussi à Klervi et Neven pour l’accompagnement musical parfait pour écrire des textes scientifiques. Trugarez and Yec'hed mat !

And finishing with the most important person of all - Liza, I don’t have any words to express the gratitude I feel for doing this silly, little life with you. You make me happy, happy, happy every day.